



University
of Glasgow

<https://theses.gla.ac.uk/>

Theses Digitisation:

<https://www.gla.ac.uk/myglasgow/research/enlighten/theses/digitisation/>

This is a digitised version of the original print thesis.

Copyright and moral rights for this work are retained by the author

A copy can be downloaded for personal non-commercial research or study,
without prior permission or charge

This work cannot be reproduced or quoted extensively from without first
obtaining permission in writing from the author

The content must not be changed in any way or sold commercially in any
format or medium without the formal permission of the author

When referring to this work, full bibliographic details including the author,
title, awarding institution and date of the thesis must be given

Enlighten: Theses

<https://theses.gla.ac.uk/>
research-enlighten@glasgow.ac.uk

**Elucidating the Biological Role of
Actin Cytoskeletal Proteins
in the Budding Yeast *Saccharomyces cerevisiae***

by

Fiona Claire Gardiner

A thesis submitted for the degree of Doctor of Philosophy

Department of Biochemistry and Molecular Biology

Institute of Biomedical and Life Sciences

University of Glasgow

July 2005

© Copyright by Fiona C. Gardiner, 2005

ProQuest Number: 10390777

All rights reserved

INFORMATION TO ALL USERS

The quality of this reproduction is dependent upon the quality of the copy submitted.

In the unlikely event that the author did not send a complete manuscript and there are missing pages, these will be noted. Also, if material had to be removed, a note will indicate the deletion.



ProQuest 10390777

Published by ProQuest LLC (2017). Copyright of the Dissertation is held by the Author.

All rights reserved.

This work is protected against unauthorized copying under Title 17, United States Code
Microform Edition © ProQuest LLC.

ProQuest LLC.
789 East Eisenhower Parkway
P.O. Box 1346
Ann Arbor, MI 48106 – 1346

**GLASGOW
UNIVERSITY
LIBRARY:**

ABSTRACT

The dynamic, co-ordinated remodelling of the actin cytoskeleton is attributed to the interaction of actin with a wide variety of actin regulating proteins. The remodelling of actin is central to many cellular processes including endocytic uptake, polarisation of growth, cell motility, and is important for the ability of cells to respond to many intracellular and extracellular signals. Therefore, the study of individual actin regulating proteins enables a greater understanding of the complex overall control of the actin network and many cellular processes.

Sla1p is an endocytic adaptor protein with several known roles in the cytoplasm, which include linking proteins involved in the early stages of endocytic uptake with those required for the actin polymerisation at endocytic sites. The data presented in this thesis however details the nuclear localisation of Sla1p. In addition to this initial observation, further analysis has allowed the proposal of a mechanism for the nuclear translocation of Sla1p. This was achieved by analysis of potential nuclear transport signals in wild-type and *sla1* mutants, consideration of phosphorylatory mechanisms, and by detailed studies of nuclear transport receptor mutants. Finally, results of microarray analysis undertaken between wild-type and *sla1* mutant strains were used to elucidate potential roles of nuclear Sla1p. These studies suggest that Sla1p localises both to the cytoplasm and the nucleus in *S. cerevisiae* and that its activity and cellular localisation may be regulated primarily through phosphorylation.

The key to the dynamic remodelling of the actin cytoskeleton is the coordinated control of filament nucleation, polymerisation and disassembly. Data presented in this thesis demonstrates the association of the cortical patch protein Ysc84p with actin filaments, and the ability of Ysc84p to both sever and cap these filaments *in vitro*. A possible regulatory mechanism for the protein is also considered. Additionally, a Ysc84p homologue is localised to dynamic actin structures in mammalian cells and studies suggest that this protein may have a similar actin regulatory mechanism. These studies therefore suggest an exciting role for the cortical patch protein Ysc84p in the regulated control of branched actin filaments in *S. cerevisiae*.

ACKNOWLEDGEMENTS

I wish to first thank my supervisor, Dr. Kathryn Ayscough for guiding me through the Ph.D process and for all her help, advice and patience. I would also like to thank all members of both the Ayscough lab and the Winder lab, but specifically: Campbell Gourlay, Rosaria Costa, Dana Georghe and Derek Warren for all their help and support and for cheering me up when the going got tough. I also wish to thank Dr. Steve Winder for carrying out subsequent studies and for his advice. Additionally, I wish to thank my parents, family and friends for their encouragement, their help with my continual moving and the promise of a good celebration when I finally leave university!

I hereby declare that this submission is my own work and contains no material written by another person, nor material which has been accepted for the award of any other degree or diploma of the university or other institute of higher learning.

TABLE OF CONTENTS

ABSTRACT	ii
ACKNOWLEDGEMENTS	iii
TABLE OF CONTENTS	iv
LIST OF FIGURES	viii
LIST OF TABLES	x
ABBREVIATIONS	x
1 INTRODUCTION.....	1
1.1 General introduction.....	2
1.2 Actin	2
1.3 Structure of G-actin	3
1.4 Structure of F-actin.....	4
1.5 Polymerisation of actin	7
1.6 Regulation of actin	11
1.6.1 Monomer binding proteins	11
1.6.2 Filament stabilising proteins.....	13
1.6.3 Capping proteins.....	13
1.6.4 Bundling and cross-linking proteins.....	14
1.6.5 Severing proteins	14
1.6.6 Nucleating proteins.....	15
1.6.7 The Arp2/3 complex in more detail.....	16
1.7 Chemical tools used to study actin.....	17
1.7.1 Phalloidin.....	17
1.7.2 Cytochalasin D	18
1.7.3 Latrunculin-A	18
1.7.4 Jasplakinolide	18
1.8 Actin in eukaryotic cells.....	19
1.9 Yeast as a model organism	23
1.10 Polarisation of growth in <i>S. cerevisiae</i>	23
1.11 Actin structures in <i>S. cerevisiae</i>.....	24
1.11.1 Actin cables	27
1.11.2 Cortical actin patches	27
1.11.3 The cytokinetic ring.....	29
1.12 Polarisation of actin in <i>S. cerevisiae</i>	29
1.13 Cortical patch proteins	30
1.14 Actin and endocytosis	31
1.15 The endocytic adaptor protein Sla1p	37
1.15.1 Phenotypes of Δs_{la1} cells	40

1.15.2	Interactions of Sla1p.....	41
1.16	The cortical patch protein Ysc84p.....	43
1.16.1	Phenotypes of Δ y _{sc84} cells	44
1.16.2	Interactions of Ysc84p.....	44
1.17	Aims of this project.....	45
2	MATERIALS AND METHODS	47
2.1	Materials	48
2.2	Yeast Strains, Plasmids and Oligonucleotides.....	48
2.3	Molecular Biology Techniques.....	53
2.3.1	Restriction enzyme digestion of DNA.....	53
2.3.2	Electrophoresis of DNA using agarose gels.....	53
2.3.3	Removal of terminal 5' phosphate groups using calf intestinal alkaline phosphatase (C.I.P.).....	54
2.3.4	Extraction of DNA from an agarose gel slice using the QIAquick Gel Extraction Kit™	54
2.3.5	Amplification of DNA using the polymerase chain reaction	54
2.3.6	Ligation of DNA fragments.....	55
2.3.7	Integration of DNA fragments into the pTrcHis-TOPO® vector.....	55
2.3.8	Preparation of calcium competent DH5 α cells	56
2.3.9	Transformation of calcium competent DH5 α cells	56
2.3.10	Plasmid DNA purification using the QIAprep Spin Miniprep Kit™	56
2.4	Yeast Methods	58
2.4.1	Mating yeast strains	58
2.4.2	Sporulation and tetrad analysis.....	58
2.4.3	Yeast transformations	59
2.4.4	'Knock in' strategy of generating integrated gene deletions or tagged strains.....	59
2.4.5	Screening for integrated tags or gene deletions by colony PCR	60
2.4.6	Testing for temperature sensitivity	60
2.4.7	Overexpression of hSh3yl-1 in a Δ y _{sc84} Δ lsb5 strain.....	60
2.4.8	Induction of the mating response.....	61
2.4.9	Glycerol stocks	61
2.5	Yeast 2-hybrid analysis.....	61
2.5.1	Yeast 2-hybrid cloning and transformation	61
2.5.2	Yeast 2-hybrid analysis	61
2.5.3	β -galactosidase assay	62
2.6	Protein Methods	63
2.6.1	Whole cell yeast extracts	63
2.6.2	Preparation of protein preps by grinding in liquid nitrogen	63
2.6.3	SDS-PAGE electrophoresis.....	64
2.6.4	Western blotting	65
2.6.5	Western blot detection using Enhanced Chemi-Luminescence (ECL)	65
2.6.6	2-Dimensional gel electrophoresis using the ZOOM® IPG Runner System	66
2.6.7	Induction of a tagged protein in bacterial cells.....	67
2.6.8	Purification of GST tagged proteins using Glutathione Sepharose® 4B Beads	67
2.6.9	F-actin sedimentation assays	68

2.6.10	Falling ball assays.....	69
2.6.11	Fluorescent actin assays	69
2.6.12	Coomassie staining of SDS-polyacrylamide gels.....	70
2.6.13	Determination of protein concentration by spectrometry.....	70
2.7	Microscopy methods	71
2.7.1	Equipment details	71
2.7.2	Indirect immunofluorescence	71
2.7.3	Rhodamine phalloidin staining.....	72
2.7.4	Lucifer Yellow uptake assay	72
2.7.5	FM4-64 assay	72
2.7.6	Latrunculin-A treatment of cells	73
2.8	Antibody Production.....	73
2.8.1	Raising an immune response in rabbits	73
2.8.2	Purification of serum over a Protein A column.....	73
2.9	RNA Methods	74
2.9.1	Yeast RNA extraction using the Promega SV Total RNA Extraction Kit and Qiagen RNeasy Mini Kit	74
2.9.2	Quantification of RNA using an Agilent Bioanalyzer2100.....	75
2.9.3	RNA concentration using Pellet Paint® co-precipitant.....	75
2.9.4	DS cDNA Synthesis and cleanup	76
2.9.5	Synthesis of Biotin Labelled cRNA using a High Yield RNA Transcript Labelling Kit	77
2.9.6	Cleanup of labelled cDNA using the RNeasy™ Mini Kit	77
2.9.7	Quantification of labelled cDNA.....	78
2.9.8	Fragmentation of RNA	78
2.9.9	Hybridisation of RNA to oligonucleotide arrays.....	79
2.9.10	Analysis of RNA data using SAM software.....	79
2.9.11	RT-PCR using the Titan One Tube RT-PCR System	79
3	CHARACTERISATION OF NUCLEAR SLA1.....	81
3.1	Introduction.....	82
3.2	Results	87
3.2.1	The localisation of Sla1p to the nucleus is not a cell-cycle associated event	87
3.2.2	Nuclear Sla1p response to heat shock	90
3.2.3	Nuclear Sla1p is not affected by induction of the mating response	92
3.2.4	The localisation of <i>Sla1</i> -ΔG2 and <i>s1a1</i> -ΔII8-5II mutants	94
3.2.5	<i>Sla1</i> -ΔG2-myc and <i>s1a1</i> -ΔII8-5II-myc mutants have endocytic and actin defects	98
3.2.6	The sequence of Sla1p suggests multiple NLSSs and NESSs	100
3.2.7	Characterisation of karyopherin mutants.....	102
3.2.8	Generation of Sla1-myc in specific karyopherin mutant strains	105
3.2.9	Sla1p mislocalisation in an <i>rsl1</i> mutant.....	106
3.2.10	Mutation of <i>cml1</i> does not affect the nuclear localisation of Sla1p.....	108
3.2.11	Microarray analysis of gene expression in wild-type and Δ <i>s1a1</i> cells.....	110
3.2.12	RT-PCR confirmation of microarray data.....	115
3.3	Discussion.....	119
4	CHARACTERISING THE ROLE OF YSC84.....	128

4.1	Introduction.....	129
4.2	Results	131
4.2.1	hSH3yl-1 can partially replace the function of Ysc84p	131
4.2.2	Generation of Ysc84p fusion proteins.....	134
4.2.3	Ysc84p and the conserved N-terminal region of Ysc84p bind directly to F-actin.....	137
4.2.4	Analysis of the Ysc84p sequence for actin binding regions.....	141
4.2.5	Analysis of the severing activity of Ysc84p.....	143
4.2.6	Ysc84p severs fluorescently labelled actin filaments.....	145
4.2.7	Ysc84p can both sever and cap fluorescently labelled actin filaments	150
4.2.8	Generation of Ysc84p antibodies	156
4.2.9	Ysc84p analysis by 2D-gel electrophoresis.....	159
4.3	Discussion.....	161
5	GTS1 IS AN Arf-GAP HOMOLOGY PROTEIN THAT INTERACTS WITH SLA1 AND YSC84	170
5.1	Introduction.....	171
5.2	Results	174
5.2.1	Gts1p interacts with Sla1p and Ysc84p, as determined by yeast two hybrid analysis.....	174
5.2.2	Gts1p interacts with the N-terminal SH3 domains of Sla1p and the SH3 domain of Ysc84p	177
5.2.3	Gts1p localises to punctate structures at the plasma membrane, independently of both Sla1p and F-actin.....	179
5.2.4	GTS1 deletion indicates that the protein plays a role in endocytosis and actin organisation.....	182
5.3	Discussion.....	185
6	THESIS SUMMARY AND FUTURE DIRECTIONS	190
6.1	Thesis Summary	191
6.2	Future Directions	195
6.2.1	Investigating the nuclear translocation of Sla1p.....	195
6.2.2	Examining the regulatory mechanism of Sla1p.....	195
6.2.3	Identifying Sla1p protein-protein interactions.....	196
6.2.4	Investigating the effect of Ysc84p on actin polymerisation	196
6.2.5	Investigating the <i>in vivo</i> function of Ysc84p and protein-protein interactions	197
6.2.6	Analysis of the Arf-GAP activity of Gts1p	197
6.2.7	Investigating protein-protein interactions and the localisation of Gts1p.....	198
7	REFERENCES	199

LIST OF FIGURES

Table	Title	Page
Figure 1-1. The structure of an actin monomer in a TMR bound state		5
Figure 1-2. The Holmes filament model		6
Figure 1-3. The structure of an actin filament		7
Figure 1-4. The time course of actin polymerisation <i>in vitro</i>		9
Figure 1-5. Filament generation and treadmilling		10
Figure 1-6. Overview of actin regulating proteins		12
Figure 1-7. Actin structures in lamellipodia and filopodia.		20
Figure 1-8 Model of dendritic nucleation for protrusion of the leading edge		22
Figure 1-9. The life cycle of <i>S. cerevisiae</i>		25
Figure 1-10. Polarisation of the actin cytoskeleton in <i>S. cerevisiae</i>		26
Figure 1-11. Proposed roles for the actin cytoskeleton in endocytosis		34
Figure 1-12. Current model demonstrating the proposed role of actin in endocytosis		36
Figure 1-13. Schematic representation of domains present in Sla1p		39
Figure 1-14. Schematic representation of domains present in Ysc84p and its homologues		39
Figure 3-1. Active transport across the nuclear membrane		85
Figure 3-2. Sla1p shows both a partial co-localisation with cortical actin patches and a nuclear co-localisation.		88
Figure 3-3. The nuclear localisation of Sla1p-myc is cell-cycle independent.		89
Figure 3-4. The localisation of Sla1p-myc is unaffected in heat shocked cells		91
Figure 3-5. The nuclear localisation of Sla1p is unaffected during the mating response.		93
Figure 3-6. Diagram of Sla1p mutant constructs, <i>sla1</i> - Δ <i>I18-511</i> and <i>sla1</i> - Δ <i>G2</i>		96
Figure 3-7. Localisation of <i>sla1</i> - Δ <i>G2</i> -myc and <i>sla1</i> - Δ <i>I18-511</i> -myc mutants constructs.		97
Figure 3-8. F-actin structures in haploid yeast strains expressing <i>sla1</i> - Δ <i>I18-511</i> -myc and <i>sla1</i> - Δ <i>G2</i> -myc.		99
Figure 3-9. Fluid phase endocytosis assays in haploid yeast strains expressing <i>sla1</i> - Δ <i>I18-511</i> -myc and <i>sla1</i> - Δ <i>G2</i> -myc.		99
Figure 3-10. Sla1p contains several possible NLS and NES motifs, several of which are absent in <i>sla1</i> - Δ <i>I18-511</i> and <i>sla1</i> - Δ <i>G2</i> mutants		101
Figure 3-11. Three karyopherins mutants displayed distinct endocytic and actin defects.		104
Figure 3-12. Expression of myc-tagged Sla1p in an <i>rsl1</i> mutant as determined by Western blotting		107
Figure 3-13. Sla1p-myc is mislocalised in an <i>rsl1</i> -1 mutant		107
Figure 3-14. Sla1p-myc localisation in a <i>cml1</i> mutant.		109
Figure 3-15. Graphical display of microarray results showing functional groupings		114
Figure 3-16. RT-PCR results confirm the trends in gene expression change identified by microarray analysis		117
Figure 3-17. Fold changes in gene expression as identified by RT-PCR		118
Figure 3-18. Proposed mechanism for Sla1p entry into the nucleus		124
Figure 3-19. The flexible cytoskeletal network found in red blood cells.		126
Figure 4-1. hSH3yl-1 expression in yeast rescues the temperature dependent growth phenotype of a Δ <i>Ysc84A</i> <i>lsb5</i> strain.		132
Figure 4-2. hSH3yl-1 expression in yeast partially rescues the endocytic defect but not the actin defect of a Δ <i>Ysc84A</i> <i>lsb5</i> strain.		133
Figure 4-3. <i>YSC84</i> amplified by RT-PCR		136
Figure 4-4. Diagram of Ysc84p and the Ysc84-Nt fragment fused to GST		136
Figure 4-5. Purification of GST-Ysc84 and GST-Ysc84-Nt fusion proteins		139
Figure 4-6. Analysis of GST-Ysc84 and GST-Ysc84-Nt interaction with F-actin		140
Figure 4-7. Ysc84p has two potential actin binding regions		142
Figure 4-8. Biochemical analysis of GST-Ysc84-Nt with actin		144

Figure 4-9. GST-Ysc84-Nt and GST-Ysc84-Nt are able to sever actin filaments	147
Figure 4-10. GST-Ysc84 and GST-Ysc84-Nt sever fluorescent actin filament in the presence of phalloidin	149
Figure 4-11. GST-Ysc84-Nt and GST-Ysc84 both cap and sever labelled actin filaments	152
Figure 4-12. GST-Ysc84-Nt demonstrates filament capping activity in dual labelling fluorescent actin assays	154
Figure 4-13. Analysis of Alexa Fluor ⁴⁸⁸ labelled filaments in dual labelling experiments	155
Figure 4-14. Purified GST-Ysc84-Nt	158
Figure 4-15. Specificity of Ysc84 antisera as determined by western blotting	158
Figure 4-16. 2-Dimensional gel analysis of wild-type extracts with anti-Ysc84 antibodies.	160
Figure 4-17. The Ysc84-*Nt fragment fused to GST	166
Figure 4-18. Proposed involvement of Ysc84p in endocytosis	169
Figure 5-2. Gts1p interacts with Ysc84p and Sla1p by 2-hybrid.	176
Figure 5-4. GFP-Gts1p localises to punctuate patches at the cell cortex.	180
Figure 5-5. GFP-Gts1p localisation is unaffected in a $\Delta s\text{la}1$ strain.	180
Figure 5-6. GFP-Gts1p localises to punctuate patches at the cell cortex in Latrunculin-A treated cells.	181
Figure 5-7. Deletion of GTS1 causes a mild actin defect and defects in the endocytic internalisation of membranes.	183
Figure 5-8. Deletion of GTS1 causes defects in fluid phase endocytosis.	184
Figure 5-9. Proposed Gts1p interactions at the cell cortex	189

LIST OF TABLES

Table	Title	Page
Table 1-1	Known cortical patch proteins	31
Table 2-1	Plasmids used in this study	49
Table 2-2	Oligonucleotides used in this study	50
Table 2-3	Yeast strains used in this study	52
Table 2-4	Antibodies used in this study	52
Table 3-1	Consensus sequence of conserved NLS and NES elements.	86
Table 3-2	Phenotypic analysis of karyopherin and nuclear transport mutants	103
Table 3-3	Genes identified by microarray and SAM analysis.	113
Table 3-4	Genes selected for RT-PCR analysis.	116
Table 5-1	2-hybrid constructs assayed	175

ABBREVIATIONS

Lengths and volumes are indicated using the International Systems of Units symbols.

Δ	deletion
::	genomic disruption
°C	degrees Celcius
α -factor	alpha factors mating pheromone
aa	amino acids
ADP	adenosine diphosphate
Arf	ADP ribosylation factor
Arp2/3 complex	actin-related protein 2/3 complex
ATP	adenosine 5'-triphosphate
bp	base pair(s)
BSA	bovine serum albumin
CA	connector and acidic
C-terminus	carboxy-terminus
CH	calponin homology
CLR	calponin like repeat
DAPI	4',6-diamino-2-phenylindole
<i>Dictyostelium</i>	<i>Dictyostelium discoideum</i>
DNA	deoxyribonucleic acid
DTT	dithiothreitol
ECL	enhanced chemiluminescence
EDTA	ethylenediaminetetraacetic acid
EH	epsin homology
ENTH	epsin N-terminal homology
F-actin	filamentous actin

FITC	fluorescein isothiocyanate
G1	Gap 1 phase (of the cell cycle)
G-actin	globular (monomeric) actin
GAP	GTPase activating protein
GFP	green fluorescent protein
GST	glutathione-S-transferase
GTPase	guanosine triphosphatase
IP	immunoprecipitation
kb	kilobase pair(s)
kDa	kilodaltons
Lat A	latrunculin A
MAT _a	mating type a
MAT _α	mating type α
min	minute(s)
mM	millimolar
Mwt	molecular weight
NES	nuclear export sequence
NLS	nuclear localisation signal
NPF	nucleation promoting factor
N-terminus	amino terminus
Oligos	oligonucleotides
ORF	open reading frame
PAGE	polyacrylamide gel electrophoresis
PBS	phosphate buffered saline
PCR	polymerase chain reaction
PEG	polyethylene glycol
pH	potential of hydrogen
pi	isoelectric point
PMSF	phenylmethylsulfonyl fluoride
PVDF	polyvinylidene fluoride
RanGAP	Ran-specific GTPase activating protein
RanGEF	Ran-specific guanine nucleotide exchange factor
RNA	ribonucelic acid
SC	synthetic complete media
<i>S. cerevisiae</i>	<i>Saccharomyces cerevisiae</i>
SD	synthetic dropout
SDS	sodium dodecyl sulphate
SGD	Saccharomyces Genome Database
TAE	TRIS-acetate-EDTA
TMR	Tetramethylrhodamine-5-maleimide
TRIS	tris (hydroxymethyl)-aminomethane
μM	micromolar
uv	ultra-violet
WASP	Wiskott-Aldrich Syndrome protein
N-WASP	neural Wiskott-Aldrich Syndrome protein
YPAD	rich media
<i>Xenopus</i>	<i>Xenopus Laevis</i>

1 INTRODUCTION

1.1 General introduction

The ability of cells to grow and replicate is fundamental to the development of organic life. Remodelling of the cytoskeleton is central to both cellular growth and replication, enabling both the polarised transport of organelles and vesicles to specific sites, cellular remodelling and division.

Cytoskeletal networks are also of interest in the study of disease. The lack of regulated cellular growth and division displayed in tumour cell lines enables such cells to proliferate in an unrestrained manner, and consequently involves cytoskeletal components, which regulate cellular polarisation and remodelling. Understanding the control of cytoskeletal networks will therefore enable greater insight into cellular dysregulation, while also providing important information on the growth, motility, polarity and development of cells.

Actin is an important component of the cytoskeletal network. This introductory chapter provides an initial overview of the composition of the cytoskeletal network and integral actin filaments. The focus then turns to the actin molecule, polymerisation of actin and the control of polymerising actin structures by additional proteins. I will then introduce the various cellular structures formed by filamentous actin, concentrating finally on the control of actin in the budding yeast *Saccharomyces cerevisiae* and the reasons for choosing to study cytoskeletal networks in this model organism.

1.2 Actin

Central to our understanding of cell polarisation and growth is an appreciation of the control of cytoskeletal networks. Actin is a highly conserved and ubiquitously expressed protein in eukaryotic cells and is an important component of such cytoskeletal networks. The conservation of the actin protein throughout eukaryotes reflects the importance of this molecule in cellular function. Actin is involved in many diverse roles including intracellular organisation, organelle movement and inheritance, cell structure, endocytosis, transcription, cell division and polarisation. Composing approximately 10% of total cellular protein in the highly motile amoeba *Dictyostelium* (Hug *et al.*, 1995), actin is regarded as a crucial cellular cytoskeletal protein, with roles in a wide variety of general and cell-specific processes. In motile cells, actin is an essential component of the machinery required for cell contractility and motility. While in the non-motile budding yeast *S. cerevisiae* however, actin is involved in events including

bud site selection and bud emergence. Actin is present therefore in all cells and has roles both in conserved cellular processes and also in cell specific activities.

Cytoskeletal actin exists in two basic forms, as monomeric G-actin and polymeric, filamentous F-actin. Actin monomers polymerise to form actin filaments which are then organised into higher order cellular structures. The diversity of actins' cellular roles is primarily dependent on the association of a wide variety of proteins with both G- and F-actin which control and generate intricate, highly regulated filamentous actin networks. These actin binding proteins regulate nucleation, polymerisation and organisation of filamentous actin at specific sites, allowing the actin structures and the force generated by actin polymerisation to be harnessed and utilised in the cell.

The cytoskeleton is composed of an array of protein filaments which not only maintain cellular structure but which also enable changes in cell shape and intracellular reorganisation and remodelling. In *S. cerevisiae*, the cytoskeleton is composed of only two types of protein filament, actin filaments and microtubules. Microtubules are similar to F-actin in that polymerisation occurs from monomeric proteins; alpha and beta tubulin. Microtubules are however hollow cylindrical filaments, whereas actin filaments polymerise in helical pairs and form thin filaments. Cytoskeletal networks in most species generally however contain intermediate filaments, in addition to microtubules and actin filaments. The components of intermediate filaments are diverse and cell specific but are known to include keratins in epithelial cells, vimentins, nuclear lamins which are involved in the stabilisation of the nuclear envelope and neurofilaments.

1.3 Structure of G-actin

An actin monomer is composed of 375 amino acid residues. Analysis of the crystal structure of actin has revealed that actin monomers are organised into two major domains (Kabsch *et al*, 1990). Each domain is then composed of a further two smaller sub-domains (figure 1-1). Actin monomers contain a divalent cation and nucleotide binding site in the deep cleft between the two large domains. Comparison of ADP-bound and ATP-bound actin structures has demonstrated conformational changes between sub-domains 2 and 3 (Otterbein *et al*, 2001; Graceffa and Dominguez, 2003). These rotational changes are thought to increase the stability of actin monomer incorporation in filaments when in the ATP-bound form. Hydrolysis of ATP bound to actin monomers promotes monomer release from a filament.

The preference of actin monomers to polymerise at high concentrations rather than form crystals, slowed the study of the structure of actin. The crystal structure of actin was therefore initially determined from crystallised 1:1 complexes of actin with profilin (Schutt *et al*, 1993), DNase I (Kabsch *et al*, 1990) and a fragment of gelsolin (McLaughlin, 1993; Robinson, 1999). Both profilin and DNase1 are relatively small proteins which inhibit the polymerisation of actin. Recent studies have however enabled the crystallisation of ADP-bound G-actin monomers alone, using the fluorescent probe tetramethylrhodamine-male imide (TMR) to inhibit polymerisation by interaction with the Cys³⁷⁴ residue of the actin molecule (Otterbein *et al*, 2001) (figure 1-1). Interference with the Cys³⁷⁴ residue renders the actin monomer polymerisation deficient. The debate is ongoing however with regard to whether the binding of this molecule prevents movement of the actin monomer into its true ADP-bound state. Attachment of the TMR molecule partially blocks the hydrophobic cleft between sub-domains 1 and 3 of the actin monomer. This hydrophobic cleft has recently been demonstrated to be important for binding of several ABPs (for review see Dominguez, 2004).

1.4 Structure of F-actin

The hydrophobic cleft between sub-domains 1 and 3 of actin is proposed to mediate binding to other actin monomers, enabling the generation of actin filaments. The DNase1 binding loop (figure 1-1), encompassing the His⁴⁰-Gly⁴⁸ residues of subunit 2, is proposed to bind in this hydrophobic cleft. This binding is demonstrated in the filament model shown in figure 1-2, proposed by Holmes and colleagues (Holmes *et al*, 1990; Lorenz *et al*, 1993). This loop region has been shown to interact with DNase1 in an Actin:DNase1 complex and in the TMR-bound crystallised monomer assumes an alpha-helical structure (Otterbein *et al*, 2001).

Crystallisation studies of filamentous actin in combination with myosins or F-actin binding proteins have not so far been achieved. The crystallisation of G-actin alone however paves the way for these studies. F-actin has been studied in combination with several F-actin binding proteins by electron microscopy. These binding proteins include utrophin (Moores *et al*, 2000), tropomyosin (Xu *et al*, 1999), and myosin (Volkmann *et al*, 2000). These studies have however provided limited resolution.

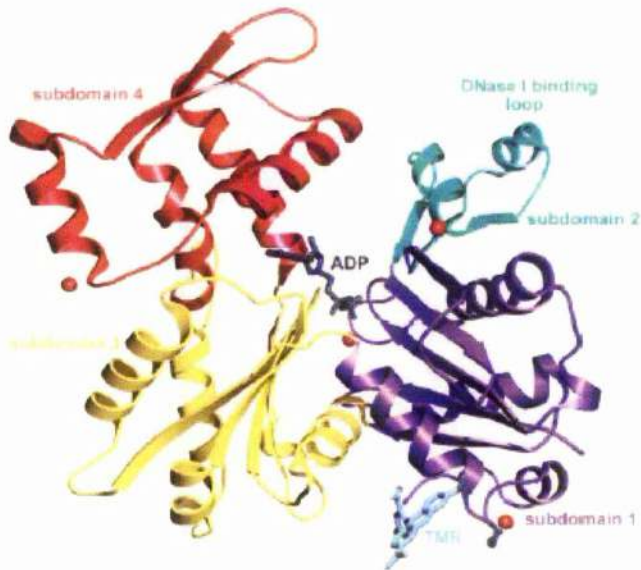


Figure 1-1. The structure of an actin monomer in a TMR bound state.

ADP binds in the centre of the actin monomer, in the deep cleft formed. Sub-domain 1 is shown in purple, sub-domain 2 in green, 3 in yellow, and sub-domain 4 in red. The DNase I binding loop in sub-domain 2 is known to form an alpha-helix in this ADP bound state. Potential cations binding sites identified in these crystals are shown as spheres. The binding site of Tetramethylrhodamine-5-maleimide (TMR) is also shown. Figure adapted from Otterbein and colleagues, 2001.

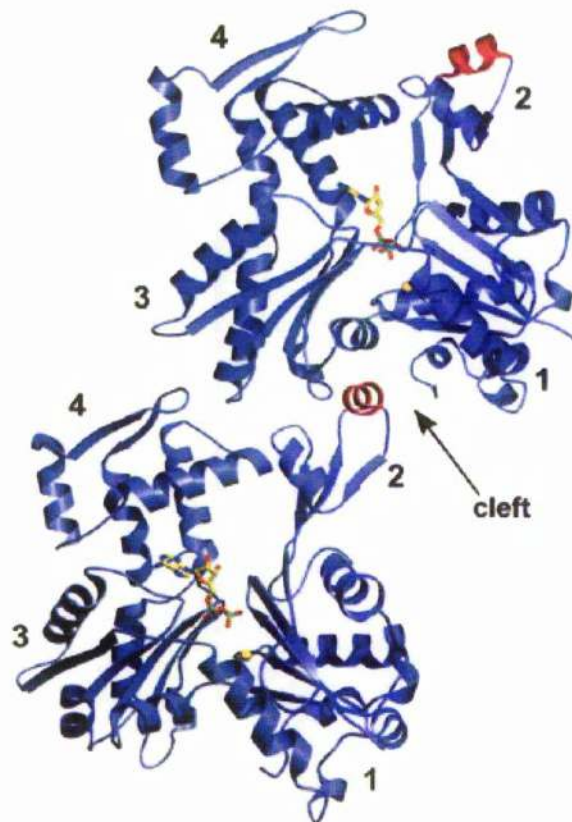


Figure 1-2. The Holmes filament model.

The proposed regions of interaction between two actin monomers in an actin filament are shown. Sub-domains 1-4 on each actin monomer are numbered. The alpha-helical DNase1-binding loop in sub-domain 2 is shown in red and is proposed to interact with the hydrophobic cleft found between sub-domains 1 and 3 on an adjacent actin monomer. ADP and a spherical cation are also shown bound in the centre of each monomer. Figure adapted from Dominguez, 2004.

The helical nature of actin filaments (F-actin) was determined by X-ray crystallography and electron microscopy studies (Holmes *et al*, 1990; Milligan *et al*, 1990 respectively). Filaments are known to consist of two proto-filaments attached by lateral contacts and which wind around each other to form a helix. A full helical twist in the actin filament is formed every 37 nm (figure 1-3).

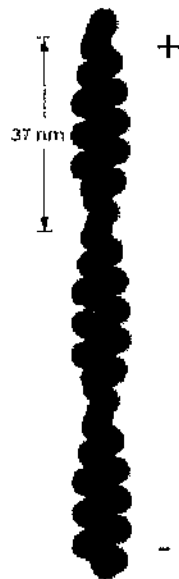


Figure 1-3. The structure of an actin filament

Actin filaments are composed of two proto-filaments of polymerised actin monomers, held together by lateral contacts. Each proto-filament lies in the same orientation and the two rotate around each other to form a helix. One helical turn is occurs every 37 nm. The barbed (plus) and pointed (minus) ends of the filament are shown. Figure adapted from Alberts *et al*, 2002.

1.5 Polymerisation of actin

Actin filaments are formed by the polymerisation of actin monomers, a process which requires ATP, monovalent (K^+) and divalent (Ca^{2+} , Mg^{2+}) cations. Polymerisation occurs when ATP bound G-actin monomers incorporate into an existing actin filament. Hydrolysis of ATP and the release of inorganic phosphate (P_i) follow monomer incorporation. ATP hydrolysis induces a conformational change in the newly incorporated actin monomer and this is thought to play a critical role in actin dynamics due to the preference of specific actin binding proteins for ATP or ADP bound actin. Hydrolysis of ATP is also known to reduce the binding affinity of the monomer for the adjacent actin monomers, promoting eventual dissociation of monomers from the filament (Alberts *et al*, 2002).

Nucleation describes the formation of a new actin filament from free actin monomers and is a two step process. The initial step, formation of an actin dimer is energetically unfavourable and dimers are therefore unstable. *In vivo*, additional factors are involved in overcoming this kinetic barrier. The second step towards nucleation is formation of an actin trimer or 'nucleus' from which polymerisation proceeds by sequential addition of actin monomers to both ends of the new filament. The time course of polymerisation *in vitro* is shown in figure 1-4. Following addition of ATP, monovalent and divalent cations to a solution of monomeric actin, polymerisation is seen to progress in three stages. During lag phase the slow process of filament nucleation occurs. This is followed by a period of rapid filament growth as monomers incorporate at both ends of the filaments, termed the elongation phase. Finally an equilibrium or 'steady state' is achieved when the filament remains at a constant length due to monomer incorporation occurring at the same rate as monomer loss.

Actin filaments are highly dynamic due to the rapid loss and addition of actin monomers from both filament ends. While both filament ends are able to incorporate or dissociate monomers, filaments are however polarised due to the orientation of monomers in each proto-filament. The barbed (fast growing) end favours addition of monomers over the pointed end, leading to a 'treadmilling' effect with actin monomers moving through the filament as polymerisation occurs preferentially at the filament barbed end. This treadmilling effect is seen during the equilibrium stage of polymerisation. During this stage, filaments remain at a constant length while still experiencing a net flux of actin subunits through the filament (figure 1-5). The equilibrium phase occurs when the concentration of free monomers in solution is above the critical concentration for the barbed end of the filament but below that of the pointed end. The critical concentration at each filament end differs as it takes into account the number of monomers added to the filament per second; dependent on the concentration of free monomers in solution, and loss of monomers from the filament end, which is not dependent on the concentration of free monomers. Thus as the filament lengthens, the number of free monomers decreases until the addition of monomers slows to the same rate as that lost from the filament end, due to a lack of free monomers available for incorporation. At this point the concentration of free actin monomers is constant and this is termed the critical concentration. When this occurs, monomers are added to the barbed end of the filament and lost from the pointed end at the same rate, allowing the filament to stay at a constant length while still experiencing a net flux of monomers.

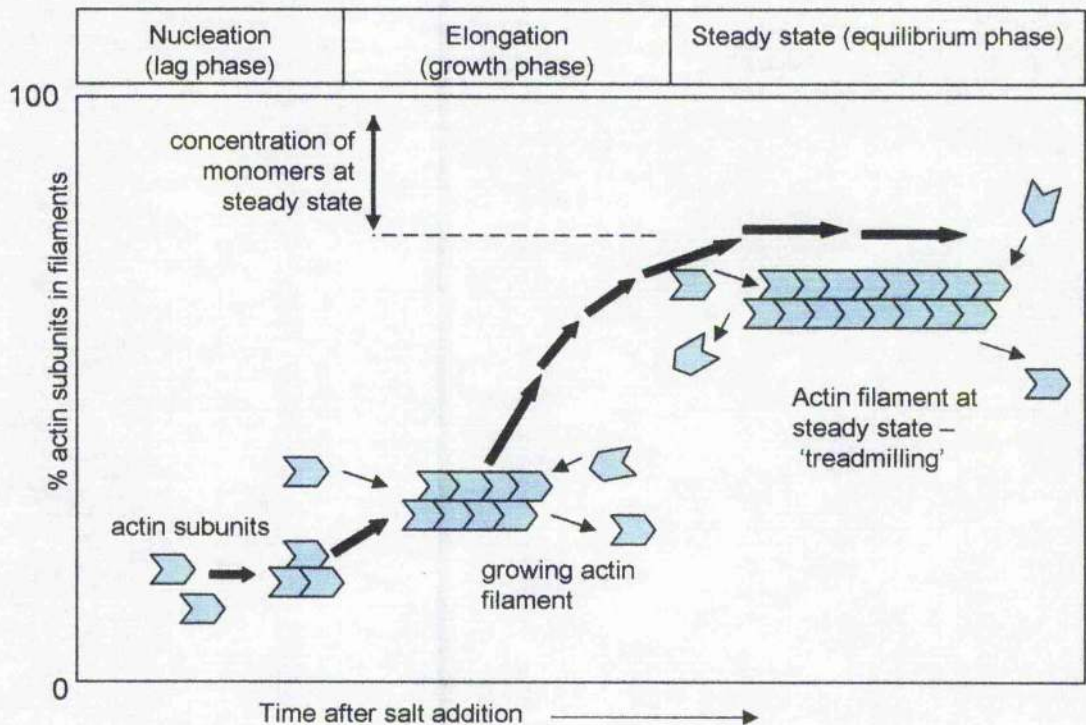


Figure 1-4. The time course of actin polymerisation in vitro. Polymerisation is initiated by increasing the salt concentration in a monomeric actin solution. The formation of trimer complexes from actin monomers is termed nucleation. The formation of this nucleus is relatively slow, producing the lag phase of polymerisation. Growth phase occurs as monomers are added to elongating filaments, while the equilibrium phase is reached when growth of the polymer is balanced by monomer loss. (Figure adapted from Alberts *et al*, 2002).

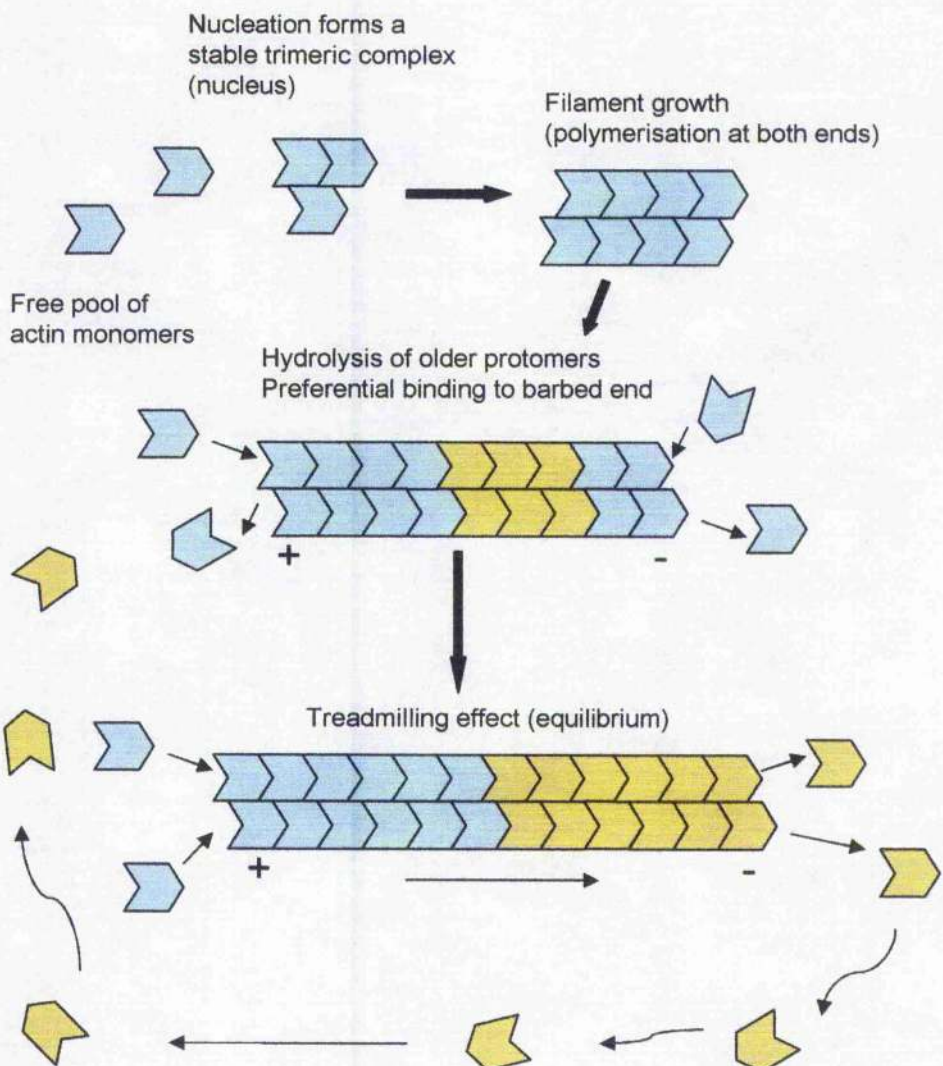


Figure 1-5. Filament generation and treadmilling. ATP-bound G-actin monomers (blue) initially form trimeric nucleation complexes onto which actin filaments are assembled. Assembly occurs by incorporation of additional ATP-G-actin monomers at both ends of the filament. Following incorporation into the filament ATP bound 'protomers' hydrolyse releasing inorganic phosphate and generating ADP-bound protomers (yellow). These protomers will eventually be released from the filament and they will be free to cycle back into actin filaments following exchange into the ATP bound form. Due to the preferential addition of ATP-G-actin to the barbed (+) end of a filament and the preferential dissociation of hydrolysed protomers from the pointed (-) end and a difference in critical concentration, a treadmilling effect is seen.

1.6

Regulation of actin

Polymerisation and organisation of actin filaments is regulated *in vivo* by a large number of actin binding proteins (ABPs) (Engel *et al*, 1977). Filament dynamics are controlled by these proteins in a variety of ways. Specific ABPs cap, uncaps and sever filaments, while yet others affect the rates of integration or dissociation of actin monomers or promote nucleation of actin filaments. Additionally, filament stabilising, bundling and cross-linking proteins promote incorporation of actin filaments into higher order structures. Many actin regulating proteins bind directly to actin in its monomeric or filamentous form. These proteins have been classified into several general groups depending on their mechanism of actin regulation (figure 1-6). Most actin regulating proteins however regulate actin in a number of ways and classification of ABPs into groups is therefore further complicated. Additionally, actin regulating abilities determined *in vitro* in many cases differ from activities seen in an *in vivo*. For this reason the precise functions of many actin binding proteins in a cellular environment are not fully defined.

1.6.1

Monomer binding proteins

Monomer binding proteins regulate actin polymerisation by binding directly to actin monomers and affecting their availability for incorporation into filaments. As the rate of filament elongation is directly proportional to the concentration of actin monomers available in solution (Pollard, 1986), these proteins exert significant control over actin polymerisation and remodelling in the cell. The small actin binding protein profilin has been shown to inhibit actin filament growth *in vitro* by monomer binding and sequestration (Carlsson *et al*, 1977). *In vivo* however, the preference of profilin to bind to ATP-actin monomers is thought to promote filament polymerisation by maintaining a pool of free actin monomers, ready for incorporation into a filament. Additionally, profilin is also known to bind to ADP-actin monomers, promoting the exchange of ADP for ATP, and thereby increasing polymerisation rates by increasing the number of actin monomers available in a ‘polymerisation ready’ state. Members of the ADP/cofilin family also regulate actin monomers directly. These proteins accelerate dissociation of actin monomers from filaments using two mechanisms. Depolymerisation is promoted by monomer sequestration with preferential binding to ADP-actin (Aizawa *et al*, 1995, Carlier *et al*,

Filament Branching

7 - (e.g. Arp2/3)

Monomer Binding

1 – Monomer sequestration (e.g. thymosins)

2 – Nucleation (e.g. Arp2/3, formins)

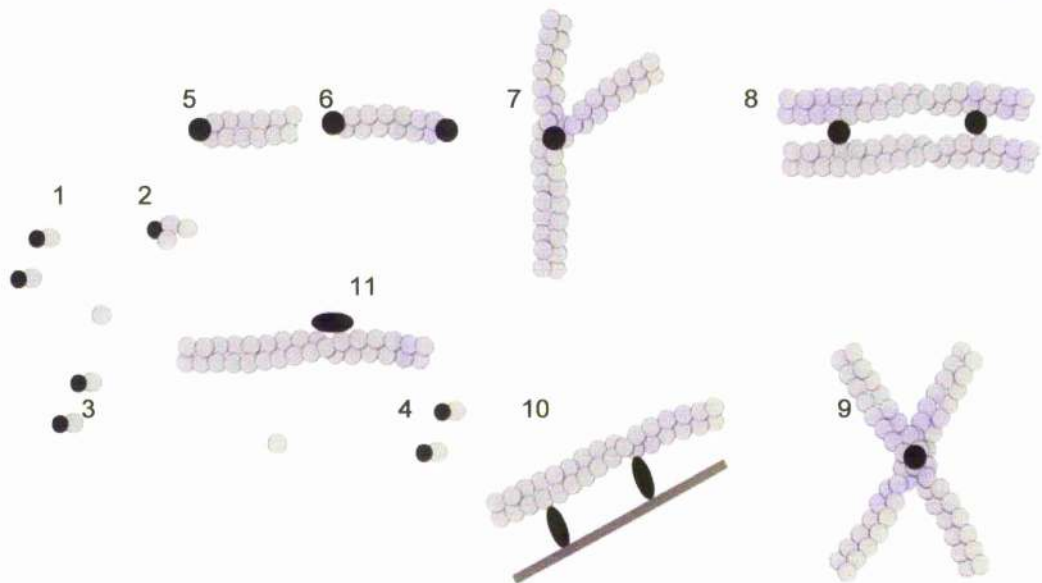
3 – Nucleotide exchange (e.g. profilin)

4 – Depolymerising and severing ADF/cofilin, AIP1)

Filament Bundling and Crosslinking

8 – bundling (e.g. fimbrin, Sac6p)

9 – Crosslinking (e.g. spectrin, transgelin)



Capping and Severing

5 – Barbed end capping (e.g. capping protein, formins)

6 – Severing and capping (e.g. gelsolin, fragmin, villin)

Filament stabilising

11 – (e.g. tropomyosins)

Filament linkers

10 – membrane anchors (e.g. dystrophin, utrophin ERM proteins)

- cytoskeletal linkers (e.g. plectin, spectrin)

Figure 1-6. Overview of actin regulating proteins. Previous studies have enabled the classification of actin binding proteins into functional groups, each with specific effects on actin polymerisation or organisation. Proteins specific to *S. cerevisiae* are underlined.

1997), while filament severing increases the number of filament ends, thereby promoting monomer exchange from these sites. Proteins of this family were first recognised for their ability to rapidly depolymerise actin and are found at the leading edge of motile cells and in ruffling membranes (Aizawa *et al*, 1995). Cofilin and profilin therefore act together in the control of available G-actin monomers.

1.6.2 Filament stabilising proteins

Several groups of actin binding proteins regulate actin by stabilising filamentous structures. Many achieve this by preventing further incorporation or loss of monomers from filaments, while others promote the incorporation of filaments into bundles or intricate networks of filaments. Filament side-binding proteins stabilise actin by binding along the length of actin filaments and making contact with multiple subunits, as in the case of tropomyosins. Additionally, some filament side-binding proteins, including tropomyosin, decrease the rate of subunit loss from filament ends by filament binding. Tropomyosins in yeast associate with actin cables and are encoded by *TPM1* and *TPM2*.

1.6.3 Capping proteins

Capping proteins stabilise actin filaments by ‘capping’ filament ends and preventing monomer exchange at these sites. Studies have shown that most actin filament barbed ends are not freely accessible in the cell (Hug *et al*, 1995), and most filament barbed ends are therefore thought to be capped. A model proposing selective uncapping of specific sites has been proposed by Carlier and Pantaloni (Carlier and Pantaloni, 1997). Selective uncapping of filaments to promote localised actin polymerisation at specific sites is a very attractive model. By selective uncapping, polymerisation would be restricted and confined to areas containing uncapped filaments, a process termed ‘funnelling’ of polymerisation. Uncapping of filament barbed ends by dissociation of capping protein (CP) has been shown to be an activity of the polyphosphoinositides, PIP₂ and PIP *in vitro* (Schafer *et al*, 1996). CP is ubiquitously expressed in all eukaryotes and co-localises with filamentous actin. In *S. cerevisiae* CP is a heterodimeric protein encoded by *CAP1* and *CAP2*.

1.6.4 Bundling and cross-linking proteins

Actin bundling proteins stabilise filaments by dual filament binding. These proteins bring actin filaments into close proximity and generate thick bundles of actin filaments, termed actin cables. Actin cross-linking proteins however promote the incorporation of actin filaments into intricate networks. Fimbrin, villin and α -actinin are examples of actin bundling proteins. Fimbrin contains two pairs of calponin homology (CH) domains (deArruda *et al*, 1990) which mediate actin binding. Sac6p (yeast fimbrin) is required for normal actin organisation, endocytosis and cell polarisation in yeast. Deletion of *SAC6* destabilises actin cables (Karpova *et al*, 1995). The calponin homology domain has been identified in many actin-associating proteins such as, spectrin, filamin and plectin. Pairs of CH domains have well-documented actin binding capabilities, however it is still unclear as to whether a single CH domain alone can bind to actin. Recently, another actin bundling protein, Scp1p has been identified in yeast. Scp1p is the yeast homologue of transgelin and contains a single CH domain and calponin-like repeat (CLR). Scp1p has been shown to bundle actin filaments *in vitro* and is found to localise primarily to cortical actin patches in yeast, suggesting the protein may have additional roles in the regulation of actin, as actin filaments do not bundle at this location (Goodman *et al*, 2003; Winder *et al*, 2003).

1.6.5 Severing proteins

Actin severing proteins cleave actin filaments and promoting both filament disassembly and filament polymerisation by the generation of free filament ends. The generation of free filament ends promotes filament breakdown or filament polymerisation depending on the availability of actin monomers and the action of actin regulating proteins at these sites. Gelsolin, villin, fragmin and adseverin are well-studied calcium regulated, actin severing proteins. All require high levels of calcium for actin severing. Intriguingly, the structure of yeast cofilin suggests the protein may have severing activity (Maciver, 1998), although this activity has yet to be shown *in vitro* and is debatable. Cofilin localises to cortical actin structures in *S. cerevisiae* (Moon *et al*, 1993). Additionally, many actin severing proteins also cap actin filaments, as in the case of gelsolin. Gelsolin activity is regulated by pH and phosphatidylinositol 4,5-biphosphate (PIP₂), in addition to calcium. To date no gelsolin family members have however been identified in yeast or plant cells.

1.6.6 Nucleating proteins

Actin nucleating proteins promote the formation of actin dimers and trimers which act as the starting blocks for polymerisation. The Arp2/3 complex nucleates new actin filaments and promotes branching of existing filaments, and is a highly conserved key regulator of actin (for review see Higgs and Pollard, 2001). This seven subunit complex contains two protein subunits which are structurally similar to actin and which are thought to mimic an actin dimer. The relatively weak intrinsic nucleating activity of the Arp2/3 complex is dramatically increased in conjunction with a number of nucleation promoting factors (NPFs) (Winter *et al.*, 1999a; Goode *et al.*, 2001). Overexpression of the NPFs: WASP and N-WASP and the yeast WASP homologue Las17p/Bee1p generate large actin aggregates in the cell, presumably due to an increase in the nucleating activity of Arp2/3 (Madania *et al.*, 1999; Symons *et al.*, 1996, Miki *et al.*, 1998).

The Arp2/3 complex is not the only factor able to mediate actin nucleation. Recently, formin proteins have also been shown to have nucleating ability (Evangelista *et al.*, 2002; Sagot *et al.*, 2002b). Filaments nucleated by formins are proposed to generate the unbranched actin filaments which collectively form actin cables in yeast. Arp2/3 complex nucleated filaments are however thought to form the branched filaments specifically found in actin patches at the cell cortex (Lew, 2002, Sagot *et al.*, 2002a). These proposals are supported by cellular studies, in which the loss of the yeast formins Bni1p and Bnr1p result in a rapid, reversible loss of actin cables, while cortical actin patches remain unaffected (Evangelista *et al.*, 2002, Sagot *et al.*, 2002a). Formins are Rho-GTPase effectors that communicate Rho-GTPase signals to the cell cytoskeleton. These proteins are multi-domain and are defined by the presence of a conserved FH2 (formin homology 2) domain. The FH2 domain alone is able to mediate actin filament nucleation *in vitro* (Pruyne *et al.*, 2002, Sagot *et al.*, 2002b), although this domain is usually flanked by a FH1 domain which binds profilin, SH3 domains or WW domains. Diaphanous related formins contain both a DAD (Diaphanous Autoregulatory Domain) and a GBD (GTPase binding domain) domain which associate to inhibit the activity of the protein. Rho-GTPase binding to the GBD domain inhibits this regulatory interaction and promotes an active conformation (Alberts *et al.*, 2001, Evangelista *et al.*, 2002). The mechanism of actin nucleation mediated by formin proteins is under investigation. Yeast Bni1p however nucleates filaments at the bud tip in *S. cerevisiae*, while Bnr1p localises to the bud neck during bud development. Each of these formins is

thought to nucleate filaments which emanate from these specific sites and form the polarised actin cables seen during bud development (Evangelista *et al*, 2002; Pruyne *et al*, 2004). Filament nucleation by formins is known to occur in a profilin dependent manner with the formation of actin cables from these filaments involving tropomyosin (Evangelista *et al*, 2002)

1.6.7 The Arp2/3 complex in more detail

The Arp2/3 complex mediates nucleation and actin filament branching. The complex was first isolated from *Acanthamoeba castellanii* (Machesky *et al*, 1994) and studies have shown the complex to be a central component of the actin regulatory network. Arp2/3 has since been identified in a variety of other species including *Xenopus* (Ma *et al*, 1998), *S. cerevisiae* (Winter *et al*, 1997) and human cell lines (Welch *et al*, 1997). The structure of this seven subunit complex is highly conserved throughout eukaryotes and includes two actin related protein subunits, Arp2p and Arp3p. Arp2/3 is able to nucleate actin filaments while also mediating branching of existing filaments. Filament branching generates Y-branched filaments from existing filaments, by nucleation of a new filament at a 70° angle as shown in figure 1-8. The ability of Arp2/3 to nucleate actin filaments is thought to depend on the Arp2p and Arp3p actin related protein subunits of Arp2/3. These actin related subunits mimic an actin dimer, thereby forming a template for actin nucleation and bypassing the energetically unfavourable formation of an actin dimer from actin monomers (Robinson *et al*, 2001, Volkmann *et al*, 2001). The nucleating ability of the Arp2/3 complex is stimulated from a low basal level by a variety of NPFs proteins (for review see Higgs and Pollard, 2001). Known NPFs in yeast include the yeast WASP homologue Las17p/Beel1p (Li, 1997; Winter *et al*, 1999a; Madania *et al*, 1999), Abp1p (Goode *et al*, 2001), Pan1p (Duncan *et al*, 2001), Myo3p and Myo5p (Evangelista *et al*, 2000) all of which localise to actin structures at the cell cortex with Arp2/3. Mammalian NPFs include WASP (Wiskott Aldrich Syndrome protein) and N-WASP. NPFs contain a CA (connector and acidic) region; a short stretch of basic and acidic residues which can induce a conformational change in the Arp2/3 complex. Additionally, NPFs also contain an F-actin (Class II NPFs) or G-actin (Class I NPFs) binding site adjacent to the CA region.

Immunogold labelling experiments have confirmed that the Arp2/3 complex remains at the 'Y' junctions following branching (Svitkina and Borisy, 1999). The

mechanism by which Arp2/3 forms 'Y' branched filaments is however disputed. Two mechanisms have been proposed. The 'dendritic nucleation' model (Pollard *et al*, 2000) proposes binding of the activated form of Arp2/3 to the side of an existing filament and nucleation of a new filament branch. In addition, a 'barbed end branching' model (Pantalone *et al*, 2000) has been proposed, suggesting integration of the actin related subunits directly into an existing filament at the barbed end during polymerisation. Subsequent electron cryomicroscopy studies have supported the dendritic nucleation model; 2-dimensional reconstructions of *Acanthamoeba* Arp2/3 with F-actin demonstrated that the existing filament is unperturbed following filament branching (Volkmann *et al*, 2001). Investigation into the mechanism of filament branching is however ongoing, with the study of branch polymerisation kinetics providing further support for the filament side binding model (Carlsson *et al*, 2004).

Deletion of Arp2/3 subunits in yeast generated severe growth defects or lethality, suggesting the importance of this complex in the yeast cell (Winter *et al*, 1999b). Studies of the motile bacterial pathogen *Listeria monocytogenes* have also implicated the Arp2/3 complex in the generation of cellular motility and intracellular movement. Following invasion of the bacterial cell, an actin 'comet tail' was seen to develop on the surface of the pathogenic cell, and appeared to drive movement of the pathogen both within the host cell and from one host cell to the next. These comet tails were shown to consist of various actin binding proteins (Loisel *et al*, 1999; Theriot *et al*, 1994; Carlier *et al*, 1997; Rosenblatt *et al*, 1997) and actin filaments orientated with their barbed ends towards the bacterial surface (Tilney *et al*, 1990; Gouin *et al*, 1999). These studies suggested that polymerisation of actin was either occurring on or close to the surface of the bacterial cells, and that polymerisation was the driving force for motility. Additionally, studies in *Listeria* have shown that the ActA surface protein (an NPF) recruits and activates the Arp2/3 complex (Welch *et al*, 1997) at the bacterial surface; driving motility by actin assembly and the formation of an actin comet tail.

1.7 Chemical tools used to study actin

1.7.1 Phalloidin

Filamentous actin can be visualised using rhodamine labelled phalloidin. This fluorochrome-labelled phallotoxin binds to actin filaments, preventing their depolymerisation and enabling direct visualisation of actin filaments in permeabilised cells by fluorescence microscopy (Adams and Pringle, 1991). Phalloidin was originally

obtained from the fungus *Amanita phalloides*. Binding is specific for filamentous actin and occurs at the junction between two subunits, stabilising the association of actin monomers (Barden *et al*, 1987).

1.7.2 Cytochalasin D

Cytochalasin D is a cell permeant fungal alkaloid which promotes filament depolymerisation by binding to the barbed end of an actin filament. This action blocks further addition or loss of actin monomers at this site (Cooper *et al*, 1987). Cytochalasin D is obtained from the fungus *Zygosporium mansonii*.

1.7.3 Latrunculin-A

Latrunculin-A is used to disrupt the actin cytoskeleton and has similar effects to cytochalasin, although the toxins are unrelated (Ayscough *et al*, 1997). Latrunculin-A inhibits actin polymerisation by binding to actin monomers preventing their incorporation into actin filaments (Morton *et al*, 2000). This membrane permeable macrolide toxin is obtained from the sea-sponge *Latrunculia magnifica*.

1.7.4 Jasplakinolide

Jasplakinolide is the most commonly used actin stabilising drug. This toxin is cell permeant and stabilises the association of actin monomers in filaments in a manner similar to phalloidin. Jasplakinolide is obtained from the marine sponge *Jaspis johnstoni*.

Control of actin nucleation, polymerisation and disassembly is required for cytoskeletal remodelling, polarisation of growth and many cell-specific processes. Studies have demonstrated a large intracellular pool of actin monomers in many motile cells, suggesting actin could be directly involved in and central to cell motility. A large pool of freely available actin monomers would enable actin polymerisation and turnover to occur at higher rates than in cells with limited amounts of freely available actin. The highly motile amoeba *Dictyostelium discoideum* is known to share many physiological functions with mammalian cells and is widely used as a model organism. *Dictyostelium* cells have been shown to contain approximately 100 times more actin than *S. cerevisiae* cells (Hug *et al.*, 1995). Actin in *S. cerevisiae* composes 0.1% of the total protein. Additionally approximately 50% of this actin in *Dictyostelium* cells exists as free or buffered monomers compared to 0.3% found in the monomeric form yeast cells (Karpova *et al.*, 1995). This reduction in monomer availability in yeast is thought to reflect the lack of cellular motility, and thus the need for rapid filament assembly as seen at the leading edge of motile cells. Actin filament assembly is thought to enable intracellular movement and cell motility by generating a pushing force that is harnessed by the cell at specific sites. Motile cells require a highly dynamic cytoskeletal network, with actin polymerisation focusing at the leading edge; potentially generating the force required to push the leading edge of the cell forward.

Cell motility can be broken down into specific processes, which include the forward movement produced by initial protrusion of the leading edge, cellular attachment to a surface, and retraction of the rear of the cell. The leading edge of motile fibroblasts does not proceed forward uniformly; instead showing shows cycles of protrusion followed by retraction. In protrusions at the leading edge, actin filaments are polarised with the barbed end of the filament orientated toward the edge of the cell. This polarisation orientates the fast growing (barbed) filament ends in the direction of growth and subsequently orientates the branching of filaments. Two forms of actin containing structures co-exist at the leading edge of motile cells, lamellipodia and filopodia (see figure 1-7). Lamellipodia are persistent protrusions, such as would be required for the forward movement of the leading edge of a cell. Lamellipodia appear as flat, sheet-like continuous protrusions punctuated with filopodia. Filopodia are individual protrusions which are thought to form sensory and exploratory tasks in the surrounding extracellular environment. Filopodia are composed of densely packed parallel bundles of actin

filaments (figure 1-7), while in contrast, several studies of lamellipodia have shown actin to assume a densely packed, branched structure (Svitkina and Borisy, 1999; Abraham *et al*, 1999). Branching of actin filaments at the leading edge is thought to strengthen the filamentous network, allowing it to sustain a pushing force on the plasma membrane without the filaments flexing substantially (Svitkina and Borisy, 1999). Filament branching is known to be an activity of the Arp2/3 complex as previously discussed.

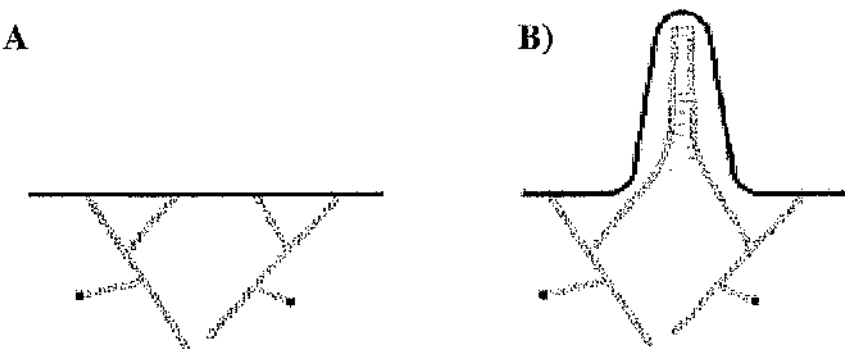


Figure 1-7. Actin structures in lamellipodia and filopodia.

A) Actin filaments are found in a branched form in lamellipodia. Branching of actin filaments is thought to strengthen filament structures, allowing the force of actin polymerisation to be transmitted to the edge of the cell to push the membrane forward, without significant flexing of filaments. B) Proposed mechanism of actin bundling in filopodia. Inhibition of filament capping would enable filaments to lengthen and merge to produce filopodial protrusions. Figure adapted from a paper by Vignjevic and colleagues, (Vignjevic *et al*, 2003).

Branched actin structures in lamellipodia, and bundled actin filaments specific to filopodia are generated by the action of many actin regulating proteins. The generation of branched actin filaments in lamellipodia requires both the branching activity of the Arp2/3 complex and the action of capping proteins to regulate filament length. Elongated actin filaments in filopodia are however thought to be generated by the inhibition of filament capping and branching at such sites. Arp2/3 has been localised to the leading edge of motile cells in studies by Welch and colleagues (Welch *et al*, 1997) and has been shown to be rapidly recruited to the leading edges of fibroblasts following chemoattractant stimulation (Bailly *et al*, 1999). In addition, capping proteins such as gelsolin have also been shown to localise to the leading edge of such cells and are thought to act both by filament capping which ensures short filaments, and by

promoting polymerisation by filament severing and the generation of new barbed ends (for review see Borisy *et al*, 2000; Carlier *et al*, 1998). The Arp2/3 complex has been shown to be excluded from filopodia (Svitkina and Borisy, 1999).

The ‘dendritic nucleation’ model of Arp2/3 filament branching has been extended to propose a model for the regulation of dynamic actin structures at the leading edge of a motile cell (for review see Pollard and Borisy, 2003) (figure 1-8). The initial stage of filament nucleation proceeds with the action of nucleation promoting factors (NPFs) which promote actin filament nucleation by Arp2/3. Following initial polymerisation, filament branching occurs by attachment of the Arp2/3 complex to the side of an existing actin filament, and subsequent nucleation of a new filament branch at a 70° angle to the existing ‘mother’ filament. Growth of both the mother and daughter filaments is thought to generate the force required to push the cellular membrane forward. Filament polymerisation at the leading edge is also thought to require the actin binding protein profilin, which binds to free ADP-actin monomers and promotes exchange of ADP for ATP. Profilin thereby presents recycled actin monomers for subsequent reincorporation into filaments in the ATP-bound form. Polymerisation is thought to proceed until capping proteins binds to the barbed end of the actin filaments, preventing further attachment or dissociation of monomers at these sites. Filament recycling also occurs, as actin monomers dissociate from the uncapped, pointed end of the filament, an action which is promoted by members of the ADF/cofilin family, thereby releasing ADP-actin monomers back into the available pool to be recycled back into newly growing filaments. ADF/Cofilin is also known to sever filaments, an action which may be useful both in the breakdown of filaments and for promoting further polymerisation, as severing generates free filament ends.

The ‘convergent elongation’ model has been proposed to explain the formation of the unbranched actin bundles seen in filopodia. In this model filopodia are generated from the lamellipodial actin network by the action of a tip complex which remains tightly associated with the barbed ends of actin filaments, preventing filament capping. Regulation of polymerisation at the barbed end of actin filaments is therefore central to both models. The importance of barbed end capping at the leading edge has recently been demonstrated in studies by Mejillano and colleagues (Mejillano *et al*, 2004) in which RNA interference was used to study the effects of capping protein depletion; which generated a striking phenotype of overproduction of filopodial protrusions and inhibition of lamellipodial components such as the Arp2/3 complex at the leading edge.

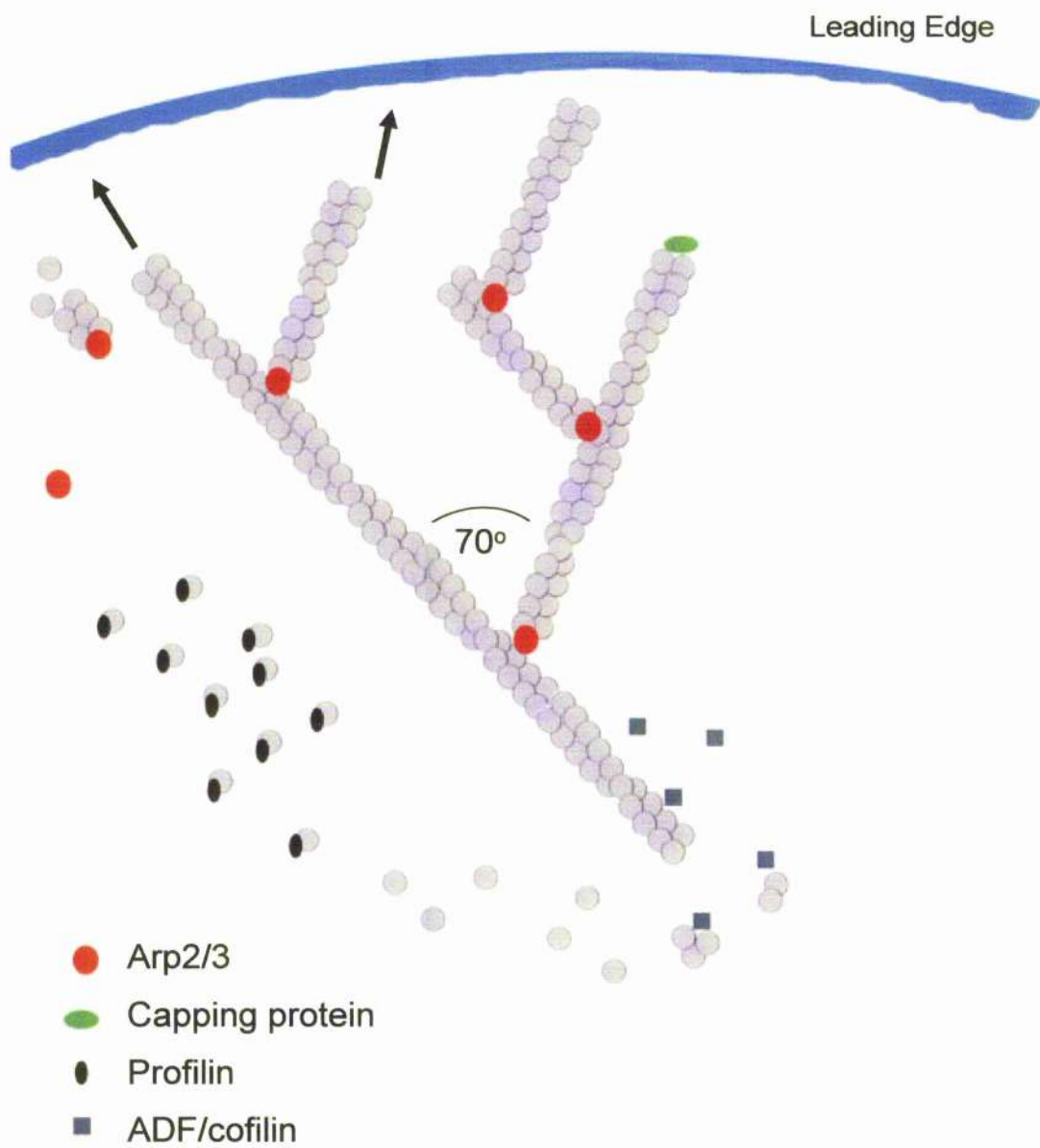


Figure 1-8 Model of dendritic nucleation for protrusion of the leading edge. The polymerisation of actin filaments at the leading edge of motile cells is thought to generate the mechanical force required to push the cell membrane forward. Activated Arp2/3 nucleates new filaments and promotes filament branching at these sites. Profilin promotes polymerisation by catalysing the exchange of ADP for ATP on actin monomers and presenting ‘polymerisation ready’ monomers at sites of polymerisation. Polymerisation and filament length is controlled by the action of capping proteins, which terminate filament elongation. Recycling of filaments and filament breakdown is promoted by the action of ADF/cofilin which severs and preferentially depolymerises ADP-actin filaments. Figure adapted from Pollard and Borisy, 2003

Actin structures are not however limited to the leading edge of motile cells. Actin polymerisation at the cell cortex has recently been shown to be intimately linked to the endocytic uptake in *S. cerevisiae*, and actin is also seen to associate with endocytic structures in higher cells. Actin polymerisation at these sites is proposed to generate the force required for vesicle fission and movement into the cell during endocytosis. Actin is also known to be central to the polarisation of cellular growth, providing a structural basis for polarisation throughout the cell. Additionally, actin is seen to associate with the nuclear matrix in *Xenopus* oocytes (Kiseleva et al, 2004) and chromatin remodelling complexes (for review see Olave et al, 2002), and as such is proposed to play a structural role in the nucleus. Diverse cellular actin structures are however linked by the filamentous nature of actin, the polymerisation and organisation of which is tightly controlled by the plethora of actin regulating proteins which act together to control the generation and disassembly of actin structures in response to both intracellular and extracellular cues.

1.9 Yeast as a model organism

The expression of actin is ubiquitous throughout eukaryotes, suggesting the importance of this structural protein. The study of proteins and cellular processes is undertaken in model organisms such as the budding yeast *S. cerevisiae* due to the ease with which classical genetic and molecular genetic manipulations can be performed. The knowledge gained in these systems can additionally, in many cases, be extrapolated to higher organisms, through the conservation of proteins, signalling pathways and cellular mechanisms. The identification of yeast counterparts of many mammalian actin regulatory proteins indicates a high degree of conservation in cytoskeletal networks across these species, and confirms that *S. cerevisiae* is an excellent model organism in which to study cytoskeletal components.

1.10 Polarisation of growth in *S. cerevisiae*

The budding yeast *S. cerevisiae* is commonly used for genetic analysis and the study of protein to protein interactions. *S. cerevisiae* cells grow well in culture and are stable in both haploid and diploid states. Conversion between these states occurs by the mating and sporulation of yeast cells. Both haploid and diploid cells polarise their growth during specific growth phases, enabling the development of buds and the formation of the mating projection (figure 1-9). Polarisation of growth to specific sites

involves the asymmetric delivery of components required for cellular growth and involves the polarisation of cytoskeletal structures including actin. Remodelling of the actin network is involved in the development of asymmetric growth, by directing localised vesicle fusion and cell wall synthesis to specific sites (for review see Pruyne and Bretscher, 2000b). Polarisation of the actin cytoskeleton towards sites of cell growth has been demonstrated by the localisation of GFP-tagged Act1p in living cells (figure 1-10) (Doyle and Botstein, 1996). Punctate actin patches were seen to accumulate at sites of bud development during the G1 growth phase, and remained polarised towards the bud tip during the early stages of bud growth. Thin cellular actin cables were also seen to polarise along the mother-bud axis during budding. During the later stages of bud development, a switch from apical to isotropic growth occurs within the bud, following the isotropic redistribution of actin. Finally, synthesis of new cell wall occurs at the bud neck during cytokinesis, allowing cellular fission to occur. Actin is seen to repolarise towards this site at the onset of cytokinesis.

1.11 Actin structures in *S. cerevisiae*

Yeast actin is the product of a single gene, *ACT1*, which encodes the globular protein G-actin. Yeast actin is 88% identical at the amino acid level to rabbit muscle actin and has been shown to have similar biochemical properties (Nefsky and Bretscher, 1992; Gallwitz and Sures, 1980). Yeast actin polymerises to form filaments with a 7 nm diameter and which show a high degree of similarity to purified, polymerised rabbit muscle actin (Greer and Schekman, 1982). Due to a decrease in the time taken for nucleation to occur however, yeast actin has been shown to polymerise more rapidly than muscle actin. Additionally, polymerisation is inhibited in the presence of the barbed end capping protein gelsolin; which is known to increase the rate of polymerisation of muscle actin due to its nucleating ability (Buzan and Frieden, 1996). While yeast actin retains a high degree of conservation with muscle actin therefore, differences are however apparent.

Tight regulation is required to control the assembly and organisation of actin filaments into the three types of filament-based actin structure seen in the yeast cell. F-actin structures can be visualised using rhodamine phalloidin, and such studies highlight distinct actin structures termed actin cables, cortical actin patches and the cytokinetic ring (Adams and Pringle, 1991).

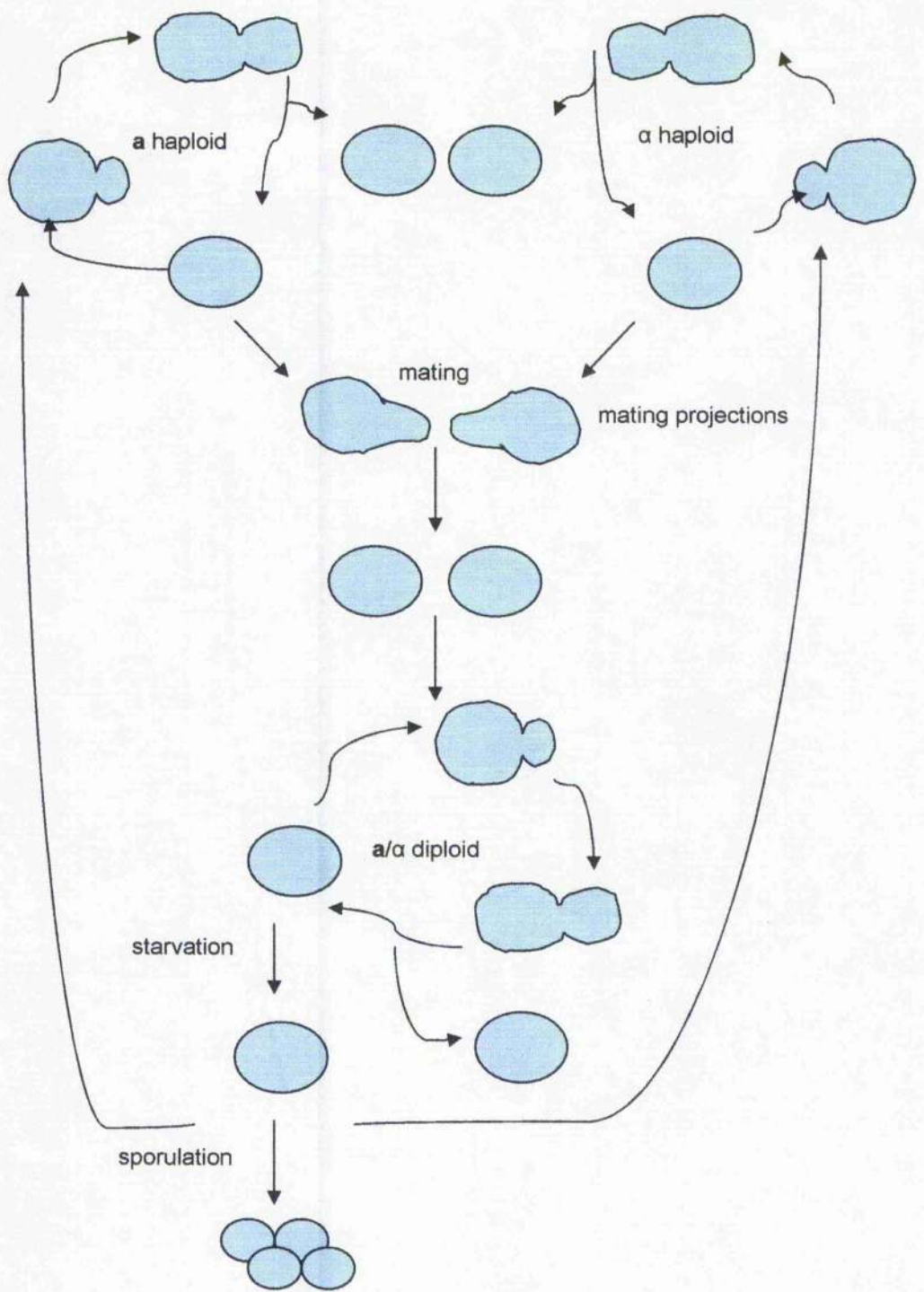


Figure 1-9. The life cycle of *S. cerevisiae*. Haploid and diploid cells are generated by sporulation and mating respectively. Polarisation of growth is required for the formation of the mating projection and growth of new buds.

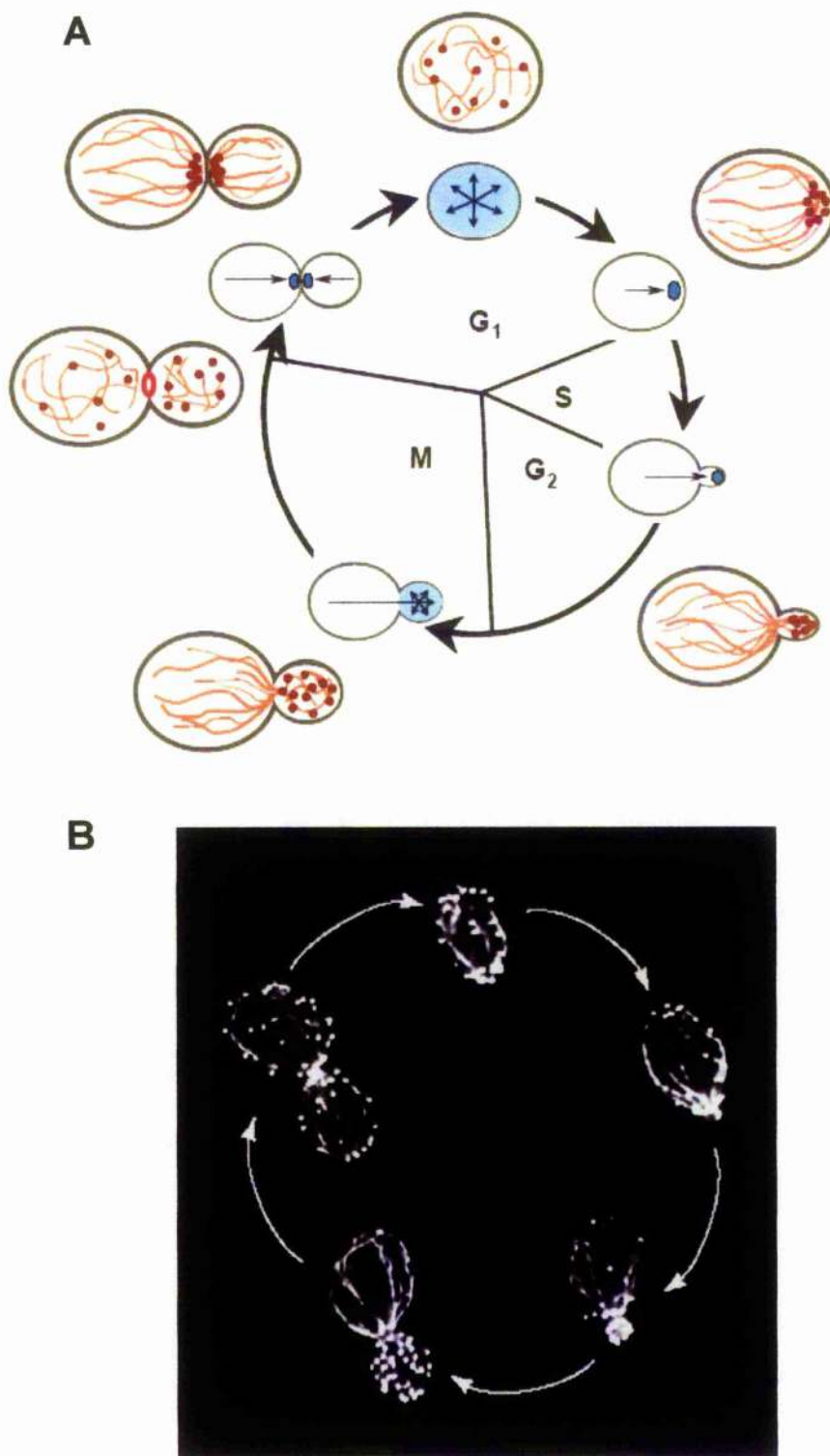


Figure 1-10. Polarisation of the actin cytoskeleton in *S. cerevisiae*. Polarisation of actin throughout the cell cycle. **A)** The location of proteins known to direct cell polarisation are shown in blue. These proteins signal to the cytoskeletal network and direct the polarisation of actin filaments (red) and cortical patches (red spots) throughout the cell cycle. Arrows on the inner circle demonstrate the direction of growth during polarisation. Polarised growth is thought to be dependent on the transport of secretory vesicles along polarised actin cables. The cell cycle stages, M =mitosis, G =growth phase, S =synthesis phase are also shown. Figure adapted from Pruyne and Bretscher, 2000b. **B)** Actin containing structures visualised throughout the cell cycle. Image obtained from David Amberg.

1.11.1 Actin cables

Actin cables are bundles of actin filaments which appear as thin filaments in the unbudded yeast cell, and which align along the mother-bud axis during budding (figure 1-10) (Karpova *et al*, 1998; Pruyne and Bretscher, 2000a). Actin cables are known to act as ‘tracks’ for the movement of secretory vesicles to sites of cellular growth. Sac6p (yeast fimbrin) and Scp1p are both known to be able to bundle actin *in vitro* in *S. cerevisiae* (Adams *et al*, 1989; Winder *et al*, 2003). Sac6p has been shown to co-localise with all actin structures in yeast, while Scp1p localises to punctate patches at the cell cortex, suggesting Scp1p may have additional actin regulatory roles (Winder *et al*, 2003). Crn1p, the yeast homology of coronin also bundles actin filaments *in vitro* and regulates the filament nucleating activity of the Arp2/3 complex (Goode *et al*, 1999; Humphries *et al*, 2002). Coronin localises to sites of dynamic actin assembly and Crn1p localises to cortical actin patches. Actin cables can be difficult to visualise in yeast, therefore the localisation of actin bundling proteins to these sites is sometimes difficult to visualise directly.

1.11.2 Cortical actin patches

Cortical actin patches are F-actin rich structures which appear as 0.1–0.2 µm diameter punctuate spots at the cell cortex. Patches are composed of branched actin filaments (Young *et al*, 2004) and over thirty additional proteins (Pruyne and Bretscher, 2000b). Actin patches associate with plasma membrane invaginations (Muiholland *et al*, 1994) and their localisation is seen to polarise to sites of cell growth throughout the cell-cycle. In unbudded cells, actin patches localise randomly at the cell cortex. Following the onset of bud development, patches then accumulate at the predetermined bud site in early G1 (see figure 1-10) and localise to the bud tip during the early stages of bud growth. Following substantial bud growth, patch localisation remains polarised towards the bud, however patches appear evenly around the cell cortex after the onset of isotropic growth. Completion of bud growth sees the redistribution of actin patches randomly throughout the mother and bud cell, with patch accumulation at the bud neck during cytokinesis. Actin patches therefore accumulate at all sites of cell growth throughout the cell cycle (Adams and Pringle, 1984). This correlation between the localisation of actin patches to sites of cell growth and recent studies which have linked patch generation to endocytic uptake, demonstrate the role of actin patches in membrane

turnover and endocytosis during cellular development. The polarised distribution of cortical actin patches is not strictly required for bud development however, as demonstrated in mutants which show depolarised cortical actin patches but which are still able to bud normally (Gourlay *et al*, 2003). Such studies therefore indicate the importance of actin cables rather than actin patches in maintaining cell polarisation and enabling polarised cell growth (Evangelista *et al*, 2002; Sagot *et al*, 2002a).

Initial studies suggested that actin patches were independent motile entities, with studies of the GFP-tagged actin patch protein Cap2p, reporting that patch movement occurred at an average rate of $0.31\mu\text{m/s}$ (Waddle *et al*, 1996), although both highly motile phases and relatively stationary phases were seen (Doyle and Botstein, 1996; Waddle *et al*, 1996). Original proposals also included the suggestion that patch movement occurred along tracks or filaments such as actin cables or microtubules, this was however disproved following studies which demonstrated that patches moved independently of each other and that movement was unaffected by the mutation of known myosins (Carlsson *et al*, 2002; Waddle *et al*, 1996). Subsequent studies have now demonstrated the dynamically changing composition of cortical actin patches, their rapid assembly and disassembly, and an association with endocytic structures. Assembly and disassembly of cortical actin patches was initially studied by Smith and colleagues (Smith *et al*, 2001). By following the GFP-labelled cortical actin patch proteins Abp1p and Sac6p, actin patches were shown to persist for on average only 4 seconds, suggesting the rapid assembly and disassembly of actin patches at specific sites, as oppose to pre-formed, motile patches.

Mutation of the Arp2/3 complex has been shown to block movement of actin patches and to block endocytic uptake (Winter *et al*, 1997), implicating actin regulation by Arp2/3 and cortical patches in the progression of endocytic uptake. Proteins including Sla1p and Sla2p have also been shown to link the regulation of actin at the cell cortex with endocytic components (Warren *et al*, 2002; Gourlay *et al*, 2003). Additionally, recent studies using tagged endocytic components have demonstrated the recruitment of actin and actin regulating proteins to endocytic sites (Kaksonen *et al*, 2003). Actin patches are now therefore regarded as integral components of the endocytic machinery.

1.11.3 The cytokinetic ring

The cytokinetic ring forms at the bud neck following completion of bud growth and contracts to enable mother and bud cell separation. The cytokinetic ring contains both actin and myosin II, but while the formation of branched actin filaments at cortical patches has been attributed to the activity of the Arp2/3 complex, and the formation of actin cables to the yeast formins Bnr1p and Bni1p, the mechanism of actin filament generation at the cytoplasmic ring is less clear. Latrunculin-A studies have demonstrated the dynamic nature of actin in the cytokinetic ring, suggesting that actin filaments are directly generated at this site (Tolliday *et al*, 2002). Additionally, the cytokinetic ring has been shown to form independently of the Arp2/3 complex (Winter *et al*, 1999b). Ring formation was however affected in tropomyosin mutants and a temperature sensitive profilin mutant, suggesting that the yeast formins may mediate nucleation of actin filament at this site (Tolliday *et al*, 2002). The rescue of actin ring defects in a *rhol-2* mutant by an activated Bni1p encoding plasmid construct suggests that Bni1p may mediate actin assembly at the cytokinetic ring, in addition to filament generation at the bud tip (Tolliday *et al*, 2002)

1.12 Polarisation of actin in *S. cerevisiae*

Cell polarisation is central to cellular development. Polarisation of the yeast actin cytoskeleton during bud development is maintained by a variety of proteins at the bud tip; including Cdc42p. Cdc42p is a member of the Rho family of guanosine triphosphatase (GTPase) proteins. These proteins participate in signalling events by cycling between an active (GTP-bound) and inactive (GDP-bound) form. Cdc42p is essential for the maintenance of cell polarisation and activates several signalling cascades, which signal directly to the actin cytoskeleton. *S. cerevisiae* has five Rho-related GTPases, Cdc42p, Rho1p, Rho2p, Rho3p, and Rho4p that enable the coordinated reorganisation of the cytoskeleton and control cell surface growth. Additional proteins localised to the bud tip are also known to be involved in the nucleation and anchoring of actin cytoskeletal filaments, providing a direct link between the cell cycle and actin remodelling. In addition to that seen during cell cycle progression, polarisation and remodelling of the actin cytoskeleton occurs in response to various intracellular and extracellular signals. In *S. cerevisiae*, haploid cells remodel in response to mating pheromones, generating a characteristic 'shmoo' phenotype by the development of a mating projection and polarisation of cell growth. Pseudohyphal

growth in response to nutrient deprivation also involves polarisation of cell growth. This response enables the exploration of the surrounding extracellular environment in an attempt to find a nutrient source. Cdc42p is again central to the polarisation of growth during this polarised growth phase (for review see Gancedo, 2001).

1.13 Cortical patch proteins

Cortical actin patches are composed of a network of branched actin filaments (Young *et al*, 2004) and many associated proteins (Pruyne and Bretscher 2000b). Many of these proteins have been studied individually and have defined roles in the regulation of actin, while the precise function of others remains unknown. Known cortical patch proteins are summarised in table 1-1. The function of proteins *in vivo* is often difficult to determine. This is in part due to the use of *in vitro* studies which may demonstrate protein activities that are unseen in a cellular environment. Additionally, upon gene deletion many mutants lack specific phenotypic defects due to partial redundancy with other proteins. Therefore, understanding the function of cytoskeletal proteins *in vivo* is often a significant challenge, requiring the analysis of regulatory and biochemical interactions in addition to *in vitro* studies.

Cortical patch proteins include the Arp2/3 complex activators Las17p, Abp1p, and Pan1p and the Arp2/3 complex itself. Many patch proteins are known to play direct or indirect roles in the regulation of the actin (for review see Pruyne and Bretscher, 2000b). The rapid assembly and disassembly of cortical patches is thought to be achieved by the co-ordinated action of these proteins.

Protein	Known activities	Mammalian orthologue/ Homologue	Known interactions with actin cytoskeletal components	Selected References
Abp1p	Activates the Arp2/3 complex. Binds actin	mABP1	Arp2/3, Act1p Ark2p, Prk1p, Rvs167p, Srv2p	Goode <i>et al</i> , 2001 Lila <i>et al</i> , 1997
Act1p	G-actin monomer, forms F-actin	Actin	Cof1p, Las17p, Pfylp, Rvs167p, Srv2p	Amberg <i>et al</i> , 1995 Adams and Pringle, 1984
Ark1p/ Prk1p	Phosphorylates actin regulating proteins	AAK1/GAK	Abp1p, Sla2p, Pan1p	Zeng <i>et al</i> , 2001 Smythe and Ayscough, 2003
Arp2p	Nucleates actin filaments	Arp2/3 subunit	Las17p, Abp1p, Pan1p, Crn1p, Bni1p, Myo3/5	Moreau <i>et al</i> , 1996
Arp3p		Arp2/3 subunit		Winter <i>et al</i> , 1997
Arc15p		Arp2/3 subunit		Winter <i>et al</i> , 1999b
Arc18p		Arp2/3 subunit		

Arc19p		Arp2/3 subunit		
Arc35p		Arp2/3 subunit		Schaerer-Brodbeck and Reizman, 2000
Arc40		Arp2/3 subunit		
Cap1/2	Caps filament barbed ends	Capping proteins	Bzz1p	Amatruda <i>et al</i> , 1992
Cmd1p	May complex with Arp2/3	Calmodulin	Arp2/3	Schaerer-Brodbeck and Reizman, 2003
Cof1p	Severs and disassembles F-actin	Cofilin	Act1p, Cmd1p, Aip1p, App1p, Srv2p, Crn1p	Rodal <i>et al</i> , 1999
Crn1p	Inhibits Arp2/3	Coronin	Arp2/3	Humphries <i>et al</i> , 2002
End3p	Inhibits Pan1p phosphorylation	Eps15 homology	Pan1p, Sla1p	Tang <i>et al</i> , 2000
Ent1-4p	Endocytic component	Epsins	Pan1p	Aguilar <i>et al</i> , 2003
Las17p	Binds activates Arp2/3	WASP	Arp2/3, Vrp1p, Sla1p, Myo3/5p, Rvs167p	Madania <i>et al</i> , 1999
Lsb3p	Unknown		Las17p	Gavin <i>et al</i> , 2002
Myo3/5	Actin filament motor	Myosin I	Act1p, Arp2/3, Vrp1p, Las17p, Cmd1p	
Pan1p	Activates Arp2/3	Eps15	End3p, Sla1p	Tang and Cai, 1996
Pfy1p	Sequesters actin monomers	Profilin	Act1p, Bni1p, Bnr1p, Srv2p	Sagot <i>et al</i> , 2002b
Rvs161p/ Rvs167p	Regulates endocytosis	Amphiphysins	Abp1p, Act1p, Las17p, Sla1p, Sla2p, Srv2p	Lila and Drubin, 1997 Colwill <i>et al</i> , 1999
Sac6p	Actin bundling	Fimbrin	Act1p	Karpova <i>et al</i> , 1995
Sla1p	Endocytic component, adaptor protein	Cin85 homology	Las17p, Ysc84p, Rvs167p, Srv2p, End3p, Pan1p, Sla2p	Stamenova <i>et al</i> , 2004 Tang <i>et al</i> , 2000
Sla2p	Binds actin monomers	IHip1R	Sla1p, Act1p, Rvs167p, Ark1p	Wesp <i>et al</i> , 1997 Gourlay <i>et al</i> , 2003
Srv2p	Binds actin monomers	CAP	Abp1p, Act1p, Aip1p, Pfy1p, Rvs167p, Sla1p	
Twf1p	Caps filament barbed ends		Act1p	Goode <i>et al</i> , 1998
Vrp1p	WIP homologue,	WIP	Las17p, Act1p, Myo3/5p	Evangelista <i>et al</i> , 2000
Ysc84p		SH3yl-1	Sla1p, Las17p	Madania <i>et al</i> , 1999

Table 1-1 Known cortical patch proteins

1.14 Actin and endocytosis

Endocytosis describes the internalisation of membrane components and extracellular material by invagination of the plasma membrane and formation of intracellular vesicles. These membranous vesicular compartments form the early and late endosomes which are trafficked to the vacuole for degradation (for review see Shaw

et al, 2001). Only a proportion of internalised molecules are however targeted for degradation in the vacuole; many escape this fate and are recycled due to the presence of a recycling/retention signal. Endocytic uptake has been classified into three distinct types, depending on the type of molecules internalised. Fluid-phase endocytosis describes the internalisation of particles which do not require direct binding, receptor-mediated endocytosis describes the uptake of plasma membrane receptor bound ligands (for review see Munn, 2000; Wendland *et al*, 1998), while phagocytosis describes the uptake and degradation of large particles. The study of endocytosis in *S. cerevisiae* was initially hindered by the presence of the yeast cell wall, which blocked the uptake of labelling molecules used successfully in other systems to study the process. The fluorescent dye lucifer yellow carbohydrazide (LY) was however shown to undergo internalisation and is now used widely as a marker for fluid-phase endocytosis, due to the inability of the dye to permeate the cell membrane (Reizman, 1985). LY therefore accumulates in the vacuole in wild-type yeast cells. The fluorescent dye FM4-64 is also used to study endocytosis as the dye labels the endocytosed plasma membrane (Vida and Emr, 1995).

Although the individual components of cortical patches have in most cases been well studied, the function of the cortical patch was unclear until recently. Localisation of cortical patches at the cell cortex and their association with plasma membrane invaginations (Mulholland *et al*, 1994) had previously suggested participation in endocytic events. Additionally, studies demonstrated actin defects in many endocytic mutants and vice versa (Munn *et al*, 1995; Moreau *et al*, 1997; Rath *et al*, 1993; Tang *et al*, 1997), while the Arp2/3 complex was associated with motile endosomal vesicles (Kaksonen *et al*, 2000), suggesting a link between the two processes. Endocytosis was also shown to require functional actin patches and not actin cables during a study of tropomyosin mutants. Yeast tropomyosins (Tpm1p and Tpm2p) bind along the length of actin filaments and stabilise filamentous structures. The major isoform of yeast tropomyosin, Tpm1p is a component of actin cables but does not co-localise with cortical actin patches (Lui and Bretscher, 1989). Deletion of *tpm1* generated cells which lacked detectable actin cables but in which endocytosis was not affected. This study suggested that actin patches alone played a crucial role in maintaining endocytic function.

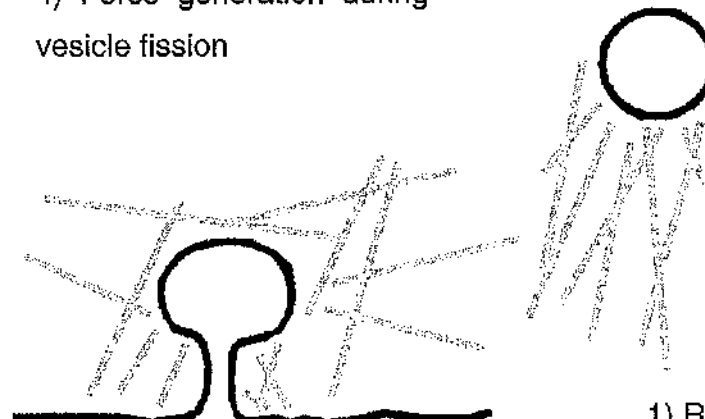
A number of potential roles for the actin cytoskeleton in endocytic uptake have been suggested (figure 1-11). Endocytosis can be divided into early events, which include invagination of the plasma membrane and the formation of vesicles, and later

events such as vesicle fission and vesicle movement into the cell. Actin has been proposed to have roles both early and late endocytic events. Potential roles include the recruitment or retention of components of the endocytic machinery at endocytic sites, and generation of the force required for membrane invagination by actin polymerisation. Actin has also been proposed to act as a barrier which prevents endocytic events and which is absent at specific endocytic sites. The polymerisation of actin has also been suggested to generate the force required for pinching off of vesicles and/or movement of vesicles into the cell (for review see Qualmann *et al*, 2000). Data demonstrating that the region around clathrin-coated pits lacks actin filaments (Fujimoto *et al*, 2000) provided evidence for a potential barrier effect of actin. Data also suggests that ENTH domain containing proteins such as epsin may effect membrane curvature during endocytosis (for reviews see Hurley and Wendland, 2002; Nossal and Zimmerberg, 2002), implying that actin involvement as a driving force for invagination of cell membrane may not be required. The epsin homologues in yeast, Ent1p and Ent2p contain ENTH domains and are required for endocytic uptake, suggesting the involvement of these proteins in plasma membrane invagination. Actin therefore is known to have an important, but poorly understood role in endocytosis.

Recent data has provided strong experimental evidence to link the function of actin at the cell cortex with endocytic uptake. A study by Kaksonen and colleagues (Kaksonen *et al*, 2003) has been significant in the study of endocytic uptake and cortical actin patch components. In this study, real time cell imaging was used to enable the movement of fluorescently tagged cortical patch and endocytic components to be followed. The proteins studied were Las17p, Sla1p, Sla2p, Pan1p, Abp1p and Arc15p; a component of the Arp2/3 complex. Strikingly, this study demonstrated the late recruitment of actin to endocytic sites, following recruitment of the cortical patch proteins Las17p, Sla1p, Sla2p and Pan1p to pre-existing endocytic sites. This report therefore suggested that actin does not recruit endocytic machinery to specific sites. This study also determined the pattern of sequential

- 3) Dissolution of a cortical actin barrier
- 5) Vesicle movement into the cytoplasm

- 4) Force generation during vesicle fission



- 1) Recruitment of endocytic machinery to specific sites



- 2) Invagination of the plasma membrane

Figure 1-11. Proposed roles for the actin cytoskeleton in endocytosis

Many possible roles for actin during endocytosis have been proposed. 1) The actin cytoskeletal may direct movement of endocytic machinery to specific sites or may retain endocytic machinery at these locations. 2) Actin polymerisation may generate a force required for invagination of the cell membrane. 3) The actin cytoskeleton may perform an inhibitory role preventing invagination of the membrane, except at endocytic sites. 4) Actin polymerisation may generate a force required to enable the 'pinching off' of vesicles. 5) Actin polymerization may promote vesicle movement into the cytoplasm by forming actin 'comet tails' (figure adapted from Qualmann *et al*, 2000).

recruitment of cortical patch and endocytic proteins to endocytic sites (figure 1-12). Accumulation of actin regulating proteins before the recruitment of actin to endocytic sites implies additional roles for these proteins. During the initial stages of endocytosis, the Arp2/3 activating protein Las17p is seen at endocytic sites. The delay in the recruitment of the Arp2/3 complex, which arrives along with actin, however suggests Las17p has additional roles during the early stages of endocytosis. As Las17p interacts with Slalp (Li, 1997), but co-localisation of Las17p with cortical actin patches is not dependent on Slalp (Ayscough *et al*, 1999), a proposed role for Las17p at endocytic sites therefore is the recruitment of proteins including Slalp. Following

Las17p recruitment, endocytic development continues with recruitment of Sla1p, Sla2p and Pan1p. Sla2p is known to localise to the cell cortex independently of actin and potentially via interactions mediated by its ENTH domain. Sla2p interacts with Sla1p (Gourlay *et al*, 2003), and as such may interact with the trimeric, endocytic Sla1p/Pan1p/End3p complex. The Arp2/3 complex, actin and Abp1p were the last proteins in the study by Kaksonen and colleagues to be recruited to endocytic sites. Recruitment of these proteins coincides with endocytic complexes moving away from the plasma membrane towards the interior of the cell. The ability of Pan1p to bind to and activate Arp2/3, suggests that Pan1p may recruit Arp2/3 to these sites (Duncan *et al*, 2001). Interestingly, by studying the sequential recruitment of proteins to endocytic sites, it has been shown that changes in patch motility correlate with changes in patch composition; with the appearance of actin at these sites coinciding with an increased in motility. Additionally, Sla2p has been shown to be crucial in linking endocytic components with actin polymerisation. Deletion of *sla2* is known to block endocytosis in yeast, and this study demonstrates the mechanism by which this is achieved. Deletion of *sla2* is shown to uncouple the association of actin with the endocytic machinery, an effect first seen in a study by Ayscough and colleagues (Gourlay *et al*, 2003). In a Δ *sla2* strain, actin polymerisation is not associated with components of the endocytic machinery; a block in endocytic uptake occurs and actin ‘tails’ are seen to form at the cell cortex. These studies propose a detailed early endocytic model in which actin, Arp2/3 and Abp1p accumulate at pre-determined endocytic sites and promote endocytic uptake through the polymerisation of actin.

Inhibition of endocytosis occurs in both in yeast and mammalian systems when cells are exposed to drugs which inhibit actin polymerisation, such as latrunculin-A and jasplakinolide (Ayscough *et al*, 1997; Ayscough, 2000). Evidence linking the actin cytoskeleton with endocytosis in higher eukaryotes is not as strong as in yeast (for review see Engqvist-Goldstein and Drubin, 2003). In mammalian cells, endocytic uptake shows an increased complexity due the existence of several endocytic pathways including: the clathrin-dependent pathway, a caveolar pathway, a clathrin and caveolar-independent pathway, phagocytosis and micropinocytosis. A direct role for actin polymerisation in all types of endocytic internalisation is however suggested by studies such as that by Merrifield and colleagues, which demonstrates the association of actin with clathrin coated vesicles and macropinosomes (Merrifield *et al*, 1999; Merrifield *et al*, 2002)

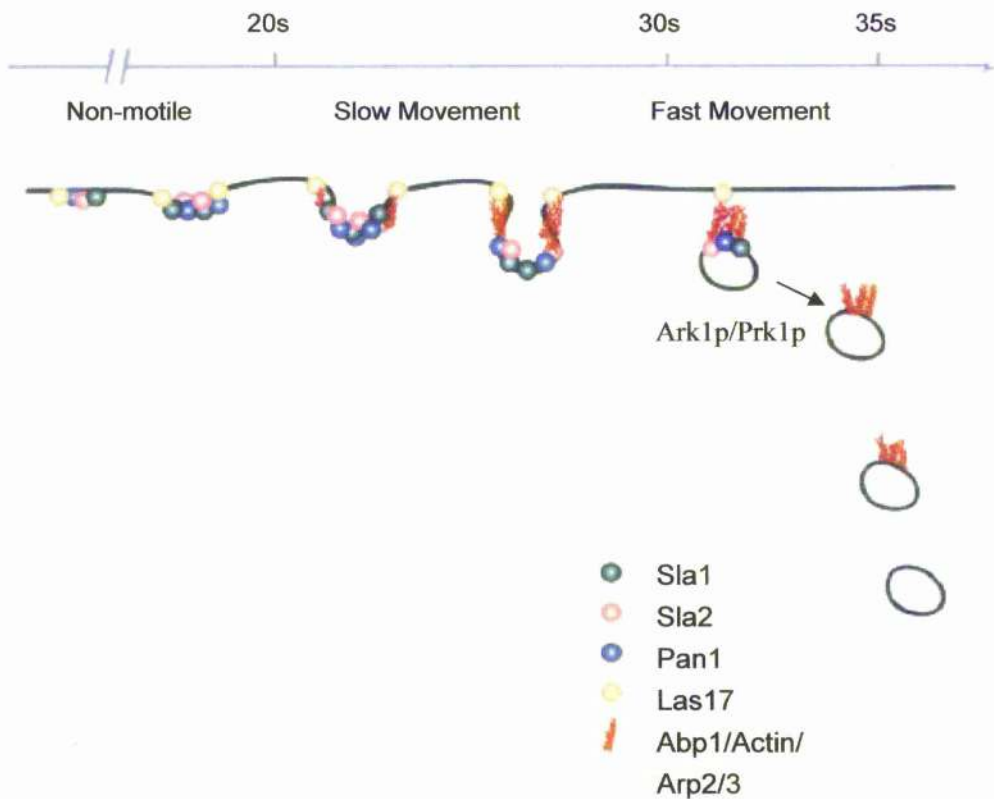


Figure 1-12. Current model demonstrating the proposed role of actin in endocytosis

A study by Kaksonen and colleagues has determined the pattern of sequential recruitment of cortical patch and endocytic proteins to sites of endocytosis. During early stages of developments Las17, Sla1, Sla2 and Pan1p are seen at sites of endocytosis. Later stages are defined by the recruitment of actin, Abp1 and the Arp2/3 complex to sites and coincide with movement of specific component away from the plasma membrane and into the cell. Following vesicle fission, disassembly of endocytic complexes is thought to be mediated by action of actin regulating kinases, Ark1/Prk1 (Zeng et al 2001), while actin polymerisation continues to mediate vesicle movement. Time taken for patch development is shown in seconds. Figure adapted from Kaksonen et al, 2004.

The importance of the Pan1p/End3p/Sla1p trimeric complex in actin and endocytic regulation in yeast is well established (Tang *et al*, 2000). Pan1p localises to cortical actin patches and is required for normal polarisation of the actin cytoskeleton, fluid phase and receptor mediated endocytosis, and is known to be required for the internalisation step of endocytosis (Tang and Cai, 1996; Tang *et al*, 1997). End3p is also required for endocytosis, with *end3* mutation causing depolarisation of the cortical actin network and the appearance of abnormal clumps of F-actin in the cytoskeleton (Benedetti *et al*, 1994). The epsin homology (EH) domain containing proteins Pan1p and End3p are therefore involved in both the regulation of actin and endocytosis. Pan1p, End3p and Sla1p have been shown to form a ternary complex, which may potentially include other factors. The actin regulating kinases, Prk1p and Ark1p are known to regulate this complex and other actin regulatory components in yeast by phosphorylation (Cope *et al*, 1999; Zeng and Cai, 1999). Ark1p and Prk1p localise to cortical actin patches and their activities partially overlap (Cope *et al*, 1999; Zeng and Cai, 1999). These kinases are proposed to promote actin patch disassembly by phosphorylation of specific cortical patch proteins, as suggested by the accumulation of large actin clumps in an $\Delta arkl\Delta prk1$ double mutant (Cope *et al*, 1999). Prk1p negatively regulates interactions in the Sla1p/End3p/Pan1p trimeric complex by phosphorylation of both Pan1p and Sla1p (Zeng and Cai, 1999; Zeng *et al*, 2001).

Essentially, recent data demonstrates that cortical patches generation occurs as an integral part of endocytic uptake. Actin is therefore an integral component of the endocytic machinery, while studies suggest that its polymerisation promotes the movement of endocytic vesicles into the cell.

1.15 The endocytic adaptor protein Sla1p

Sla1p was identified during analysis of the first protein shown to bind to actin in *S. cerevisiae*, actin binding protein-1 (Abp1p). Abp1p was shown to interact with actin by affinity chromatography using an actin column (Drubin *et al*, 1988). Abp1p co-localised with cortical actin patches in yeast, suggesting a role in actin regulation, while overexpression of Abp1p produced severe depolarisation of the actin cytoskeleton. Deletion of *abp1* however produced no obvious cellular phenotypes, suggesting a functional overlap with other yeast proteins. In order to identify functionally overlapping proteins, a synthetic lethal screen was performed to allow the identification of genomic mutations that caused cells to become dependent the expression of Abp1p

(Holtzman *et al*, 1993). Three genes were identified in this screen as being essential in strains lacking Abp1p. These genes were *SLA1* (synthetic lethal with *abp1-1*), *SLA2* (synthetic lethal with *abp1-2*) and *SAC6* (ycast fimbrin).

The amino-terminus of Sla1p contains three SH3 (Src homology-3) domains (figure 1-13). These domains are highly conserved protein to protein binding domains of approximately 60 amino acids in length. SH3 domains interact with proline-rich motifs including PxxP, and are found in a variety of proteins including the cytoskeletal proteins, Abp1p and myosin I, and many proteins involved in signal transduction (for review see McPherson, 1999; Macias *et al*, 2002). The central region of Sla1p contains two regions with high homology to the Sla1p homologues in other fungal species. These regions are termed homology domains 1 and 2 (SHD1 and SHD2) and show 58% and 60% identity respectively between *S. cerevisiae* and *S. pombe*. The carboxy-terminal region of Sla1p contains 26 repeats rich in proline, glutamine, glycine and threonine with the consensus sequence LxxQxTGGxxxPQ (Holtzman *et al*, 1993; Ayscough *et al*, 1999). This C-terminal repeat region contains many potential Prk1p phosphorylation motifs (Zeng *et al*, 2001). This carboxy-terminal repeat region has in addition been shown by immunoprecipitation to interact with the N-terminal EH domain of End3p and the LR2 domain of Pan1p. Sla1p therefore forms a trimeric endocytic complex with End3p and Pan1p (Tang *et al*, 2000).

A recent study by Stamenova and colleagues (Stamenova *et al*, 2004) has proposed the mammalian protein CIN85/CD2AP/CMS (Cbl-interacting protein of 85 kDa; CD2 associated protein; Cas ligand with multiple SH3 domains) as a functional homologue of Sla1p. The CIN85/CD2AP/CMS protein is significantly smaller than Sla1p and shows 34% similarity across the corresponding amino-terminal region of Sla1p. The structure of CIN85/CD2AP/CMS is similar to the amino-terminus of Sla1p; containing three amino-terminal SH3 domains with similar spacing to that found in Sla1p. CIN85/CD2AP/CMS is not however a direct homologue of Sla1p, but the protein does show comparable interactions and has been shown to be involved in endocytosis in mammalian cells (Kowanetz *et al*, 2003; Kowanetz *et al*, 2004).

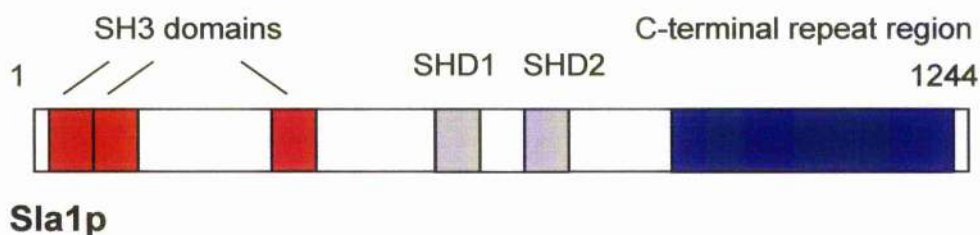


Figure 1-13. Schematic representation of domains present in Sla1p. Sla1p contains three amino-terminal SH3 domains (red), two regions of high homology to Sla1p homologues, SHD1 and SHD2 (grey) and a carboxy terminal repeat region containing 26 repeats of consensus sequence LxxQxTGGxxxPQ (blue).

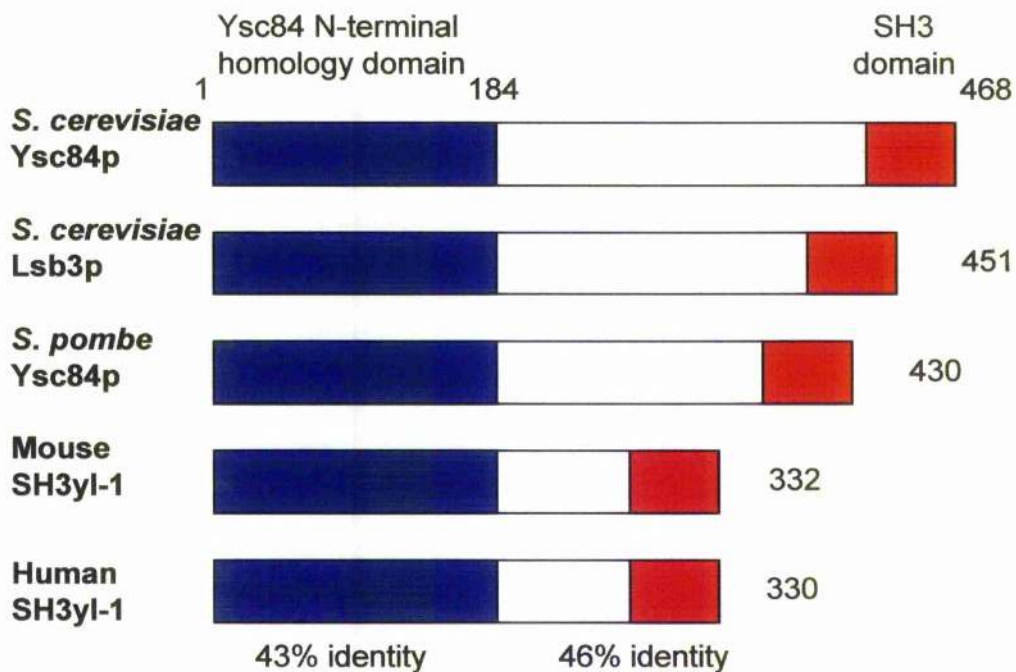


Figure 1-14. Schematic representation of domains present in Ysc84p and its homologues. Selected Ysc84p homologues are shown. Ysc84p in *S. cerevisiae* contains an amino terminal region (blue) highly conserved amongst its homologues (43% identity) but which shows no similarity to known motifs. In addition a highly conserved (46% identity) carboxy-terminal SH3 domain (red) is present in Ysc84p and its homologues.

1.15.1 Phenotypes of Δ *sla1* cells

Cells lacking *SLA1* display an aberrant cortical actin phenotype, with fewer but enlarged cortical actin patches. This strain also shows a temperature dependent growth defect when grown at 37°C, and a dependence on *ABP1* expression. (Holtzman *et al*, 1993). Additionally, a Δ *sla1* strain shows an increased resistance to the actin-disrupting drug latrunculin-A, suggesting a less dynamic actin cytoskeleton (Ayscough *et al*, 1997). Studies of *sla1* mutants have demonstrated the importance of the Gap1 and third SH3 domain for the regulation of the actin cytoskeleton. Deletion of the Gap1+SH3#3 region (residues 118-551) of Sla1p generated cells with actin cytoskeletal defects but which were not Abp1p dependent (Ayscough *et al*, 1999). Deletion of the C-terminal region of Sla1p (*sla1ΔCt* expression) does not generate actin defects but these cells are Abp1p dependent. In addition, growth of this mutant at 37°C demonstrates that *sla1ΔCt* is partially functional (Warren *et al*, 2002). These studies demonstrate the importance of the Gap1 and third SH3 domain of Sla1p for normal actin organisation, while determining that the region required for the rescue of Abp1p dependence lies in the C-terminal repeat region of Sla1p.

Studies show that deletion of *SLA1* caused mislocalisation of Sla2p and Rho1p (Ayscough *et al*, 1999), and that Sla1p is required for the localisation of Sla2p to cortical actin patches (Gourlay *et al*, 2003; Kaksonen *et al*, 2003). Sla2p is required for normal actin organisation and endocytic uptake, while Rho1p is a component of the β -glucan synthase enzyme. β -glucan synthase is involved in the synthesis of the cell wall material and consequently, cells lacking *SLA1* demonstrate an abnormal deposition of cell wall material (Ayscough *et al*, 1999). The combination of Δ *sla1* and Δ *sla2* deletion has also been reported to generate an interesting actin phenotype. Deletion of both genes causes accumulation of cortical actin patches primarily at the distal end of the mother cell, far removed sites of cell growth (Gourlay *et al*, 2003). Budding appears to progress normally in these enlarged cells and additional cortical patch components have also been localised to the aberrant patch sites. The mechanism for this localisation is not clear; however this study does demonstrate that polarised cell growth continues following the loss of actin patch accumulation at sites of cell growth.

1.15.2 Interactions of Sla1p

Characterisation of Sla1p has determined that the protein acts as a multifunctional adaptor, required for both the organisation of the cortical actin cytoskeleton and endocytic uptake. Sla1p interacts with a plethora of actin regulating, endocytic proteins and several additional factors, including the Arp2/3 activating proteins Las17p/Beel1p (Li, 1997) and Abp1p. Sla1p is thought to regulate actin dynamics through Las17p and Abp1p (Warren *et al.*, 2002), which localise to cortical actin patches in *S. cerevisiae*. Additionally, Sla1p has also been shown to interact with the cortical patch protein Ysc84p (Uetz *et al.*, 2000; Drees *et al.*, 2001; Dewar *et al.*, 2002). The interaction between Sla1p and several cortical patch proteins, and the partial co-localisation of Sla1p to cortical patches suggested a strong link between Sla1p and the regulation of actin.

Sla1p forms a trimeric complex with the endocytic proteins End3p and Pan1p (Tang *et al.*, 2000). This complex is important for actin organisation, endocytosis and cell wall morphogenesis (Benedetti *et al.*, 1994; Tang and Cai, 1996; Tang *et al.*, 1997; Ayscough *et al.*, 1999). Sla1p binds to the LR1 (Long Repeat 1) region of Pan1p and the N-terminus of End3p (Tang *et al.*, 2000). The C-terminal region of End3p also binds to the LR2 region of Pan1p (Tang *et al.*, 1997). Prk1p, an actin regulating kinase phosphorylates Pan1p (Zeng and Cai, 1999) and is proposed to phosphorylate motifs in the carboxy-terminal repeat region of Sla1p (Tang *et al.*, 2000). Protein interactions in this complex appear to be regulated primarily by phosphorylation, with binding of the C-terminal repeat region of Sla1p to the LR1 domain of Pan1p inhibited by Prk1p phosphorylation (Zeng *et al.*, 2001). Both regions contain multiple Prk1p phosphorylation motifs. Mislocalisation of Sla1p in an *end3-1* mutant, suggests End3p is required for the localisation of Sla1p to the cell cortex (Warren *et al.*, 2002).

The Sla1p protein has been shown to associate with Sla2p (Gourlay *et al.*, 2003). The minimal interacting regions of these proteins, as determined by 2-hybrid analysis are residues 118-361 of Sla1p, and the central region of Sla2p from residues 310-768. Sla2p is the yeast homologue of the mammalian protein HIP1R (Huntingtin interacting protein-1), a protein involved in endocytic function in mammalian cells (Engqvist-Goldstein *et al.*, 1999). A C-terminal region of Sla2p shows homology to the mammalian actin binding protein, talin (Hemmings *et al.*, 1996), while an N-terminal ENTH domain has been shown to bind to membrane inositol phospholipids and to mediate localisation of Sla2p to the cell cortex. The talin homology domain of Sla2p

binds F-actin *in vitro* (McCann and Craig, 1997). Expression of this C-terminal region of Sla2p in yeast also localises the fragment to cortical actin patches (Yang *et al*, 1999). Full-length Sla2p however localises only to subset of cortical patches (Yang *et al*, 1999), which only partially co-localise with actin but which co-localise to a large extent with Sla1p (Yang *et al*, 1999; Gourlay *et al*, 2003). Sla1p is required for the localisation of Sla2p to cortical actin patches. In the absence of Sla1p, Sla2p localises to patch like structures at the cell cortex rather than the aberrant actin in 'chunks' seen in this mutant (Ayscough *et al*, 1999).

Recent work has demonstrated binding of Sla1p to the ubiquitin ligase Rsp5p through the central domain of Sla1p (residues 420-720) (Stamenova *et al*, 2004). Rsp5p mediates mono-ubiquitination of many plasma membrane components including permeases, transporters and receptors, specifying internalisation of these proteins (Galan *et al*, 1996; Dunn and Hicke, 2001). Ubiquitin mediated endocytosis is emerging as an important pathway for the removal of plasma membrane components. Rsp5p is also required for fluid phase endocytosis and as such is proposed to have multiple functions in the regulation of endocytosis (Dunn and Hicke, 2001). GFP-tagging has localised Rsp5p to membrane invaginations and peri-vacuolar structures (Wang *et al*, 2001a). The vacuolar localisation of Rsp5p is dependent on its catalytic activity and Sla2p, suggesting Rsp5p may be transported to this location via endocytic uptake. The interaction of Rsp5p with Sla1p also raised the possibility that Sla1p recruits Rsp5p to proteins requiring ubiquitination, or in some way facilitates the process of ubiquitination. This however appears unlikely as ubiquitination and endocytosis of the Ste2p receptor occurs normally in Δ s $la1$ cells (Stamenova *et al*, 2004). In addition to interacting with Rsp5p, Sla1p interacts with Rvs167p, which in turn interacts with Rsp5p (Stamenova *et al*, 2004). A Δ s $la1$ strain has previously been shown to be synthetically lethal with Rvs167p (Tong *et al*, 2004), and work by Stamenova and colleagues confirmed a direct interaction between the two proteins. Rvs167p forms a dimer with Rvs161p in an analogous manner to mammalian amphiphysins. Amphiphysins are endocytic and actin regulatory proteins of which Rvs167p is proposed to be an orthologue. Rvs167p is known to bind to the Arp2/3 complex NPF, Las17p (Colwill *et al*, 1999; Madania *et al*, 1999). The interaction of Sla1p with End3p, Pan1p, Sla2p and Rsp5p therefore demonstrate links between Sla1p and endocytosis.

Recent data from our lab has also demonstrated the interaction of Sla1p with Lsb5p and subsequently, an interaction between Lsb5p and Arf3p (Dewar *et al*, 2002; Costa *et al*, 2005). Lsb5p shows similarity to the GGA family of membrane trafficking

proteins which are known to bind ADP-ribosylating factor (Arf) proteins both in mammalian and yeast systems (Zhdankina *et al*, 2001; for review see Boman, 2001). Similarity was determined by the identification of an N-terminal Vps27p, Hrs, Stam (VHS) domain and an Arf-interacting GGA and Tom1 (GAT) domain in the Lsb5p sequence. Arf binding by GGA proteins is known to be mediated by GAT domains (Zhdankina *et al*, 2001). In mammalian cells, activated Arf proteins with the exception of Arf6, recruit specific coat proteins and GGAs to sites of vesicle development at the trans-golgi network (TGN) (Puertollano *et al*, 2001; Takatsu *et al*, 2002). The yeast homologue of mammalian Arf6, Arf3p, additionally localises predominately to the plasma membrane (Huang *et al*, 2003), while yeast Arf1p and Arf2p are Golgi localised. Arf3p is linked to endocytosis at the plasma membrane by interaction with Lsb5p. In addition to a potential role as a membrane trafficking protein, Lsb5p has been implicated in endocytic regulation through a genetic interaction with the gene encoding Ysc84p (Dewar *et al*, 2002). Lsb5p localises to the cell cortex in punctuate spots, a localisation which is affected by *sla1* deletion (Dewar *et al*, 2002) and interacts with Las17p by 2-hybrid (Madania *et al*, 1999). Sla1p may therefore interact indirectly with Arf3p, which is plasma membrane associated in its GTP bound form (Huang *et al*, 2003), through Lsb5p. Additionally, Sla1p is proposed to recognise and mediate the uptake of plasma membrane proteins containing NPFX_(1,2)D motifs. These motifs are found in proteins including Ste2p, Ste3p and Kex3p (Howard *et al*, 2002).

1.16 The cortical patch protein Ysc84p

Ysc84p is a 468 amino acid protein which localises to cortical actin patches in *S. cerevisiae* (Dewar *et al*, 2002). Ysc84p has a conserved amino terminal domain and a conserved SH3 (Src homology 3) domain in the carboxy-terminal region of the protein (figure 1-14). SH3 domains are known to mediate protein to protein interactions with proline rich regions including containing PxxP motifs (for reviews see McPherson, 1999; Macias *et al*, 2002). The amino-terminal domain of Ysc84p does not show homology to known motifs or domains, but is highly conserved between Ysc84p homologues. This N-terminal domain encompasses amino acids 1-184 of the protein and is conserved with 43% identity across the species. The mouse homologue of Ysc84p was identified by Aoki and colleagues (Aoki *et al*, 2000) and shows 53% identity across the amino terminal region, and 50% identity across the carboxy terminal SH3 domain. Ysc84p also has a homologue in *S. cerevisiae* which shows 59% identity

at the protein level. This *S. cerevisiae* homologue, Lsb3p is also known to co-localise with cortical actin patches (Dewar *et al*, 2002). Additionally, studies have demonstrated phosphorylation of Ysc84p on serine residue 301 by phosphoproteome analysis (Ficaro *et al*, 2002).

1.16.1 Phenotypes of Δ *ysc84* cells

Deletion of *YSC84* generates no obvious cellular phenotype (Dewar *et al*, 2002). The association of phenotypes with single mutations or deletions can indicate the importance of a gene in cellular function. In conjunction with deletion of *LSB5* however, which also shows no distinct phenotypes upon single deletion, depolarisation of actin, endocytic defects and growth defects at high temperature however become apparent (Dewar *et al*, 2002). Severe phenotypic defects upon deletion of both *YSC84* and *LSB5* suggest that the encoded proteins may act in functionally redundant pathways. Lsb5p localises to the cell cortex in punctate patches, a localisation which is partially dependent on Sla1p (Dewar *et al*, 2002). Lsb5p is implicated in vesicle trafficking due to similarity to yeast GGA proteins and the presence of an NPFXD motif, which are known to bind to epsin homology (EH) domains present in the endocytic proteins Pan1p and End3p (deBeer *et al*, 2000). Additionally, Lsb5p has been shown to interact with Arf3p at the plasma membrane (Costa *et al*, 2005) and the Arp2/3 regulating factor Las17p (Madania *et al*, 1999). The ADP-ribosylation factors (Arfs) are a family of small ubiquitously expressed Ras-like GTPases that are central to many vesicular transport processes.

1.16.2 Interactions of Ysc84p

The function of Ysc84p at cortical patches sites has so far remained unstudied. Localisation of Ysc84p to cortical actin patches however suggests a role in the regulation of actin, as many patch proteins regulate actin directly (see table 1-1). Ysc84p localisation is dependent on actin, with Latrunculin-A treatment causing rapid mislocalisation of GFP-Ysc84p (Dewar *et al*, 2002). Lack of a conserved actin binding motif in the Ysc84p sequence however suggested that co-localisation with actin was mediated by additional cortical patch proteins. In addition, the localisation of Ysc84p to cortical actin patches was shown to be dependent on Abp1p and to a lesser extent on Las17p/Beel, the yeast WASP homologue (Dewar *et al*, 2002), suggesting potential

mechanisms for Ysc84p recruitment and localisation to cortical patches. Furthermore, Ysc84p has been shown to interact with Las17p by 2-hybrid (Madania *et al*, 1999) and to immunoprecipitate in a complex containing Abp1p (Ho *et al*, 2002). As previously discussed, genomic wide yeast 2-hybrid screens initially reported an interaction between Ysc84p and Sla1p (Uetz *et al*, 2000; Drees *et al*, 2001). Domains mediating this interaction were subsequently localised to residues within amino acids 118-511 of Sla1p and the C-terminal region of Ysc84p from residues 229-468. Interaction between Sla1p and Ysc84p has also been confirmed biochemically (Dewar *et al*, 2002).

1.17 Aims of this project

The dynamic nature of the actin cytoskeleton is attributed to the interaction of actin monomers and filaments with a plethora of actin regulating proteins. Regulation of individual actin filaments and their co-ordinated organisation into higher order structures allows the participation of actin in a wide variety of dynamic cell processes. Actin is involved in structural roles, in the polarisation of growth and development, in endocytic uptake, and in generating cellular and intracellular movement; enabled by harnessing the force generated by actin polymerisation. Previous studies have enabled the classification of actin regulating proteins into generalised functional groupings and overall actin regulatory mechanisms to be investigated. The study of individual actin regulatory proteins therefore contributes to the overall understanding of the regulation of actin, allowing regulatory pathways and complexes to be examined.

The aim of this project was to further investigate two proteins implicated in the regulation of the actin cytoskeleton in yeast. The cortical adaptor protein Sla1p had been the focus of many studies and was known to have several roles at the cell cortex. In addition however, we had observed this protein in the yeast nucleus (Kathryn Ayscough, unpublished observations). As Sla1p was already known to be a multi-functional protein, an addition role for nuclear Sla1p was an interesting possibility. In order to further investigate and characterise nuclear Sla1p, a variety of cellular and proteomic techniques were used. In addition, this project aimed to investigate the cortical patch protein Ysc84p. Previous studies had provided little insight into the function of the Ysc84p protein, having not defined either a specific role for Ysc84p, or a mechanism for its localisation to cortical patches. In order to gain further insight into the function of Ysc84p, extensive biochemical and cellular analysis were carried out. Studies were also extended to include analysis of the Ysc84p homologue, hSH3yl-1.

In chapter 3 of this thesis, I describe the advances that I have made in the study of nuclear Sla1p, which include examining the nucleocytoplasmic trafficking of Sla1p and investigating potential nuclear roles. I will additionally demonstrate that nuclear Sla1p is not affected by cytoplasmic actin remodelling and will propose a mechanism for the nuclear translocation of Sla1p. Localisation of Sla1p to the nucleus has not been described prior to this work.

In chapter 4, I detail my investigation of the yeast protein Ysc84p and its human homologue, hSH3yl-1. My studies suggest a direct role for both proteins in the regulation of actin, and detail the biochemical analysis of Ysc84p, which has identified the actin binding, severing and capping abilities of this protein. My studies identify specific activities of Ysc84p *in vitro* which promote interesting possibilities for the role of the protein at cortical patch sites.

In chapter 5, I describe my study of Gts1p in *S. cerevisiae*. Previous 2-hybrid analysis had suggested that Gts1p may interact both with Ysc84p and Sla1p *in vivo*. My work confirms these 2-hybrid studies and further defines the domains mediating this interaction. I additionally demonstrate that localisation of Gts1p to the cell cortex occurs independently of Sla1p and actin, and provide evidence for a role for Gts1p in the regulation of both actin and endocytosis.

In chapter 6, I provide a summary of my thesis and propose additional experiments which would provide additional insight into the roles of Ysc84p, Gts1p and nuclear Sla1p.

2 MATERIALS AND METHODS

2.1 Materials

All chemicals and media used in this study were obtained from Merck or Sigma unless otherwise stated. Enzymes used in this study were obtained from New England Biolabs unless otherwise stated.

2.2 Yeast Strains, Plasmids and Oligonucleotides

All plasmids, oligonucleotides, yeast strains and antibodies generated and used during the course of this study are listed in tables 2-1, 2-2, 2-3 and 2-4 respectively.

Plasmid	Description	Origin
pCR®4-TOPO	TOPO cloning	Invitrogen
pGAD-C2 (pKA163)	2-hybrid Gal4 empty activation domain	(James <i>et al</i> , 1996)
pGBDU-C1	2-hybrid Gal4 empty binding domain	(James <i>et al</i> , 1996)
pFA6-3xHA-HIS3MX6	For C-terminal 3xHA tagging (<i>HIS3</i> marked)	(Longtine <i>et al</i> , 1998)
pFA6-13xmyc-TRP1	For C-terminal 13xmyc tagging (<i>TRP1</i> marked)	(Longtine <i>et al</i> , 1998)
pFA6-HIS3MX6	For <i>HIS3</i> marked gene deletions	(Longtine <i>et al</i> , 1998)
pTrcHis	For N-terminal 6x histidine tagging	Invitrogen
pWZV86 (pKA119)	For <i>TRP1</i> marked gene deletions	K. Nasmyth (IMP, Vienna)
pWZV87 (pKA159)	For C-terminal myc tagging (<i>TRP1</i> marked, pFA6-13xmyc)	K. Nasmyth (IMP, Vienna)
pWZV89	For C-terminal 3xHA tagging (<i>TRP1</i> marked)	K. Nasmyth (IMP, Vienna)
pKA32	<i>Sla1-Δ118-511</i> plasmid generated from pKA53	(Ayscough <i>et al</i> , 1999)
pKA53	pRS313 + <i>sla1ΔGI+SH3#3</i>	(Ayscough <i>et al</i> , 1999)
pKA55	pRS313 + <i>sla1</i> BamH1 fragment	(Ayscough <i>et al</i> , 1999)
pKA142	pGEX4T1	Pharmacia
pKA143	pGEX4T2	Pharmacia
pKA151	For C-terminal myc tagging (<i>HIS</i> marked, pFA6-13xmyc)	
pKA241	Gal4-AD-Ysc84-229-468 (<i>LEU</i> marked)	This study
pKA242	Gal4-AD-Ysc84-181-468 (<i>LEU</i> marked)	This study
pKA243	Gal4-AD-Ysc84-143-468 (<i>LEU</i> marked)	This study
pKA251	Gal4-AD-Ysc84-(-SH3) pKA241 minus SH3 domain (<i>LEU</i> marked)	This study
pKA252	pME18S-FL + hSH3yl-1 cDNA	Dr Hata (University of Tokyo)

pKA256	p416MET25 methionine inducible <i>CEN URA</i> (pMET25)	(Mumberg <i>et al.</i> , 1994)
pKA259	pCR®4-TOPO + <i>YSC84</i>	This study
pKA275	pCR®4-TOPO + <i>hSH3YL-1</i>	This study
pKA276	pCR®4-TOPO + <i>ysc84 (1-654)</i>	This study
pKA277	pCR®4-TOPO + <i>ysc84 (1-552)</i>	This study
pKA278	pGEX4T1 + <i>ysc84 (1-654)</i>	This study
pKA279	pGEX4T1 + <i>YSC84</i>	This study
pKA328	Gal4-AD-Sla1-SH3#1-3 (<i>LEU</i> marked)	This study
pKA388	Gal4-BD-Gts1 (<i>TRP</i> marked)	This study
pKA392	pK416MET25 + <i>hSH3YL-1</i> (pMET25- <i>hSH3yl-1</i>)	This study
pKA394	pGEX4T2 + <i>ysc84 (259-552)</i>	This study

Table 2-1 Plasmids used in this study

oKA	Sequence	Description
2	TGCTGCTCCGGTTTCATCTGCTCCGGTTTC ATCTGCTCCCGCTCCATTGGATCCATTCAA TCCGGITCTGCTGCTAG	Tagging and deleting C-terminal repeats of <i>SLAI</i> (5')
3	GTAATCATTGGCATCATCACAAAGCCAGTA GATAAGGGTAAGATATTGTGCCACCGGTT CCTCGAGGCCAGAAGAC	Tagging and deleting C-terminal repeats of <i>SLAI</i> (3')
7	CCTCAACAATCAAGGCAAGCCAACATATTCAA TGCTACTGCATCAAATCCGTTGGATTCTCCGG TTCTGCTGCTAG	<i>SLAI</i> N-terminal 3' tagging
8	ACGAAACTATTTCATATAAGCTTGTTTAGTTAT TATCCTATAAAAATCTTAAAATACATTAATCGG AGCTCCGGTCTTCTG	<i>SLAI</i> N-terminal 5' tagging
13	CATTATTGGACTGAGAACG	<i>SLAI</i> -tag C-terminal check (5')
14	CCATTGGATCCATTCAAAACC	<i>SLAI</i> -tag C-terminal check (3')
124	GCATGGCCTTGCAGGGC	pGEX cloning checking oligo, forward
132	ACGAAACTATTTCATATAACGTGTTTAGTTAT TATCCTATAAAAATCTTAAAATACATTAATCGA ATTGAGCTCGTTAAAC	(3') amplification of 9x Myc tag for <i>SLAI</i>
133	CTCAACAATCAAGGCAAGCCAACATATTCAAAT GCTACTGCATCAAATCCGTTGGATTGCTGCA GCCGCTGCAGCTGCACGGATCCCCGGGTTAAT TAA	(5') amplification of 9x Myc tag for <i>SLAI</i>
153	ATACCACTACAATGGATGATG	pGAD (5') sequencing
154	AGATGGGCATTAATTCTAGTC	pGAD (3') sequencing
182	ACATCATCATCGGAAGAGAG	pGBD (5') sequencing
183	AATGAAAGAAATTGAGATGG	pGBD (3') sequencing
231	GACCGGATCCATGAATAACCTATACCTTCC	<i>hSH3YL-1</i> (3') amplification
232	GAGCGGATCCAGTATACGCTTTAATTCATGG	<i>hSH3YL-1</i> (5') amplification
236	GATCGGATCCATGGGTATCAATAATCCAATT	<i>YSC84</i> (5') amplification

237	GATCGGATCCACCAATCATTTGAGAATCTGA	YSC84 (3') amplification
239	GATCGGA'CCCTTAAAAGTTGAACGCTCTGAA	YSC84 (3') amplification from bp 654
251	GATCGAATTCTTAGAAAACCTTCGATTAGC	YSC84 (3') amplification from bp 552
349	GATCGGATTCATGTCCCATCCGCACTCACAT	GGA2 (5') amplification
350	GATCGGATCCCTATACATTAGGTAAACGTAAA	GGA2 (3') amplification
351	GATCGGATTCATGGACCCACATAATCCAATT	ARP2 (5') amplification
352	GATCGGA'CCCTATCTTGGACCAAATTAGT	ARP2 (3') amplification
353	GATCGGATTCATGTATTCTTGGAAAGTCAAAG	YPK1 (5') amplification
354	GATCGGATCCCTATCTAATGCTTCTACCTTG	YPK1 (3') amplification
355	GATCGGATTCAATGTCTGATGCGGCTCCTCA	STE2 (5') amplification
356	GATCGGATCCGTATAAATTATTATTATCTTC	STE2 (3') amplification
357	GATCGGATTCAATGCAGACGTCAATGGTGAGC	WSC4 (5') amplification
358	GATCGGATCCGTTATCGTCATTAGCCGCAG	WSC4 (3') amplification
364	GATCGAATTCATGAGAGAAGTTATTAGTATT	TUB1 (5') amplification
365	GATCGGATCCCTAAAATTCCCTTCCTCAGC	TUB1 (3') amplification
366	GATCGGATCCATGGCAGGTGCTGGTGCAGGT	YSC84 (5') amplification from bp 259
377	GATCGAATTCATGGCTGATAAGATAGATGAGG	SLT2 (5') amplification
378	GCGCGGATTCCCTAAAAATTTTCTATC	SLT2 (3') amplification
410	TACAGACAAGCTGTGACC	pGEX cloning checking oligo, reverse

Table 2-2 Oligonucleotides used in this study

Strain	Genotype	Origin/Reference
pJ69-2a	MAT α trp-901, leu2-3,112, ura3-52, his3-Δ200, gal4Δ, gal80Δ, GAL2::ADE2, GAL1::HIS3	Clontech
pJ69-4a	MAT α trp-901, leu2-3,112, ura3-52, his3-Δ200, gal4Δ, gal80Δ, LYS2::GAL2 _{UAS} -GAL1 _{TATA} -HIS3, GAL2 _{UAS} -GAL2 _{TATA} -ADE2	Peter Piper (University of Sheffield), (James <i>et al</i> , 1996)
pJ69-4α	MAT α trp-901, leu2-3,112, ura3-52, his3-Δ200, gal4Δ, gal80Δ, LYS2::GAL2 _{UAS} -GAL1 _{TATA} -HIS3, GAL2 _{UAS} -GAL2 _{TATA} -ADE2	Peter Piper (University of Sheffield), (James <i>et al</i> , 1996)
KAY300	MAT α trp1-1 leu2-3,112 his3-Δ200 ura3-52 Δslal::URA3	(Ayscough <i>et al</i> , 1999)
KAY301	MAT α trp1-1 leu2-3,112 his3-Δ200 ura3-52 Δslal::URA3	(Ayscough <i>et al</i> , 1999)
KAY302	MAT α , trp1-1, leu2-3,112, lys2-801, his3-Δ200, ura3-52	(Ayscough <i>et al</i> , 1999)
KAY303	KAY302 + integrated SLA1-9xmyc::TRP	(Ayscough <i>et al</i> , 1999)
KAY367	MAT α , trp1-1, his3-Δ20, leu2-3,112, ura3-52 Δslal::LEU2, slalΔ118-511-9xmyc::TRP	(Gourlay <i>et al</i> , 2003)
KAY382	MAT α his3-Δ200, ura3-52, leu2-3,112, trp1-1 Δslal::URA3 SLA1ΔG2::HIS3	Kathryn Ayscough (University of Sheffield)
KAY387	MAT α , trp1-1, his3-Δ20, leu2-3,112, ura3-52 Δslal::LEU2, slalΔG2-9xmyc::TRP	(Gourlay <i>et al</i> , 2003)
KAY389	MAT α , trp1-1, leu2-3,112, lys2-801, his3-Δ200, ura3-52	(Ayscough <i>et al</i> , 1999)
KAY429	MAT α leu2Δ, his3Δ, trp1-1, ura3Δ Δerm1/xpo1::KanMX +	M. Rashbash

pDC-crmI (<i>LEU2</i> CEN)		
KAY430	MAT α <i>leu2Δ, his3Δ, trp1-1, ura3Δ ΔcrmI/xpo1::KanMX</i> + pDC-crmI/TS39C (<i>LEU2</i> CEN)	M. Rashbash
KAY443	KAY429 + <i>SLA1-9xmyc::TRP</i>	This study
KAY444	KAY430 + <i>SLA1-9xmyc::TRP</i>	This study
KAY446	MAT α <i>his3Δ1, leu2Δ, ura3Δ, met 15Δ</i> (also BY4741)	Research Genetics
KAY447	MAT α <i>his3Δ1, leu2Δ, ura3Δ, met 15Δ</i> (also BY4742)	Research Genetics
KAY480	MAT α/α , <i>his3Δ1/his3Δ1, leu2Δ1/leu2Δ1, ura3Δ/ura3Δ, Met15/MET15, LYS2/LYS2Δ</i>	Research Genetics
KAY510	MAT α <i>his3-Δ200, ura3-52, leu2-3,112, trp1-1, lys2-801 Δysc84::HIS</i>	(Dewar <i>et al</i> , 2002)
KAY516	MAT α <i>his3Δ, leu2Δ, ura3Δ, lys2Δ, Δlsb5::KanMX, Δysc84::HIS3</i>	(Dewar <i>et al</i> , 2002)
KAY554	MAT α <i>his3Δ, leu2Δ, ura3Δ, trp1-1, lys2-801 Δysc84::HIS Δlsb3::URA3</i>	(Dewar <i>et al</i> , 2002)
KAY606	MAT α , <i>rna1-1, ura3-52, trp1Δ63, leu2Δ1</i>	(Koepp <i>et al</i> , 1996)
KAY607	MAT α , <i>srp1-31, leu2-3, 112, ura3-52, his3, ade2, trp1</i>	Paul Ko Ferrigno (University of Cambridge)
KAY608	MAT α , <i>kap123Δ::HIS3, ura3-52, his3Δ200, leu2Δ1</i>	(Seedorf <i>et al</i> , 1997)
KAY609	MAT α , <i>lph2Δ::HIS3, ura3-52, leu2Δ1, his3Δ200</i>	Paul Ko Ferrigno (University of Cambridge)
KAY610	MAT α , <i>rs11-4, ura3-52, leu2Δ1, trp1Δ63</i>	Paul Ko Ferrigno (University of Cambridge)
KAY612	MAT α , <i>xpolΔ/crmI::LEU2, pKW440 (XPO1/CRM1, HIS3)</i>	Karsten Weis (University of California)
KAY613	MAT α , <i>mtr10-1, ura3-52, lys2-301</i>	Alan Tartakoff
KAY614	MAT α , <i>msn5Δ::HIS3, ura3-52, his3Δ200, leu2Δ1</i>	Paul Ko Ferrigno (University of Cambridge)
KAY615	MAT α , <i>los1-1, SUP4, ade2-1, can1-100, lys1-1, trp5-48, ura3-1, his5-2</i>	Anita Hopper (Pennsylvania State University)
KAY616	MAT α , <i>xpolΔ/crmI::LEU2 pKW440 (xpol-1/crmI-1, HIS3)</i>	Karsten Weis (University of California)
KAY617	MAT α , <i>ura3-52, his3Δ200, leu2-3,112, trp1Δ1, lys2-801</i>	Günter Blobel (Rockefeller University, New York)
KAY619	MAT α , <i>nmd5Δ::HIS3</i>	Paul Ko Ferrigno (University of Cambridge)
KAY620	MAT α , <i>sxn1Δ::HIS3, leu2Δ1, his3Δ200, trp1Δ63, ura3-52</i>	Paul Ko Ferrigno (University of Cambridge)
KAY621	MAT α , <i>pse1-1, ura3-52, leu2Δ1, trp1Δ63,</i>	(Seedorf <i>et al</i> , 1997)
KAY622	MAT α , <i>prp20-1, ura3-52, leu2Δ1, trp1Δ63</i>	(Seedorf <i>et al</i> , 1997)
KAY709	MAT α/α <i>his3Δ1/his3Δ, leu2Δ/leu2Δ, ura3Δ/ura3Δ, Met15/MET15, LYS2/lys2Δ Δgts1::KanMX/Δgts1::KanMX</i>	Invitrogen
KAY710	MAT α <i>his3Δ, leu2Δ, ura3Δ, Met15 Δgts1::KanMX</i>	Invitrogen
KAY725	MAT α <i>his3Δ, leu2Δ, ura3Δ, Met 15 GFP-Gts1p</i>	Research Genetics
KAY750	pJ694a + Gal4AD-Sla1	Invitrogen
KAY751	pJ694a + Gal4AD-Ysc84	Invitrogen

KAY752	MAT α <i>his3Δ, leu2Δ, ura3Δ, Met 15, Als1::URA3</i> GFP-Gts1p	This study
KAY767	MAT α <i>his3Δ, leu2Δ, ura3Δ, lys2Δ, Als2::KanMX, Δyse84::HIS3 + pMET25-SH3yl-1</i>	This study
KAY768	MAT α <i>his3Δ, leu2Δ, ura3Δ, lys2Δ, Als2::KanMX, Δyse84::HIS3 + pMET25</i>	This study

Table 2-3 Yeast strains used in this study

Application	Antibody	Dilution Factor	Source/Reference
Anti-Ysc84p	Primary antibody: rabbit anti-Ysc84p	1:2000	This study
	Secondary antibody: anti-rabbit-HRP	1:10000	Vector Labs
Anti-myc immunostaining	Primary antibody: rabbit anti-myc (A14)	1:100	Santa Cruz Biotechnology Inc.
	Secondary antibody: goat anti-rabbit FITC	1:100	Vector Labs
	Secondary antibody: anti-rabbit-AP	1:10000	Vector Labs

Table 2-4 Antibodies used in this study

Bacterial Media

2x YT	1% yeast extract	(Difco Laboratories)
	0.5% NaCl	(Sigma)
	1.6% tryptone	(Difco Laboratories)

For solid media, 2xYT was supplement with 2% bacteriological agar (Oxoid Ltd). Ampicillin resistance was identified by addition of ampicillin at 100 µg/ml (Melford Laboratories).

2.3.1 Restriction enzyme digestion of DNA

Restriction enzyme digests were carried out according to the manufacturer's instructions using the buffers supplied. Double digests were performed as required and where similar digestion conditions allowed, and as recommended by the manufacturer. Reactions were typically performed in a final volume of 20 µl using 3-4 U of enzyme per reaction. All digests were carried out at 37°C for 2 hours unless otherwise recommended by the manufacturer.

2.3.2 Electrophoresis of DNA using agarose gels

DNA fragments were separated and visualised using agarose gel electrophoresis. A 0.8% agarose gel was prepared using 0.8% powdered agarose (Melford Laboratories) in 100 ml of a 1 x TAE (10 mM Tris-HCl pH 7.5, 5 mM Acetic acid, 1 mM EDTA pH7.5) solution. Typically 0.4 g of powdered agarose was added to 50ml of 1 x TAE. The agarose/TAE solution was melted and allowed to cool to approximately 50°C. 2 µl of a 10 mg/ml stock of ethidium bromide was then added to the solution and the solution poured into a gel casting tray and sample wells inserted. Following complete cooling and solidification of the gel, 6 x gel loading buffer (0.25% Bromophenol Blue, 0.25% Xylene Cyanol FF, 30% glycerol (Merck) in water) was added to the DNA samples to a final 1x concentration. The agarose gel was then immersed in electrophoresis buffer (1 x TAE) in a suitable tank and the DNA samples loaded into the wells of the gel. Samples were electrophoresed at 100 Volts for 50 minutes. The DNA was then visualised by illuminating the gel with a uv light source.

2.3.3 Removal of terminal 5' phosphate groups using calf intestinal alkaline phosphatase (C.I.P.)

0.5 U of C.I.P. and a quantity of 10X C.I.P. buffer (New England Biolabs) which gave a final 1x concentration, was added to appropriate amounts of DNA requiring dephosphorylation. Samples were then incubated at 37°C for 30 minutes, electrophoresed on an agarose gel and the DNA purified as described in section 2.3.4.

2.3.4 Extraction of DNA from an agarose gel slice using the QIAquick Gel Extraction Kit™

DNA extraction from an agarose gel was performed using the QIAquick Gel Extraction Kit™ (Qiagen). DNA samples were first electrophoresed on an agarose gel (as described in section 2.2.6). The DNA to be extracted could be visualised by illuminating the gel with a UV source, enabling the DNA band to be identified and cut from the gel. The gel slice was then placed in a 1.5 ml microfuge tube, weighed, and 3 volumes of Buffer QG added. The tube was then incubated at 50°C for 10 minutes to solubilise the agarose and one volume of absolute ethanol added to the tube, if the DNA fragment to be extracted was larger than 500 bp but smaller than 4 Kb. This tube was then inverted 3 times and the sample applied to a spin column held in a 2 ml collection tube. The column was then centrifuged at top speed in a benchtop centrifuge for 1 minute. After discarding the flow-through, 750 µl of wash buffer was also added to the column and the centrifugation repeated. This was step was again repeated using a further 250 µl of wash buffer and centrifugation for 2 minutes to allow drying of the membrane. The collection tube was then discarded, the column placed in a 1.5 ml microfuge tube and 35 µl of sterile water applied directly to the column membrane. Plasmid DNA was then eluted into the 35 µl of water by centrifuging the membrane at top speed for 1 minute.

2.3.5 Amplification of DNA using the polymerase chain reaction

Specific sequences of DNA were amplified using the polymerase chain reaction (PCR). Specific oligonucleotide primers complementary in sequence to regions flanking the sequence of interest were first generated using a commercial service at MWG Biotech. A plasmid containing the region to be amplified was then obtained, and was termed the template DNA. The PCR method described here is a general method

used to amplify both fragments of genes for cloning, and sequences from plasmids designed to allow deletion or tagging of genes within the yeast genome. All PCR reactions were performed using Bioline reagents.

For each PCR reaction, 0.5 pmols primer 1, 0.5 pmols primer 2, 200 nM dNTP's, 1 X NH₄ reaction buffer (Bioline), 1.5 mM MgCl₂ (Bioline), 1 μ l template DNA and sterile water to a total volume of 99.5 μ l was added to a 0.2 ml thin walled PCR tube held on ice. The components were mixed gently and centrifuged briefly to concentrate the liquid in the base of the tube. The tube was then transferred to a pre-heated PCR machine (Biometra TGradient Thermocycler) at 94°C, to which 5 U of BioTaq DNA polymerase enzyme (Bioline) was added after 60 seconds. The PCR was performed using 30 cycles of amplification. Each cycle contained an initial denaturing step of 94°C for 1 minute, followed by a variable annealing temperature of approximately 55°C for 1 minute, and finally an extension step at 72°C for 1 minute per Kb of DNA to be amplified. The temperature of annealing was varied in order to optimise annealing of the oligonucleotide primers used. A final step of 72°C for 5 minutes was used at the end of the amplification cycles. The PCR product was then visualised by electrophoresis on an agarose gel to check for amplification of a product of the correct size.

2.3.6 Ligation of DNA fragments

DNA ligation was performed using T4 DNA Ligase (New England Biolabs). Fragments to be ligated were incubated at ratios varying between 1:1 – 1:3 of vector to insert DNA, in order to optimise ligation, whilst ensuring that the insert DNA was in excess. The total amount of DNA in the reaction did not exceed 1 μ M. DNA was added to a 1.5ml microfuge tube containing 1 μ l of 10x T4 DNA ligase reaction buffer (New England Biolabs), 0.5 μ l (200 U) of T4 DNA Ligase (New England Biolabs) and sterile water to produce a total reaction volume of 10 μ l. The contents of the tube were then mixed gently and incubated overnight at 4°C. 2 μ l of the ligation mix was then transformed into bacterial cells (section 2.3.9).

2.3.7 Integration of DNA fragments into the pTrcHis-TOPO® vector

The pTrcHis-TOPO®TA Expression Kit (Invitrogen) uses the single deoxyadenosine (A) overhangs generated on the 3' ends of DNA fragments amplified by PCR to enable direct recombination of fragments into the pTrcHis-TOPO® vector.

Cloning of fragments into this vector enabled a 6x His tag to be fused onto the encoded protein of interest. Expression of recombinant proteins in this vector is regulated by the Trc promoter. 1 μ l of a fresh PCR amplified fragment was mixed with 3 μ l of sterile water and 1 μ l of pTrcHis-TOPO[®] vector in a 0.5ml microfuge tube. The contents were mixed gently and left to incubate for 5 minutes at room temperature. 2 μ l of the reaction was then transformed into calcium competent DH5 α cells.

2.3.8 Preparation of calcium competent DH5 α cells

A 0.5 ml overnight culture of DH5 α cells was used to inoculate a further 100 ml of 2x YT liquid media which was grown for approximately 2 hours until the optical density was between OD₆₀₀=0.5-0.6. The culture was then divided into two 50 ml Falcon tubes and placed on ice for 10 minutes. Cells were then harvested by centrifugation at 1000g for 5 minutes at 4°C. The cell pellets were then resuspended in 50 ml of ice cold 100 mM CaCl₂ and the tubes placed on ice for 30 minutes. Cells were again centrifuged at 1000g for 5 minutes at 4°C and the cell pellet resuspended in 5 ml CaCl₂ containing 15% glycerol. From this suspension, 100 μ l aliquots were snap frozen in liquid nitrogen and stored at -80°C.

2.3.9 Transformation of calcium competent DH5 α cells

A 100 μ l aliquot of calcium competent cells for each transformation to be performed, was removed from the -80°C freezer and allowed to thaw on ice for 5 minutes. To this cell suspension, 1 μ l of transforming DNA was added, the cells gently mixed and the tubes incubated on ice for 10 minutes. A pre-heated water-bath was then used to heat shock the cells at 42°C for 35 seconds and the tubes placed back onto ice for 2 minutes. 200 μ l of 2x YT was then added to tubes and the culture incubated with shaking at 37°C for 1 hour. Cells were then spread onto plates containing bacterial media and a selective antibiotic at a working concentration, and incubated overnight at 37°C.

2.3.10 Plasmid DNA purification using the QIAprep Spin Miniprep KitTM

Plasmid DNA was purified using the QIAprep Spin Miniprep KitTM (Qiagen). 1.5 ml of cells from a 2 ml overnight bacterial culture was harvested by centrifugation for 2 minutes at top speed in bench top microfuge. The cell pellet was then resuspended in 250 μ l of Buffer P1, following which 250 μ l of Buffer P2 was also added to the tube.

Samples were mixed by inversion 6 times and incubated at room temperature for 5 minutes. 350 μ l of Buffer N3 was then added and the tubes again inverted 6 times. Samples were then centrifuged at top speed in a bench top microfuge for 10 minutes after which a white precipitate was visible. The supernatants were then transferred into a QIAprep Spin Column™ held in a 2 ml collection tube and the tubes spun at top speed for 1 minute. After discarding the flow through, spin columns were washed with 750 μ l of Buffer PE and centrifuged at top speed in a bench top microfuge for 1 minute. The flow through was again discarded and tubes centrifuged for an additional 1 minute to remove residual wash buffer. The QIAprep Columns™ were then placed in a fresh 1.5 ml microfuge tube and DNA eluted from the columns by adding 35 μ l of sterile water to the membrane, incubating at room temperature for 1 minute and centrifuging at top speed for 1 minute.

2.4

Yeast Methods

Yeast media

YPAD	1% yeast extract (Merck) 2% Bacto-peptone (Merck) 40 µg/ml adenine (Sigma) 2% glucose (Merck) For solid media supplement with 2% agar (Oxoid Ltd)
Synthetic drop-out	0.67% nitrogen base without amino acids (Sigma) 0.2% drop-out mix (lacking variable amino acids) (Qbiogene Inc) 2% glucose (Merck) For solid media supplement with 2% agar (Oxoid Ltd)
Sporulation	1% potassium acetate 2% agar (Oxoid Ltd)
5-FOA	0.67% nitrogen base (Difco Laboratories) 0.2% drop-out uracil mix (Difco Laboratories) 2% glucose (Merck) 0.1% 5-FOA (Melford Laboratories) 2% agar (Oxoid Ltd)

2.4.1 Mating yeast strains

Two strains of opposite mating type were grown overnight on YPAD plates. A small amount of cells taken from these plates were patched on top of the other on a fresh YPAD plate and the plate incubated at 30°C for 5 hours. Cells were then transferred onto selective media that would allow only the growth of diploids.

2.4.2 Sporulation and tetrad analysis

Following growth of a diploid strain on YPAD plates overnight at 30°C, cells from this plate were patched onto a plate containing sporulation media and incubated at 30°C for three to five days. During this time cells were exposed daily to microscopic analysis to monitor the development of four spored ascii. Cells were then removed from

the plate, resuspended in 100 μ l filter sterilised 0.1 M potassium phosphate buffer + 0.5 mg/ml 100T zymolyase and incubated for 10 minutes at room temperature. Digested spores were then struck onto YPAD plates and the four spores separated using a micromanipulator (Singer) which allowed the precise positioning of the spores using a grid system to enable simple placing of each set of four. At least 10 tetrads from each diploid were separated due to genetic variability. The plates were then incubated at 30°C to allow growth of the spores. The number of viable spores was noted and spores were then patched onto YPAD and selective media to test for the presence of genetic markers.

2.4.3 Yeast transformations

A 10 ml culture of cells were grown to mid log phase OD₆₀₀ = 0.5 for each transformation to be performed. Cells were harvested in 15 ml falcon tubes at 3000 rpm for 2 minutes, washed once in 5ml of 0.1 M TE (10 mM TRIS-HCl pH7.5, 1 mM EDTA) and once in 5 ml of 0.1 M Lithium acetate/TE. Cells were then resuspended in 100 μ l 0.1 M Lithium acetate/TE and transferred to a 1.5 ml microfuge tube. 15 μ l of 10 mg/ml of herring sperm DNA previously boiled for 15 minutes, was added to the tube in addition to 0.1-1 μ g of transforming DNA. Cells were then gently swirled and 700 μ l 40 % PEG-4000 (Polyethylene Glycol - Merck) in 0.1 M lithium acetate/TE added, followed by gentle mixing of the cells by pipetting. Cells were incubated at room temperature for at least one hour on a vertical rotator, followed by incubation at 42°C for 15 minutes in a water-bath. Following harvesting by centrifugation at 5000 rpm for 2 minutes, cells were resuspended in 100 μ l of sterile water and plated onto selective media.

2.4.4 'Knock in' strategy of generating integrated gene deletions or tagged strains

Plasmids previously generated (Longtine *et al*, 1998) were used to allow the tagging or deletion of specific genes within the yeast genome by the use of a simple strategy. PCR (section 2.3.5) was used to amplify specific tags or deletion cassettes from these plasmids using oligonucleotides designed with homology to the regions flanking a specific site in the yeast genome, and homology to the tagging/deletion cassette. PCR products generated were then transformed into yeast cells and were thus incorporated into a specific site in the yeast genome by homologous recombination. The

transformed cells were then plated onto selective media which enabled only the growth of cells which contain the transformed DNA. Integration of the deletion/tagging DNA at the correct site was confirmed by colony PCR as described in Section 2.4.7.

2.4.5 Screening for integrated tags or gene deletions by colony PCR

Following growth of yeast transformants for approximately three days at 30°C on selective media, colonies were struck out onto YPAD plates and incubated overnight at 30°C. Several single colonies were selected using a toothpick, and were resuspended in 20 µl of SPZ Buffer (1.2 M sorbitol, 0.1 M Potassium Phosphate buffer pH7.5 and 2.5 mg/ml zymolyase) in a 0.2 ml thin walled PCR tube. Cell suspensions were then incubated at 37°C for 30 minutes in a PCR machine followed by incubation at 95°C for 5 minutes. This cell preparation formed the DNA template used for standard PCR reactions (section 2.3.5), using oligonucleotides homologous to regions flanking the inserted DNA. PCR reactions either produced a DNA fragment of the size of the wild type region of genomic DNA, or a fragment corresponding to the size of the integrated tag or inserted DNA. PCR products were visualised by agarose gel electrophoresis (section 2.3.2).

2.4.6 Testing for temperature sensitivity

Cells to be tested for temperature sensitivity were struck onto YPAD plates and incubated at both 30°C and 37°C for 1-2 days to assess if growth was affected at the higher temperature.

2.4.7 Overexpression of hSh3yl-1 in a Δ ysc84 Δ lsb5 strain

KAY516 cells were transformed with plasmid pKA392 which encoded hSH3yl-1, expression of which was under the control of a methionine inducible promoter. The same strain was also transformed with empty yeast expression vector, pKA256. Cells from both transformations were grown overnight in 2 ml of YPAD at 30°C and 0.2 ml of the cultures used to inoculate 2 ml of YPAD which was then grown for 4 hours at 30°C. Cells were harvested by centrifugation at 3000 rpm for 5 minutes, and the cell pellet resuspended in liquid synthetic media lacking methionine. For overexpression studies on plates, cells from both transformations were also struck onto YPAD plates and grown overnight at 30°C. A small amount of these cells was then struck onto

synthetic media lacking methionine and the cells examined for phenotypic defects following 4 hours of growth at 30°C.

2.4.8 Induction of the mating response

A haploid MAT_a strain expressing Slal-myc (KAY303) was incubated with a strain of the opposite mating type to induce the mating response (KAY389). Strains were initially grown individually on YPAD plates at 29°C overnight. A small amount of each strain was then patched on top of the other on a fresh YPAD plate. The plate was then placed in the 29°C incubator for 2 hours. Cells were then removed from the plate and resuspended in 1 ml of liquid YPAD media. This culture was then processed for immunofluorescence as described in section 2.7.1. Cells which formed mating projections were identified by microscopy, by identification of the characteristic, elongated 'shmoo' phenotype.

2.4.9 Glycerol stocks

Stocks of specific yeast strains were generated by the addition of 25% sterile glycerol to log phase cultures. Stocks were then frozen at -80°C in plastic cryovials.

2.5 Yeast 2-hybrid analysis

2.5.1 Yeast 2-hybrid cloning and transformation

A plasmid containing the *GTS1* coding sequence fused N-terminally to a sequence encoding the Gal4-binding domain (pKA388) was transformed into the 2-hybrid MAT_a strain pJ69-4a. Positive transformants were selected by growth of the transformed cells on drop-out tryptophan plates. 2-hybrid strains of the opposite mating type, pJ69-4 α , transformed with plasmids encoding protein and protein fragments of interest fused N-terminally to Gal4-activation domains, were either obtained commercially or the plasmids transformed individually into the pJ69-4 α strain. Positive transformants were selected by growth of the transformed cells on drop-out leucine plates

2.5.2 Yeast 2-hybrid analysis

Mating of the 2-hybrid pJ69-4a strain containing the *GTS1*-N-terminal Gal4-binding domain encoding plasmid, with cells from the opposite mating type strain pJ69-

4α which contained plasmids encoding proteins of interest fused N-terminally to Gal4-activation domains, was performed. Diploids were selected by growth of the resulting cells on drop-out leucine and tryptophan plates. These strains were then tested for activation of the Gal4 protein by plating onto drop-out histidine, leucine and tryptophan synthetic drop-out media.

2.5.3 β -galactosidase assay

5 ml of cells were grown overnight at 30°C in synthetic media to ensure the retention of both 2-hybrid plasmids in the diploid strain. The optical density of this culture was noted (OD_{600}) and 2 ml of cells harvested by centrifugation. Cells were then resuspended in 0.5 ml of Z Buffer (60mM Na₂HPO₄, 40mM NaH₂PO₄, 10mM KCl, 1mM MgSO₄, 50mM β -Mercaptoethanol, pH7) to which 3 drops of chloroform and 2 drops of 1% SDS was added. The suspension was vortexed for 10 seconds, incubated at 28°C for 5 minutes, and 0.2 ml of ONPG added (Melford)(4mg/ml in Z Buffer) to start the reaction. The reaction was stopped by addition of 0.5ml 1M Na₂CO₃ after the solution showed a colour change to pale yellow. The time from the start of the reaction until addition of Na₂CO₃ was recorded. Samples were then centrifuged for 10 minutes at 5000 rpm and the OD_{420} of the supernatant recorded. Assay results were calculated in β -galactosidase units and plotted, using the equation shown below. Assays were performed in triplicate.

$$\beta\text{-galactosidase units} = \frac{OD_{420}}{\text{Time}}$$

2.6 Protein Methods

2.6.1 Whole cell yeast extracts

Cells were grown in liquid YPAD media (section 2.4.1) overnight in a shaking incubator at 29°C. 1.5 mls of this culture was harvested by centrifugation in a bench top microfuge at 5000 rpm for two minutes and the supernatant discarded. 100 µls of acid washed glass beads were then added to the cell pellet in addition to 50 µls of 2 x SDS sample buffer (62.5 mM Tris-HCl (pH 6.8), 20 % glycerol, 2 % SDS, 0.0025 % bromophenol blue). Cell suspensions were boiled for three minutes and vortexed for one minute. An additional 100 µls of 2 x SDS sample buffer (20% glycerol, 100 mM TRIS pH 6.8, 4% SDS, 0.2 % Bromophenol Blue, 2 % β -mercaptoethanol) was then added and the sample vortexed again briefly. Before loading the protein containing supernatants onto SDS-page gels, samples were boiled for an additional five minutes.

2.6.2 Preparation of protein preps by grinding in liquid nitrogen

100 ml of cells were cultured until the optical density was approximately OD₆₀₀ = 0.5. Cells were harvested by centrifugation at 3500 rpm for 5 minutes at 4°C and the pellet resuspended in 2 ml of UBT buffer (50 mM KHEPES, pH 7.5, 100 mM KCl, 3 mM MgCl₂, 1 mM EGTA, 0.5% Triton X-100) to which protease inhibitors (0.5 mg/ml leupeptin, aprotinin, chymostatin, pepstatin A) and 1 mM of PMSF (phenylmethylsulfonyl fluoride) had been added. The cells were then slowly dripped into a 50 ml falcon tube previously pre-frozen in, and containing, approximately 20 ml of liquid nitrogen. Excess liquid nitrogen was then poured from the falcon tube and the frozen cells transferred to a pestle and mortar for grinding. To ensure the cells were kept frozen throughout grinding a small amount of liquid nitrogen was repeatedly poured onto the cells. The cells were ground to a fine powder which was then either transferred to microfuge tubes and stored in the -80°C freezer for use later, or transferred to a fresh 50ml falcon tube and the powder allowed to thaw at 4°C. Once thawed, the solution was centrifuged at 45,000rpm for 20 minutes at 4°C and the supernatant retained for use.

2.6.3 SDS-PAGE electrophoresis

The appropriate percentage of acrylamide gel was poured according to the recipes below.

Separating gel:			
	7.5 %	10 %	12 %
Sterile water	4.10 ml	3.44 ml	2.69 ml
30 % acrylamide (BioRad), 0.8 % bisacrylamide (37.5:1) (BioRad)	2.25 ml	3.00 ml	3.75 ml
Resolving Buffer (1.5 M Tris-HCl (pH 8.8), 0.4 % SDS)	2.25 ml	2.25 ml	2.25 ml
10 % ammonium persulfate	31 µl	31 µl	31 µl
TEMED (N,N,N',N' – tetramethylethylene-diamine)	5 µl	5 µl	5 µl
5 % Stacking gel:			
Sterile water		1.71 ml	
30 % acrylamide (BioRad), 0.8 % bisacrylamide (37.5:1) (BioRad)		0.50 ml	
Stacking buffer (0.5 M Tris-HCl (pH 6.8), 0.4 % SDS)		0.75 ml	
10 % ammonium persulfate		35 µl	
TEMED (N,N,N',N' – tetramethylethylene-diamine)		3.5 µl	

Following loading of protein samples held in 1x sample buffer (10% glycerol, 50 mM TRIS pH 6.8, 2% SDS, 0.1 % Bromophenol Blue, 1 % β -mercaptoethanol), gels were run in 1 x Running buffer (0.025 M Tris, 0.192 M Glycine, 0.1 % SDS, pH 8.6) at 90 Volts for 30 minutes, and then 120 Volts for approximately 1 hour, until the dye front had run off the bottom of the gel.

Pre-cast NuPAGE® gradient gels (Invitrogen) were also used. These were obtained as 4-12% NuPAGE® Bis-Tris gradient gels and 3-8% NuPAGE® Novex Tris-Acetate gels. Gels were run in 1x NuPAGE® MOPS buffer SDS Running Buffer (Invitrogen) and 1x NuPAGE® Tris-Acetate SDS Running Buffer (Invitrogen) at 200 Volts for 50 minutes, and 150 Volts for 1 hour respectively.

2.6.4 Western blotting

Semi-dry blotting was performed as described. Proteins were separated by SDS-PAGE gel electrophoresis, the gel removed from the apparatus and immersed in 1x NuPAGE[®] transfer buffer (Invitrogen) containing 10% methanol. PVDF (Polyvinylidene Difluoride) membrane (Schleicher and Schuell) and 4 layers of 3 mm filter paper were cut to the approximate size of the gel to be transferred and the membrane immersed directly in methanol. The filter paper was then soaked in 1x NuPAGE[®] transfer buffer (Invitrogen) containing 10% methanol. The blot sandwich was quickly assembled with the exclusion of air bubbles between the gel and PVDF which would prevent transfer. The sandwich was then placed into the semi-dry blotter (Biorad) and a limiting voltage of 25 Volts applied for 50 minutes. The membrane was removed and immersed in TBS-T (10 mM Tris-HCl pH8, 150 mM NaCl, 0.2% Tween-20).

Wet blotting was performed as described. Proteins were separated by SDS-PAGE gel electrophoresis, the gel removed from the apparatus and immersed in 1x CAPS buffer (10 mM CAPS pH11, 10% methanol). PVDF (Polyvinylidene Difluoride) membrane was cut to the approximate size of the gel to be transferred and the membrane immersed directly in methanol. Four foam pads were then soaked in 1x CAPS buffer. The blot sandwich was quickly assembled with the exclusion of air bubbles between the gel and PVDF which would prevent transfer. The sandwich was then placed into a wet blotting tank (BioRad), the tank filled 1x CAPS buffer and a limiting voltage of 400 mAmps applied for 60 minutes. The membrane was then removed and immersed in TBS-T (10 mM Tris-HCl pH8, 150 mM NaCl, 0.2% Tween-20).

2.6.5 Western blot detection using Enhanced Chemi-Luminescence (ECL)

Proteins were blotted as described (section 2.6.4) and the PVDF membrane immersed in 1x TBS-T (10 mM Tris-HCl pH8, 150 mM NaCl, 0.2% Tween-20) containing 5% milk for 1 hour on a rocker. The membrane was removed from this blocking solution, immersed in 1 x TBS-T for 5 minutes on a rocker and sealed in polythene, to ensure contact with 5 mls of 1x TBS-T containing 1% milk and the primary antibody (usually at 1000x dilution). The membrane was then left to incubate in this solution overnight at 4°C on a rotor, enabling slow rotation. The blot was then removed and washed three times in 50 ml of 1 x TBS-T for 15 minutes at room

temperature on a rocker. The membrane was then placed sealed in polythene for a second time with 5 ml 1x TBS-T containing 1% milk and a horseradish peroxidase (HRP) conjugated secondary antibody (usually 5000 x dilution) for one hour at room temperature with on a rotor. The membrane was then removed and washed as described previously. ECL solution I (250 mM luminol (3-aminophthalhydrazide (Fluka) in DMSO, 90 mM p-coumaric acid (Sigma) in DMSO, 0.1 M Tris-HCl pH 8.5) and solution II (0.18% hydrogen peroxide, 0.1 M Tris-HCl pH 8.5) were prepared. Equal volumes of these solutions were mixed and the blot immersed in the resulting solution for one minute. The membrane was then briefly rinsed in TBS-T, placed inside two thin layers of plastic in a cassette and exposed to X-ray film (Konica) which was developed in an automatic developer.

2.6.6 2-Dimensional gel electrophoresis using the ZOOM® IPG Runner System

1 ml of cells was obtained from a culture grown until the optical density of the culture was approximately OD₆₀₀ = 0.5. Cells were harvested by centrifugation at full speed for 2 minutes in a benchtop microfuge. The cell pellet was then washed twice in 200 µl of Rehydration Buffer (8 M Urea, 2% CHAPS, 0.5% (125 µl) ZOOM® Carrier Ampholytes of the appropriate pH (Invitrogen) and 0.002% Bromophenol Blue). 100 µl of glass beads was then added to the pellet, in addition to 50µl of Rehydration Buffer, and the cells vortexed for 60 seconds. A further 100 µl of Rehydration Buffer was added and the sample centrifuged at 10000 rpm for 2 minutes to clarify the extract. 8 µl of this lysate was then added to 155 µl of Rehydration Buffer, a ZOOM® strip of the appropriate pH gradient placed in a ZOOM® Cassette and the solution added to the cassette to allow strip hydration overnight in accordance with the manufacturer's protocol.

After rehydration overnight, the ZOOM® strip was then removed from the cassette and prepared for Isoelectric Focusing (IEF). The first dimension was run under the following conditions: STEP1, 175 V for 15 minutes; STEP2, 175-2000 V ramping for 45 minutes; STEP3, 2000 V for 1 hour. Before running the second phase, the ZOOM® strip was first equilibrated by soaking in 5 ml Reducing Solution (500 µl NuPAGE® Sample Reducing Agent (Invitrogen), 4.5 ml NuPAGE® LDS Sample Buffer (Invitrogen) for 15 minutes, followed by 5 ml Alkylation Solution (116 mg iodoacetamide in 5 ml 1x NuPAGE® LDS Sample Buffer (Invitrogen)) for 15 minutes. The ZOOM® strip was then placed on top of a 4-20% NuPAGE® Novex Bis-Tris SDS

gradient gel and encased in 0.6% agarose in 1xMOPS buffer (Invitrogen). The gel was then placed in a XCell SureLock™ Mini-Cell tank and electrophoreses at 200 V for 1 hour. Western blotting was then performed (section 2.6.4).

2.6.7 Induction of a tagged protein in bacterial cells

Transformation of an appropriate plasmid into bacterial cells was performed as described (section 2.3.9). Cells were then grown overnight at 37°C in 5 ml of YT containing ampicillin at 100 µg/ml to enable the selection of plasmid containing cells. This culture was then used to inoculate 20 ml of YT containing ampicillin which was grown for 1 hour at 37°C. This culture was used to inoculate 1 litre of YT containing ampicillin which was grown for approximately 4 hours at 37°C until the OD₆₀₀ was between 0.5-0.6. Expression of the tagged protein was induced by the addition of 1 mM IPTG (Isopropyl-β-D-thiogalactopyranoside) and the cultures grown at 37°C for 2 hours. Cultures were then pelleted by centrifugation at 4000 rpm for 30 minutes at 4°C, the supernatants discarded and the pellets frozen at -20°C until required.

2.6.8 Purification of GST tagged proteins using Glutathione Sepharose® 4B Beads

Bacterial cultures were induced as described in section 2.6.7. Fusion proteins containing a glutathione S-transferase (GST) tag were purified using glutathione sepharose® 4B Beads (Amersham Pharmacia). Cell pellets from induced cultures were thawed on ice, washed once in 20 ml of PBS (20 mM phosphate, 50 mM NaCl, pH7.5) and the pellet resuspended in 4 ml of PBS containing 20 µg of lysozyme, Protease Inhibitors (0.5 mg/ml leupeptin, aprotinin, chymostatin, pepstatin A) and 1 mM PMSF (phenylmethylsulfonyl fluoride). This cell suspension was then sonicated for 5 seconds to lyse the cells and the lysate incubated at room temperature for 30 minutes on a horizontal rotor. Following addition of 1 µM MnCl₂, 10 µM MgCl₂ and 4µl of 10mg/ml DNase I (Boeringer Mannheim) and a further 10 minute incubation, the lysate was centrifuged at 45000 rpm for 20 minutes at 4°C. The supernatant from this spin was added to 0.5ml of pre-washed glutathione sepharose® 4B Beads and incubated on a rotor for one hour at 4°C. Beads were then washed three times with for 15 minutes with PBS + 1% Triton-X-100, transferred to a column, allowed to drain and the column capped. The fusion protein was eluted from this column by addition of 1 ml glutathione elution buffer (10 mM reduced glutathione, 50 mM Tris-HCl pH 8) to the column. The

elution buffer was allowed incubate with the beads for 10 minutes at room temperature, before removal of the cap and collection of the elutant. This elution step was repeated five times and each fraction analysed by SDS-Page gel electrophoresis.

2.6.9 F-actin sedimentation assays

Purified fusion proteins were tested for binding to actin by high speed sedimentation assays. F-actin was prepared from a known concentration of purified rabbit muscle G-actin (Cytoskeleton Inc.) in G-buffer (5 mM TRIS pH7.5, 0.2 mM ATP, 0.2 mM DTT, 0.2 mM CaCl₂) by resuspension in 1 x KME (50mM KCl, 1mM MgSO₄, 1mM EGTA, 10mM TRIS-HC, pH 7.5) overnight at 4°C. The solution became viscous overnight due to the formation of actin filaments. The concentration of the protein of interest was then accurately determined by spectrophotometry, and increasing amounts tested for F-actin binding ability. Assays were carried out using TL100 centrifuge tubes (Beckman). To each tube 5 µl of 10 x ABB (200 mM TRIS-HCl pH8, 1 M NaCl, 20 mM MgCl₂, 10 mM ATP, 10 mM DTT, 1 mM CaCl₂) was first added. Known concentrations of the protein of interest held in 35 µl of glutathionine elution buffer (GEB; 10mM Reduced Glutathionine, 50mM Tris-HCL pH 8) were then added to tubes in duplicate. Finally 10µl of F-actin was added to every second tube while the remaining tubes received the same volume of 1 x KME. In addition control reactions containing either actin alone or protein alone, in addition to buffers, were also prepared. Tubes were then left to incubate at room temperature for 15 minutes after which all tubes were centrifuged at 100,000 rpm for 20 minutes at 4°C in an Optima TL Benchtop Ultracentrifuge (Beckman) to pellet F-actin. Following centrifugation, the supernatant from each tube was removed and added to 50µl of 2x SDS Sample Buffer (20% glycerol, 100 mM TRIS pH 6.8, 4% SDS, 0.2 % Bromophenol Blue, 2 % β-mercaptoethanol). In addition, 50 µl of 2x Sample Buffer was added to each tube and left to incubate with, and soften, the very viscous pellet for 15 minutes at room temperature. The pellets were then resuspended in this solution and transferred to fresh microfuge tubes containing an additional 50 µl of 1:9 10x ABB: 1x GEB. 10µl aliquots from supernatant and pellet fractions from each tube was then analysed by SDS page gel electrophoresis. Standard assay conditions are also described by Winder and Walsh, 1990.

2.6.10 Falling ball assays

The effect of a specific ligand on the polymerisation of an actin gel was assessed by analysis of the time taken for a metal ball to pass through 10 cm of actin, polymerised in the presence and absence of the ligand. Monomeric actin was resuspended in G-Buffer (5 mM TRIS pH7.5, 0.2 mM ATP, 0.2 mM DTT, 0.2 mM CaCl₂) at a concentration of 7.5 μM. 80 μl aliquots of actin were then added to 10μl of known concentration of ligand held in glutathione elution buffer (GEB; 10mM Reduced Glutathionine, 50mM Tris-HCL pH 8). To this 10 μl of 10x Polymerisation Salts (10x; 20 mM MgCl₂, 5 mM ATP, 1 M KCl) was added and the 100 μl reactions vortexed to allow mixing of the solutions. Reactions were used to fill a 10 cm length of glass capillary tube, capped at the base using a small plasticine bung. Tubes were then left overnight to allow polymerisation of the actin matrix. The time taken for passage of a metal ball bearing through 10 cm of the actin was then recorded.

2.6.11 Fluorescent actin assays

Alexa Fluor labelled actin monomers were incorporated into polymerising actin filaments allowing visualising of actin filaments using fluorescence microscopy. Alexa Fluor®⁴⁸⁸ and Alexa Fluor®⁵⁶⁸ labelled actin monomers (Molecular Probes) were used to allow visualisation of filaments at two wavelengths. Rabbit skeletal muscle G-actin (Cytoskeleton Inc.) was resuspended in general actin binding buffer (5 mM Tris-HCl pH8, 0.2 mM CaCl₂, 0.002% Chlorohexidine (Cytoskeleton Inc.)) at 7.2 μM. 10 μg of Alexa Fluor® 488 labelled actin monomers was added to 25 μl of unlabelled G-actin and 2.5 μl of 10 x polymerisation salts (100 mM Tris-HCl pH 7.5, 500 mM KCl, 20 mM MgCl₂, 10 mM ATP) added to the solution. Incubation of the reaction for 1 hr at room temperature enabled polymerisation of labelled actin filaments. Prior to this incubation the actin stabilising drug phalloidin (Cytoskeleton Inc.) was added as detailed in sections 4.2.7 and 4.2.8, at equimolar concentrations to actin. Known concentrations of the proteins of interest were then added to the polymerised, labelled actin and the effect on polymerisation examined by fluorescence microscopy after a 30 minute incubation at room temperature. If dual labelling experiments were to be performed, following this 30 minute incubation time with the protein of interest, a further 10 μg of Alexa Fluor®⁵⁶⁸ labelled actin monomers were added to the reaction and allowed to incubate for a further 1 hour at room temperature before visualisation of dual labelled filaments.

2.6.12 Coomassie staining of SDS-polyacrylamide gels

Proteins separated by SDS-PAGE gel electrophoresis were visualised by staining of protein with Coomassie Brilliant Blue. Gels were fixed and stained in a solution of 40% methanol, 10% acetic acid and 50% water which contains 0.1 % (w/v) Coomassie Brilliant Blue R250 for 5 minutes at room temperature. Gels were then transferred to a de-staining solution (40% methanol, 10% acetic acid and 50% water) for 30 minutes. This de-staining solution was then refreshed and de-staining allowed to proceed until the background of the gel was clear of stain.

2.6.13 Determination of protein concentration by spectrometry

The concentration of purified proteins in solution was calculated using Beer's Law, following determination of the absorbance of the protein sample at 280 nm by spectrophotometry. Concentrations were calculated using the equation:

$$A = \epsilon c l$$

where 'c' is the concentration of protein in the sample in moles/liter, 'A' is the Absorbance of the sample at 280 nm, 'ε' is the extinction coefficient for the protein of interest as determined by analysis of protein residues in the protein of interest, and 'l' is length of the light path in centimetres. The extinction coefficient of a protein at 280 nm was estimated by identification of the number of tyrosine, tryptophan and cysteine residues present in the protein, and multiplication of these numbers by 1280, 5690 and 120 respectively.

2.7 Microscopy methods

2.7.1 Equipment details

Microscopy was performed using an Olympus microscope BX-60 fluorescence microscope with a 100 W mercury lamp and an Olympus 100' Plan-NeoFluar oil-immersion objective. Images were captured using a Roper Scientific Micromax 1401E cooled CCD camera using IP lab software (Scanalytics, Fairfax, VA) on an Apple Macintosh G4 computer.

2.7.2 Indirect immunofluorescence

5 ml of cells were grown to mid-log phase ($OD_{600} = 0.5$), formaldehyde added to a final volume of 5 % and the cultures incubated at room temperature for at least 1 hour. Cells were then harvested by centrifugation at 2500 rpm for 3 minutes in a 15 ml falcon tube and washed twice in 2 mls of sorbitol buffer (1.2 M sorbitol, 0.1 M potassium phosphate buffer, pH 7.5). After resuspending the cell pellet in 0.5 ml of sorbitol buffer and transferring the sample to a 1.5 ml microfuge tube, 1 μ l of β -mercaptoethanol and 20 μ l 1 mg/ml 100T zymolyase was then added. Tubes were incubated at 37°C for 30 minutes and 20 μ l of the resulting cell suspension placed onto a poly-L-lysine coated slide well. The suspension was left on the slide for 10 minutes at room temperature to allow the cells to settle, after which the excess solution was gently aspirated from the well and the slide immersed for 6 minutes in -20°C methanol. The slide was then transferred to -20°C acetone for 30 seconds and left to air-dry. Wells were washed 10 times with 1x PBS/1 mg/ml BSA (Bovine Serum Albumin) and 20 μ l of 1x PBS/1 mg/ml BSA containing the primary antibody at a 1:100 dilution added to the well and allowed to incubate overnight at 4°C. The well was then again washed 10 times with 1x PBS/1 mg/ml BSA and 20 μ l of 1x PBS/1 mg/ml BSA containing the secondary antibody at a 1:100 dilution added. This was allowed to incubate with the fixed cells for a further hour in the dark at 4°C. Following incubation the well was again washed 10 times with 1x PBS/1 mg/ml BSA and drop of mounting solution (90 ml glycerol, 10 ml 1x PBS, 100 mg DAPI) containing DAPI (4',6'-diamidino-2-phenylindole hydrochloride) was placed onto each well. A cover slip was placed over the wells, and the edges sealed with nail polish and the slides examined by fluorescence microscopy.

2.7.3 Rhodamine phalloidin staining

2 ml of cells were grown to an $OD_{600}=0.2\text{-}0.4$, formaldehyde added to a 5 % final volume and the culture left to incubate for one hour at room temperature. 1 ml of this culture was then harvested at 5000 rpm in a microfuge, the supernatant discarded and the cell pellet washed three times in 1x PBS/1 mg/ml BSA/0.1 % Triton-X-100. After resuspending the pellet in 40 μl of 1x PBS/1 mg/ml BSA/1 % Triton-X-100, 5 μl (1U) of rhodamine phalloidin (Molecular Probes) was added and the cells incubated at room temperature for 30 minutes in the dark. Following incubation, the cells were washed three times with 0.1 M PBS/1 mg/ml BSA and resuspended in 100 μl of the solution. 20 μl of cell suspension was then placed in a poly-L-lysine coated slide well and allowed to settle for 10 minutes. The well was then washed twice with 0.1 M PBS/1 mg/ml BSA, a drop of mounting solution placed into the well and covered with a coverslip. The edges of the coverslip were then sealed with nailpolish and the slide was viewed by fluorescence microscopy.

2.7.4 Lucifer Yellow uptake assay

2 ml of cells were grown to an optical density of approximately $OD_{600} = 0.25$. 0.5 ml of these cells were harvested by centrifugation at 5000 rpm for 3 minutes and resuspended in 40 μl YPAD liquid. 5 μl of 40 mg/ml lucifer yellow (Fluka) was then added and the suspension left to incubate at room temperature for one hour in the dark. 1 ml of ice-cold succinate/azide buffer (50 mM succinic acid, 20 mM NaN_3 , pH adjusted to 5 with NaOH) was then added to the suspension, the tube inverted to mix the contents and a cell pellet obtained by centrifugation at 5000 rpm for 3 minutes. After discarding the supernatant, this succinate/azide buffer wash was repeated twice. Cells then resuspended in 10 μl of buffer and 2 μl of the suspension placed on a slide for immediate observation. This method is adapted from a method described by Dulic and colleagues (Dulic *et al* 1991). For quantitative analysis of lucifer yellow uptake, 200 cells from each strain were examined.

2.7.5 FM4-64 assay

2 ml of cells were grown to an optical density of approximately $OD_{600} = 0.1$. 1 ml of these cells was harvested by centrifugation at 5000 rpm for 3 minutes and resuspended in 0.5 ml YPAD liquid. 20 μM FM4-64 (Molecular Probes) was added to the suspension and the cells incubated with shaking for 15 minutes at 29°C. Following

this incubation, cells were again harvested by centrifugation at 5000 rpm for 3 minutes and resuspended in 0.5 ml of fresh YPD media. Cells were then incubated with shaking at 29°C for 30 minutes, following by harvesting by centrifugation, resuspension in 40 µl YPAD, and 5 µl of this suspension placed onto a slide for viewing. This method is adapted from a method described by Vida and Emr (Vida and Emr, 1995). For quantitative analysis of FM4-64 internalisation, 200 cells from each strain were examined.

2.7.6 Latrunculin-A treatment of cells

The strain to be examined was first grown in liquid culture in 2 ml of YPAD media at 29°C until in log phase growth. To this culture Latrunculin-A (a generous gift from Phil Crews, University of California, CA) was added at a concentration of 400 µM and the culture incubated with shaking for a further 15 minutes at 29°C. 1 ml of this culture was then fixed and processed for visualisation of actin structures by rhodamine phalloidin staining to confirm disruption of the actin cytoskeleton (section 2.7.3), while 1 ml of the culture was used for the localisation of GFP-tagged proteins by direct microscopic observation of GFP fluorescence.

2.8 Antibody Production

2.8.1 Raising an immune response in rabbits

The GST-Ysc84-Nt fusion protein was purified over a Glutathione Sepharose column as previously described in section 2.6.8. This purified protein was then used to generate polyclonal rabbit antisera. Four injections of approximately 50 µg of protein were administered to two rabbits (R1414 and R1415) at 28 day intervals (Diagnostics Scotland). An initial pre-immune serum was obtained from these animals as were subsequent primary and secondary serums taken 7 days after each injection. A final exsanguination bleed was performed 13 weeks after the first injection and the serum obtained.

2.8.2 Purification of serum over a Protein A column

Protein A sepharose™ CL-4B beads (Amersham Pharmacia) were prepared by allowing 0.75 g of Protein A sepharose™ CL-4B bead powder to incubate with 30 ml of distilled water for 30 minutes at room temperature. The swollen beads were then

centrifuged at 1000 rpm for 2 minutes, the supernatant discarded and the beads washed in 30 ml of 50 mM Tris-HCl pH 7.0 and centrifuged as before. 0.3 ml of 1 M Tris-HCl pH 7.0 was then added to 3 mls of serum from the final bleed of rabbit R1415. This serum was then added to the Protein A sepharoseTM CL-4B beads in a 15ml Falcon tube and left to incubate for 1 hour at room temperature on a rotor. The beads were pelleted by centrifugation at 1000 rpm for 5 minutes and the supernatant removed and retained. Beads were then transferred to a 50 ml Falcon tube, 30 ml of 50 mM Tris-HCl pH 7.0 added and the beads left to wash in this solution for 20 minutes on a rotor. This solution of beads and wash buffer was then applied to a column and the wash buffer allowed to drain from the beads. Beads were washed with a further 60ml of 50 mM Tris-HCl pH 7.0 applied directly to the column, before proceeding to the elution of the antibodies. 10 ml of elution buffer (0.1 M glycine pH 2.5) was applied to the column in 1 ml fractions. Each fraction was collected separately in a 1.5 ml microfuge tube containing 100 μ l of 1 M Tris-HCl pH 8.8 to neutralise the solution. The concentration of protein in the sample was then measured by spectrophotometry and 10 μ l samples of each fraction analysed by SDS-page gel electrophoresis. Specificity of these antibodies was determined by testing these aliquots at 1:1000 and 1:2000 dilutions by western blotting against whole cell extracts as described in section 4.2.9. Antibodies were also tested for identification of protein *in vivo*, however the specificity of these antibodies was not high enough to enable this, and a high level of background staining was seen.

2.9 RNA Methods

2.9.1 Yeast RNA extraction using the Promega SV Total RNA Extraction Kit and Qiagen RNeasy Mini Kit

This method for RNA isolation from yeast cells uses reagents from both the SV Total RNA Isolation Kit (Promega) and the RNeasy Mini Kit (Qiagen). 0.25ml of cells from an overnight yeast culture were used to inoculate 4.5 ml of YPD media which was grown for 4 hours until the optical density was approximately OD600 = 0.5. 2 ml of this culture was then harvested by centrifugation at 5000 rpm and the pellet resuspended in 2 ml of buffer Y1 (1 M sorbitol, 0.1 M EDTA pH 7.4 (Qiagen), containing 0.1% β -mercaptoethanol and 250 μ l of 2mg/ml 100T zymolase). Spheroplasts were generated by incubating the cells in this solution for 20 minutes at 30oC in a water-bath. Spheroplasts were pelleted by centrifugation at 1000 rpm for 5 minutes, the supernatant discarded and resuspended in 350 μ l of buffer RLT (Qiagen) containing 1% β -mercaptoethanol.

Spheroplasts were then lysed by vigorous vortexing, 350 μ l of absolute ethanol added to the lysate and gently mixed by pipetting, and the lysate poured into a spin column assembly (Promega). The isolation proceeded from this stage according to the SV Total RNA Isolation Kit (Promega) Protocol. The assembly was centrifuged at top speed for 1 minute, flow-through discarded and the column washed with 600 μ l of SV RNA wash solution (60 mM potassium acetate, 10 mM Tris-HCl pH 7.5 and 60% ethanol (Promega). Following centrifugation and discarding of the wash flow-through, the spin column was left at room temperature while a mixture containing 40 μ l yellow core buffer (0.0225M Tris pH 7.5, 1.125M NaCl (Promega)), 5 μ l 0.09M MnCl₂ and 5 μ l DNase1 was prepared. This solution was then applied directly to the membrane and the column left to incubate at room temperature for 15 minutes. Following this incubation 200 μ l of SV DNase Stop Solution (2 M guanidine isothiocyanate, 4 mM Tris-HCl pH 7.5, 57% ethanol (Promega)) was added to the membrane and the assembly centrifuged for one minute. The column was then washed twice with 600 μ l SV RNA wash solution, and then with 250 μ l of SV RNA wash solution, after which the column was centrifuged for an additional one minute to dry the membrane. RNA was eluted by applying 100 μ l of Nuclease Free Water (Qiagen) to the membrane and centrifuging for one minute into a fresh 1.5 ml microfuge tube. RNA was then immediately placed on dry ice and transferred to the -80°C freezer.

2.9.2 Quantification of RNA using an Agilent Bioanalyzer2100

Quantification of the RNA (section 2.9.1) using an Agilent BioAnalyzer2100 was performed, as it was recommended that 10 μ g of high quality total RNA be used for each GeneChip® Array. Quantification was performed at the Sir Henry Wellcome Functional Genomic Facility (SHWFGF) at Glasgow University according to Agilent BioAnalyzer2100 protocols.

2.9.3 RNA concentration using Pellet Paint® co-precipitant

Suitable RNA preps (section 2.9.1-2.9.2) were concentrated using the Pellet Paint® Co-precipitant Kit (Novagen). 2 μ l of Pellet Paint® was added to each sample, followed by the addition of 0.1x volume of 3 M sodium acetate. 2 volumes of absolute ethanol were then added and the samples vortexed briefly followed by a 2 minute incubation at room temperature. Samples were then spun at top speed in a benchtop microfuge for 5 minutes after which the supernatant was removed and discarded. The

pellet was washed with 70% ethanol, vortexed briefly and spun again at top speed for 5 minutes. The supernatant was removed and this step was repeated using 100% ethanol to wash the pellet. The pellet was then left to air dry and once suitably dry, the pellet was resuspended in a volume of RNase free water to give a concentration of 2 µg per µl of RNA.

2.9.4 DS cDNA Synthesis and cleanup

Double stranded cDNA was synthesised from the RNA preps (section 2.9.3) using the SuperScript™ Double-Stranded cDNA Synthesis Kit (Invitrogen). First strand synthesis was performed by adding 1 µl of T7-(dT)24 primer (100 pmol/µl) to a RNase free microfuge tube, 10 µg of total RNA from the pellet paint precipitation and sterile water to increase the sample volume to 10 µl. The sample was then incubated at 70°C for 10 mins, spun at top speed in a benchtop microfuge for 10 seconds and placed on ice. 4 µl of first strand cDNA buffer, 2 µl 0.1 M DTT and 1 µl 10 mM dNTP was added to the tube and the tube contents mixed by gentle vortexing, again spun for 10 seconds and then incubate at 42°C for 2 mins. 1 µl of Superscript™ II RT enzyme was added, the samples mixed by gentle pipetting and incubated at 42°C for 1 hour, after which the tubes were placed on ice.

Second stranded synthesis was performed by adding to the tube, 91 µl of nuclease free water, 30 µl of 5x second strand reaction buffer (100 mM Tris-HCl pH 6.9, 450 mM KCl, 23 mM MgCl₂, 0.75 mM β-NAD+, 50 mM (NH₄)₂SO₄), 3 µl of 10 mM dNTPs, 10 U *E.coli* DNA ligase, 40 U *E.coli* DNA Polymerase I and 2U RNase H to a final volume of 150 µl. The contents of the tube were mixed by gentle tapping, spun briefly in a benchtop microfuge and incubated at 16°C for 2 hours. After this step 2ul (10U) of T4 DNA Polymerase was added and the tube incubated for a further 5 mins at 16°C, followed by the addition of 10µl of 0.5 M EDTA (pH8). The samples were then transferred to 1.5 ml microfuge tubes and used in the DS cDNA cleanup protocol.

Cleanup of the double stranded cDNA was achieved using the Phase Lock Gel™ system (Eppendorf). 162 µl of (25:24:1) phenol:chloroform:isoamylalcohol (saturated with 10 mM Tris-HCl pH8/1 mM EDTA) and the cDNA synthesis preparation was mixed in a 1.5 ml microfuge tube by vortexing. The mixture was then transferred to the Phase Lock Gel™ tube and immediately spun at full speed in a benchtop microfuge for 2 mins. The upper aqueous layer held the cleaned DS cDNA which was then transferred to a fresh 1.5 ml tube.

DS cDNA was then concentrated by repeating the Pellet Paint® (Novagen) protocol and resuspending the pellet by gentle pipetting in 12 µl RNase free water. The sample was then left on the benchtop for 30 minutes.

2.9.5 Synthesis of Biotin Labelled cRNA using a High Yield RNA Transcript Labelling Kit

The BioArray™ HighYield RNA Transcript Labelling kit (T7) (Enzo Life Sciences) was used to produce Biotin labelled cRNA. To a 0.2 ml RNase free microfuge tube the following components were added: 5 µl of DS cDNA (section 2.9.4), 17 µl of nuclease free water, 4 µl of 10x HY Reaction Buffer, 4 µl of 10x Biotin labelled ribonucleotides, 4µl of 10x DTT, 4µl of 10x RNase Inhibitor Mix and 2µl of 20x T7 RNA polymerase. The mixture was then mixed by gentle pipetting and collected in the base of the tube by a pulse spin in a benchtop microfuge. An *in vitro* transcription (IVT) reaction was performed by transferring the tube into a PCR machine set to incubate the sample at 37oC for 5 hours. The sample was then stored at -20°C overnight before cleanup and quantification of the product.

2.9.6 Cleanup of labelled cDNA using the RNeasy™ Mini Kit

Unincorporated dNTPs were removed so that the concentration of RNA could be measured accurately via absorbance at 260nm. The IVT reaction (section 2.9.5) was thawed and transferred into a 1.5 ml microfuge tube and the sample made up to a total volume of 100 µl by addition of RNase-free water. To this sample 350 µl Buffer RLT (Qiagen) containing 1% β-mercaptoethanol was added and mixed thoroughly. 250 µl of absolute ethanol was then added and mixed by pipetting only. This sample was added to a RNeasy minispin column in a 2 ml collection tube and centrifuged at 12000 rpm for 15 seconds, after which the flow through was reapplied to the column and the centrifugation repeated. Flow-through held in the collection tube was then discarded and the RNeasy column transferred into a new 2 ml collection tube. 500 µl of wash buffer RPE (Qiagen) was added to the column and the column centrifuged for 15 seconds at 12000 rpm, the flow-through discarded and the column wash repeated by the addition of another 500 µl of buffer RPE. Again the column was centrifuge for 2 minutes at full speed to dry the RNeasy membrane, the flow-through discarded and the column centrifuged for an addition 1 minute at 12000 rpm.

The RNeasy column was then eluted by transfer of the column into a 1.5 ml microfuge tube and the addition of 30 µl of RNase-free water onto membrane. The column was then left to stand for 1 minute at room temperature, followed by centrifugation for 1 min at 12000 rpm to elute the first fraction which was stored on ice. A second elution was then performed as before, using again 30 µl of RNase-free water. A 0.5 µl aliquot of both elutions was used for analysis of the cleaned IVT product on the Agilent Bioanalyser2100. The remaining IVT fractions were stored on at -20oC

2.9.7 Quantification of labelled cDNA

Quantification of the product was performed on the Agilent BioAnalyzer 2100 at a 1:4 dilution (0.5 µl IVT reaction (section 2.9.5-2.9.6) + 1.5 µl H₂O) of the first elution and an undiluted 0.5 µl aliquot of the second elution. An OD of 1 at 260 nm is known to equate to 40 µg/ml RNA. A A260/A280 ratio close to 2 suggests good quality, pure RNA.

The formula:

$$\text{Adjusted cRNA yield} = \text{RNAm} - (\text{total RNAi})(y)$$

was used to quantify the cRNA while allowing for adjustment to reflect carryover of unlabelled total RNA. Carryover of 100% was estimated. RNAm = amount of cRNA measured after IVT (µg, unpurified). Total RNAi = starting amount of RNA (µg, prior to cDNA synthesis). Y = fraction of cDNA reaction used in IVT reaction (i.e. 3.3 µl/12 µl)

2.9.8 Fragmentation of RNA

Fragmentation of the labelled RNA sample must be performed before hybridisation to the Affymetrix GeneChip® Arrays. This was done by referring to the unadjusted cRNA concentration of the sample and using 20.5 µg of RNA to which a volume of RNase free water was added to bring the total to 32 µl. To the 32 µl, 8 µl of 5x Fragmentation Buffer (200 mM Tris-acetate pH 8.1, 500 mM KOAc, 150 mM MgOAc) was added and the sample mixed by pipetting. Incubation at 94°C for 35 minutes was followed by placing the sample on ice. This fragmentation produced a distribution of RNA fragments the size of which varied from approximately 35 to 200 bases. These fragments formed the probe used for hybridisation.

2.9.9 Hybridisation of RNA to oligonucleotide arrays

Hybridisation of the probe to Genechip Yeast Microarrays was performed at the Sir Henry Wellcome Functional Genomic Facility (SHWFGF) at Glasgow University by Catriona Young.

2.9.10 Analysis of RNA data using SAM software

SAM (Significance Analysis of Microarrays) is a statistical technique for finding significant genes in a set of microarray experiments. It was proposed by Tusher, Tibshirani and Chu (Tusher et al, 2001). The software was written by Balasubramanian Narasimhan and functions as an add-on to the Microsoft Excel program.

Data inputs into the SAM program are in the form of gene expression measurements from a set of microarray experiments. Data from our three wild type arrays and three *slal* null arrays were input into the program. SAM generates a statistic d_i for each gene i , measuring the strength of the relationship between gene expression and each group. Repeated permutations of the data are then used to determine if expression of any genes are significantly related to each group. The cut-off for significance was determined by a tuning parameter δ , chosen in this case as a 1% false positive rate.

2.9.11 RT-PCR using the Titan One Tube RT-PCR System

RT-PCR was performed using approximately 400 ng of total RNA from a yeast RNA isolation (section 2.9.1) held in a volume not exceeding 3 μ l. The Titan One Tube RT-PCR system (Roche) was used. The reaction was initially setup on ice in two 0.2 ml thin walled PCR tubes. 4 μ l of 10 mM dNTPs (Bioline), 0.5 μ l of each primer at 50 pmol/ μ l, 400 ng of RNA, 2.5 μ l of 100 mM DTT and sterile water to make up the total volume to 25 μ l was added to the first tube. 5 μ l of 25 mM MgCl₂, 5 μ l of 5x RT-PCR Reaction buffer, 1 μ l Titan One Tube enzyme mix and sterile water to make up the total volume to 25 μ l was then added to tube 2. The contents of both tubes were then added to a fresh 0.2 ml thin walled PCR tube on ice and mixed by gentle pipetting. This tube was transferred immediately to a pre-heated PCR machine which would incubate the sample initially for 30 minutes at 50°C, followed by denaturation of the sample at 94°C for 2 minutes and 27 PCR cycles. The first ten cycles consisted of thermocycling at 94°C

for 10 seconds, 53°C for 30 seconds and a 68°C extension step of 45 seconds for a transcript less than 1 Kb or 60 seconds for transcripts between 1Kb and 1.5 Kb. The following 17 cycles were identical except from the 68°C extension step which was set to add an additional 5 seconds to the length of this step after every cycle. Thermocycling was ended with a five minute incubation at 68°C. The temperature of the 53°C annealing step was variable to allow optimum annealing of oligonucleotide primers to the template. 10 µl of the 50 µl reaction was then analysed by agarose gel electrophoresis (section 2.3.1).

3 CHARACTERISATION OF NUCLEAR SLA1

Abstract

Prior characterisation of Sla1p has shown the protein to function as an adaptor molecule linking endocytic proteins with the actin cytoskeleton in *S. cerevisiae* (Ayscough *et al.*, 1999; Tang *et al.*, 2000; Warren *et al.*, 2002). In this chapter I further the study of Sla1p with an analysis of nuclear Sla1p. Two particular aspects of nuclear Sla1p have been the focus of this study. Firstly, the nucleocytoplasmic trafficking of Sla1p has been investigated and additionally, an investigation into the possible roles of Sla1p in the nucleus has been undertaken. Briefly, in this study it is shown that remodelling of the actin cytoskeleton, both during cell-cycle progression, and during the mating response does not affect the nuclear localisation of Sla1p. This suggests that nuclear accumulation of Sla1p occurs independently of the cytoplasmic actin network. Sla1p is also shown to contain several potential nuclear localisation and nuclear export motifs and following analysis of *sla1* mutants, we identify specific regions of Sla1p important for nuclear localisation. Furthermore, mutation of the nuclear transport receptor Rsl1p is shown to prevent nuclear accumulation of Sla1p, suggesting the mechanism of Sla1p nuclear entry. To investigate the possible role of nuclear Sla1p, microarray analysis of both a Δ *sla1* strain and a wild-type strain was performed. This technique was used to provide insight into the roles of nuclear Sla1p.

3.1 Introduction

Prior analysis of Sla1p has demonstrated that the protein is multifunctional and is required for normal cortical actin patch structure and organisation. Previous studies have shown that Sla1p links the regulation of the cortical actin cytoskeleton to endocytic proteins, through interactions with several proteins regulating these processes (Ayscough *et al.*, 1999; Zeng and Cai, 1999; Uetz *et al.*, 2000; Drees *et al.*, 2001; Warren *et al.*, 2002; Gourlay *et al.*, 2003). Sla1p localises to punctate patches at the cell cortex, which partially co-localise with cortical actin patches (Ayscough *et al.*, 1999).

Sla1p has been shown to interact with the Arp2/3 complex regulating proteins Abp1p and Las17p/Beel1p (Warren *et al.*, 2002). These proteins enhance actin polymerisation by increasing the activity of the Arp2/3 complex (Madania *et al.*, 1999; Winter *et al.*, 1999a; Goode *et al.*, 2001). The involvement of Sla1p in the regulation of actin dynamics is further demonstrated by studies demonstrating the increased resistance of a Δ *sla1* strain to Latrunculin-A treatment and the identification of aberrant

actin structures in *sla1* mutant strains (Ayscough *et al*, 1997; Ayscough *et al*, 1999). Increased resistance to Latrunculin-A suggests a decrease in the dynamic nature of the actin cytoskeleton in these cells. Sla1p is also involved in endocytic uptake and has been shown to form a trimeric complex with the endocytic proteins Pan1p and End3p (Tang *et al*, 2000). Additionally, localisation of Sla1p to the cell cortex is dependent on End3p (Warren *et al*, 2002). These interactions demonstrate the role of Sla1p as an adaptor protein at the cell cortex, while multiple interactions suggest many interactions made by Sla1p may be transient. Recent studies have also shown Sla1p to have a role in ubiquitination of proteins by interaction with Rsp5p, a ubiquitin ligase (Stamenova *et al*, 2004). Sla1p may also have a role in the regulation of vesicle trafficking as Sla1p has been shown to interact with Lsb5p, a protein with homology to the GGA proteins (Dewar *et al*, 2002). To date only cytoplasmic roles of Sla1p have been described.

Prior localisation studies performed in this lab suggested that Sla1p is also found in yeast nucleus (Kathryn Ayscough, unpublished data). Immunofluorescence studies using Sla1p specific antibodies demonstrate a diffuse immunofluorescence signal which co-localises with DAPI fluorescence of nuclear DNA, in addition to the previously reported cortical fluorescence. Additionally, and in support of nuclear Sla1p, previously unpublished data from this lab has identified an interaction between Sla1p and the nuclear protein Cin5p by a yeast 2-hybrid screen (Hilary Dewar, unpublished data). Large scale screen have also shown synthetic lethality between a *ctf4/pob1* mutant and deletion of *SLA1* (Tong *et al*, 2004), and a two hybrid interaction between Sla1p and Slx2p (Uetz *et al*, 2000), a nuclear protein with endonuclease activity. CTF4/POB1 encodes a nuclear chromatin associated protein. A nuclear role for Sla1p is also suggested by genetic interactions with the gene encoding the nuclear protein Taf14p/Anc1p (Welch and Drubin, 1994). The *TAF14/ANC1* (actin noncomplementing) gene was identified during screening for mutations that enhanced the defect caused by mutation of the actin gene. In addition *taf14/anc1* mutants were shown to have defects in the organisation of cortical actin cytoskeleton (Welch *et al*, 1993; Welch and Drubin, 1994) and to be defective in mating projection formation, suggesting a role for Anc1p in the regulation of the cytoskeleton. An *anc1Δ1::HIS* mutation has been shown to be synthetically lethal in combination with *SLA1* deletion (Welch and Drubin, 1994), suggesting the two proteins may perform overlapping cellular roles. The localisation of Taf14p/Anc1p occurs independently of Sla1p and overexpression of neither Sla1p nor Anc1p is able to rescue the phenotypic defects caused by deletion of the other protein, which suggests similar but not identical roles for these proteins (Welch and Drubin,

1994). Taf14p/Anc1p is a component of the yeast TFIID and yeast TFIIF complexes (Cairns *et al*, 1996; Auty *et al*, 2004). These are two factors required for basal transcription by RNA Polymerase II. The aims of this study were therefore to examine the nuclear localisation of the Sla1p protein and investigate the potential roles of nuclear Sla1p.

Due to the localisation of Sla1p to the nucleus, a brief overview of the mechanisms of nuclear entry in *S. cerevisiae* is detailed here. In contrast to mammalian cells, the nuclear envelope of *S. cerevisiae* remains intact throughout the cell cycle. Molecules are able to enter the nucleus at the time of nuclear envelope reformation, while also undergoing active transport in mammalian cells. In *S. cerevisiae* however, nuclear entry and export always involves translocation across the nuclear membrane. Cargo molecules enter and exit the yeast nucleus by two mechanisms. Passive diffusion occurs when molecules smaller than 40 kDa freely diffuse through the nuclear envelope. Larger molecules must however be translocated across the membrane by active transport. Active import and export of molecules is mediated by a family of nuclear transport receptors collectively termed karyopherins (importins and exportins). These proteins recognise specific sequences on cargo molecules and transport the cargo into or out of the nucleus via the nuclear pore complexes (NPCs), as determined by signal sequences in the cargo (figure 3-1). NPCs are large complexes which span the nuclear envelope and which are composed of approximately 40 proteins in *S. cerevisiae* (nucleoporins) (for review see Weis, 2003). Many nuclear import and export signal sequences have been identified and this has led to the classification of nuclear localisation signals (NLSs) which specify nuclear import of cargo molecules, and nuclear export signals (NESs), which specify nuclear export. Additionally, many proteins are known to undergo nuclear transport but which do not show homology to known signal sequences, suggesting that several as yet unidentified signal sequences may exist or that another mechanism controlling nuclear translocation may be active. Known NLS and NES sequences are summarised in table 3-1. Nuclear translocation is additionally dependent on the gradient of the small Ras-like GTPase Ran, which cycles between the nucleus and cytoplasm, assuming a predominantly GTP bound form in the nucleus and a GDP bound form in the cytoplasm. This gradient is a consequence of the different cellular localisations of the yeast Ran-specific GTPase activating protein (RanGAP) and guanine-nucleotide exchange factor (RanGEF).

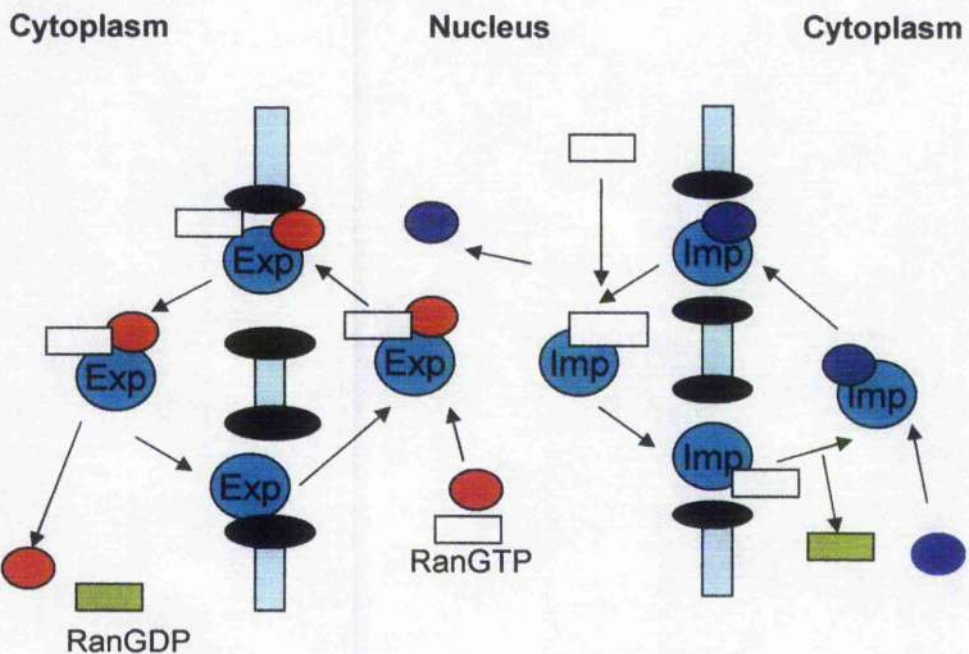


Figure 3-1 Active transport across the nuclear membrane. Transport occurs via nuclear pore complexes (black) which span the nuclear membrane. The direction of transport is determined by sequence signals in the cargo known as nuclear localisation sequences (NLSs) and nuclear export signals (NESs). Transport receptors or karyopherins; importins (Imp) or exportins (Exp) recognise cargo either directly or indirectly, escorting the cargo through the NPC. Transport is dependent on a RanGTPase gradient across the nuclear membrane.

Sequence element	Conserved Sequence	NLS source
Monopartite NLS- Lys rich	PKKKRKV	SV40 T-antigen
Monopartite NLS	PAAKRVKLD	c-myc
Monopartite Consensus	KKxK	
Bipartite NLS -Lys rich	KRPAATKKAGQAKKKKL	Nucleoplasmia
Bipartite Consensus	2K/R (10-12 aa) 3K/R	
Leu-rich NES	LQLPPLERLTL	HIV-1 Rev

Table 3-1 Consensus sequence of conserved NLS and NES elements.

Examples of known NLS and NES sequences from specific proteins are shown with the general consensus sequence also demonstrated. Essential residues are shown in bold. The SV40 NLS was identified by Kalderon and colleagues (Kalderon *et al*, 1984), c-myc NLS by Dang and Lee, (Dang and Lee, 1988) and the nucleoplasmia NLS by Robbins and colleagues (Robbins *et al*, 1991).

The monopartite or classical NLSs were initially identified and characterised as a short cluster of basic amino acids. Bipartite NLSs, composed of two short stretches of basic amino acids separated by a linker sequence were then identified. NESs identified to date are rich in hydrophobic amino acids such as leucine or isoleucine.

In order to investigate the localisation of Sla1p in the nucleus, Sla1p localisation during the *S. cerevisiae* cell-cycle was examined (sections 3.2.1 – 3.2.3) and the phenotypes of the *sla1* mutants, *sla1*-ΔG2 and *sla1*Δ-118-511 studied (sections 3.2.4 – 3.2.5). Sla1p localisation in a specific nuclear transport receptor (Karyopherin) mutant strain was examined and was shown to be abnormal (sections 3.2.7 – 3.2.10), suggesting the mechanism of Sla1p nuclear uptake. Microarray analysis of gene expression changes in a *SLA1* deletion strain and a wild-type strain was also performed in order to examine potential nuclear Sla1p roles (section 3.2.11). Determining the effects of *SLA1* deletion on gene expression should provide new insight into the functions of nuclear Sla1p.

3.2 Results

3.2.1 The localisation of Sla1p to the nucleus is not a cell-cycle associated event

Nuclear Sla1p was initially identified during localisation of myc-tagged Sla1p in the wild-type strain KAY303 (Kathryn Ayscough, unpublished data). This strain was generated by integration of a short region of DNA encoding a 9x myc tag (9 x EQKLISEEDL) into the wild-type strain (KAY302) at the 3' end of the *SLA1* gene. Localisation of the Sla1-myc fusion protein was then performed by indirect immunofluorescence (section 2.7.2). Polyclonal rabbit anti-myc primary antibodies were used to label the myc-tagged protein, while goat anti-rabbit FITC labelled secondary antibodies allowed the localisation of the primary antibodies by fluorescence microscopy. Pictures were obtained using an Olympus BX-60 fluorescence microscope as described in section 2.7.1. The immunofluorescence pattern in this strain clearly shows accumulation of Sla1-myc at punctate structures at the cell cortex as previously reported. Additionally, a diffuse fluorescence across the yeast nucleus is seen (figure 3-2A). The location of the nucleus in these cells was confirmed by DAPI fluorescence, which incorporates into the nuclear DNA (figure 3-2B). This data suggested that Sla1-myc localises both to the nucleus and the cell cortex.

Due to the lack of previous reports of nuclear Sla1p, nuclear Sla1p has remained unstudied. Several possibilities exist regarding the nuclear localisation of Sla1p. Accumulation of the protein at this localisation could be a transient occurrence, with accumulation occurring at specific points in cell-cycle or during specific cell processes. This may potentially occur as a sequestering event to remove the active protein from the cytoplasm. Sla1p may also however be consistently found in the nucleus with a definable specific role. In order to study nuclear Sla1p in more detail, localisation of the protein was performed under specific conditions to ascertain if nuclear Sla1p was apparent throughout. Due to the confirmed roles of Sla1p in the regulation of actin dynamics, localisation of the protein was performed throughout the cell cycle, when extensive cytoskeletal remodelling occurs, and which may have affected nuclear Sla1p. During budding and cytokinesis, the actin cytoskeleton polarises towards sites of cell growth, in the developing bud and at the bud neck respectively. Sla1p-myc localisation was therefore examined by immunofluorescence at specific points in the cell-cycle in the wild-type strain (KAY 303). Data demonstrated that 78% of unbudded cells demonstrated a co-localisation of Sla1p-myc fluorescence with

nuclear DAPI fluorescence (figure 3-3). Similarly, 76% of budded cells showed a co-localisation of Sla1p-myc fluorescence with nuclear DAPI fluorescence. Remodelling of the actin cytoskeleton and other cell-cycle specific processes did not therefore affect the percentage of cells demonstrating nuclear Sla1-myc, suggesting that nuclear Sla1p accumulates independently of cell-cycle progression.

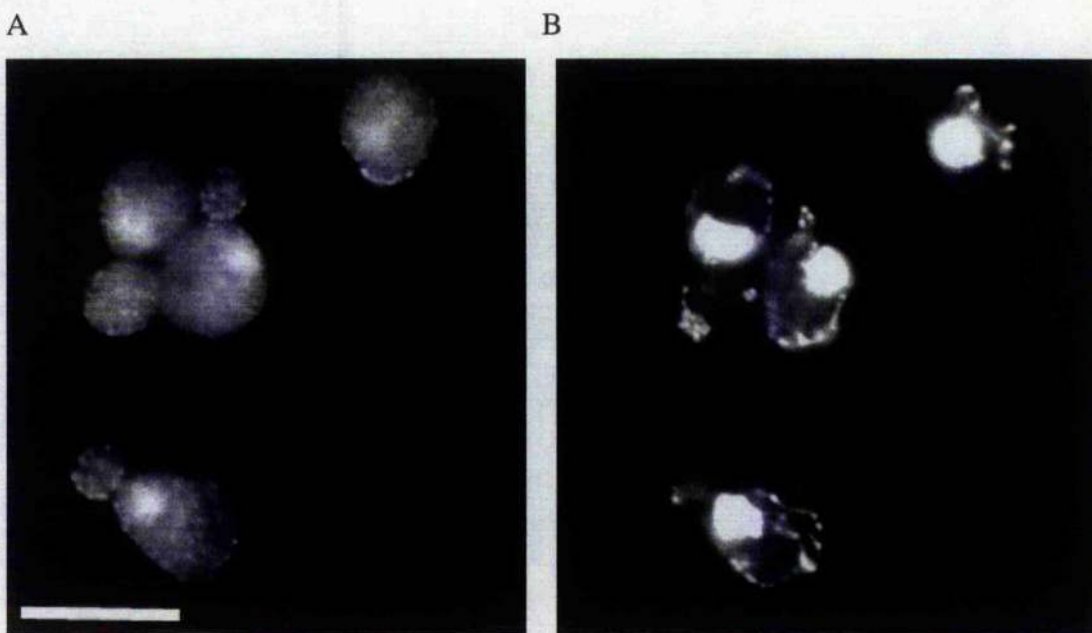


Figure 3-2. Sla1p shows both a partial co-localisation with cortical actin patches and a nuclear co-localisation.

The localisation of Sla1-myc as determined by immunofluorescence in a wild-type (KAY 303) strain. A) The KAY303 strain expresses myc-tagged Sla1p and was processed for immunofluorescence by methanol fixation during log-phase growth. Examination of Sla1-myc localisation was undertaken by immunofluorescence with rabbit polyclonal anti-Myc A-14 antibodies (1:100). B) DAPI fluorescence allows the localisation of the yeast nucleus by DAPI incorporation into nuclear DNA.

Localisation of Sla1p

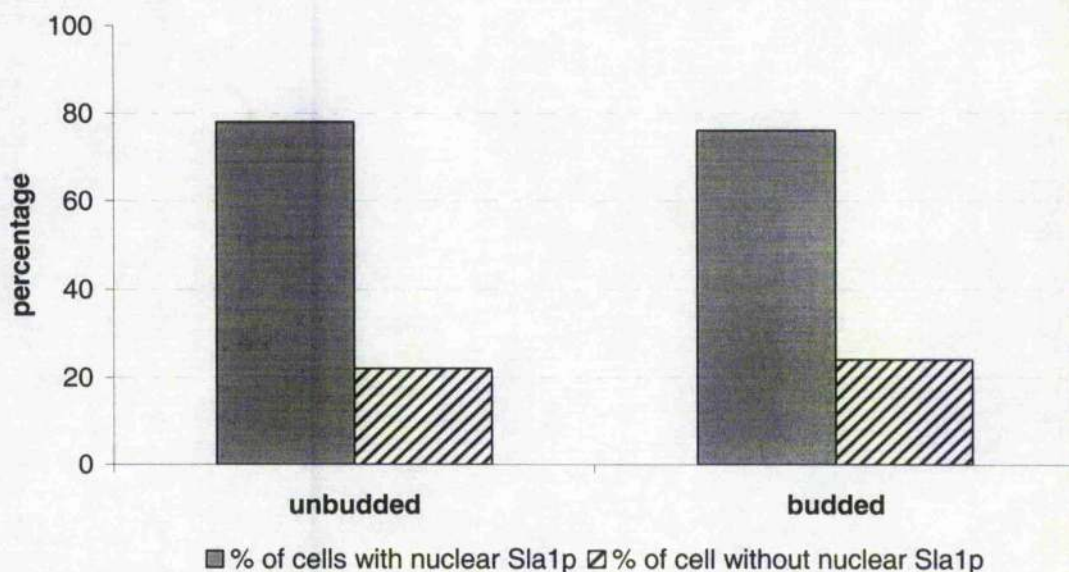


Figure 3-3. The nuclear localisation of Sla1p-myc is cell-cycle independent.

KAY303 cells expressing myc-tagged Sla1p were processed for immunofluorescence during log-phase growth and the localisation of Sla1-myc examined using anti-myc rabbit polyclonal A-14 antibodies. Localisation of Sla1p-myc was examined in over 200 cells at specific cell-cycle stages. The presence of nuclear Sla1p recorded as shown. 78% of unbudded cells demonstrated nuclear Sla1-myc, while 76% of unbudded cells demonstrate nuclear Sla1-myc.

3.2.2 Nuclear Sla1p response to heat shock

To examine the effect of the heat-shock response on the localisation of nuclear Sla1-myc, the wild type, Sla1-myc expressing strain (KAY 303) was incubated at 37°C, following initial 29°C growth. Extensive remodelling of the actin cytoskeleton occurs in response to heat shock. Previous studies have demonstrated the substantial depolarisation of cortical actin patches and loss of actin cables in budding yeast cells, following heat shock (Gu *et al*, 1997). In addition, the heat shock response is associated with the increased expression of proteins involved in specific stress response pathways.

To examine the effect of heat shock and the associated depolarisation of the actin cytoskeleton on the localisation of nuclear Sla1-myc, a strain expressing Sla1-myc was first grown normally at 29°C, and then transferred to incubation at 37°C, in order to induce the heat shock response. Cells were then examined by immunofluorescence to localise Sla1-myc. The wild-type strain (KAY303) was cultured overnight in liquid YPAD media, and this culture used to inoculate 5 ml of fresh media which was grown for a further four hours at 29°C, to allow cells to enter log phase growth. These cultures were then transferred to incubation at 37°C and examined by immunofluorescence at time points 5, 15, and 30 minutes after temperature shift. The immunofluorescence pattern of Sla1p-myc at these time points demonstrates the continuing co-localisation of Sla1-myc fluorescence with nuclear DAPI fluorescence (figure 3-4). Sla1-myc also continued to localise to partially polarised punctuate patches at the cell cortex. The immunofluorescence pattern of nuclear Sla1p-myc was therefore unaffected by induction of the heat-shock response.

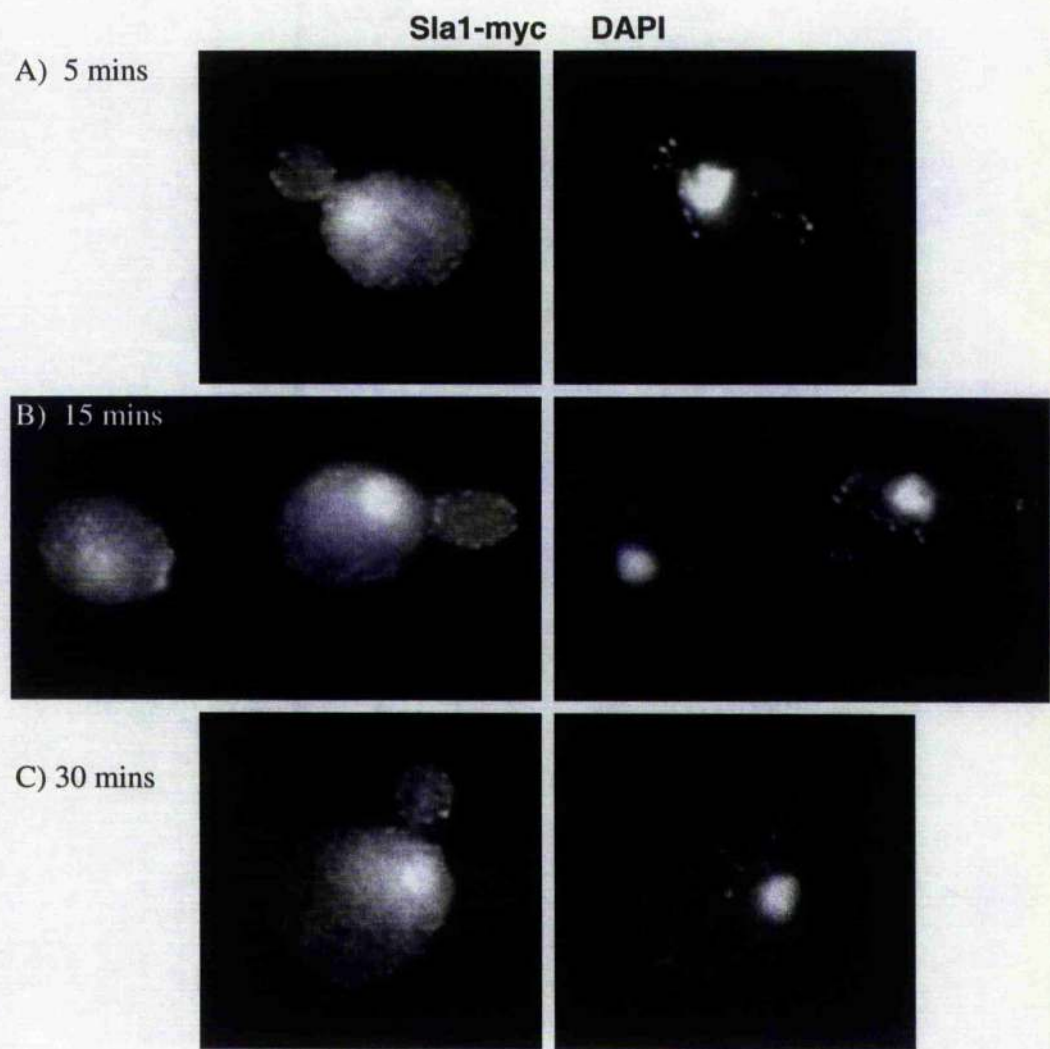


Figure 3-4. The localisation of Sla1p-myc is unaffected in heat shocked cells

Haploid cells expressing myc-tagged Sla1 (KAY 303) were initially grown into log-phase at 29°C, followed by transfer to 37°C for 30 minutes. Cells were fixed and examined by immunofluorescence microscopy at time points A) 5 minutes B) 15 minutes and C) 30 minutes following temperature shift. Sla1-myc immunofluorescence (left) and DAPI fluorescence (right) is shown.

3.2.3

Nuclear Sla1p is not affected by induction of the mating response

In order to continue examining the effect of specific cellular responses on the localisation of Sla1p, the effect of inducing the mating response and the associated actin remodelling on Sla1-myc localisation was examined. During mating, haploid cells secrete cell-type specific mating pheromones. MAT α cells secrete α -factor, while MAT α cells secrete α -factor. These peptide pheromones bind to receptors on the surface of cells of the opposite mating type, initiating a response which enables the formation of a mating projection. In this way, haploid cells are able to detect cells of opposite mating type with which they can successfully mate to form diploids. Mating pheromones bind to membrane bound G-protein coupled pheromone receptors which initiate activation of a signalling pathway, which promotes the remodelling of the actin cytoskeleton and the activation of Ste12p, a transcription factor which promotes the expression of mating factor response genes. Cells responding to mating pheromones have a characteristic ‘shmoo’ appearance due to the formation of the mating projection and the associated polarisation of cellular growth.

A MAT α strain expressing the Sla1-myc fusion protein (KAY303) was incubated with cells of the opposite mating type but which did not express Sla1p-myc (KAY389) to induce the mating response in both strains (section 2.4.10). Strains were initially grown individually on YPAD plates at 29°C. A small amount of one strain was then patched onto the other on a fresh YPAD plate, and the cells returned to the 29°C incubator for a further 2 hours. Cells were then removed from this plate and resuspended in 1ml of liquid YPAD media. This culture was then fixed and examined by immunofluorescence microscopy with anti-myc antibodies as described in section 2.7.2. Cells undergoing the mating response were identified by the formation of the characteristic elongated, mating projection as shown in figure 3-5. The immunofluorescence pattern shows Sla1p-myc localising both to punctuate patches at the cell cortex, and also to the nucleus in cells with undergoing the mating response. These images demonstrate that the nuclear localisation of Sla1p-myc is unaffected by the induction of mating response.

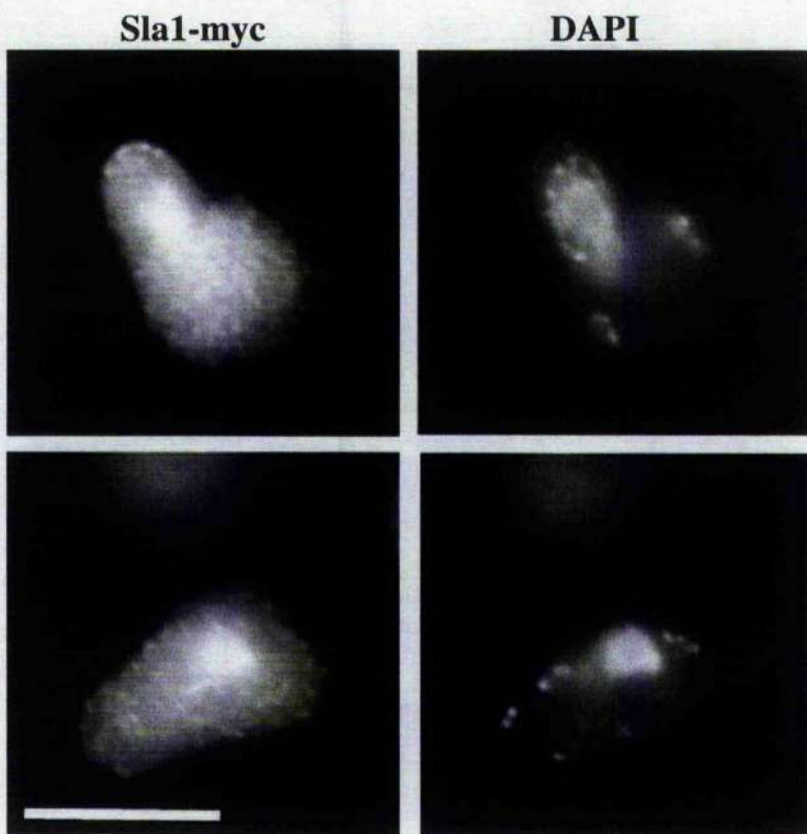


Figure 3-5. The nuclear localisation of Sla1p is unaffected during the mating response.
MAT α cells expressing myc-tagged Sla1 (KAY 303) formed the characteristic mating projection following incubation with strain of the opposite mating type (KAY389). Sla1-myc was then localised in the MAT α , KAY303 strain by immunofluorescence using anti-myc A14 antibodies (left panels). Nuclear DNA was also identified by DAPI incorporation and fluorescence (right panels). Bar = 10 μ M.

3.2.4

The localisation of *Sla1*-ΔG2 and *sla1*-Δ118-511 mutants

Given that the co-localisation of nuclear Sla1p-myc was unaffected during cell-cycle progression, the induction of the mating response and the heat shock response, the localisation of previously generated Sla1p mutants was undertaken. Removal of specific regions of Sla1p was known to affect the organisation of the actin network and endocytic function in these mutant strains (Ayscough *et al.*, 1999; Gourlay *et al.*, 2003). These regions may therefore also be important for mediating nuclear interactions or in localising Sla1p to the nucleus.

Sla1p mutant strains lacking specific regions of the protein were examined. These strains carry functionally inactive genomic copies of *SLA1*, disrupted by integration of the *LEU2* at the *SLA1* locus. The first strain examined additionally carried a carboxy-terminal myc-tagged *sla1*-Δ118-511 construct (KAY 367) (Ayscough *et al.*, 1999). This *sla1*-Δ118-511-myc mutant construct was inserted into the genome by homologous recombination at the *URA3* locus. The deleted region of Sla1p was 393 amino acids in length and encompassed the last 10 amino acids of the second SH3 domain, the Gap1 region, third SH3 domain and a small section of the Gap2 region, including the first 20 amino acids of SHD1 (figure 3-6). This region of Sla1p has been previously shown to be required for the actin regulating activity of the Sla1p (Ayscough *et al.*, 1999). *Sla1*-Δ118-511 was shown to localise to small punctuate spots at the cell cortex which did not co-localise with the aberrant actin structures generated in this mutant (Ayscough *et al.*, 1999; Gourlay *et al.*, 2003). This strain is temperature sensitive in addition to its actin phenotype, which shows fewer, and enlarged cortical actin patches; an actin phenotype similar to that seen in a *SLA1* deletion strain. *Sla1*-Δ118-511 is however able to rescue the Abp1p dependence associated with *SLA1* deletion, suggesting some functionality of the protein is retained (Ayscough *et al.*, 1999). The nuclear localisation of *Sla1*-Δ118-511-myc had not previously been examined.

The second strain to be examined carried a carboxy-terminally tagged *sla1*-ΔG2 construct (KAY 387) (Ayscough *et al.*, 1999). This *sla1*-ΔG2 construct lacks a 1495 bp fragment (figure 3-6), and was inserted into the genome by homologous recombination at the *URA3* locus. The Gap2 (G2) region of Sla1p is partially removed in this mutant. This region contains the SHD1 region reported to interact with Lsb5p (Dewar *et al.*, 2002; Costa *et al.*, 2005).

The *sla1-Δ118-511-myc* and *sla1-ΔG2-myc* mutant strains were grown in liquid YPAD media at 29°C until in log phase growth, then fixed and processed for immunofluorescence with anti-myc A14 antibodies. The immunofluorescence pattern of *sla1-Δ118-511-myc* and *sla1-ΔG2-myc* is shown in figure 3-7. *Sla1-ΔG2-myc* fluorescence co-localises primarily with nuclear DAPI fluorescence and demonstrates an almost total loss of fluorescence at cortical patch sites (figure 7A). Only a very low level of fluorescence is apparent in the cytoplasm in these cells. *Sla1-Δ118-511-myc* has been previously reported to localise to punctate patches at the cell cortex, indicating that the protein still retains the ability to localise to cortical sites (Gourlay *et al*, 2003). Our data confirms the localisation of *sla1-Δ118-511-myc* to punctate cortical patches (figure 3-7B), however a partial loss of co-localisation with the nucleus was also noted. Removal of the Gap1 and third SH3 domains of Sla1p in this *Sla1-Δ118-511* mutant caused a marked decrease in the intensity of nuclear staining in all cells examined. This data suggests the importance of the Gap1 and SH3#3 region, and the Gap2 region for normal localisation of the Sla1p to the cell cortex and nucleus. Deletion of either region has a marked effect on Sla1p localisation.

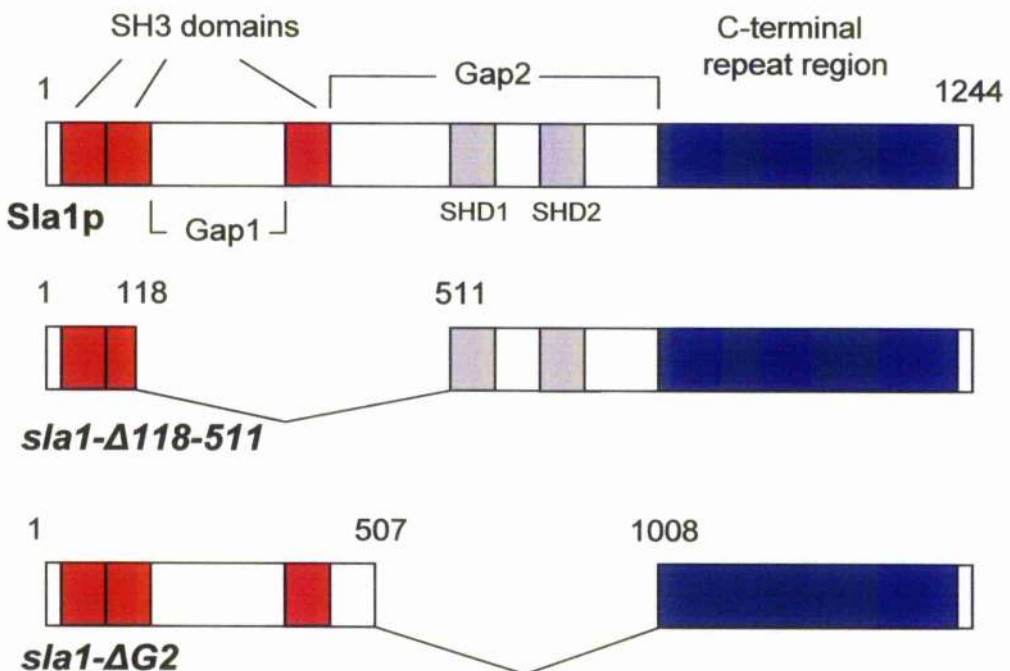


Figure 3-6. Diagram of Sla1p mutant constructs, *sla1*-Δ118-511 and *sla1*-ΔG2.

Previously generated genomic Sla1 constructs lacking residues 118-511 and the ΔG2 region (amino acids 507-1008) were used in this study. The Sla1p mutants encoded are shown in the diagram and termed *sla1*-Δ118-511 and *sla1*-ΔG2. A carboxy-terminal 9xmyc tag was also fused to these constructs. Constructs are thus expressed as myc-tagged fusions in KAY 351 (*sla1*-Δ118-511) and KAY 387 (*sla1*-ΔG2) strains. Deletion of amino acids 188-511 removes the last 10 amino acids of SH3#2, the Gap1 region, SH3#3, and the first 20 amino acids of SHD1. In the *sla1*-ΔG2 mutant a significant region of the Gap2 domain is lost including homology domains 1 and 2 (SHD1+SHD2). SH3 domains are shown in red, homology domains in grey and the carboxy-terminal repeat region in blue.

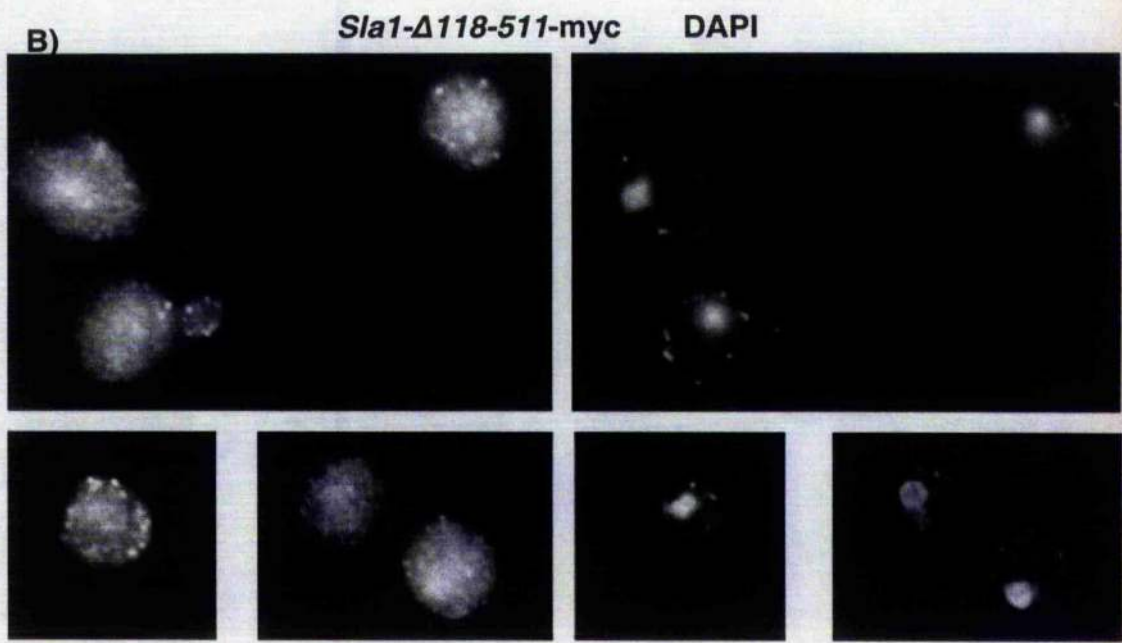
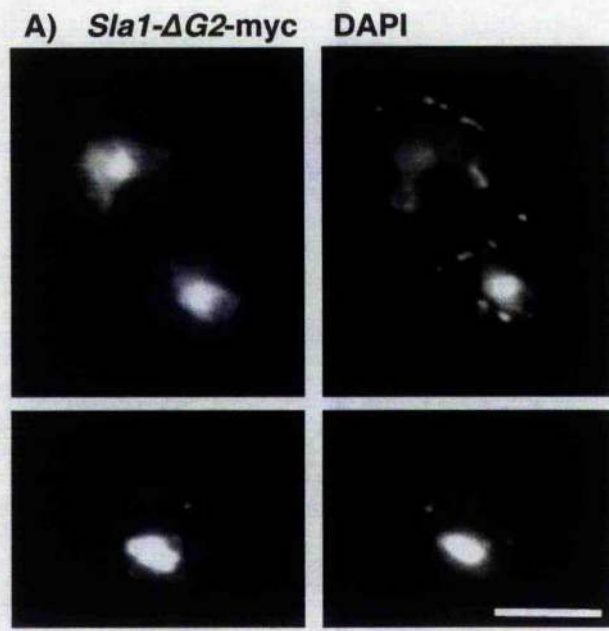


Figure 3-7. Localisation of *sla1*- Δ G2-myc and *sla1*- Δ 118-511-myc mutants constructs.

Haploid cells expressing A) *sla1*- Δ G2-myc (KAY 387) and B) *sla1*- Δ 118-511-myc (KAY 367) were examined by immunofluorescence microscopy using anti-myc A-14 antibodies (left panels) and DAPI fluorescence (right panels).

3.2.5 *Sla1*- Δ G2-myc and *sla1*- Δ 118-511-myc mutants have endocytic and actin defects

Given the mislocalisation of the *sla1*- Δ 118-511-myc and *sla1*- Δ G2-myc mutants, with accumulation occurring primarily in the nucleus in the *sla1*- Δ G2 mutant, and predominantly in the cytoplasm in the *sla1*- Δ 118-511-myc mutant, additional effects of the deletion of these regions of Sla1p were examined. Effects on the actin cytoskeleton were studied by rhodamine phalloidin staining (section 2.7.3), while lucifer yellow uptake assays were then performed to examine endocytic uptake (section 2.7.4) in these mutant strains.

A *sla1*- Δ 118-511 and Δ *sla1* strain have previously been shown to display an aberrant actin cytoskeleton, with fewer and enlarged cortical actin patches (Holtzman et al 1993, Ayscough et al 1999). A *sla1* deletion strain expressing plasmid borne *sla1*- Δ G2 has however been previously reported to display a normal actin phenotype in 90% of cells studied (Ayscough, 1999). Results of experiments performed during this study confirm these actin phenotypes (figure 3-8). 85% of *sla1*- Δ 118-511-myc cells examined displayed enlargement of, and a decrease in the number of cortical actin patches. 80% of *sla1*- Δ G2-myc cells examined however displayed a normal actin phenotype. The region of Sla1p from residues 118-511, has previously been shown to act as the actin regulatory region within Sla1p (Ayscough et al, 1999). *Sla1*- Δ 118-511-myc retains partially functionality however, with the ability to rescue Abp1p dependence of a Δ *sla1* strain but lacking the ability to rescue the temperature sensitive growth phenotype associated with Δ *sla1*. The *sla1*- Δ G2 mutant is able to rescue both the growth defect and Abp1p dependence of a *sla1* deletion strain and exhibits a generally wild-type actin cytoskeletal staining (Ayscough et al, 1999).

Endocytic uptake is intimately linked with the function of the cortical actin cytoskeleton. Given the aberrant actin phenotypes displayed in our *sla1*- Δ 118-511-myc mutant and the mild actin defect displayed in our *sla1*- Δ G2-myc mutant, effects on endocytosis were assayed. Uptake of the dye Lucifer Yellow from the growth medium is used to quantify the extent of fluid phase endocytic activity occurring in a specific strain (section 2.7.4). Lucifer Yellow uptake assays performed on the *sla1*- Δ 118-511-myc mutant showed an approximate 50% reduction in uptake in all cells examined, as determined qualitatively (figure 3-9). Assays performed on the *sla1*- Δ G2-myc mutant showed approximately a 90% decrease in uptake in all cells examined, as determined qualitatively, similar to that seen in a Δ *sla1* strain (Warren et al, 2002).

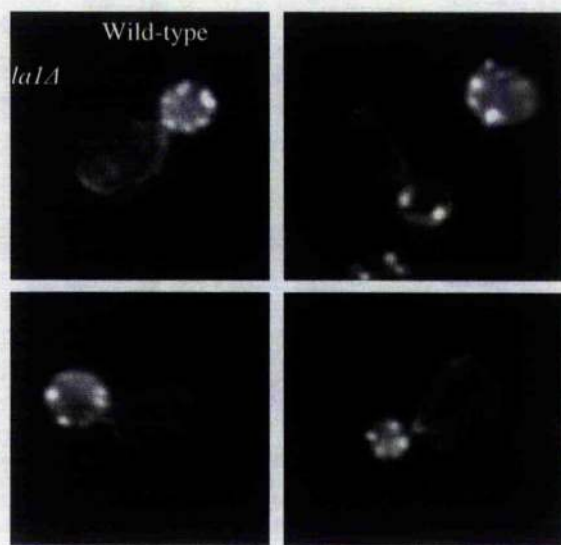


Figure 3-8. F-actin structures in haploid yeast strains expressing *slal-Δ118-511-myc* and *slal-ΔG2-myc*.

Strains expressing *slal-Δ118-511-myc* (KAY367) and *slal-ΔG2-myc* (KAY387) were cultured into log-phase growth and stained with rhodamine phalloidin to visualise the F-actin structures. Wild-type (KAY302) and Δ *sla1* (KAY300) strains were also examined.

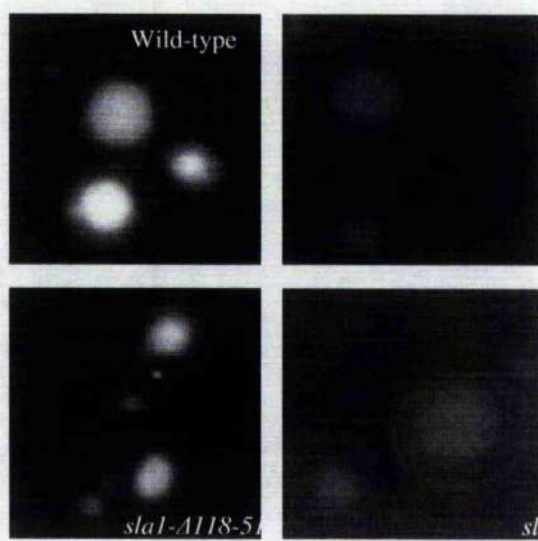


Figure 3-9. Fluid phase endocytosis assays in haploid yeast strains expressing *slal-Δ118-511-myc* and *slal-ΔG2-myc*.

Uptake of the dye Lucifer Yellow was assayed to identify defects in fluid phase endocytosis in wild-type (KAY302), Δ *sla1* (KAY300), *slal-Δ511-811-myc* (KAY367) and *slal-ΔG2-myc* (KAY387) strains.

3.2.6

The sequence of Sla1p suggests multiple NLSs and NESs

Sla1- Δ G2-myc localises predominantly to the nucleus, while *sla1*- Δ 118-511-myc demonstrates a decrease in nuclear co-localisation, as shown previously (section 3.2.3). In order to determine the mechanism of nuclear entry of Sla1p, the amino acid sequence of Sla1p was examined for the presence of known nuclear localisation signals (NLSs) and nuclear export signals (NESs). The Sla1p sequence contained six regions with significant homology to known NLS, and two regions with a high degree of homology to known NES. Regions were identified by motifs scanning at http://myhits.isb-sib.ch/cgi-bin/motif_scan. Three of the potential NLSs identified displayed similarity to monopartite NLSs, characterised by a short stretch (5-20 residues) of basic amino acids (Dingwall and Laskey, 1991). The remaining three NLS regions showed similarity to bipartite NLSs, which are composed of two short stretches of basic amino acids separated by a linker sequence. Two regions were also identified that showed significant homology to leucine rich NESs. The localisation of the residues forming these potential signal sequences in Sla1p are shown in figure 3-10. NLSs are generally recognised and imported by the importin α and importin β homologues in yeast, Kap60p/Srp1p and Kap95p/Rsl1p respectively. While Kap95p/Rsl1p can import cargo directly, Kap60p/Srp1p requires Kap95p/Rsl1p to cross the NPC, forming a Kap60p/Srp1p-Kap95p/Rsl1p complex following identification of an NLS. Signal mediated nuclear import is not however exclusively carried out by Kap60p/Srp1p and Kap95p/Rsl1p, and many Kap95p/Rsl1p isoforms exist in yeast which mediate the uptake of specific molecules. Leucine rich NES sequences are thought to be primarily recognised by, and exported by the Crm1p exportin protein in *S. cerevisiae* (for review see Jans *et al*, 2000). Identification of these sequences suggests a mechanism for the uptake and export of Sla1p from the nucleus.

The loss of several potential NLS or NES motifs in the *sla1* mutants, *sla1*- Δ 118-511 and *sla1*- Δ G2 is demonstrated in figure 3-10. Specifically, five potential nuclear import signals are lost in the *sla1*- Δ 188-511 mutant, while one potential nuclear import signal and both nuclear export sequences are lost in the *sla1*- Δ G2 mutant.

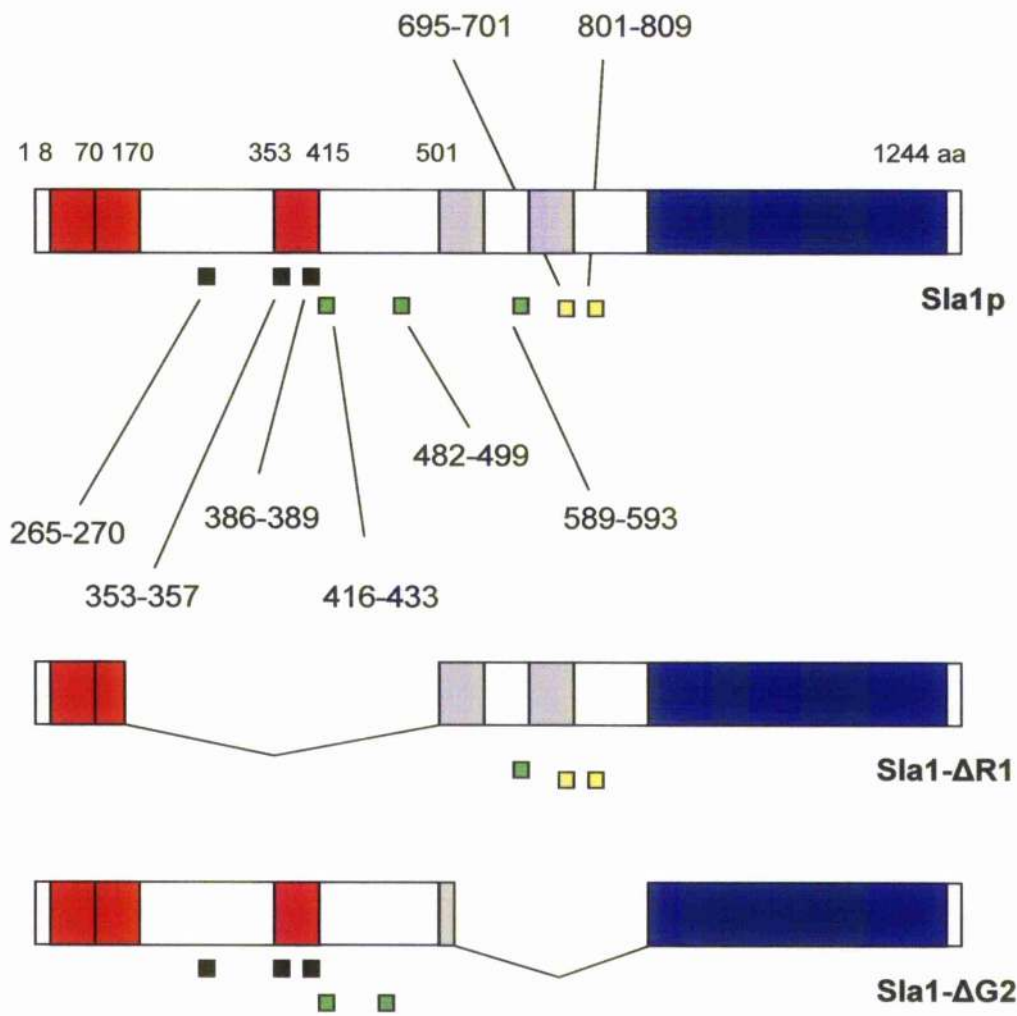


Figure 3-10. Sla1p contains several potential NLS and NES motifs, several of which are lost in the *sla1*- Δ I18-511 and *sla1*- Δ G2 mutants. The location of SH3 domains (red), HD1 and HD2 domains (grey) and the C-terminal repeats region (blue) in *sla1*- Δ I18-511 and *sla1*- Δ G2 mutants is demonstrated. Possible NLS and NES sites identified by analysis of the protein sequence are shown as small boxes shown at the appropriate location in the protein. Black boxes represent the location of monopartite NLSs, green represents Bi-partite NLSs and yellow demonstrates possible NESs. The residues numbers at which these motifs are located are also shown.

3.2.7

Characterisation of karyopherin mutants

Following the identification of several potentially functional NLSs and NESs in the Sla1p sequence (section 3.2.6) and the abnormal localisation of the *sla1-Δ118-511-myc* and *sla1-ΔG2-myc* mutants (section 3.2.4), mechanisms which may control the nuclear translocation of Sla1p were examined. In order to determine whether a specific karyopherin protein mediated nuclear translocation of Sla1p, several karyopherin and nuclear transport mutants were studied, as listed in table 3-2. These strains were a generous gift from Dr Paul Ko Ferrigno (University of Cambridge). 14 β-karyopherins and 1 α-karyopherin have been identified in yeast (for review see Mosammaparast and Pemberton, 2004). 11 karyopherin mutants are examined here. Additionally, *prp20/srm1* and *rna1* mutants are examined. *PRP20/SRM1* and *RNA1* encode the yeast RanGEF and RanGAP respectively. The small GTPase Ran is crucial to the nuclear transport process, existing predominantly in the GTP bound form in the nucleus and in the GDP bound form in the cytosol due to the action of nuclear Prp20p and cytosolic Rna1p. Ran is a highly conserved protein which is essential for cell viability. Interfering with the cyclic nature of Ran has been shown to produce many pleiotropic phenotypes, due in part to the role of Ran in nuclear transport, but also due to the role of Ran in other cell processes (for review see Sazer and Dazzo, 2000).

Nuclear transport mutants were examined by rhodamine phalloidin staining for visualisation of F-actin structures and identification of actin cytoskeletal abnormalities (section 2.7.3), and lucifer yellow uptake (section 2.7.4), to assess fluid phase endocytic defects. In each strain over 200 cells were examined by rhodamine phalloidin staining, while lucifer yellow uptake assays were performed in triplicate and over 200 cells examined in each strain. Results of these assays are summarised in table 3-2. Mutation of the RanGAP and RanGEF, Prp20p/Srm1p and Rna1p produced significant depolarisation of the actin cytoskeleton but did not affect fluid phase endocytic uptake. Actin defects were identified in all mutants examined with varying degrees of severity.

Strains for further study were selected on the basis that mutation of proteins involved in the normal localisation of Sla1p may cause actin and endocytic defects, as seen in *Asla1* and *sla1* mutant strains. Strains selected contained mutations in the *CRMI/XPO1*, *RSL1* and *SRP1* genes (strains KAY616, KAY610 and KAY607 respectively). Uptake of the dye lucifer yellow was defective in 100% of *srm1-1* and *crm1/xpo1* mutant cells examined, while 60% of *rsl1-1* mutant cells showed defects in

fluid phase endocytosis (table 3-2 and figure 3-11). Images demonstrating the results of rhodamine phalloidin straining performed on these mutants are shown in figure 3-11.

Mutation	KAY number	% with actin defect	Defects identified	Endocytic defect
<i>kap123</i>	608	7.1	Enlargement of cells Depolarisation Some multibudding	decreased uptake Fragmentation of vacuoles
<i>los1</i>	615	27	Enlargement of dividing cells and depolarisation	No
<i>iph2</i>	609	8.9	Depolarisation	No
<i>msn5</i>	614	2	Polarisation defects	No
<i>mtr10</i>	613	6	Enlargement of dividing cells and depolarisation	No
<i>nmd5</i>	619	8.5	Depolarisation in budding Eulargement of dividing cells	No
<i>prp20/srm1</i>	622	27	Enlarged of cells Depolarisation	No
<i>pse1</i>	621	25.6	Elongated budding cells Some multibudding	No
<i>rna1</i>	606	2.5	Depolarisation	No
<i>rsl1</i>	610	3	Polarisation defects	40% no defect 60% defective
<i>srp1</i>	607	5.4	Polarisation defects, some enlarged unbudded cells	100% defective
<i>sxm1</i>	620	2.9	Depolarisation	No
wild-type	617	3.6	Polarisation defects	No
<i>xpo1/crm1</i>	616	38	Polarisation defects	100% defective

Table 3-2 Phenotypic analysis of karyopherin and nuclear transport mutants

Rhodamine phalloidin staining and lucifer yellow uptake assays were performed the nuclear transport mutants listed. *PRP20/SRM1* and *RNA1* encode the yeast RanGEF and RanGAP respectively. All other mutants listed encoded known yeast karyopherins. Assay results are summarised in the table. The gene mutated is listed in the first column, strain identifiers are listed in the second column, while assay results for actin phenotype (columns 3 + 4) and endocytic uptake (column 5) are also listed.

Mutation of *XPO1/CRM1*, the gene encoding the general yeast exporter Crm1p/Xpo1p, produced severe defects in both actin organisation and fluid phase endocytosis. This was perhaps unsurprising due to the variation and number of molecules which Crm1p is known to export from the nucleus. Deletion of *CRM1/XPO1* is lethal, while mutation of the protein has been shown to produce severe phenotypic defects. Severe endocytic defects were also seen in *srp1* and *rsl1* mutants. In addition, each of these strains also displayed defects in polarisation of the actin cytoskeleton.

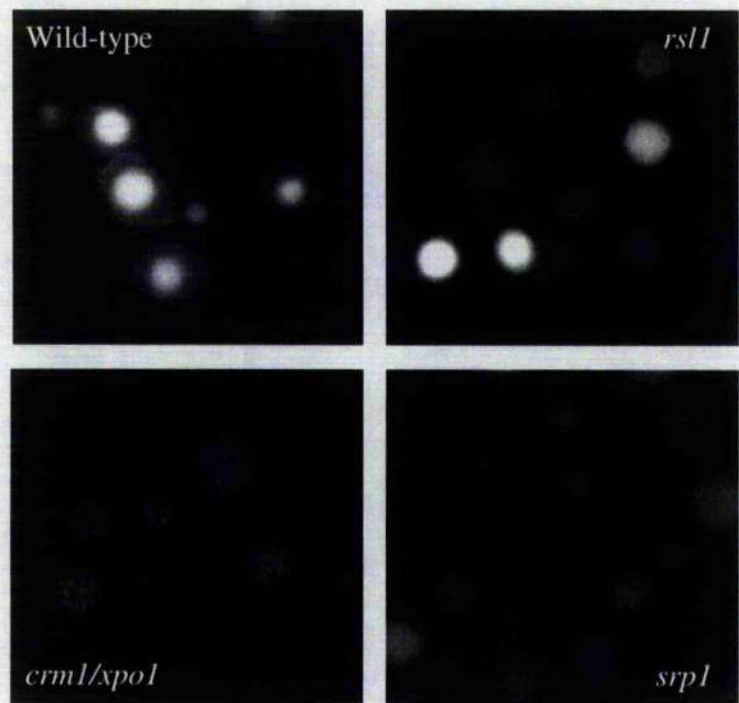
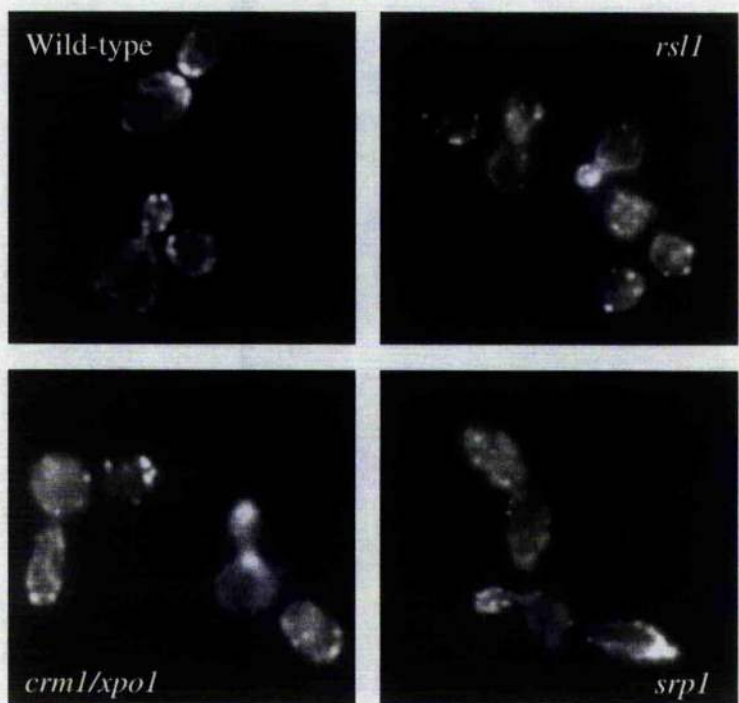
A)**B)**

Figure 3-11. Three karyopherins mutants displayed distinct endocytic and actin defects.

Lucifer yellow uptake assays and rhodamine phalloidin staining was performed on wild-type (KAY302) *rs11* (KAY610), *srp1* (KAY607) and *crml/xpo1* (KAY616) mutant strains. A) Images obtained from lucifer yellow uptake assays B) Images obtained from rhodamine phalloidin staining.

3.2.8

Generation of Sla1-myc in specific karyopherin mutant strains

Following the identification of karyopherin mutants which displayed marked endocytic and actin defects, and with reference to data showing the correlation of mislocalised *sla1-Δ118-511-myc* and *sla1-ΔG2-myc* (section 3.2.4) with defects in fluid phase endocytosis (section 3.2.5), I proposed that Sla1p may also mislocalise in these karyopherin strains. Three karyopherin mutant strains, *crml/xpol*, *rsl1* and *srp1* (KAY616, KAY610 and KAY607 respectively) were examined for localisation of Sla1p. To examine the localisation of Sla1p in these mutants, 13x myc-tagging of Sla1p was attempted using a PCR product integration method, in both the *srp1* and *rsl1* mutant strains (section 2.4.6). Oligos oKA132 and oKA133 were used to PCR (section 2.3.5) a short sequence of DNA from the pFA6-13xmyc-TRP1 plasmid, which contains a region encoding a 13x myc-tag and a selectable *TRP* marker, integration of which would allow cells to grow on drop-out tryptophan media. Oligonucleotides were designed to amplify the *TRP* marked myc-tagging cassette so as to allow specific integration of the product at the C-terminus of the genomic *SLA1* gene, by homologous recombination. Using this method Sla1p was myc-tagged in the *rsl1* mutant strain (KAY610). Myc-tagging of Sla1p in the *srp1* strain was not however achieved, as the tagging cassette consistently integrated at incorrect sites in the genome of this strain.

Localisation of Sla1-myc in a *crml* strain was performed using a previously generated strain, KAY 444 (K. Ayscough unpublished work). The *CRML* gene is required for viability in *S. cerevisiae*. This strain therefore carried a plasmid copy of *CRML* to maintain viability in a *crml* genomic deletion strain. This strain also contained genetically tagged Sla1-myc. The action of plasmid borne Crm1p was inhibited by cell growth in the presence of the potent cytotoxin Leptomycin B (Fornerod *et al*, 1997; Fukuda *et al*, 1997). Data suggests that Leptomycin B acts by blocking the formation of Crm1p/cargo/RanGTP nuclear export complex by interaction with Crm1p (Daelemans *et al*, 2005).

3.2.9 Sla1p mislocalisation in an *rsll* mutant

Expression of myc-tagged Sla1p was verified in the *rsll* mutant (KAY610) by Western blot analysis with anti-myc antibodies. Identification of a band at 190 KDa in this mutant suggested specific integration and expression of myc-tagged Sla1p (figure 3-12). Myc tagging allowed localisation of Sla1-myc in this *rsll* mutant strain. To examine the localisation of *sla1*-myc in this *rsll* mutant, the strain was cultured into log-phase growth, and was then processed for immunofluorescence with anti-myc antibodies (section 2.7.2). Fluorescence was predominantly seen in the cytoplasm with no significant nuclear accumulation of Sla1-myc (figure 3-13). The cytoplasmic fluorescence identified small, punctuate structures in the cell cortex, suggesting that the cortical localisation of Sla1p-myc is unaffected in this mutant, however nuclear accumulation was lost in all cells examined.

Rsllp (Kap95p) is the homologue of mammalian Importin β 1. β -karyopherins can identify and transport cargo directly following NLS recognition. Rsllp is however also known to import cargo in conjunction with the adaptor protein Srp1p. Srp1p (Kap60p) is the homologue of mammalian Importin α and identifies and binds to cargo molecules containing classical and bipartite NLSs. Srp1p and bound cargo then form a complex with Rsllp (Kap95p), which is only then actively imported into the nucleus. Following import, cargo and importins dissociate and the importins are recycled back to the cytosol to continue functioning as importing transport receptors (for review see Yoneda, 2000).

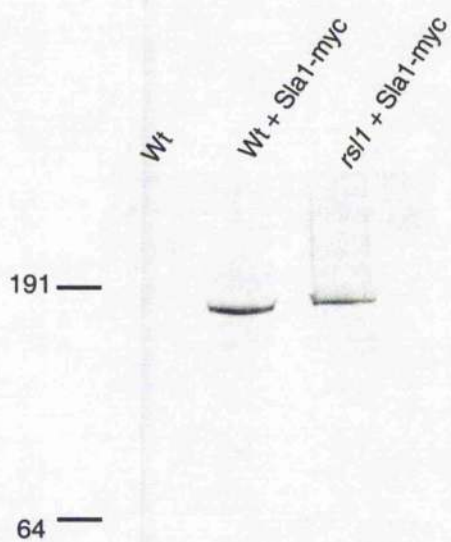


Figure 3-12. Expression of myc-tagged Sla1p in an *rs11* mutant as determined by western blotting. An immunoblot of total cellular extracts from: Lane 1) wild type cells (KAY 302), Lane 2) a Sla1-myc strain (KAY303) and Lane 3) *rs11* mutant strain (KAY610) which expresses Sla1-myc. Blots were probed with anti-myc A-14 primary antibodies. Molecular weight markers (KDa) are also shown on the left of the image.

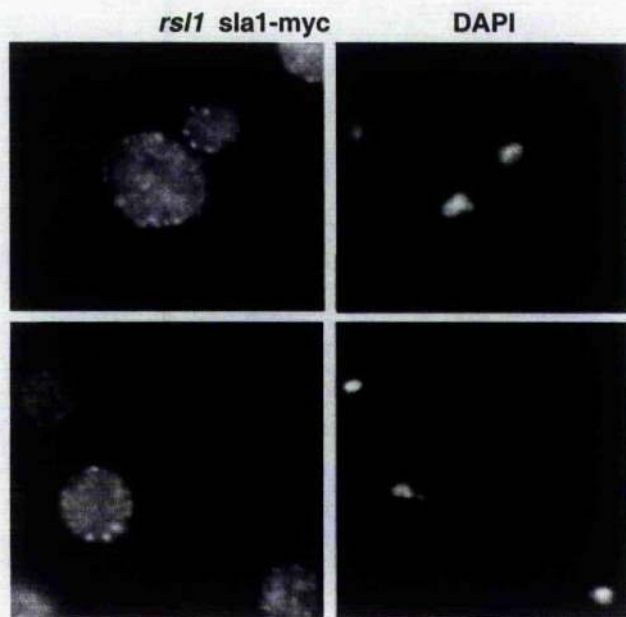


Figure 3-13. Sla1p-myc is mislocalised in an *rs11-1* mutant. Localisation of myc-tagged Sla1p in *rs11* mutant strain (KAY610) was performed by immunofluorescence with anti-myc antibodies.

3.2.10 Mutation of *crm1* does not affect the nuclear localisation of Sla1p

To examine the localisation of Sla1-myc in the *crm1/xpo1* mutant strain (KAY 444), the strain was cultured into log-phase growth in drop-out Leucine synthetic media to retain the *CRM1* encoding plasmid during growth. Cells were then resuspended in drop-out leucine media containing Leptomycin B at a working concentration of 100ng/ml for two hours to inhibit the formation of Crm1p nuclear export complexes. Cells were then processed for immunofluorescence with anti-myc antibodies. Fluorescence images obtained are shown in figure 3-14. The immunofluorescence pattern demonstrates a punctate cortical fluorescence, suggesting that the localisation of Sla1p-myc to cortical sites is unaffected. Due to the effects of Crm1p inhibition, cortical actin patches do not however polarise correctly in this strain (K.Ayscough unpublished data). Fluorescence is also seen to accumulate and co-localise with the nucleus in this strain. Sla1p-myc localisation therefore appears unaffected by Crm1p inhibition.

Crm1p/Xpo1p is a general exporter of cargo from the nucleus in *S. cerevisiae*. Crm1p/Xpo1p homologues are known to be involved in export of various proteins including: mRNAs, ribosomes and snRNAs (Jans *et al*, 2000), and while less studied in yeast, this broad substrate specificity of Crm1p is thought to be retained. Crm1p recognises cargo by identification and interaction with leucine rich NESs present in cargo molecules.

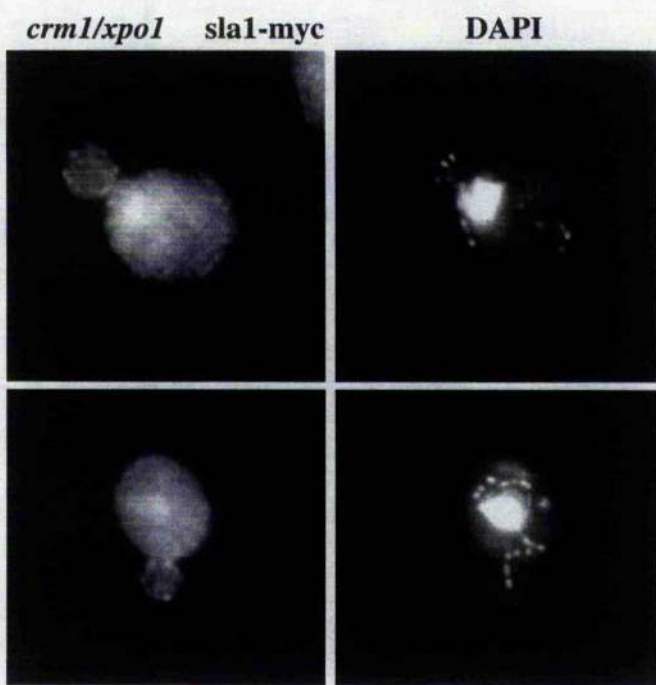


Figure 3-14. Sla1p-myc localisation in a *crm1* mutant.

Localisation of Sla1p-myc in the *crm1* mutant strain (KAY444) was performed by immunofluorescence using anti-myc antibodies. Crm1p activity was inhibited by growth of the strain in synthetic media containing Leptomycin B for 2 hours.

3.2.11 Microarray analysis of gene expression in wild-type and *Asla1* cells

Identification of nuclear Sla1p and the identification of a potential nuclear import mechanism raise many questions as to the possible function of nuclear Sla1p. An investigation into the function of nuclear Sla1p was therefore undertaken. Several possibilities for Sla1p accumulation in the nucleus exist. Nuclear accumulation of the protein could be a regulatory mechanism, controlling the cytoplasmic action of the Sla1p and rendering the protein inactive by sequestering to the nucleus. Equally, Sla1p may be retained in the nucleus by direct interaction with a nuclear protein, and may have a structural or transcriptional role in the nucleus. A nuclear role for the Sla1p is plausible, particularly in light of data detailing the existence of actin and many other actin regulating proteins in the nucleus. As with the cytoplasmic role of Sla1p, the potential for Sla1p to play several overlapping roles in the nucleus was also considered.

Microarray analysis is a relatively new technique which provides invaluable data on levels of gene expression. Such data can be used to elucidate both signalling pathways and the mechanistic function of molecules. Total cellular RNA is first isolated from a strain of interest, from which biotin labelled cRNA probes are generated. Probes are then used to hybridise and label oligonucleotide arrays which contain short oligonucleotides sequences from genes spanning the entire genome of the species of interest. Several control oligonucleotides are also present and are used for normalisation of results. By comparing the hybridisation levels of probes to individual oligonucleotides, changes in gene expression levels can be compiled when compared to other strains.

Microarray analysis of a *sla1* deletion mutant (KAY300) was performed. For analysis and comparison of gene expression levels, a wild-type strain (KAY302) was selected due to having a congenic genetic background, opposing mating type and having undergone prior cellular analysis. Yeast GeneChip® Arrays were used (Affymetrix). Total RNA was prepared in triplicate from each strain as described in section 2.9.1. Quantification and quality checks were then performed on each preparation (section 2.9.2) and this starting material used to generate double stranded cDNA (Section 2.9.4). Biotin labelled cRNA was produced directly from these cDNA preparations (section 2.9.5 - 2.9.6), and was then quantified (sections 2.9.7) and fragmented (section 2.9.8) in preparation for hybridisation to Genechip® Arrays (section 2.9.9).

The analysis and the normalisation of microarray data is a highly specialised technique. Analysis of this data was therefore kindly performed for us by Dr Paweł Herzyk at the Sir Henry Wellcome Functional Genomics Facility (SHWFGF) in the University of Glasgow. As hybridisations were performed in triplicate for each strain, data from six arrays was normalised using SAM (Significance Analysis of Microarrays) software. SAM uses a statistical technique to finding significant gene expression changes in a set of microarray experiments (Tuscher *et al*, 2001). 95 gene identifiers were selected using this software. These genes showed a significant change in expression level between the wild type and *slal* deletion strain. A false positive rate of 1 % was chosen to limit both the number of genes identified and possible errors. Of these 95 genes, 9 duplicates were removed; identified through recognition of different oligonucleotides derived from the same gene. A further 18 genes specific to mating type were also removed from our analysis. Of the 68 genes remaining, the expression of 39 was significantly upregulated in the $\Delta slal$ strain, while the expression of 29 was significantly downregulated. Results are shown in table 3-3 and are summarised in figure 3-15. The *URA3* gene shows the largest upregulation. This gene serves as an excellent control, as the *SLA1* gene was disrupted by integration of *URA3*. Equally, downregulation of *SLA1* is also identified in our analysis.

Effects on gene expression may be direct or indirect following the loss of a specific protein. For this reason microarray results require further experimental exploration before specific interactions or signalling events are conclusively identified. Several membrane transporters were however noted to be downregulated in the $\Delta slal$ strain. *SLT2* expression was also upregulated by 2.8 fold in the $\Delta slal$ strain. *SLT2* encodes Slt2p, a constituent of the cell integrity MAP kinase pathway. This pathway involves the activation of Pkc1p signalling, which is activated by Rho1p in a GTPase dependent manner. Slt2p activates the heterodimeric transcription factor, SBF, which promotes expression of SBF targets, including cell wall biosynthesis genes during the G1/S transition of the cell cycle. Slt2p is also known to activate the transcription factor Rlm1p (Jung and Levin, 1999, Zu *et al*, 2001). *WSC4* plays a role in the environmental stress response pathway and is required for viability of yeast cells under heat stress conditions (Verna *et al*, 1997; Zu *et al*, 2001). *WSC4* is also significantly downregulated.

Table 3-3A: Genes upregulated in *Δslal* strain (KAY300) as identified by SAM analysis

Fold change	Name	ORF	Role
19.86	<i>URA3</i>	<i>YEL021W</i>	Pyrimidine base biosynthesis
11.20	<i>PRM8</i>	<i>YGL053w</i>	Membrane protein
6.49		<i>YBR056W</i>	Unknown
5.36	<i>MST27</i>	<i>YGL051W</i>	Vesicle formation and organisation, Golgi and ER membrane protein
5.22	<i>PRM5</i>	<i>YIL117C</i>	Plasma membrane protein, cell integrity signalling
4.09	<i>CWP1</i>	<i>YKL096W</i>	Cell wall protein, cell wall organisation
3.78	<i>YPS4</i>	<i>YLR121C</i>	Endopeptidase (protein metabolism)
3.77	<i>DIA1</i>	<i>YMR316W</i>	Cytoplasmic protein
3.44	<i>MCH5</i>	<i>YOR306C</i>	Membrane transporter
2.79	<i>SLT2</i>	<i>YHR030C</i>	Map kinase
2.72	<i>CMK2</i>	<i>YOL016C</i>	Calmodulin dependent protein kinase, amino acid phosphorylation
2.64	<i>LSR1</i>	<i>NLT026C</i>	Nuclear mRNA splicing
2.58		<i>YGL052W</i>	Unknown
2.49		<i>YOR385W</i>	Unknown
2.48		<i>YLR152C</i>	Unknown
2.45		<i>YIL023C</i>	Unknown
2.41		<i>YBR005W</i>	Unknown
2.34		<i>YNL208W</i>	Unknown
1.99	<i>DFG5</i>	<i>YMR238W</i>	Cell wall biosynthesis, plasma membrane localised
1.98		<i>YDL027C</i>	Unknown
1.95	<i>YET1</i>	<i>YKL065C</i>	Endoplasmic reticulum protein
1.92	<i>ASG7</i>	<i>YJL170C</i>	Expression increased by alpha factor
1.90		<i>YAL053W</i>	Unknown
1.87	<i>RTS3</i>	<i>YGR161C</i>	Protein phosphatase, type 2A activity
1.86	<i>PPM1</i>	<i>YDR435C</i>	Carboxyl methyl transferase, amino acid methylation
1.86	<i>ARP2</i>	<i>YDL029W</i>	Component of Arp2/3 complex
1.85	<i>RKB1</i>	<i>YCR036W</i>	ATP binding – ribokinase activity
1.78		<i>YER163C</i>	Unknown
1.78		<i>YIL108W</i>	Unknown
1.78	<i>CRG1</i>	<i>YGR189C</i>	Cell wall glycosidase
1.71	<i>ROD1</i>	<i>YOR018W</i>	Plasma membrane protein, contains a PY motif
1.70	<i>GTT2</i>	<i>YIL060C</i>	Glutathione S-transferase, glutathione metabolism
1.69	<i>APM4</i>	<i>YOL062C</i>	Component of AP-2 adaptor complex
1.67	<i>SAM2</i>	<i>YCR502C</i>	Methionine metabolism
1.67		<i>YGR259C</i>	Unknown
1.65	<i>CMP2</i>	<i>YML057W</i>	Cyttoplasmic Ca2+ dependent serine/threonine phosphatase
1.60		<i>YER034W</i>	Unknown
1.49	<i>YPK1</i>	<i>YKL126W</i>	Serine/threonine protein kinase. Endocytosis and sphingolipid metabolism
1.46		<i>YLI058W</i>	Unknown

Table 3-3B: Genes downregulated in the $\Delta slal$ strain (KAY300) as identified by SAM analysis

Fold change	Name	ORF	Role
29.49	<i>SLA1</i>	<i>YBL007C</i>	Involvement in endocytosis and actin regulation
13.13		<i>YLR040C</i>	Unknown
8.49	<i>PHO84</i>	<i>YML123C</i>	Phosphate transporter
6.17	<i>MDH2</i>	<i>YOL126C</i>	Malic enzyme, metabolism
4.95		<i>YNL034W</i>	Unknown
4.85		<i>YCL065W</i>	Unknown
3.97	<i>GGA2</i>	<i>YHR108W</i>	Golgi to vacuole transport
3.59	<i>URA1</i>	<i>YKL216W</i>	Pyrimidine nucleotide biosynthesis
3.56	<i>RIB4</i>	<i>YOL143C</i>	Vitamin B2 biosynthesis
3.35	<i>GAP1</i>	<i>YKR039W</i>	Amino acid permease, amino acid transport
3.14	<i>LEU1</i>	<i>YGL009C</i>	Leucine biosynthesis
3.13	<i>URA4</i>	<i>YLR420W</i>	Pyrimidine nucleotide biosynthesis
2.98		<i>YLR126C</i>	Unknown
2.84	<i>FU11</i>	<i>YBL042C</i>	Uridine transporter
2.66		<i>YBL029W</i>	Unknown
2.55	<i>GAT1</i>	<i>YFL021JW</i>	RNA Polymerase II transcription
2.51	<i>COS8</i>	<i>YHL048W</i>	Unfolded protein response
2.45	<i>WSC4</i>	<i>YHL028W</i>	Trausmembrane receptor involved in actin organisation and Rho signalling
1.99	<i>SHM2</i>	<i>YLR058C</i>	One-carbon compound metabolism
1.94		<i>YJL037W</i>	Unknown
1.93	<i>RPR1</i>	<i>SCHYLEFT</i>	tRNA processing
1.88	<i>THI7</i>	<i>YLR237W</i>	Thiamine transporter
1.86	<i>TNA1</i>	<i>YGR260W</i>	Nicotinamide mononucleotide transport
1.86	<i>MDL1</i>	<i>YLR188W</i>	ABC transporter
1.79	<i>HSX1</i>	<i>TR(CC4)J</i>	Translational elongation
1.77	<i>OPT2</i>	<i>YPR194C</i>	Oligopeptide transporter
1.52		<i>YHL026C</i>	Unknown
1.37		<i>YNL181W</i>	Unknown
1.36	<i>TES1</i>	<i>YJR019C</i>	Acyl-CoA thioesterase

Table 3-3 Genes identified by microarray and SAM analysis.

Following analysis and normalisation of microarray data comparing gene expression in wild-type (KAY302) cells with $\Delta slal$ (KAY300) cells, 68 genes with significant changes in expression were identified. A) 39 genes were identified as upregulated in $\Delta slal$ cells. B) 29 genes were identified as downregulated in $\Delta slal$ cells. Genes of specific interest are highlighted.

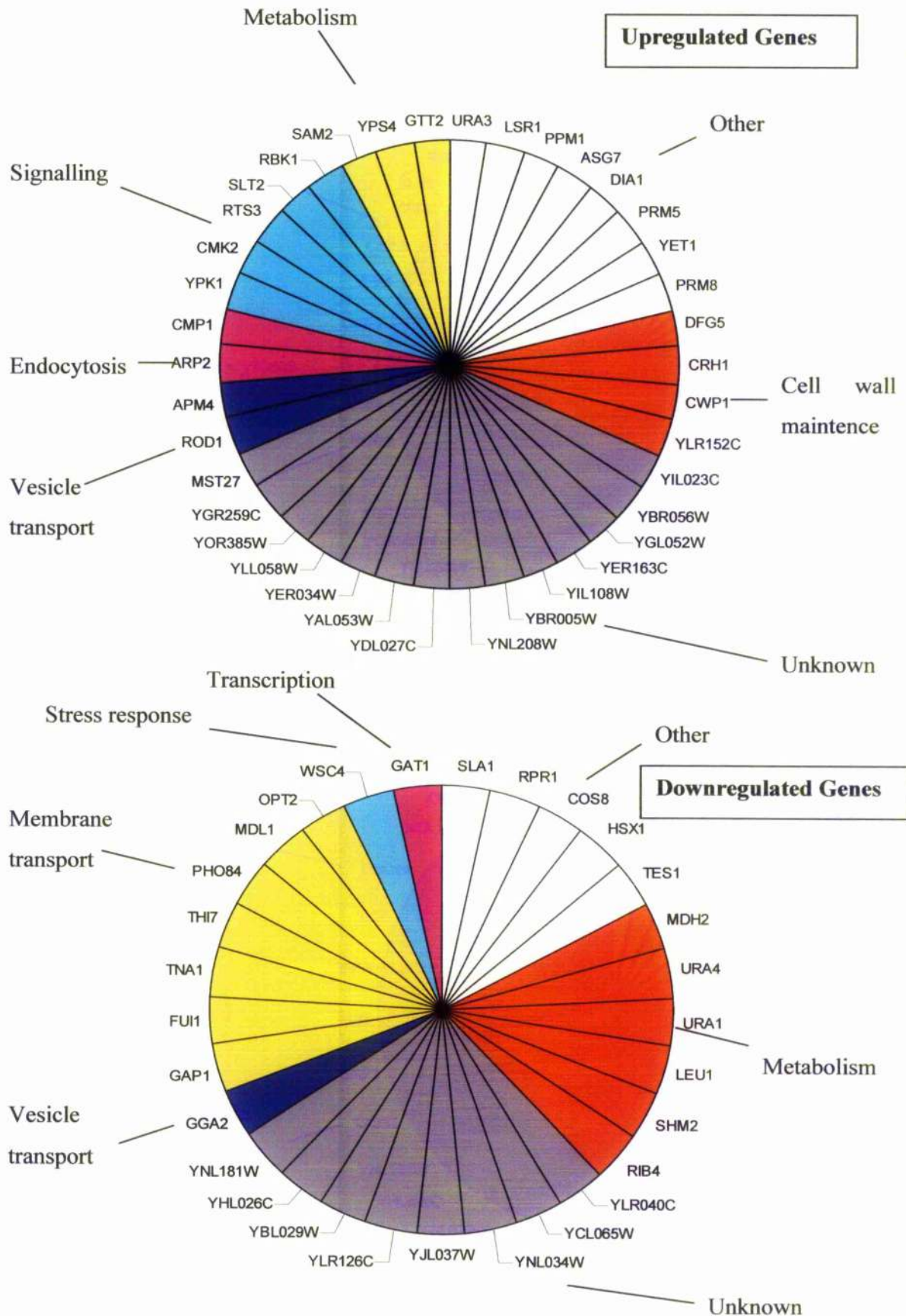


Figure 3-15. Graphical display of microarray results showing functional groupings.

3.2.12 RT-PCR confirmation of microarray data

Following the generation and normalisation of microarray data comparing gene expression levels between a wild-type and $\Delta sla1$ strain, a crucial second confirmation step was performed to in order to validate these results. Quantitative RT-PCR (real-time PCR) is a highly sensitive technique which allows the detection and quantification of mRNA levels using only small amounts of RNA. This technique was used to validate our microarray data. RT-PCR reactions use cDNA generated from total RNA isolations to provide the template for PCR reactions. In this way the amount of PCR product generated is dependent on the amount of mRNA transcript present in the RNA isolation. RT-PCR was performed using RNA isolated from our wild-type strain (KAY302), $\Delta sla1$ strain (KAY300) and the MATa $sla1\text{-}AG2$ strain (KAY382). RNA from the $sla1\text{-}AG2$ strain was included in this analysis to provide further insight into the effects of nuclear accumulation of the mutant protein, demonstrated in section 3.2.4.

RT-PCR was performed using the Titan One Tube RT-PCR System (Promega). Template cDNA was first generated from total cellular RNA isolations (section 2.9.1) using the Reverse Transcriptase enzyme. Primers specific for the gene of interest were then used in PCR reactions, to amplify transcripts from the cDNA templates using Taq DNA polymerase (Section 2.9.11). RT-PCR was performed on several control genes which included *TUB1*, as expression was unchanged in our microarray analysis. *TUB1* encodes alpha tubulin, a microtubule component. The *STE2* gene was also amplified as a control. The *YSC84* gene was also amplified as a control as expression of this gene was not reported to change significantly between the wild-type and $\Delta sla1$ strains in our microarray analysis. Expression of *STE2* was reported to increase by 33 fold in our $\Delta sla1$ strain, according to microarray analysis. Expression of *STE2* is mating type specific, as the gene encodes the alpha factor pheromone receptor. *STE2* was therefore additionally used as a control. RT-PCR was also performed on *WSC4*, *ARP2*, *YPK1*, *SLT2* and *GGA2*. Known functions of the proteins encoded by these genes are summarised in table 3-4. Products from RT-PCR reactions were analysed by agarose gel electrophoresis (Section 2.3.2) (figure 3-16). Images were then quantified using image analysis software (NIH Image) (figure 3-17).

Expression of *YSC84* and *TUB1* did not vary significantly between the $\Delta sla1$ and wild type strain, with fold changes of 1.12 and 1.02 respectively. These two control genes demonstrated slightly higher expression levels in RT-PCR analysis of the

sla1-ΔG2 strain, potentially due to a marginal increase in the amount of RNA used when performing the *sla1-ΔG2* RT-PCR reactions. This was considered upon analysis of subsequent *sla1-ΔG2* RT-PCR results. Expression of the *STE2* gene was increased by 38.11 fold between the Δ *sla1* and wild type strain, similar to the 33 fold increase identified by microarray analysis (data not shown). *GGA2* was downregulated 2.04 fold, and *WSC4* downregulated 4.35 fold, while *SLT2* was upregulated by 2.26 and *YPK1* upregulated by 1.31 fold between the Δ *sla1* and wild type strain, as determined by RT-PCR and analysis of agarose gel images. Microarray analysis reported *GGA2* to be downregulated 3.97 fold, *WSC4* to be downregulated by 2.45 fold, while *SLT2* was upregulated by 2.79 and *YPK1* upregulated by 1.49 fold between the Δ *sla1* and wild type strain. While the figures obtained from RT-PCR analysis do not directly correlate with the fold-changes reported by microarray analysis, these results do however confirm the trend in either upregulation or downregulation of specific gene expression between these strains. RT-PCR results from the *sla1-ΔG2* strain were therefore interpreted cautiously, and were used only as an indicator of the potential regulation of specific genes. *STE2* upregulation in the *sla1-ΔG2* strain confirms the mating type of this *sla1-ΔG2* strain, while *SLT2* expression also appears to be significantly upregulated in this strain.

Gene	Fold change reported by microarray	Encoded protein and known function
<i>TUB1</i>	n/a	Alpha tubulin. Microtubule component.
<i>YSC84</i>	n/a	Cortical patch protein, function unknown.
<i>STE2</i>	33.3 upregulation	α -factor mating receptor. Response to mating pheromone.
<i>SLT2</i>	2.8 upregulation	Map kinase. Involvement in PKC1 signalling pathway.
<i>ARP2</i>	1.85 upregulation	Subunit of the Arp2/3 complex. Actin nucleation, regulation and branching.
<i>YPK1</i>	1.49 upregulation	Serine/threonine protein kinase. Modification of endocytic proteins.
<i>WSC4</i>	2.45 downregulation	Membrane receptor. Involved in cell integrity pathway
<i>GGA2</i>	3.97 downregulation	Golgi localised Arf interacting protein. Golgi to vacuole transport.

Table 3-4 Genes selected for RT-PCR analysis.

Known functions of the genes selected for RT-PCR analysis are listed. Changes in gene expression, as reported by microarray analysis are also shown in the table. Expression of the control genes *TUB1* and *YSC84* were not significantly changed in our microarray analysis.

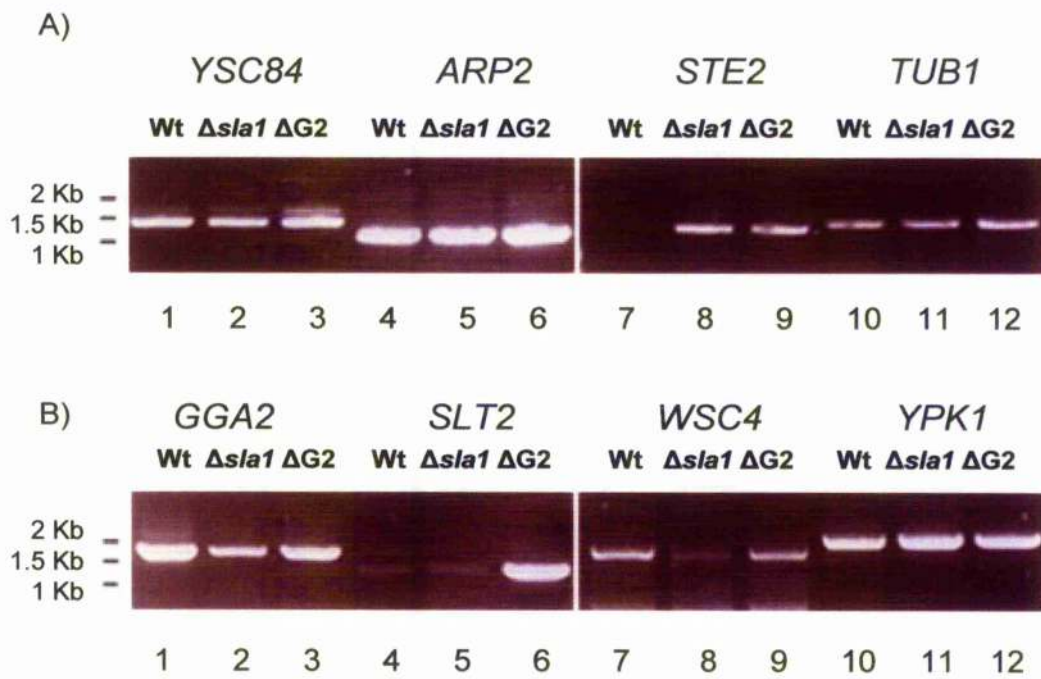


Figure 3-16. RT-PCR results confirm the trends in gene expression change identified by microarray data. To assess changes in gene expression of specific genes RT-PCR was performed using RNA from both wild-type cells (KAY 302)(lanes 1,4,7+10), *SLA1* deletion cells (KAY 300) (lanes 2,5,8+11) and *sla1ΔG2* cells (KAY382) (lanes 3,6,9+12). Primers specific for the genes, *YSC84*, *ARP2*, *STE2*, *YPK1*, *GGA2*, *SLT2*, *WSC4* and *YPK1* were used in these reactions. (A) Agarose gel showing products from *YSC84* amplification (Lanes 1,2+3), *ARP2* amplification (Lanes 4,5+6), *STE2* amplification (Lanes 7,8+9) and *TUB1* amplification (Lanes 10,11+12). (B) Agarose gel showing products from *GGA2* amplification (Lanes 1,2+3), *SLT2* amplification (Lanes 4,5+6), *WSC4* amplification (Lanes 7,8+9) and *YPK1* amplification (Lanes 10,11+12).

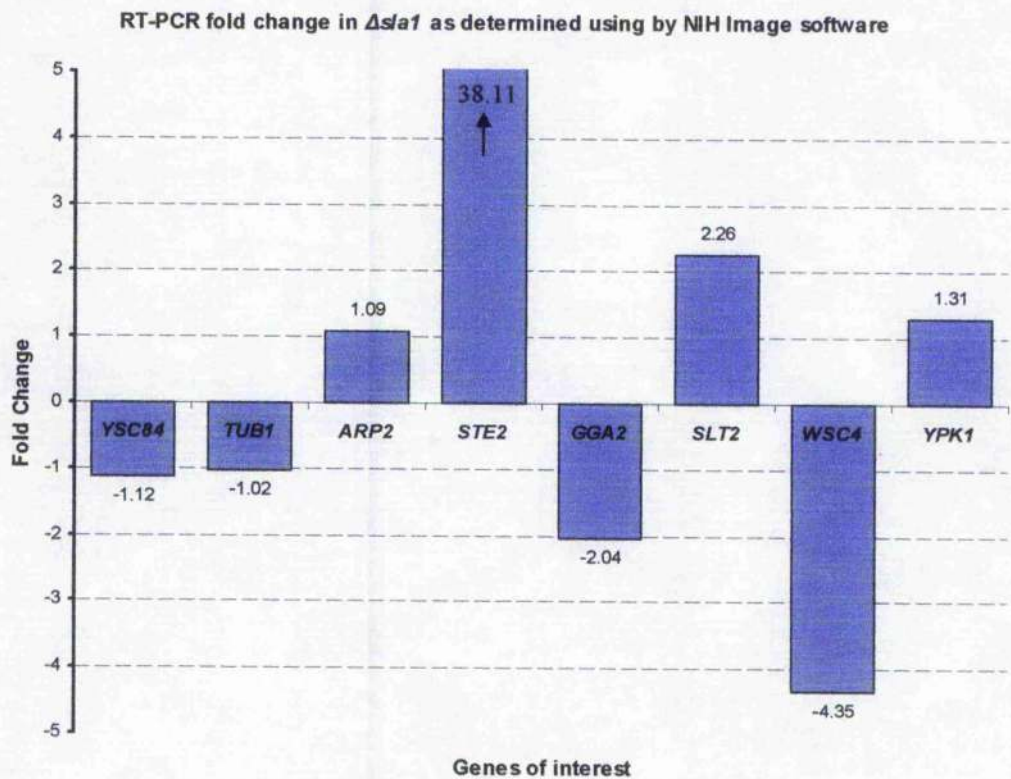


Figure 3-17. Fold changes in gene expression as identified by RT-PCR.
 Analysis of agarose gels images of specific RT-PCR products using NIH Image analysis software. The results shown demonstrate the fold change in product amplified from *sla1*/ Δ (KAY300) RNA compared to product from wild-type (KAY302) RNA.

3.3

Discussion

Sla1p is known to act as a multifunctional adaptor protein at the cell cortex, with roles in the regulation of endocytic and actin regulating proteins. Sla1p is required for the normal organisation of the cortical actin cytoskeleton in budding yeast (Holtzman *et al.*, 1993), which has recently been shown to be intimately linked to endocytic uptake. Sla1p localises to a subset of cortical patches which partially co-localise with actin patches (Ayscough *et al.*, 1999). In this chapter however, I investigate the localisation of Sla1p to the nucleus. Based on experimental results to date, a direct interaction between Sla1p and a nuclear protein has yet to be shown. Progress has however been made in the study of nuclear Sla1p, by determining the import mechanism of Sla1p and by studying the effect of gene deletion on genome-wide gene expression.

In this study Sla1p was shown to localise to the nucleus in *S. cerevisiae*. As demonstrated by myc-tagging of the protein, Sla1p shows a diffuse co-localisation with nuclear DAPI fluorescence, in addition to its previously reported co-localisation with cortical patches (section 3.2.1). Nuclear accumulation of Sla1-myc was unaffected by the cytoplasmic remodelling of actin and additional adaptive cellular responses which occurred during induction of the heat shock and mating response pathways, and during cell cycle progression. Cdc24p, the guanine nucleotide exchange factor for Cdc42p is known to export from the nucleus in response to induction of the mating response and during bud development, at which point it is known to activate the actin regulating Rho GTPase Cdc42p at sites of cell growth (Nern and Arkowitz, 2000). Nuclear Sla1p however does not respond in a similar manner.

Analysis of the *s1a1-Δ118-511-myc* deletion mutant (section 3.2.4), demonstrated the importance of residues 118-511 of Sla1p in the localisation of the protein to the nucleus. Deletion of these residues caused a decrease in nuclear co-localisation of *s1a1-Δ118-511-myc* but did not affect the localisation of the protein to cortical patches. Previous characterisation has shown that residues 118-511 of Sla1p are critical for the actin regulating abilities of Sla1p, with rhodamine phalloidin staining of a *s1a1-Δ118-511* mutant showing fewer, and enlarged cortical actin patches (Ayscough *et al.* 1999). This phenotype is similar to that seen in $\Delta s1a1$ cells, which have additionally been shown to demonstrate an increased resistance to Latrunculin-A, suggesting that the actin in these cells is less dynamic. *S1a1-Δ118-511-myc* is able to localise to patch structures at the cell cortex. These patches do not however co-localise

with the aberrant actin structures associated with this mutant (Gourlay *et al*, 2003). *Sla1-Δ118-511-myc* therefore retains the ability to localise to the cell cortex and is partially functional, as it has previously been shown to rescue the Abp1p dependence associated with *sla1* deletion (Gourlay *et al*, 2003).

Analysis of endocytic uptake in the *sla1-Δ118-511-myc* mutant demonstrated that fluid phase endocytic uptake is only marginally defective in a *sla1-Δ118-511-myc* strain (section 3.2.5). 2-hybrid analysis has shown that residues 118-511 of Sla1p interact with the central coiled-coil region of the Sla2p. This interaction has been confirmed biochemically (Gourlay *et al*, 2003). Studies suggest that Sla2p recruits the actin cytoskeleton to sites of endocytosis via interaction with Sla1p (Gourlay *et al*, 2003; Kaksonen *et al*, 2003). In support of this, in both a *sla1* deletion strain and a strain expressing *sla1-Δ118-511*, Sla2p is mislocalised; retaining a cortical localisation which does not significantly overlap with the aberrant actin structures seen in these cells (Ayscough *et al*, 1999; Gourlay *et al*, 2003). This data suggests that deletion of this region of Sla1p severs the link between Sla2p actin, blocking recruitment of actin to endocytic sites. Our study of the *sla1-Δ118-511-myc* mutant confirms a decrease in endocytic uptake, concurrent with this model. Levels of endocytosis in this mutant are however above that seen in the $\Delta s la1$ strain. In $\Delta s la1$ cells a significant reduction, but not total loss of endocytic uptake has been reported (Warren *et al*, 2002) and this observation has been confirmed in this study (section 3.2.5). Actin is less dynamic in $\Delta s la1$ cells as demonstrated by Latrunculin-A assays, however the demonstration of low levels of endocytic uptake in $\Delta s la1$ and *sla1-Δ118-511* strains suggests that the enlarged actin 'chunks' seen these cells may still be partially dynamic, allowing endocytosis to proceed at a reduced level. The increased uptake seen in the *sla1-Δ118-511* mutant when compared to $\Delta s la1$ suggests that while regulation of actin and interaction with Sla2p is lost in this mutant, the C-terminal regions of Sla1p may continue to promote endocytosis through C-terminal interactions.

Analysis of the localisation of the *sla1-Δ118-511-myc* mutant revealed a significant decrease in the nuclear localisation of the mutant protein of approximately 80%, as determined by image analysis software when compared to wild-type cells (section 3.2.4). Decreased nuclear accumulation of *sla1-Δ118-511-myc* suggests that residues 118-511 are critical for the nuclear localisation of Sla1p. Loss of this region may either prevent nuclear uptake of the protein or may prevent a nuclear interaction which normally retains the protein in the nucleus. These observations lead to an investigation of the mechanism of Sla1p uptake into the nucleus. Subsequent

investigation and sequence analysis identified several potential NLSs between residues 118-511 of Sla1p (section 3.2.6). The loss of these NLSs may prevent uptake of *sla1-Δ118-511-myc* into the nucleus due to loss of cargo recognition by karyopherins. Analysis of several karyopherin mutants was undertaken to determine the mechanism of nuclear translocation of Sla1p. Studies demonstrated that nuclear uptake of Sla1-myc was lost in an *rsl1* mutant (section 3.2.9), suggesting that the nuclear entry of Sla1p is mediated by Rsl1p. This protein is able to recognise cargo directly for nuclear translocation or in conjunction with the nuclear transport receptor, Srp1p. Due to recognition of NLSs by Rsp1p and Srp1p, one of the five NLSs identified between residues 118-511 is likely to mediate the nuclear translocation of Sla1p. Identification of the active NLS or NLSs however requires further investigation.

Analysis of the *sla1-ΔG2-myc* mutant strain was also undertaken (section 3.2.4 and 3.2.5). Partial deletion of the Gap2 region from residues 507-1008 caused a substantial increase in the nuclear accumulation of *sla1-ΔG2-myc*. Actin staining appeared similar to wild-type in these cells, as has been previously reported for a *sla1-ΔG2* strain (Ayscough et al, 1999). This lack of actin defect suggests that a low level of *sla1-ΔG2-myc* is functioning in actin regulation at the cell cortex and that this protein interacts with Sla2p, allowing recruitment of actin to endocytic sites. The *sla1-ΔG2-myc* strain however displays a reduction in endocytic uptake comparable to that seen in *Δsla1* cells. A potential mechanism for this endocytic inhibition is the abrogation of the ability of *sla1-ΔG2* to dissociate from endocytic complexes in the cytosol. Previous data has shown that the unphosphorylated form of Sla1p integrates into a trimeric Sla1/End3/Pan1 complex at the cell cortex, the dissociation of which is regulated by phosphorylation of Pan1p and Sla1p (Zeng et al, 2001). Endocytic defects have been previously reported following overexpression of GST-*Sla1-118-511* (Gourlay et al, 2003), a mutant which lacks the C-terminal repeat region thought to undergo phosphorylation by Prk1p (Zeng et al, 2001). *Sla1-118-511* is thereby predicted to be unable to dissociate from this endocytic trimeric complex. C-terminal Pan1p phosphorylation motifs are however present in the *sla1-ΔG2-myc* mutant, suggesting that *sla1-ΔG2-myc* undergoes phosphorylation. Deletion of domains in close proximity to the phosphorylated region may however interfere with the function of the phosphorylated form of *sla1-ΔG2-myc*.

Sequence analysis of the region removed in the *sla1-ΔG2* construct which encompasses residues 507 to 1008 of Sla1p, identified one potential bi-partite NLS and two potential NESs. The loss of these NESs would correlate with the nuclear

accumulation of *sla1-ΔG2-myc*, by blocking nuclear export of the mutant protein (section 3.2.6). Analysis of a *cram1/xpo1* karyopherin mutant, which encodes the general yeast exporter Crm1p/Xpo1p and which recognises and transports cargo containing leucine rich NLSs, did not however affect Sla1p localisation (section 3.2.10). Export of Sla1p may therefore be mediated by other yeast exportins. Some karyopherins are known to function bidirectionally; for example Msn5p which has been shown to export multiple proteins including Far1p, Mig1p and Pho4p (Blondel *et al*, 1999; Devit and Johnston, 1999; Kaffman *et al*, 1998) while also mediating import of the trimeric replication protein A (Yoshida and Blobel, 2001). Further analysis of both importins and exportins may therefore identify the karyopherin(s) mediating Sla1p export, as nuclear accumulation of the *sla1-ΔG2-myc* suggests Sla1p cycles through the nucleus.

Our studies suggest that Sla1p localises both to the cytosol and the nucleus in yeast. An interesting possibility is that activity and cellular localisation of Sla1p may be regulated primarily through its state of phosphorylation. Regulation may occur in a similar manner to Slt2p, whereby phosphorylation promotes nuclear entry and activity of the protein. Phosphorylation of proteins involved in actin regulation and endocytosis is mediated by members of the Ark/Prk serine/threonine family of protein kinases (for review see Smythe and Ayscough 2003). Sla1p has several potential Prk1p phosphorylation motifs found in the carboxy-terminal repeat region of the protein (Zeng *et al*, 2001). Previous data from this lab has determined 4 modified forms of Sla1p by 2-Dimensional gel analysis, suggesting modification as a mechanism of protein regulation (Derek Warren and Campbell Gourlay, unpublished data). In addition, Sla1p has been reported to interact with Glc7p, the catalytic subunit of protein phosphatase 1 (PP1), a major serine/threonine protein phosphatase, by yeast 2-hybrid analysis (Venturi *et al*, 2000). Dephosphorylation of endocytic proteins has been previously shown to involve Scd5p, a protein which partially co-localises with cortical actin patches and which interacts with Glc7p (Chang *et al*, 2002). Scd5p may be involved in targeting Glc7p to substrates that require dephosphorylation in order to regulate actin and endocytosis. Prk1p additionally negatively regulates Scd5p by phosphorylation (Henry *et al*, 2003), providing a mechanism for control of Scd5p recruitment of Glc7p to cortical patches. Sla1p may therefore be phosphorylated by the action of Prk1p and dephosphorylated by PP1 recruitment. Phosphorylation has been proposed as the mechanism of regulation for nuclear entry of a number of actin binding proteins, including cofilin (Ohta *et al*, 1989). Nuclear entry of the actin binding protein cofilin has been shown to be linked to the phosphorylation state of the protein, with dephosphorylated cofilin being transported

into the nucleus following DMSO treatment or heat shock. Based on our data and previous findings, a mechanism for Sla1p regulation and nuclear entry is proposed in figure 3-18.

Progress has also been made in the investigation of a potential nuclear role of nuclear Sla1p. Microarray analysis of total RNA from wild-type and *Asla1* cells was performed to in order to identify transcriptional effects of *sla1* deletion. Our results demonstrate significant changes in the expression of 69 genes following *sla1* deletion (section 3.2.11). Variable gene expression may be caused by a variety of mechanisms following gene deletion, including loss of direct interactions made by the protein, dysregulation of signalling cascades or adaptive changes in expression, promoted in order to counteract protein loss. Seven membrane transporters have been identified as being downregulated in the *Asla1* strain. These receptors are Opt2p, Pho84p, Thi7p, Tna1p, Fui1p and Gap1p. Previous reports have shown that *Asla1* cells fail to undergo normal cell cycle arrest in response to nutrient starvation (Care *et al*, 2004). This inability to respond to nutrient starvation may be a consequence of the downregulation of membrane transporters in this strain and an inability to sense nutritional deficiencies in the surrounding environment. Many additional actin and endocytosis mutants including *end3Δ*, *rvs161Δ*, *vrp1Δ*, and *sla2Δ* (Care *et al*, 2004), also do not undergo this cell cycle arrest, during which preparation to survive nutrient limitation and other adverse environmental conditions occurs. Sla1p may therefore be involved directly or indirectly in the regulation of transcription of membrane transport receptors.

Upregulation of *SLT2*, *ARP2* and *YPK1* occurs in *sla1* deletion cells. Arp2p is a component of the actin nucleating and filament branching complex Arp2/3. Slt2p is a component of the cell integrity MAP kinase pathway. Phosphorylated Slt2p is known to dimerise and enter the nucleus, activating the transcription factor SBF and expression of SBF targets, which include genes involved in cell wall repair. *SLA1* deletion induces upregulation of *SLT2*, potentially either by mislocalisation of Rho1p or by defects endocytic uptake, and therefore potentially in response to cell wall damage (Ayscough *et al*, 1999). Mislocalisation of Rho1p and aberrant cell wall synthesis may therefore promote *SLT2* upregulation, or potentially nuclear Sla1p may regulate gene transcription directly. Ypk1p is a serine/threonine protein kinase which has a role in the cell wall integrity pathway. Deletion of *ypk1* has been shown to cause depolarisation and enlargement of cortical actin patches and temperature sensitivity, a phenotype which was rescued by growth of cells in the presence of sorbitol, an indication of cell wall integrity defects (Roelants *et al*, 2002; Hampsey, 1997). *Sla1* deletion and cell wall

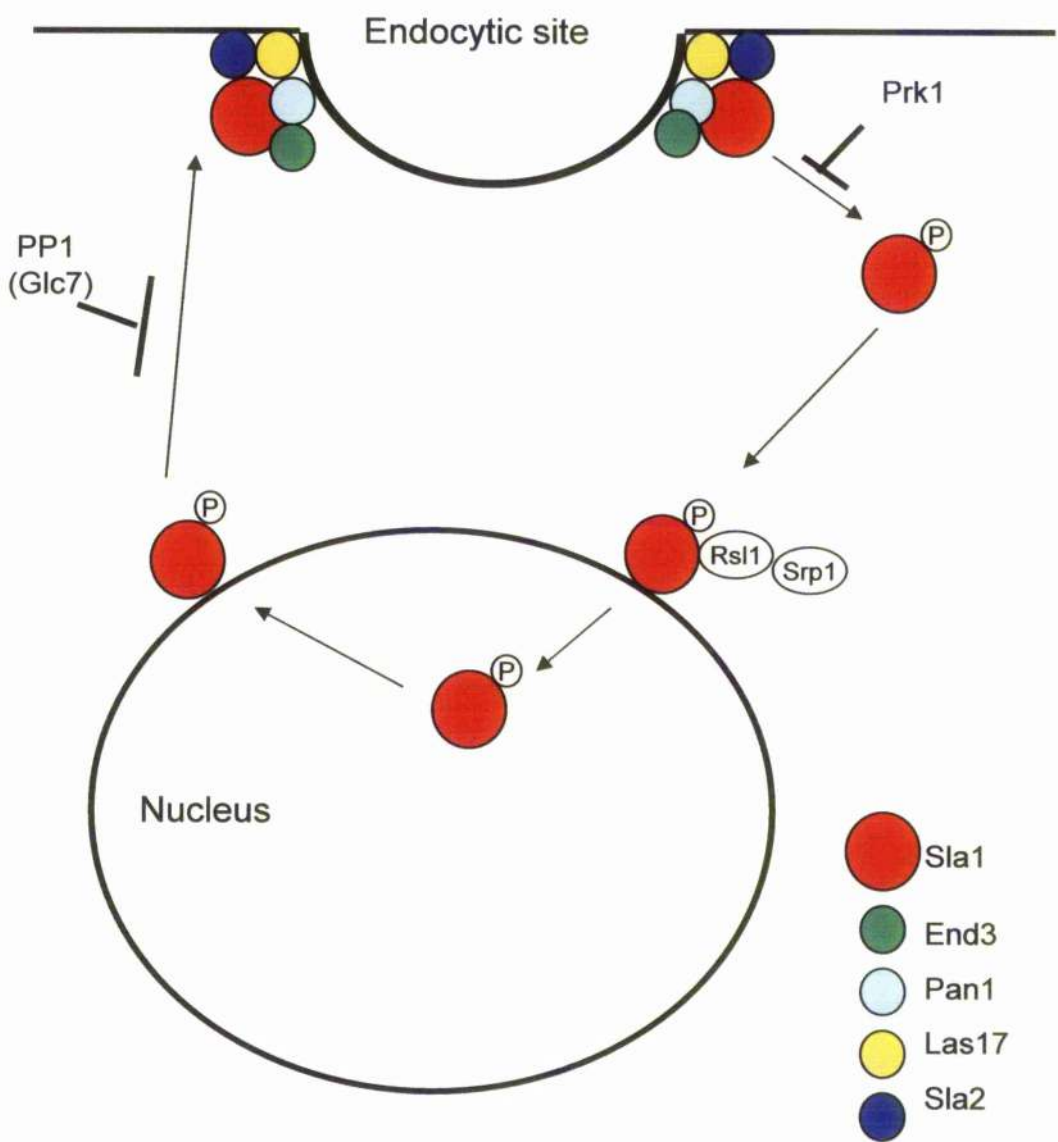


Figure 3-18. Proposed mechanism for Sla1 entry into the nucleus. Phosphorylation and dephosphorylation of Sla1p, mediated by Prk1 and a phosphatase such as Glc7p is proposed to regulate the localisation of Sla1. Translocation into the nucleus is mediated by the nuclear transport receptor Rsl1p, possibly in conjunction with Srp1p. Nuclear entry occurs by an undefined mechanism but is thought to require specific NLSs in the Sla1p sequence. Dephosphorylated Sla1p forms a trimeric complex with End3p and Pan1p, which localises to endocytic sites. Phosphorylation of Sla1p may therefore specify nuclear uptake.

defects therefore appear to be intimately linked. This may be due to a lack of Sla1p at the cell cortex or due to transcriptional effects caused by *s1a1* deletion. In addition, downregulation of *GGA2* and *WSC4* is also shown. Gga2p is involved in Golgi to vacuole transport while Wsc4p is thought to play a role in the cell wall integrity response pathway.

This study has not defined a specific role for nuclear Sla1p. It should be considered however that nuclear Sla1p may continue to regulate actin in a nuclear structural role. Studies have provided mounting evidence of actin, actin regulating proteins and actin related proteins in the nucleus (for review see Rando *et al*, 2000). Recent studies have also identified actin as a component of nuclear filaments in *Xenopus* oocytes (Kiseleva *et al*, 2004), suggesting nuclear actin may form part of a structural 'nucleoskeleton'. Rhodamine phalloidin staining does not recognise nuclear actin, which suggests that actin may either form novel structures or short filaments in the nucleus, or that additional proteins may block the phalloidin binding sites on actin filaments. Identification of nuclear actin with the monoclonal anti-actin antibody (2G2) however reveals a punctate pattern of immunogold labelling on nuclear filaments (Kiseleva *et al*, 2004), reminiscent of actin incorporation in the flexible filamentous network present in red blood cells (figure 3-19). These nuclear filaments additionally show sensitivity to the actin disrupting macrolide Latrunculin-A and the actin stabilising drug Jasplakinolide. Due to space constraints in the nucleus, any filamentous network may also require this flexible quality, of which actin may form a part. Cytoskeletal filaments found in red blood cells are composed primarily of flexible spectrin rods, linked at 'junctional complexes' containing short actin filaments and other cytoskeletal proteins including protein 4.1. The nuclear filaments with which actin was found to associate also contain protein 4.1 (Kiseleva *et al*, 2004).

Actin has also been identified as a component of chromatin remodelling complexes in the nucleus. Actin is known to form part of the mammalian BAF complex and yeast Ino80 complex, both of which are SWI/SNF-like chromatin remodelling complexes which alter the topology of nucleosomal DNA (for review see Olave *et al*, 2002; Blessing *et al*, 2004). Additionally, the NuA4 complex; a chromatin remodelling complex with histone acetylase activity, has also been shown to contain actin and recent studies have also shown the requirement of nuclear actin for transcription by RNA Polymerase II (Philimonenko *et al*, 2004). These studies demonstrate functional roles for nuclear actin.

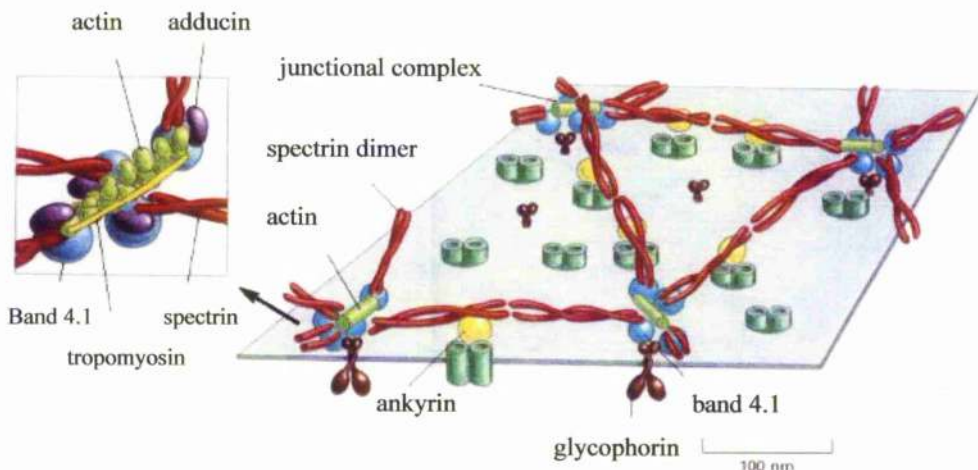


Figure 3-19. The flexible cytoskeletal network found in red blood cells.

The filamentous network present in red blood cells is composed primarily of flexible spectrin heterodimers (red). Spectrin molecules are linked at 'junctional complexes' (shown enlarged on the left) which contain small actin polymers (light green), protein 4.1 (blue), tropomyosin (yellow rods) and adducin. Additional proteins are involved in the linkage of the filamentous network to the cell membrane. Figure adapted from Alberts *et al.*, 2002.

Many ARP (actin related proteins) have been shown to form part of nuclear complexes. Although similar to actin at the amino acid level (between 16-60% sequence identity) most ARPs are not functionally similar to actin (Olave *et al*, 2002). Only Arp1p is known to be able to form filaments and interact with some actin binding proteins. The presence of nuclear ARPs does not therefore argue for the presence of actin and actin binding proteins in the nucleus. Studies have however determined the presence of many actin regulatory proteins in the nucleus (for review see Bettinger *et al*, 2004). CapG is a member of the gelsolin related capping protein family that has been localised to the nucleus (Onoda *et al*, 1993). Dephosphorylated cofilin has also been localised to the nucleus, and studies suggest it is responsible for nuclear entry of actin (Ohta *et al*, 1989; Pendleton *et al*, 2003). The actin monomer binding protein profilin is also implicated in the export of actin from the nucleus (Stuven *et al*, 2003), while emerin is a nuclear inner membrane thought to form part of the nuclear lamina, a scaffold structure thought to control chromosome architecture by anchoring chromatin components. Recent studies have shown emerin to be an actin regulatory protein which promotes actin polymerisation by binding to and stabilising the pointed ends of actin filaments *in vitro* (Holaska *et al*, 2004). It is proposed therefore that emerin stabilises and promotes formation of a nuclear actin network, involving short actin filaments and linking lamin filaments with other nuclear membrane proteins (Bengtsson and Wilson, 2004).

Actin binding proteins known to localise to the nucleus therefore include: cofilin, CapG (a gelsolin homologue), emerin, Protein 4.1, cofilin and profilin (for review see Rando *et al*, 2000; Bettinger *et al*, 2004). Many of these proteins are small enough to passively diffuse into the nucleus, however others require active transport. The identification of actin in nuclear isolations of *Xenopus* oocytes, forming part of a filamentous matrix (Kiseleva *et al*, 2004) and in filamentous structures inside the permeabilised nuclei of mouse cells (Nakayasu *et al*, 1985) suggests nuclear actin retains its structural role. The nuclear matrix is tentatively regarded as a potential homologue of the cytoplasmic cytoskeleton, and as such Sla1p and additional actin regulatory proteins may continue to regulate actin in this location.

4 CHARACTERISING THE ROLE OF YSC84

Abstract

Ysc84p is a cortical patch protein, required in conjunction with Lsb5p for the polarisation of the actin cytoskeleton, normal growth rates and growth at high temperatures (Dewar *et al*, 2002). Using purified protein, our studies show the direct binding of the Ysc84p protein to filamentous actin. In addition, we also show the first evidence of the ability of Ysc84p to both sever and cap actin filaments. Ysc84p has a highly conserved N-terminal region and C-terminal SH3 domain (figure 1-14). Our studies show the actin binding, capping and severing ability to be a function of the highly conserved N-terminal region. Data presented in this chapter suggests Ysc84p plays a direct role in the regulation of actin at cortical actin patch sites, enabling breakdown of filaments and preventing further polymerisation at filament ends.

4.1 Introduction

Ysc84p is a cortical patch protein known to interact with Sla1p (Uetz *et al*, 2000; Drees *et al*, 2001; Dewar *et al*, 2002). Ysc84p has also been shown to interact with Las17p in a 2-hybrid assay. Las17p is an Arp2/3 complex activator which also localises to cortical patches (Madania *et al*, 1999). A genetic interaction between *YSC84* and *LSB5* has also been shown. *LSB5* encodes a protein with an involvement in vesicle trafficking and similarity to the GGA (Golgi-localizing, gamma-adaptin ear homology domain, ARF-binding) proteins. This genetic interaction suggests overlapping roles for Ysc84p and Lsb5p (Dewar *et al*, 2002). Localisation of Ysc84p to cortical actin patches is dependent on F-actin but independent of Sla1p (Dewar *et al*, 2002). This localisation and its dependence on the actin network suggesting a possible role for Ysc84p in the regulation of actin.

Previous studies did not find a specific role for Ysc84p at cortical patch sites nor did they identify an actin binding domain in the protein. A phosphorylation site at serine residue S³⁰¹ of Ysc84p has however been determined by large scale phosphoproteome analysis (Ficaro *et al*, 2002), and Ysc84p homologues in *S. cerevisiae* (Madania *et al*, 1999; Dewar *et al*, 2002), mouse (Dowar *et al*, 2002; Aoki *et al*, 2000), and human cells have been identified. The N-terminus of Ysc84p, and the C-terminal SH3 domain are both highly conserved between Ysc84p homologues (figure 1-14). SH3 domains have been shown to bind specifically to proline rich regions including PxxP motifs (Macias *et al*, 2002; Cestra *et al*, 1999). It is proposed that SH3 domains are involved in regulating

the interactions of signalling molecules with cytoskeletal proteins (Drubin, 1990). SH3 domains, such as the one present in Ysc84p have been identified in many actin-associated proteins (Lila and Drubin, 1997).

Localisation of Ysc84p to cortical patches suggests a potential role in the regulation of actin. Many known cortical patch proteins affect actin dynamics by regulation of the Arp2/3 complex, as in the case of Las17p, Pan1p and Abp1p, or by direct interaction with actin, as in the case of Cof1p and Pfy1p. While an actin binding domain has not been identified in Ysc84p or its homologues in previous studies, the mammalian Ysc84p homologue, hSH3yl-1 has been shown to interact with the actin cytoskeleton of *S. cerevisiae*. Overexpression of hSH3yl-1 in wild-type yeast cells caused depolarisation of the actin cytoskeleton, indicating that the mammalian protein is able to interact with the yeast actin network, either directly or indirectly (Dewar et al, 2002).

To investigate the conservation between Ysc84p and its mammalian homologue, the ability of hSH3yl-1 to functionally replace Ysc84p in the yeast cell was examined. To examine the function of Ysc84p, fragments of Ysc84p were expressed and purified as fusion proteins, coupled to a glutathione-S-transferase (GST) tag (section 4.2.2). Fusion proteins were then used for antibody generation (section 4.2.8) and for analysis with F-actin (section 4.2.3 - 4.2.7). Our results demonstrate the ability of Ysc84p to bind directly to F-actin and to cap and sever actin filaments *in vitro* (sections 4.2.3-4.2.7). Determination of these *in vitro* abilities of the protein may provide insight into the precise role of Ysc84p at cortical patches.

4.2 Results

4.2.1 hSH3yl-1 can partially replace the function of Ysc84p

Deletion of both *YSC84* and *LSB5* generates cellular phenotypes not seen following deletion of either single gene. *YSC84* and *LSB5* deletion generates phenotypic defects including a decreased growth rate at 37°C, depolarisation of the actin network and endocytic defects. Previous studies have demonstrated the functional conservation between homologues of actin regulating proteins in different species, as in the case of profilin (Rothkegel *et al.*, 1996) and members of the ADF/cofilin family (for review see Moon and Drubin, 1995). Mammalian homologues have in many cases been able to functionally replace the yeast proteins when expressed in *S. cerevisiae*. Conservation between the conserved amino-terminal region (43% identity) and SH3 domain (46% identity) of Ysc84p and its homologues suggested functional conservation may exist between these proteins (figure 1-14) (Dewar *et al.*, 2002).

To examine the ability of human SH3yl-1 (hSH3yl-1) to functionally replace the yeast protein, hSh3yl-1 encoding cDNA (pKA252) was obtained (a generous gift from Dr. Hata, University of Tokyo) and cloned into a methionine inducible yeast expression vector which utilised the MET25 promoter. The hSH3yl-1 encoding cDNA was cloned into this yeast expression vector (pKA256) at the Xho1 restriction enzyme site. Yeast expression plasmid, pMET-hSH3yl-1 (pKA392) was therefore generated. This construct was transformed into a Δ *ysc84* Δ *lsb5* mutant (KAY516). Prior experience of the p416MET25 expression plasmid (pKA256) has demonstrated low levels of expression from the promoter, which do not require methionine induction. This 'leaky' expression of hSH3yl-1 was tested and was shown to be able to rescue the temperature dependent growth defect of the Δ *ysc84* Δ *lsb5* mutant and partially rescue its endocytic defect (figure 4-1 and figure 4-2). Induction of the protein at these levels did not however rescue the actin or slow growth phenotype (data not shown) of this strain. This data demonstrates that hSH3yl-1 is partially functional in *S. cerevisiae*. Increased expression of hSH3yl-1 by growth of the cells in media lacking methionine failed to rescue the slow growth phenotype or further rescue the endocytic defect in these cells. Overexpression of hSH3yl-1 however produced enlarged cells which showed total depolarisation of the actin cytoskeleton (data not shown). Prior analysis of Δ *ysc84* Δ *lsb5* mutants had highlighted extreme depolarisation of actin (Dewar *et al.*, 2002). Some actin patches were however seen to localise to the cytokinetic ring. This minor polarisation of

actin was however lost following overexpression of hSH3yl-1, indicating that the protein interacts with actin.

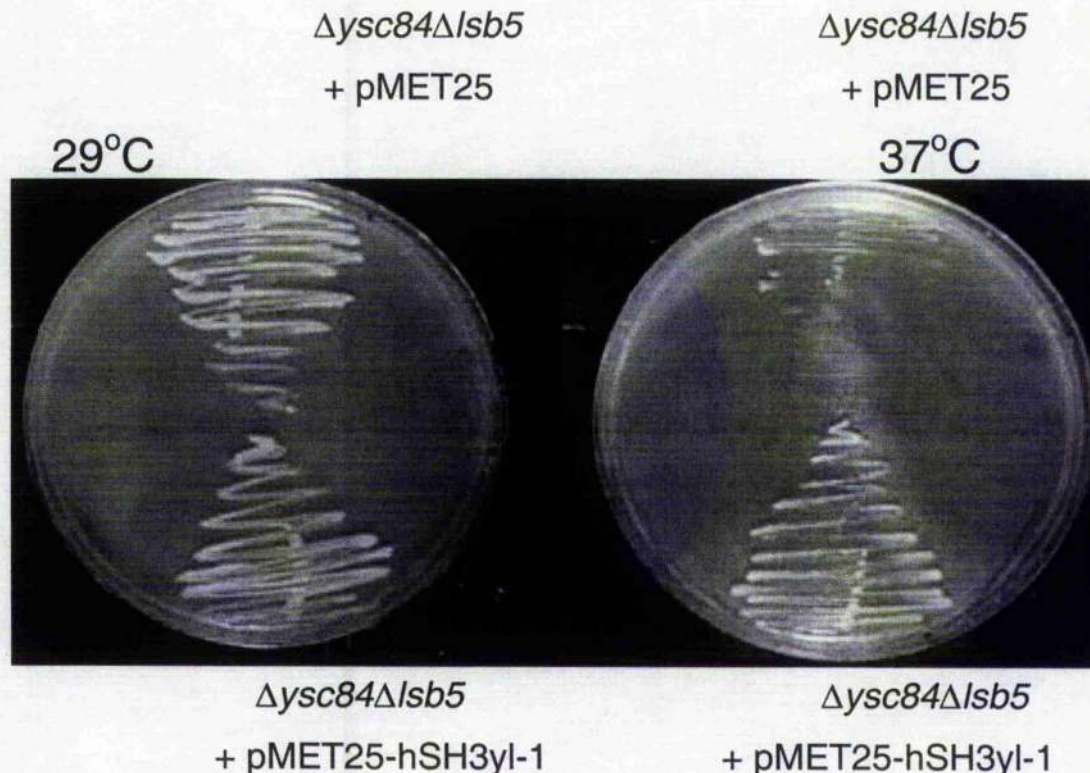
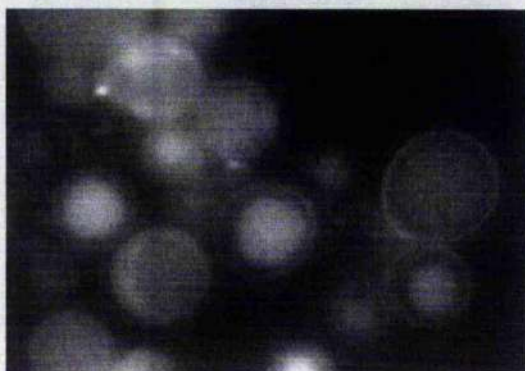
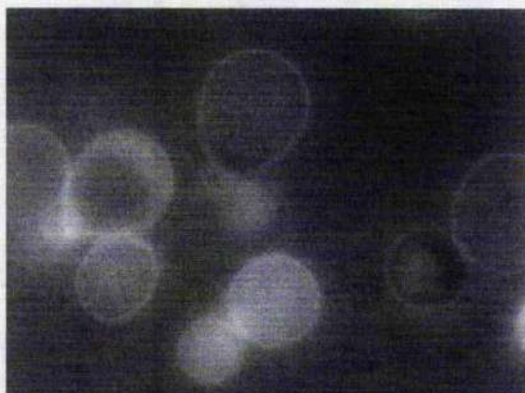


Figure 4-1. hSH3yl-1 expression in yeast rescues the temperature dependent growth phenotype of a $\Delta ysc84\Delta lsb5$ strain.

$\Delta ysc84\Delta lsb5$ (KAY516) cells transformed with, (top) empty vector (pMET25) or ,(lower) hSH3yl-1 expressing plasmid (pMET25 + hSH3yl-1) were grown on synthetic drop-out media at 29°C or 37°C for 2 days. Expression of hSH3yl-1 rescued the growth defect of the $\Delta ysc84\Delta lsb5$ strain at 37°C. This data has been published by Dewar and colleagues (Dewar *et al*, 2002).

Δ ysc84 Δ lsb5 + pMET25



Δ ysc84 Δ lsb5 + pMET25-hSH3yl-1

Figure 4-2. hSH3yl-1 expression in yeast partially rescues the endocytic defect but not the actin defect of a Δ ysc84 Δ lsb5 strain.

Δ ysc84 Δ lsb5 (KAY516) cells transformed with, (top panels) empty vector (pMET25) or, (lower panels) hSH3yl-1 expressing plasmid (pMET25-hSH3yl-1) were analysed by lucifer yellow uptake assay. Expression of hSH3yl-1 demonstrates a partial rescue of the endocytosis defects seen in this Δ ysc84 Δ lsb5 mutant strain.

4.2.2 Generation of Ysc84p fusion proteins

Functional characterisation of Ysc84p was undertaken with the generation of several Ysc84p fusion constructs. These constructs allowed high level expression and purification of specific regions of the protein. Due to the presence of an intron, the *YSC84* coding sequence was initially amplified by RT-PCR (section 2.9.11) from RNA isolated from wild-type (KAY 302) yeast cells (section 2.9.1). 1 µg of RNA and oligonucleotides oKA236 and oKA237 were used to perform this RT-PCR reaction, and the RT-PCR product obtained was analysed by agarose gel electrophoresis. The product generated was 1.4 Kb in size (figure 4-3). The intron in the *YSC84* gene lies between nucleotides 47 and 217. Introns are found infrequently in *S. cerevisiae*, although an intron is also present in the *LSB3* gene, which encodes the *S. cerevisiae* homologue of Ysc84p, Lsb3p. Amplification of *YSC84* from RNA ensured removal of the intron from the gene sequence by mRNA splicing. The size of the *YSC84* coding sequence was therefore expected to be 1407 bp.

The RT-PCR product was cloned directly into the pCR®4-TOPO-TA vector (Invitrogen), which uses the end terminal overhangs generated by PCR for cloning of the product. Integration generated plasmid pCR®4-TOPO-YSC84 (pKA259). The presence of the *YSC84* gene in the correct orientation in this plasmid was confirmed by sequencing with oligonucleotide primers M13.Rev and T7. This plasmid was then used as template for the amplification of full length *YSC84* and *YSC84* fragments. PCR amplification using oligonucleotides oKA236 and oKA237 engineered BamHI restriction enzyme sites onto the ends of *YSC84*. This PCR product from was then incubated with BamHI to digest the ends of the product and to enable cloning into the BamH1 site of a linearised pGEX4T1 GST-fusion vector (pKA142). This cloning generated plasmid pGEX4T1-YSC84 (pKA279), which encoded full-length Ysc84p in fusion with an amino-terminal GST tag (GST-Ysc84). A region encoding the highly conserved N-terminal region of Ysc84p was also amplified from the pKA259 plasmid (figure 4-4). PCR was performed using oligonucleotides oKA236 and oKA239 which generated BamH1 restriction sites at product ends, which were then used to clone the 654 bp product which encoded residues 1-218 of Ysc84p, into the BamH1 site of pGEX4T1 (pKA142). Cloning generated plasmid pGEX4T1-*ysc84(1-654)* (pKA278), which encoded a 218 amino acid fragment of Ysc84p in fusion with an amino-terminal GST tag (GST-Ysc84-Nt). An additional 24 residues of the central region of Ysc84p

was included in this fragment, in order to encompass a region highly conserved between Ysc84p and its *S. cerevisiae* homologue Lsb3p, which may have been important for the function of the N-terminal region. A diagram of the Ysc84p and the amino terminal fragment cloned is shown in figure 4-4. Clones were checked by sequencing to ensure correct amplification of the gene and integration in-frame with the encoded GST tag.

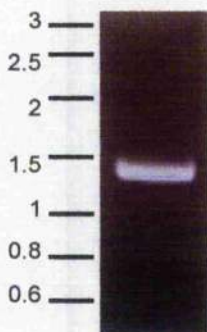


Figure 4-3. *YSC84* amplified by RT-PCR. RT-PCR was performed using oligonucleotides oK236 and oK237 and RNA from wild-type cells (KAY 302). The product was analysed by agarose gel electrophoresis as shown. The generated product was 1.4 Kb in size.

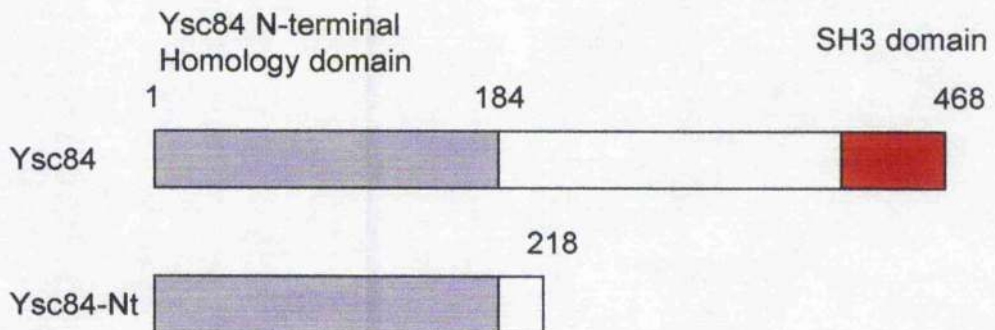


Figure 4-4. Diagram of Ysc84p and the Ysc84-Nt fragment fused to GST. Full length Ysc84p is a 468 residue protein containing a conserved amino-terminal domain and carboxy-terminal SH3 domain. The highly conserved amino-terminal of Ysc84p encompasses residues 1-184. An additional 24 residues were included in fragment Ysc84-Nt to include a region highly conserved between Ysc84 1 and Lsb3.

4.2.3 Ysc84p and the conserved N-terminal region of Ysc84p bind directly to F-actin

While previous analysis did not identify a region of Ysc84p which contained significant homology to known actin binding motifs (Dewar et al 2002), localisation of Ysc84p to cortical actin patches and the ability of hSH3yl-1 to interact with the yeast actin cytoskeleton suggested that the actin binding ability of Ysc84p should be investigated. F-actin binding abilities of GST-tagged full length Ysc84p (GST-Ysc84) and the partial coding sequence (GST-Ysc84-Nt) were determined by high speed F-actin sedimentation assays. The central principle of this assay is the ability to pellet F-actin in solution, by ultracentrifugation for 20 minutes at 100000 rpm. Unbound protein molecules will remain in the supernatant, whereas F-actin binding proteins will be found in the pellet fraction.

pGEX4T1-YSC84 (pKA279) and pGEX4T1-*ysc84*(1-654) (pKA278) expression plasmids were transformed (section 2.3.9) into bacterial *E. coli* DH5 α cells. These expression plasmids encoded GST-tagged Ysc84p fusions constructs corresponding to full length Ysc84p and a fragment encompassing residues 1-218 respectively. Expression of these fusion constructs was induced as described in section 2.6.7. Cell lysates were incubated with glutathionine sepharose[®] 4B beads and fusion proteins released by incubation of the beads with 10 mM reduced glutathionine, as described in section 2.6.8. Eluted proteins were stored at -20°C. The purity of the fusion proteins was determined by SDS-page analysis (figure 4-5) and their concentration determined by spectrometry (section 2.6.13). The expected molecular weights of Ysc84p and Ysc84-Nt are 50.2 kDa and 22 kDa respectively. Addition of the GST tag increases the molecular weight of these fusion proteins by 26 kDa. High speed F-actin sedimentation assays were performed with these purified fusion proteins as described in section 2.6.10. Increasing concentrations of GST-Ysc84 and GST-Ysc84-Nt were incubated with known concentrations of F-actin and incubations performed in actin binding buffer (ABB; 20 mM TRIS, 0.1 M NaCl, 2 mM MgCl₂, 1 mM ATP, 1 mM DTT, 0.1 mM CaCl₂) at 25°C for 20 minutes. Reactions were then centrifuged at 100,000 rpm for 20 minutes to allow F-actin to form a pellet. Equivalent volumes of supernatant and pellet fractions from each of these reactions were then analysed by SDS-page gel electrophoresis. Assays results are shown in figure 4-6.

The effect of coupling Ysc84p and a Ysc84p fragment to a GST tag was considered. GST tags have been previously reported to dimerise in solution, potentially causing aggregation of the tagged protein and invalidation of results. By performing sedimentation assays in duplicate, both in the presence and absence of actin however, this effect was examined. Significant aggregation and pelleting of the fusion proteins in the absence of actin was not seen. Recloning of the fragment into additional tagging vectors was however undertaken in order to remove this potential consideration. Expression of amino-terminally histidine tagged Ysc84p and Ysc84p fragments from the pTrCHis vector (Invitrogen) was however unsuccessful.

Analysis of the results of both F-actin sedimentation assays (figure 4-6) demonstrates a significant increase in the amount of fusion protein in the pellet fraction when incubated with F-actin. This is most obviously demonstrated in the comparison of reactions 3 and 4 (figure 4-6A) which show an increase in the quantity of GST-Ysc84 in the pellet fraction when incubated with F-actin. Equally, the same trend is seen when comparing reactions 5 and 6 (figure 4-6B) in which an increase in the quantity of GST-Ysc84-Nt in the pellet fraction is seen, when incubated with F-actin. This data demonstrates that both GST-Ysc84 and GST-Ysc84-Nt binding directly to F-actin *in vitro*. Additionally, the result shown in reaction 3 and 4 (figure 4-6B) is intriguing. Actin in reaction 3 is primarily found in the supernatant fraction suggesting a breakdown of F-actin into small filaments or monomers which would not pellet, following incubation with GST-Ysc84-Nt. This result suggests a depolymerising or severing activity in the GST-Ysc84-Nt fusion construct.

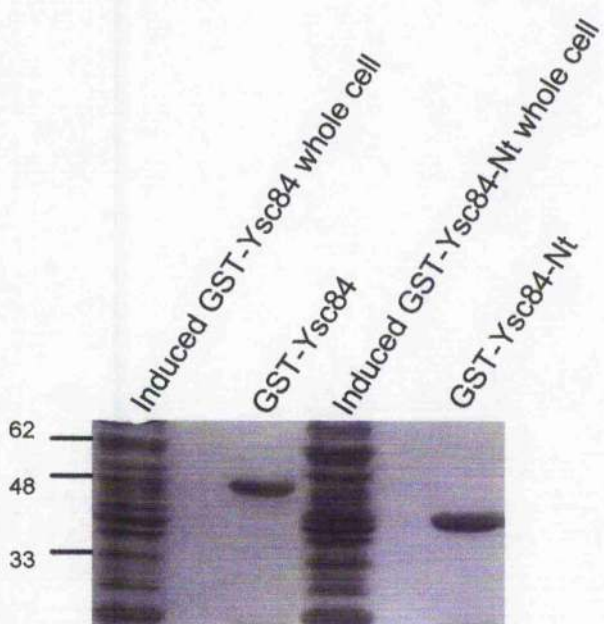
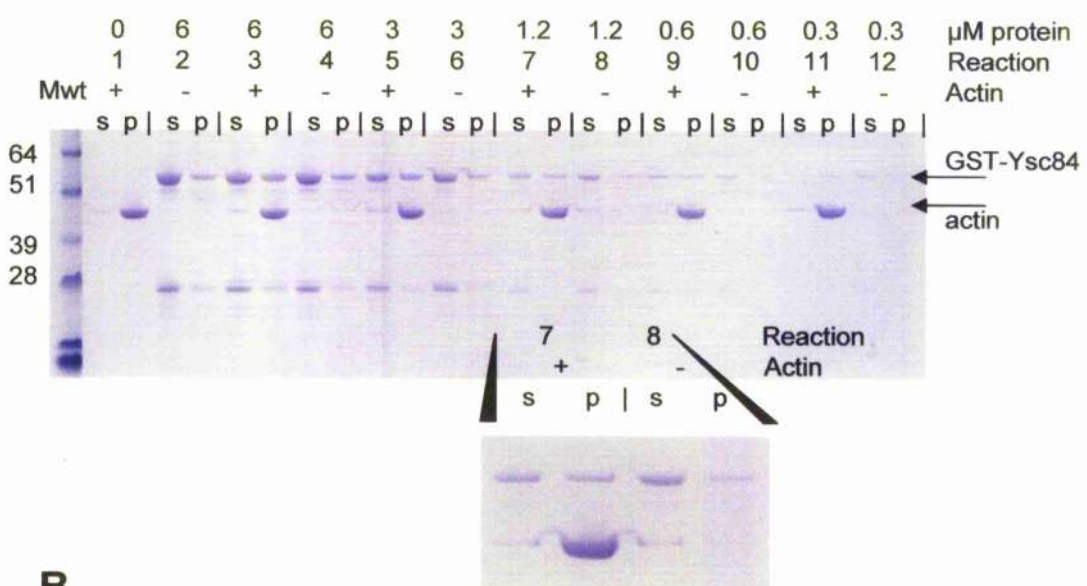
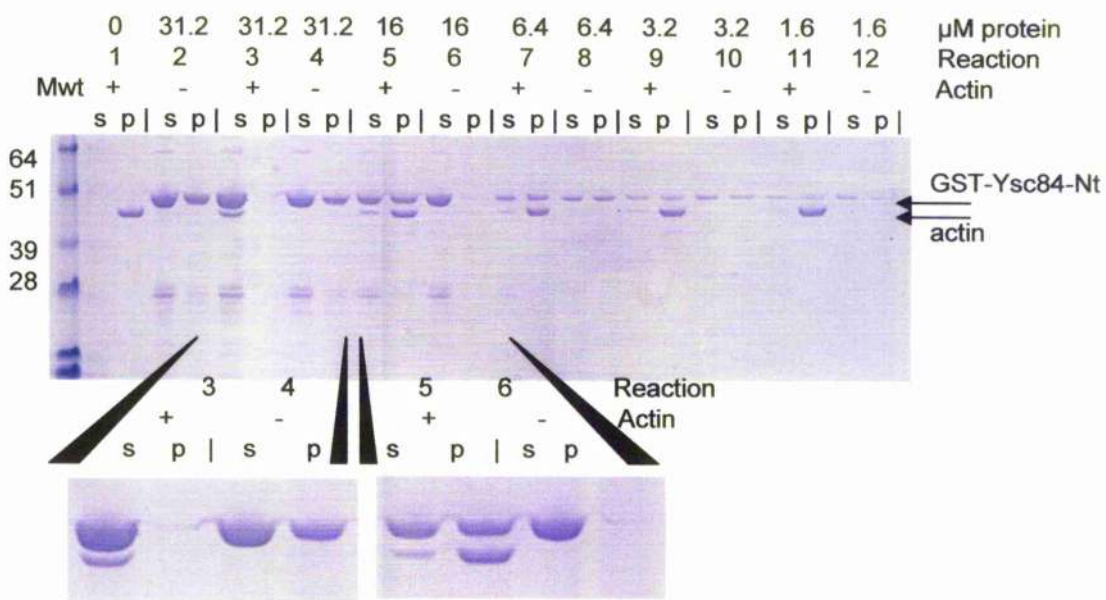


Figure 4-5. Purification of GST-Ysc84 and GST-Ysc84-Nt fusion proteins. The purity of GST-Ysc84 and GST-Ysc84-Nt was examined by electrophoresis on a 12% SDS-polyacrylamide gel and coomassie staining of the gel as shown above. The expected molecular weights of GST-Ysc84 and GST-Ysc84-Nt are 76.2 kDa and 48 kDa respectively. Whole cell extracts before purification of the induced proteins are also shown.

A**B****Figure 4-6. Analysis of GST-Ysc84 and GST-Ysc84-Nt interaction with F-actin.**

Decreasing concentrations of protein were incubated with or without F-actin and subjected to high-speed centrifugation. Equivalent amounts of the supernatant fraction (s) and pellet fraction (p) obtained were then analysed by SDS-page gel electrophoresis. Controls reaction containing actin alone (reaction 1) and protein alone (reaction 2) are also shown. (A) Decreasing concentrations of GST-Ysc84, from 6 to 0.1 μM , were incubated with or without 6.8 μM F-actin and subjected to high-speed centrifugation. An increased amount of GST-Ysc84 is seen in the pellet fraction when incubated with actin. (B) Decreasing concentrations of GST-Ysc84-Nt, from 31.5 to 0.6 μM , were incubated with or without 6.8 μM F-actin and subjected to high-speed centrifugation. Reaction 3 demonstrates the presence of actin primarily in the supernatant fraction, suggesting a severing activity for GST-Ysc84-Nt. The predicted Mwt of actin is 43 kDa. Predicted Mwts of GST-Ysc84 and GST-Ysc84-Nt are 76.2 kDa and 48 kDa respectively. A molecular weight standard is shown on the far left of the gel with standard molecular weights shown in kilodaltons (kDa).

4.2.4 Analysis of the Ysc84p sequence for actin binding regions

Previous studies had not identified regions of Ysc84p which showed homology to known actin binding motifs, and as such had not identified Ysc84p as a potential actin binding protein (Dewar *et al*, 2002). Prior cellular evidence did however suggest a close association of Ysc84p with the actin network, as demonstrated by Ysc84p mislocalisation upon depolymerisation of the actin cytoskeleton with Latrunculin-A (Dewar *et al*, 2002). Data shown in section 2.4.2 demonstrates the ability of GST-Ysc84p and GST-Ysc84-Nt to bind directly to F-actin in *vitro*. This suggested that Ysc84p localisation to cortical actin patches may be mediated by direct binding of the protein to filamentous actin and not as previously suggested, via another protein or complex. Close analysis of the Ysc84p sequence subsequently identified two regions of Ysc84p which contained a high concentration of hydrophobic residues including leucine, which are known to be highly conserved in actin binding WASP homology 2 (WH2) domains (Dominguez, 2004). These regions were thought most likely to mediate direct binding to F-actin, in the absence of significant homology to known actin binding motifs. The location and sequence of these regions is shown in figure 4-7.

A

↓

MGINNPIPRSL**KSETKKA**AKVLRSFVKPNQVFGADQVIPPYVLKRAKGLAIITVLKAGFLFS
GRAGSGVIVARLKDGTWSAPSAIAMAGAGAGGMVGVELDFVFI**NSEEAVRSFSEFGTIT**
 LGGNVSVSAGPLGRSAEAAASASTGGVSAVFAYSKSKGLFAGVSVEGSAILERREANRKFY
 |
 184 |
GDNCTSKMILSGRVKVPPAADPLLRILESRAF**NFTRHD**DDNASGDDFYDDGQYS^{*}DNTSH
 YYDDIPDSFDSTDESSTRPNTRSSRRGMSLGSRSRYDDYDDDGYGRGRGYGDFDSED
 EDYDYGRSPNRSSRNRGPIDRGTPRANTRWEDDLYDRDTEYSRPNHSGRDYDNTRG
 NRRGYGRERGYSLGHGPTHPSNMSNVDDLSHKMSKTGLGNESTATNSATPTAVALYNFA
 GEQPGDLAFKKGDVITLKKSDSQNDWWTGRTNGKEGIFPANYVRVS

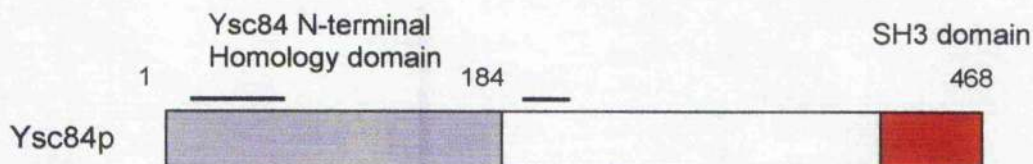
B

Figure 4-7. Ysc84p has two potential actin binding regions. A) Protein sequence of the 468 amino-acid Ysc84 protein. The conserved C-terminal SH3 domain is shown in italics. The two regions shown in bold type were identified by sequence analysis as being possible actin binding regions. The two regions encompass residues 12 – 65 and 207 – 223. Arrows demonstrate the start sites for the Ysc84-Nt fragment at residue 1 and the Ysc84-*Nt fragment at residue 89 (described in section 4.3). Residues 184 and 218 are marked. The serine residue reported to undergo phosphorylation is asterisked. **B)** Diagram of the identified possible actin binding regions.

4.2.5 Analysis of the severing activity of Ysc84p

Previous data has shown that GST-Ysc84 and GST-Ysc84-Nt interact directly with F-actin (section 4.2.3), while also suggesting an actin severing or depolymerising activity for residues 1 – 218 of Ysc84 *in vitro*. These residues encompass the highly conserved N-terminal homology domain of Ysc84p. In order to confirm and investigate the activity of this domain, further analysis was performed. Falling ball assays study the effect of ligand addition to a polymerising actin matrix. Actin is polymerised in the presence of increasing amounts of ligand and the effect on the viscosity of the filament matrix assayed (Pollard, 1982). The effect on viscosity is assayed by recording the time taken for passage of a small metallic ball through 10 cm of the polymerised actin matrix. Addition of a protein with actin severing activity would be expected to decrease the viscosity of the filament matrix allowing quicker passage of the falling ball. Conversely, addition of a protein with actin cross-linking activity would be expected to increase time of passage. 6 μ M of rabbit muscle G-actin (Cytoskeleton Inc) was polymerised in the presence of increasing concentrations of GST-Ysc84-Nt from 2 μ M to 20 μ M (section 2.6.11). Results of these falling ball assays are shown in figure 4-8.

Assays were performed in the presence of 0.2 mM CaCl₂ in light of reports of actin-severing proteins, such as villin, gelsolin and severin, which require calcium for activity (for review see Kumar and Khurana, 2004). The activity of gelsolin is additionally known to be regulated by pH (Lamb et al 1993). All assays were however carried out at pH 7.5 and performed in triplicate. The time taken for passage through an actin matrix polymerised in the absence of the protein was recorded. The addition of concentrations of GST-Ysc84-Nt between 2 and 15 μ M were seen to dramatically decrease the relative viscosity of this actin matrix. Maximum effect was seen with addition of 5 μ M of GST-Ysc84-Nt when the relative viscosity of the matrix decreased to 44%. This maximum effect was seen with addition of near equimolar amounts of GST-Ysc84-Nt to the 6 μ M of actin present in the matrix. The increase in viscosity following addition of 10 μ M and over of GST-Ysc84-Nt is potentially attributable to the ability of the GST tag to dimerise, which at high concentrations may obscure the severing effect of the fusion protein.

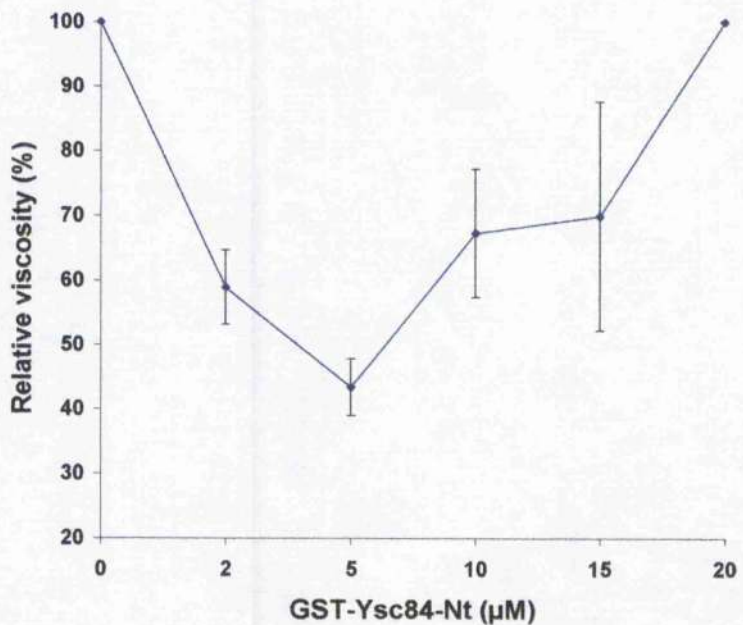


Figure 4-8. Biochemical analysis of GST-Ysc84-Nt with actin. Falling ball assays were performed to investigate the effect of addition of GST-Ysc84-Nt to an F-actin matrix. The matrix was polymerised from a solution of 6 μ M G-actin in the presence of increasing concentrations of the GST-Ysc84 from 0 – 20 μ M. Relative viscosity of the matrix was assayed by passage of a metal ball through 10 cm of the actin matrix.

4.2.6

Ysc84p severs fluorescently labelled actin filaments

Given the inhibitory effect of addition of GST-Ysc84-Nt to a polymerising actin matrix (section 4.2.5), and to examine Ysc84p in greater detail, the effect of addition of the protein to individual actin filaments was studied. The ability of the GST-Ysc84-Nt fusion protein to affect an actin matrix polymerised in the presence of calcium led to the hypothesis that Ysc84p may act in a similar manner to gelsolin or a related protein. The severing activity of gelsolin is regulated both by pH and calcium availability, and following severing of the actin filament, the protein remains attached to the newly generated filament barbed end. Gelsolin is therefore also a capping protein. In addition to regulation by calcium and pH, the severing activity of some capping proteins is inhibited by the binding of phalloidin to actin filaments. This inhibition is thought to occur by competition for a similar binding site on the actin filament. In order to visualise the effect of GST-Ysc84 and GST-Ysc84-Nt on individual actin filaments, and to test the inhibitory effect of phalloidin, the fusion proteins were incubated with fluorescently labelled Alexa Fluor[®] 568 actin filaments in the presence or absence of phalloidin. Filaments polymerised from rabbit muscle G-actin (Cytoskeleton Inc) in the presence of Alexa Fluor[®] 568 actin monomers (Molecular probes) enable the visualisation of individual filaments by fluorescence microscopy. Filaments were allowed to polymerise with or without phalloidin, and in the presence or absence of GST-Ysc84 and GST-Ysc84-Nt for 30 minutes. GST-Ysc84 and GST-Ysc84-Nt were incubated at equimolar concentrations to the actin in solution, as previously performed falling ball analysis had demonstrated the maximum depolymerising effect of GST-Ysc84-Nt was achieved at approximately equimolar concentrations to actin (4.2.5). Polymerisation of actin filaments in the presence of equimolar amounts of phalloidin was expected to increase the average filament length due to stabilisation of filaments.

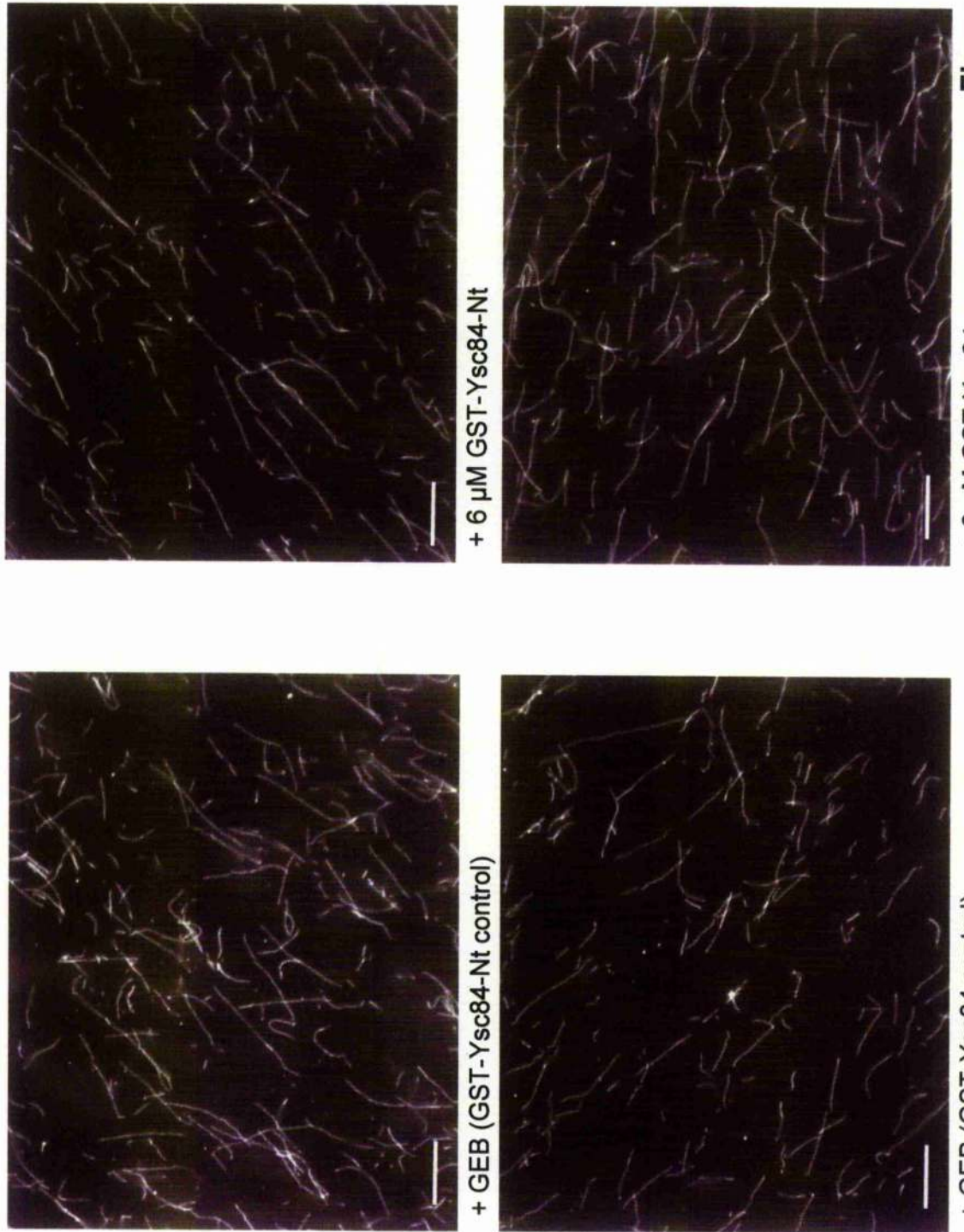
Filament lengths from several microscope field images were counted and averaged. Examples of these images are shown in figure 4-9. Figures 4-10 summarises the results these assays. Surprisingly, filaments polymerised in the presence of phalloidin did not show a significant increase in overall filament length. 21.8 % ± 2.5 of filaments exceeded 10 µM in length in the absence of phalloidin, while 23.0 % ± 3.0 exceeded 10 µM in length in the presence of phalloidin, in the GST-Ysc84-Nt control reaction. In the GST-Ysc84 control reaction, 19.5 % ± 2.0 of filaments exceeded 10 µM in length in the absence of phalloidin, with 18.5 % ± 1.1 exceeding 10 µM in length in

the presence of phalloidin (figure 4-10). Both GST-Ysc84 and GST-Ysc84-Nt were however shown to sever actin filaments. Incubation of labelled filaments with GST-Ysc84 in the presence of phalloidin demonstrated a decrease in filament length. Filaments 10 μ M and over in length decreased from $18.5\% \pm 1.1$ of total filaments to $9.6\% \pm 0.8$ in the presence of phalloidin; a decrease of approximately 48%. Incubation of filaments with GST-Ysc84 in the absence of phalloidin did not however significantly affect filament length. The presence or absence of phalloidin therefore appears to affect the severing activity of GST-Ysc84.

Incubation of labelled filaments with GST-Ysc84-Nt in the absence of phalloidin decreased the number of filaments 10 μ M and over in length by approximately 46%. Filaments 10 μ M and over in length decreased from $21.8\% \pm 2.5$ of total filaments in the absence GST-Ysc84-Nt, to $11.8\% \pm 2.2$ in the presence of GST-Ysc84-Nt. A similar activity was seen in the presence of phalloidin, with the percentage of filaments 10 μ M and over in length decreasing from $23.0\% \pm 3.0$ in the absence of the protein, to $11.0\% \pm 1.7$ in the presence of GST-Ysc84-Nt; a decrease of approximately 52%. Both GST-Ysc84 and GST-Ysc84-Nt are therefore able to sever actin filaments *in vitro* in the presence of phalloidin, but GST-Ysc84-Nt severing activity only was active in the absence of phalloidin.

Figure 4-9. GST-Ysc84-Nt and GST-Ysc84 are able to sever actin filaments. Microscope fields of fluorescently labelled, Alexa Fluor[®] 568 actin filaments are shown. Filaments were polymerised A) in the absence of equimolar amounts of phalloidin or B) in the presence of equimolar amounts of phalloidin. The addition of 0.5 μ l GEB (Glutathione Elution Buffer) acts as a control for the addition of equimolar amounts (6 μ M) of GST-Ysc84-Nt protein in GEB buffer. Addition of 1.5 μ l of GEB acts as a control for the addition of equimolar amounts (6 μ M) of GST-Ysc84. 10 μ M size bars are also shown.

Figure 4-9A



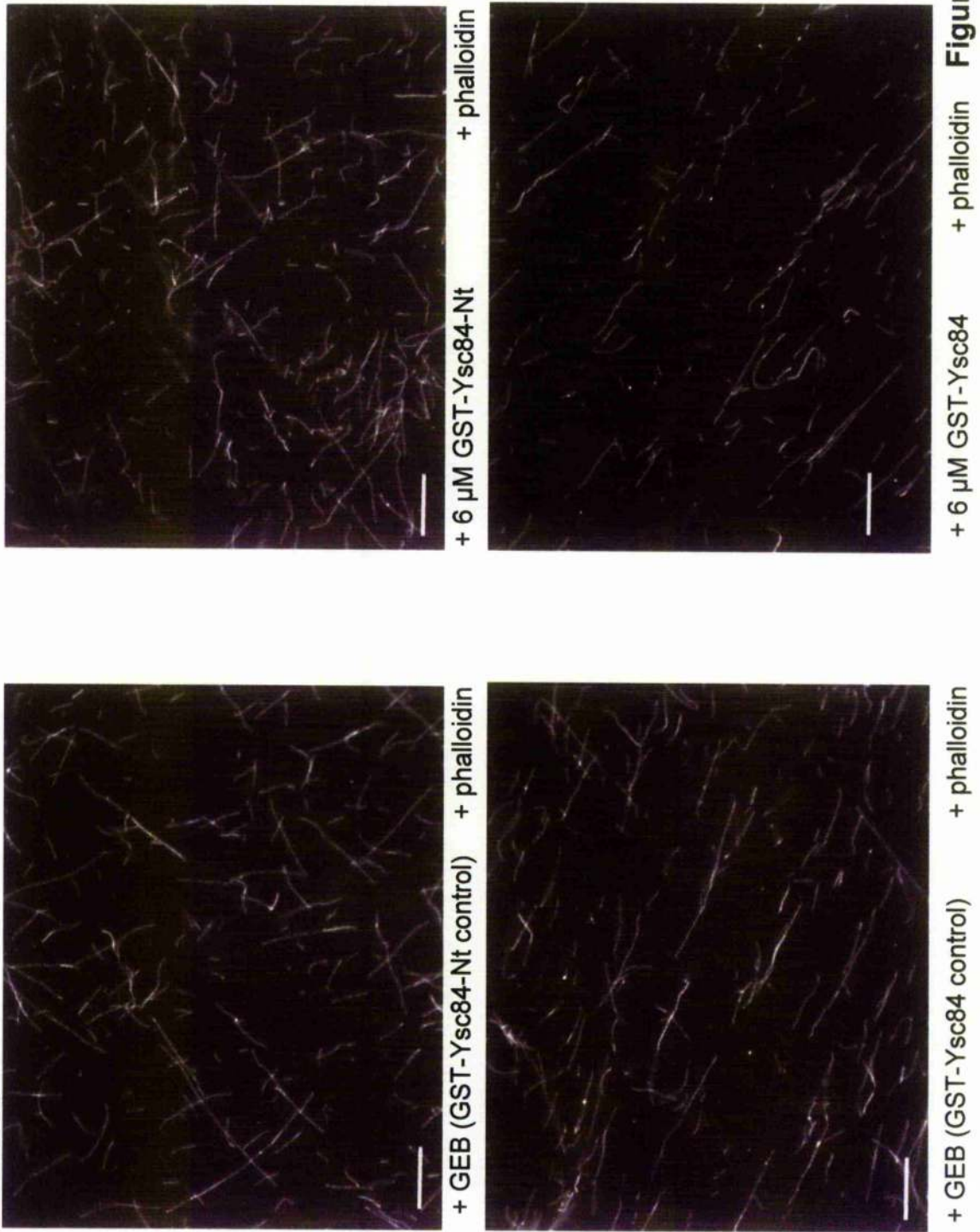
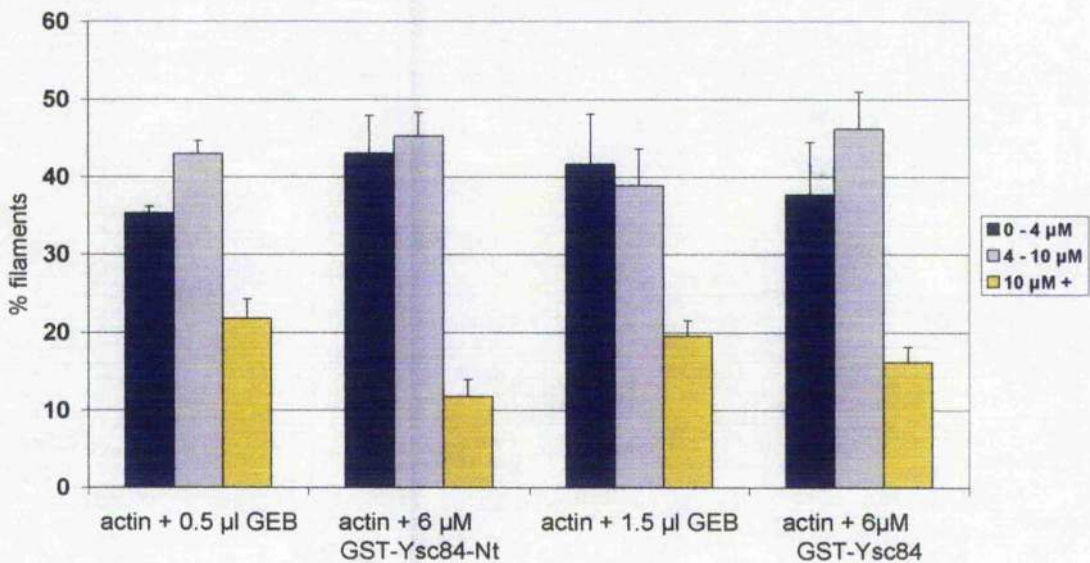


Figure 4-9B

A

filaments without phalloidin



filaments with phalloidin

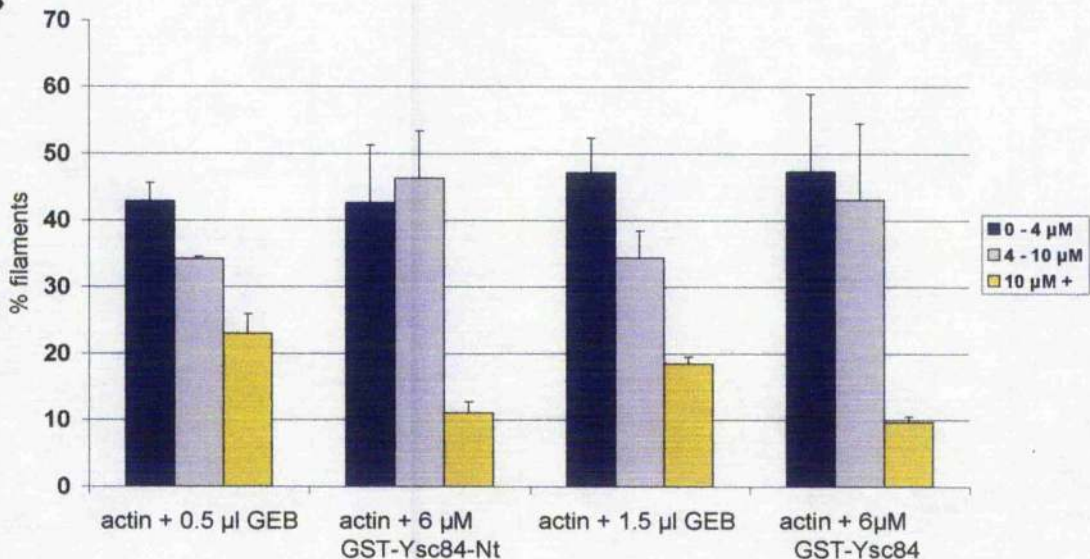
B

Figure 4-10. GST-Ysc84 and GST-Ysc84-Nt sever fluorescent actin filament in the presence of phalloidin. Filaments are grouped according to filament length and shown as a percentage of the total filaments counted in each image. Filaments 0 – 4 μM in length are shown in blue, 4 – 10 μM in grey, and those 10 μM and over in yellow. The addition of 0.5 μl GEB (Glutathione Elution Buffer) acts as a control for the addition of the 6 μM Gst-Ysc84-Nt protein held in the same buffer. Addition of 1.5 μl GEB (Glutathione Elution Buffer) acts as a control for the addition of 6 μM GST-Ysc84 protein in GEB. **A)** Actin filaments polymerised in the absence of phalloidin. **B)** Actin filaments polymerised in the presence of equimolar amounts of phalloidin. The addition of both Gst-Ysc84-Nt and Gst-Ysc84 decreases the percentage of filaments of length 10 μM and over.

4.2.7 Ysc84p can both sever and cap fluorescently labelled actin filaments

Given the ability of both GST-Ysc84 and GST-Ysc84-Nt to sever actin filaments *in vitro*, and previous reports of actin severing proteins which additionally demonstrate filament capping activity (for review see McGough, 2003), the ability of these Ysc84p fusion proteins to cap actin filaments was investigated. Fluorescently labelled Alexa Fluor[®] 568 (red) and Alexa Fluor[®] 488 (green) actin monomers (Molecular probes) were used to generate dual labelled actin filaments. Alexafluor[®] 568 and Alexa Fluor[®] 488 labelled actin monomers were sequentially incorporated into polymerising actin filaments, allowing visualising of polymerised filaments by fluorescence microscopy at two wavelengths. Filaments were initially polymerised from rabbit muscle G-actin (Cytoskeleton Inc) in the presence of Alexa Fluor[®] 488 with equimolar amounts of phalloidin for one hour, to generate filaments which fluoresced in green upon excitation. Purified fusion proteins held in Glutathione Elution Buffer (GEB) were then added to these filaments at an equimolar concentration to actin (6 µM), while GEB buffer alone was added in equivalent amounts to controls reactions. Alexa Fluor[®] 568 actin monomers were then added to these reactions and filaments allowed to polymerise for a further hour. Filaments polymerised following addition of GST-Ysc84 or GST-Ysc84-Nt would therefore fluoresce predominantly in red upon excitation, due to polymerisation in an excess of Alexa Fluor[®] 568 actin monomers. Filament severing activity exhibited by the fusion proteins would be apparent by a reduction in the length, and an increase in the number of Alexafluor⁴⁸⁸ labelled filaments (green) filaments. Filament capping activity of the fusion proteins would be apparent by comparing the number of filaments polymerised in the presence of fusion protein which demonstrated both red and green fluorescence, with the number of dual labelled filaments polymerised in the absence of fusion protein. A reduction in the number of dual labelled filaments would suggest the presence of a capping protein, as capping of initial (green) filaments would prevent filament extension following addition of Alexa Fluor[®] 568 actin monomers.

Images of filament spreads were taken using the fluorescence microscope at both wavelengths. These images were then merged and examined for the number of dual labelled filaments present, the total number of filaments, and the number and length of initial Alexa Fluor[®] 488 (green) filaments. Examples of these images are shown in figure 4-11. Results of these counts are summarised in figure 4-12. A marked

reduction in the number of dual labelled filaments is seen following addition of equimolar amounts of GST-Ysc84-Nt, as the number of dual labelled filaments drops from $42.1\% \pm 4.9$ of total filaments in the presence of GST-Ysc84-Nt, to $23.4\% \pm 2$ in the absence of GST-Ysc84-Nt; a reduction of approximately 44%. The addition of GST-Ysc84 did not however significantly affect the percentage of dual filaments seen, with dual filament accounting for $23.7\% \pm 3.4$ of total filaments when incubated in the presence of GST-Ysc84 and $24.4\% \pm 1.0$ of total filaments in the absence of GST-Ysc84. A reduction in the number of dual labelled filaments suggests that GST-Ysc84-Nt is able to cap actin filaments, preventing the addition of further actin monomers to existing filaments.

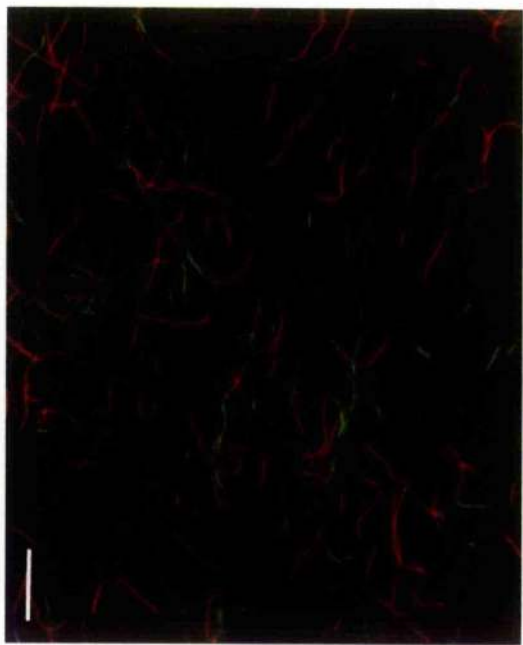
As demonstrated in section 4.2.6 both the GST-Ysc84-Nt and GST-Ysc84 proteins were able to sever Alexa Fluor^{® 568} labelled filaments, in the presence of phalloidin. In order to confirm this observation in our dual labelling assay, Alexa Fluor^{® 488} (green) labelled filaments were counted individually. Results of these counts are summarised in figure 4-13. Incubation of filaments with GST-Ysc84 in the presence of phalloidin again generated a reduction in the number of filaments 10 μM and over in length, with numbers decreasing from $21.3\% \pm 2.7$ of total filaments in the absence of the protein to $7.2\% \pm 1.2$ in the presence of GST-Ysc84; a decrease of approximately 66%. Incubation of filaments with GST-Ysc84-Nt in the presence of phalloidin also decreased the number of filaments 10 μM and over. Numbers of filaments 10 μM and over decreased from $16.4\% \pm 3.6$ of total filaments in the absence GST-Ysc84-Nt, to $10.5\% \pm 1.6$ of in the presence of GST-Ysc84-Nt; a decrease of approximately 36%.

Filament capping activity is demonstrated by a decrease in the number dual labelled filaments, and is therefore shown to be an activity of the GST-Ysc84-Nt fusion protein only. GST-Ysc84 may still cap actin filaments following severing, however significantly less efficiently than GST-Ysc84-Nt. A potential capping activity for GST-Ysc84 is proposed due to the rationale that filament severing without capping would generate an increase in the number of Alexa Fluor^{® 488} (green) filaments available for continuing polymerisation in the presence of Alexa Fluor^{® 568} (red) monomers. You might expect therefore, to see an increase in the number of dual labelled filaments polymerised in the presence of a severing protein which exhibits no capping activity, when compared to a control lacking this protein. Factors such as continued severing in the presence of Alexa Fluor^{® 568} (red) monomers and the concentration of free actin monomers in solution may however affect this proposed outcome. Low levels of filament capping by actin GST-Ysc84 however cannot be ruled out by these results.

Filament severing was demonstrated by GST-Ysc84-Nt and GST-Ysc84 in the presence of phalloidin, but for only GST-Ysc84-Nt in the absence of phalloidin (section 4.2.6). Identification of GST-Ysc84-Nt filament capping activity suggests the stable association of a proportion of the fusion protein with filament ends and an associated decrease in the concentration of freely available fusion protein in solution, when compared to experiments performed with GST-Ysc84. This rationale may explain the increased severing activity of GST-Ysc84 demonstrated in this dual labelling assay, which generated a 66% decrease in the number of Alexa Fluor® 488 (green) labelled filaments 10 µM and over in length, compared to a 36% decrease generated by the GST-Ysc84-Nt fusion protein.

Figure 4-11. GST-Ysc84-Nt and GST-Ysc84 both cap and sever labelled actin filaments

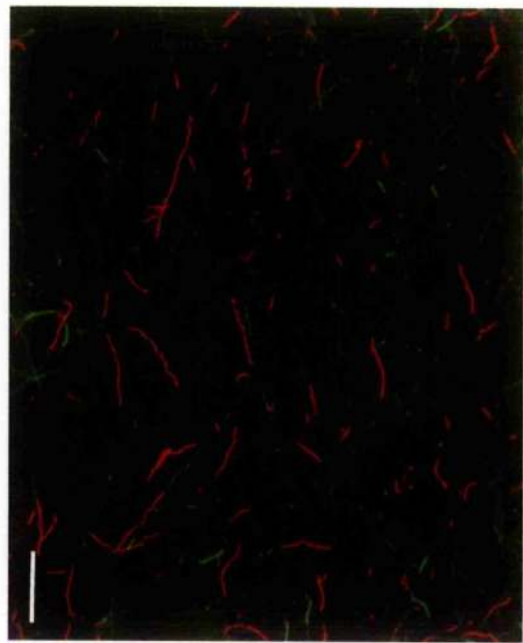
Filaments were initially polymerised in the presence of Alexa Fluor® 488. 6 µM GST-Ysc84-Nt, 6 µM GST-Ysc84 or control buffer GEB (Glutathionine Elution Buffer) was added, and the solution allowed to further polymerise in the presence of Alexa Fluor® 568 labelled actin monomers. Filament spreads were obtained by fluorescence microscopy and are shown above. The addition of 0.5 µl GEB (Glutathione Elution Buffer) acts as a control for the addition of 6 µM GST-Ysc84-Nt in GEB. Actin was polymerised in the presence of equimolar amounts of phalloidin.



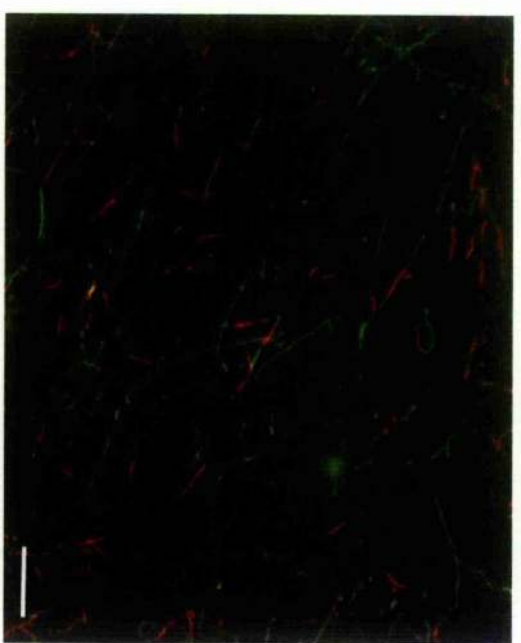
+ GEB (GST-Ysc84-Nt control)



+ GEB (GST-Ysc84 control)



+ 6 μ M GST-Ysc84-Nt



+ 6 μ M GST-Ysc84

Figure 4-11

**Labelling of actin filaments in the presence of GST-Ysc84p
and GST-Ysc84-Nt**

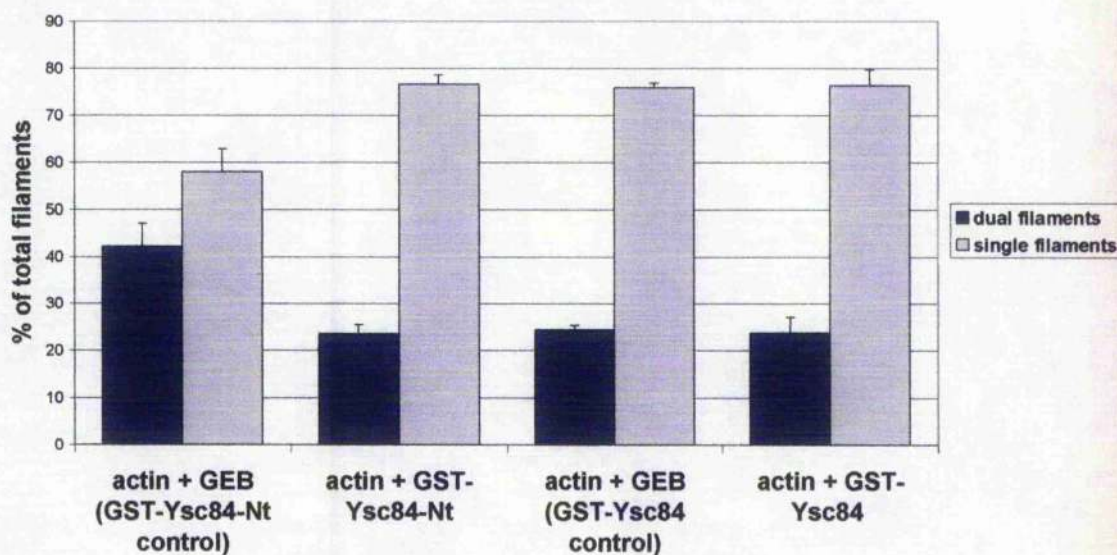


Figure 4-12. GST-Ysc84-Nt demonstrates filament capping activity in dual labelling fluorescent actin assays. Filaments were polymerised in the presence of Alexa fluor⁴⁸⁸ followed by addition of either the protein of interest or GEB buffer as a control. Filaments were then allowed to continue polymerisation following addition of Alexa fluor⁵⁶⁸ actin monomers. Filaments are grouped as continuous dual labelled filaments or as single colour filaments. Dual labelled filaments (blue) and single colour filaments (grey) are shown. The addition of 0.5 µl GEB (Glutathione Elution Buffer) acts as a control for the addition of 6 µM GST-Ysc84-Nt in GEB. Addition of 1.5 µl GEB acts as a control for the addition of the 6 µM GST-Ysc84. Actin was polymerised in the presence of equimolar amounts of phalloidin.

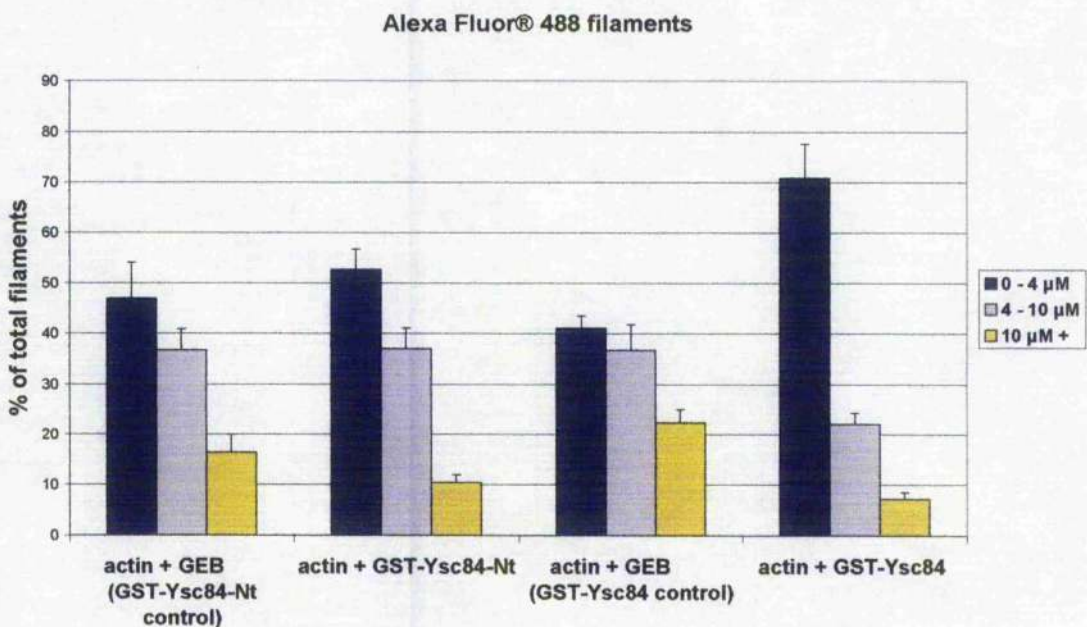


Figure 4-13. Counts of Alexa Fluor⁴⁸⁸ labelled filaments in dual labelling experiments. Filaments are grouped according to length of filament and as a percentage of the total Alexa Fluor⁴⁸⁸ filaments counted in each image. Filaments 0 – 4 μM in length are shown in blue, 4 – 10 μM in grey, and 10 μM and over in yellow. The addition of 0.5 μl GEB (Glutathione Elution Buffer) acts as a control for the addition of 6 μM GST-Ysc84-Nt in GEB. Addition of 1.5 μl GEB acts as a control for the addition of the 6 μM GST-Ysc84. Actin was polymerised in the presence of equimolar amounts of phalloidin.

4.2.8 Generation of Ysc84p antibodies

Biochemical analysis of Ysc84p fusion proteins has provided insight into the potential *in vivo* functions of Ysc84p. The generation of antibodies specific for Ysc84p would potentially however enable *in vivo* studies of protein location, immunoprecipitation and identification of Ysc84p by Western analysis to be performed, in addition to other studies. The generation of Ysc84p specific antibodies was therefore undertaken. Expression and purification of GST-Ysc84-Nt was performed as described in sections 2.6.7 and 2.6.8. Conservation of this amino terminal region between Ysc84p homologues raised the possibility generating antibodies specific not only for Ysc84p, but also for homologues in other species. The specificity of this region to Ysc84p and its homologues, as these residues showing little homology to known motifs or domains, suggested this region would act as an excellent antigen with which to raise a highly specific immune response.

Transformation of the plasmid pGEX4T1-*ysc84*(1-654) (pKA278) into DH5 α cells was performed as described in section 2.3.9. Expression and purification of the encoded fusion protein GST-Ysc84-Nt from two litres of culture was then undertaken (section 2.6.7 and 2.6.8), with GST-tagged protein purified using glutathione sepharose[®] 4B beads. The purity and concentration of the purified protein was then determined by SDS-page analysis and spectrometry respectively. Analysis of the purified fusion protein by SDS-page gel electrophoresis is shown in figure 4-14. Approximately 200 μ g of purified protein was subsequently administered to two rabbits (R1414 and R1415) in four separate injections at 28 day intervals (Diagnostics Scotland) (section 2.8.1). An initial pre-immune serum, subsequent primary and secondary serums and a final exsanguination serum was obtained from these animals. 3 ml of the final polyclonal rabbit antisera was then purified using Protein A sepharoseTM CL-4B beads (Amersham Pharmacia) which bind specifically to immunoglobulin molecules (section 2.8.2). 1 ml fractions of protein were eluted from these beads by addition of 0.1 M glycine pH 2.5, which was subsequently neutralised. 10 fractions were obtained and were analysed by spectrometry to determine the concentration of protein held in each fraction. The two most concentrated fractions (fraction 6 and 7) were tested by Western blotting against whole cell extracts (section 2.6.4) at a dilution of 1:1000 in 1% milk + TBS-T (section 2.6.4) using ECL detection (section 2.6.5).

Western blotting of lysates performed using fractions 6 and 7 (figure 4-15) identified a strong band between 60-62 kDa in wild type extracts (KAY302). Additional faint bands were identified in blots performed using fraction 6, at higher molecular weights in wild-type extracts, Δ *ysc84*/ Δ *lsb3* (KAY554) extracts and Δ *ywc84* (KAY510) extracts. The predicted size of Ysc84p is 52.2 KDa. The identification of the 60-62 KDa band in wide type extracts only, suggested the specificity of these antibodies for Ysc84p. Identification of a single band in wild-type extracts and the lack of band identification in a Δ *ysc84* extract also suggested that these antibodies did not recognise the Ysc84p homologue Lsb3p, which has a predicted molecular weight of 48.5 kDa.

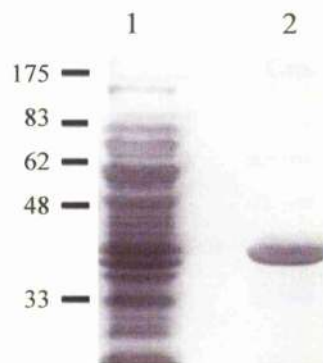


Figure 4-14. Purified GST-Ysc84-Nt. Purification of total cell lysate (lane 1) from DH5 α cells expressing GST-Ysc84-Nt using Glutathione Sepharose® 4B beads yielded a single purified protein band (lane 2) with a molecular weight of 39 kDa. Predicted size of the fusion protein was 45 kDa.

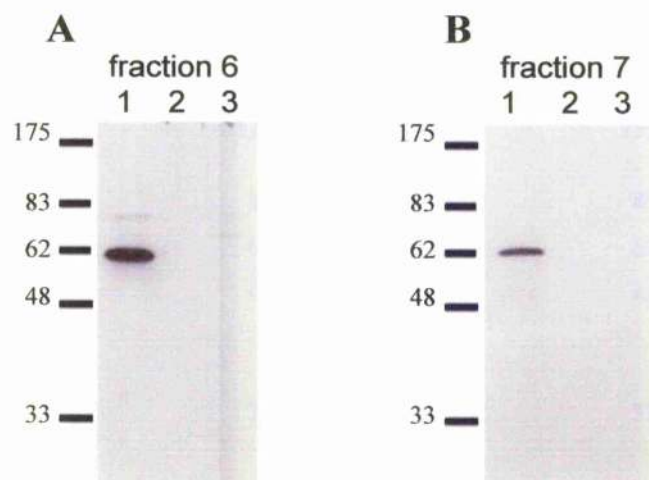


Figure 4-15. Specificity of Ysc84 antisera as determined by western blotting. Purified polyclonal rabbit antisera fractions 6 and 7, purified over Protein A Sepharose™ CL-4B beads, were tested at a 1:1000 dilution and detected by ECL. Both fraction 6 (A) and fraction 7 (B) were tested against whole cell wild-type (KAY302, Lane 1) extracts, $\Delta ysc84/\Delta lsb3$ (KAY554, lane 2) extracts and $\Delta ysc84$ (KAY510, lane 3) extracts. Standard molecular weight markers are also shown.

4.2.9 Ysc84p analysis by 2D-gel electrophoresis

Biochemical assays have localised the actin filament binding, severing and capping activity to the amino terminal 1-218 residues of Ysc84p (sections 4.2.3 - 4.2.7). Given the apparent lack of capping activity demonstrated by the full length fusion protein GST-Ysc84 (section 4.2.7), a regulatory function for the carboxy-terminal regions of the protein is suggested. In addition, a study by White and colleagues had identified a site of phosphorylation in the carboxy-terminal region of Ysc84p at serine residue 301 (Ficarro et al 2002), by phosphoproteome analysis and mass spectrometry. Phosphorylation is a widely occurring mechanism of protein regulation. Modification of Ysc84p was therefore investigated by 2-D gel analysis using our newly generated Ysc84p specific rabbit polyclonal antibodies (section 4.2.8).

Wild-type whole cell extracts (KAY302) were prepared and separated by 2-Dimensional (2-D) gel electrophoresis as described in section 2.6.6. Isoelectric focusing (IEF) strips of pH 6 – 10 were used. Ysc84p has a predicted pI of 8.38. 2-D gel electrophoresis allows the separation of proteins both by size and charge, enabling the identification of modified forms of individual proteins. Extracts separated by 2-Dimensional Gel Electrophoresis were transferred onto PVDF membrane and Western blotted using anti-Ysc84 antibodies at 1:2000 (section 2.6.5). Membranes were then analysed by ECL (enhanced chemiluminescence). The result of this analysis is shown in figure 4-16. Western blotting identified a single distinct spot at 57 KDa with a pI of approximately 7.3. The predicted molecular weight of Ysc84p is 51 KDa. This data suggest that several modified forms of Ysc84p do not exist under the experimental conditions examined.

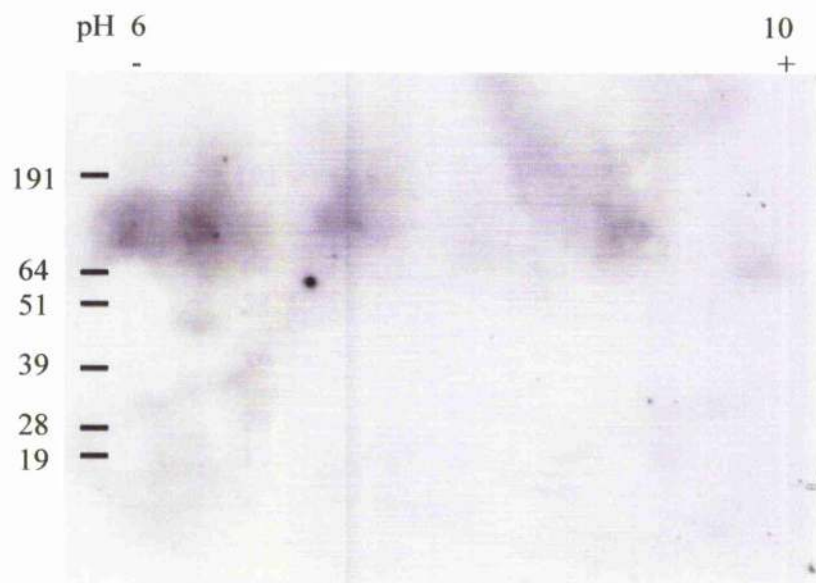


Figure 4-16. 2-Dimensional Gel analysis of wild-type extracts with anti-Ysc84 antibodies.
Extracts from wild-type strain KAY302 were separated by 2-D gel electrophoresis and Western Blotted using antibodies raised to the amino-terminus of Ysc84p. IEF strips of pH 6 – 10 were used. Ysc84p has a predicted pI of 8.38. A single spot is seen at 57 KDa (predicted size: 52.2 kDa).

4.3

Discussion

The cortical patch protein Ysc84p interacts with the cytoplasmic adaptor protein Sla1p as determined biochemically (Dewar *et al*, 2002) and the Arp2/3 complex activator Las17p as determined by yeast 2-hybrid analysis. Ysc84p co-localises with cortical actin patches, which are regarded as an integral component of the endocytic machinery, as their formation at endocytic sites is proposed to enable processes including vesicle formation, fission and transport.

In this study considerable progress has been made towards establishing the role of Ysc84p. Previous studies had shown that the localisation of Ysc84p to cortical patches was dependent on F-actin, and the Arp2/3 activators Las17p and Abp1p. A role for Ysc84p in the regulation of actin was also proposed (Dewar *et al*, 2002) but had not been investigated. Consistent with this proposal, F-actin sedimentation assays performed during this study have demonstrated the ability of both a GST-tagged N-terminal fragment of Ysc84p and full length Ysc84p to bind directly to filamentous actin *in vitro* (section 4.2.3). Additionally, studies have demonstrated the actin filament severing and capping activity of Ysc84p *in vitro*, and have localised these activities to residues 1-218 of Ysc84p (section 4.2.6 and 4.2.7).

Ysc84p shows a high degree of conservation with its human homologue hSH3yl-1, particularly across two conserved regions. These proteins show 48% identity across the conserved N-terminal domain from residues 1-184, and 58% identity across the carboxy-terminal SH3 domain. Transformation and expression of an hSH3yl-1 expression construct in a Δ y_c84 Δ lsb5 mutant strain demonstrated a partial rescue of the phenotypes associated with this double deletion. This demonstrates partial functionality of hSH3yl-1 in a yeast system, previously suggested by the high degree of conservation between Ysc84p and hSH3yl-1. Previous studies have also shown that hSH3yl-1 is able to affect the actin network in yeast, with overexpression of the protein in a wild-type strain causing depolarisation of the actin cytoskeleton (Dewar *et al*, 2002). Taken together, these studies demonstrate both conservation of function between Ysc84p and its human homologue, while also suggesting a direct role for the yeast protein in the regulation of the actin. Due to the high degree of conservation seen between Ysc84p and its *S. cerevisiae* homology Lsb3p, these studies also suggest potentially conservation of function with Lsb3p. Conservation may also extend to other Ysc84p homologues. Sequence conservation between Ysc84p and Lsb3p is extremely high, with 91% identity seen across the N-terminal homology domain and 86% identity across the SH3 domain (Dewar *et al*, 2002).

High speed sedimentation assays performed to investigate the F-actin binding abilities of Ysc84p and an N-terminal Ysc84p fragment, demonstrated the ability of both GST-Ysc84 and GST-Ysc84-Nt to bind directly to F-actin (section 4.2.3). F-actin binding does not therefore require the carboxy terminal domain of the protein from residues 218-468. These assays also suggested an actin depolymerising or severing activity for GST-Ysc84-Nt, as seen by accumulation of actin in the supernatant fraction following incubation of 6 μ M F-actin with 31.2 μ M GST-Ysc84-Nt (figure 4-5B). Total accumulation of actin in the supernatant was only seen upon incubation with 31.2 μ M GST-Ysc84-Nt, however substantial amounts of actin in the supernatant were also seen following incubation with all concentrations of the GST-Ysc84-Nt fusion protein tested. It was additionally noted that the activity of proteins tested may be substantially inhibited by experimental conditions, with activity potentially being regulated by additional factors such as pH or the availability of additional molecules. Subsequently, the prediction of two potential actin binding regions between residues 1-218 of Ysc84p was made due to a high density of hydrophobic residues at these sites. Hydrophobic residues are conserved in several known actin binding motifs and were used to suggest regions of Ysc84p which may bind directly to F-actin (Dominguez, 2004).

The suggested severing activity of GST-Ysc84-Nt was investigated using falling ball viscometry. Falling ball assays demonstrated the effect of addition of GST-Ysc84-Nt on the viscosity of an F-actin matrix polymerised in the presence of the protein. Additional studies later performed assessed the effect of addition of the fusion proteins to pre-existing actin filaments. Falling ball assays demonstrated the ability of GST-Ysc84-Nt to decrease the viscosity of a 6 μ M actin matrix by up to 44% in the presence of 0.2 mM Ca²⁺. Interestingly, the maximum severing activity of GST-Ysc84-Nt was seen to occur following addition of 5 μ M of protein; an approximately equimolar concentration to that of actin used in this study. This effect on the viscosity of a polymerising matrix confirmed a severing or depolymerising activity for the N-terminal region of Ysc84p while also suggesting that maximum severing activity of the protein may occur at equimolar concentrations to actin. Previous studies have demonstrated the regulation of actin severing proteins by factors such as pH and calcium concentration, therefore it is proposed therefore that the actin severing activity of Ysc84 may be regulated by additional factors, and further analysis needs to be performed to identify these factors. *In vivo* resting intracellular calcium levels are reported as approximately 0.2 μ M (Kinosian, 1998); however for the severing activity of previously identified severing proteins to occur *in vitro*, higher levels of calcium are known to be required. Half maximal severing activity of gelsolin was

reported in the presence of 10 μ M calcium, although this figure is variable with pH (Lamb *et al.*, 1993).

Additional analysis of the severing activity of Ysc84p was performed by studying the effects of protein addition on previously polymerised fluorescently labelled actin filaments (section 4.2.6). Filaments were polymerised either in the presence or absence of phalloidin, both to assess the effects of filament stabilisation on Ysc84p severing activity (Cooper, 1987), and also in light of reports detailing the inhibitory effect of phalloidin binding on the severing activity of proteins including cofilin and actophorin (Yonezawa *et al.*, 1988; Maciver *et al.*, 1991). Actin severing activity was demonstrated for GST-Ysc84-Nt at similar levels both in the presence or absence of phalloidin, and for GST-Ysc84 in the presence of phalloidin. Intriguingly however, a lack of phalloidin was shown to inhibit the actin severing activity of GST-Ysc84. Inhibition of the actin severing by cofilin, actophorin and gelsolin by phalloidin has been previously reported, while severing by proteins such as the *Dictyostelium* gelsolin related protein severin have been shown to be unaffected by phalloidin (Giffard *et al.*, 1984). Studies have suggested that the mechanism for inhibition of severing activity may be direct competition with phalloidin for a similar binding site on the actin filament. The presence of phalloidin has not however been previously shown to promote the activity of a filament severing protein. Stabilisation of the severing mechanism by phalloidin is however a potential explanation for this effect.

Dual labelling experiments were performed in order to assess the actin filament capping activity of GST-Ysc84 and GST-Ysc84-Nt. Filaments were polymerised in the presence of phalloidin, as lack of phalloidin had previously been shown to inhibit the severing activity of GST-Ysc84 (section 4.2.6). Filament capping activity by GST-Ysc84-Nt was clearly demonstrated (section 4.2.7). This was shown by a decrease in the number of dual labelled filaments by approximately 44% following addition of GST-Ysc84-Nt. GST-Ysc84 did not however show significant capping activity as the number of dual labelled filaments remained similar in the presence or absence of GST-Ysc84. The loss of capping activity upon incubation with the full length protein promotes interesting possibilities and suggests that the carboxy terminal regions of Ysc84p may regulate the amino terminal filament capping activity of Ysc84p. Potential regulatory mechanisms include conformational changes, which would allow the carboxy-terminal region of Ysc84p to mask the actin binding, severing and capping regions located in the amino terminus of the protein. Additionally, the possibility of protein modification as a regulatory mechanism exists. In support of this proposal, Ysc84p has been shown to undergo phosphorylation on serine residue S³⁰¹ (Ficarro *et al.*, 2002), as determined by

phosphoproteome analysis (Ficarro *et al*, 2002). This region is removed in the GST-Ysc84-Nt fragment; therefore modification by phosphorylation is a potential regulatory mechanism for Ysc84p. Initial 2-Dimensional gel analysis of Ysc84p in wild-type cells does not however support the suggestion of modified forms of Ysc84p. 2-Dimensional gel analysis identified a single spot with similar molecular weight and isoelectric point to that predicted for Ysc84p (section 4.2.9) suggesting that a single form of Ysc84p exists under the experimental conditions tested. Modification of the protein may occur under conditions not examined however, for example during a specific growth phase.

Dual labelling studies demonstrated that purified GST-Ysc84-Nt is able both to sever and cap actin filaments *in vitro*, while GST-Ysc84 is able to sever actin filaments, but does not exhibit significant capping activity. N-terminal filament severing and capping activity, coupled with potential self-regulation suggests similarity to Class I members of the gelsolin/villin family and in particular, gelsolin itself. Class I family members are known both sever and cap actin filaments, while Class II members show only severing activity. In addition to severing and barbed end capping, gelsolin is known to self-regulate. The activity of gelsolin and many related proteins is dependent on the availability of free calcium in solution. Recent X-ray crystallography studies of the inactive protein have demonstrated the arrangement of gelsolins six domains (Burtnick *et al*, 1997), which suggest regulation of the N-terminal actin binding domain by folding over of the C-terminal regions, which thereby mask the N-terminal domain in the absence of calcium. This model is supported by an earlier study in which deletion of specific carboxy terminal residues eliminated the calcium requirement for gelsolin activity (Way *et al*, 1992). To date, no gelsolin family members have been identified in yeast, despite being identified in various vertebrate and plant cells (Huang *et al*, 2005; for review see Silacci *et al*, 2004). Ysc84p and gelsolin do not show significant similarity at the amino acid level but as has been previously demonstrated, gelsolin does not always show a high level of sequence similarity to gelsolin family members (Hatanaka *et al*, 1996). This is particularly clear in the case of destin. Conservation of a similar domain structure to gelsolin is however apparent in this protein. The localisation of filament binding, severing and capping activity to the N-terminal region of Ysc84p with potential self-regulation suggests similarity to the barbed end capping protein, gelsolin. Recent studies have also demonstrated conformational changes induced by tyrosine phosphorylation of the actin severing protein villin, and this may be another mechanism of regulation for severing proteins (Kumar and Khurana, 2004). Tyrosine phosphorylation has been shown to abrogate the requirement of calcium for severing by villin. Gelsolin has also been shown to be tyrosine phosphorylated

in vivo (Wang *et al*, 2003) and this mechanism of regulation is proposed to extend to other related actin severing proteins.

Identification of two potential actin binding regions in the N-terminus of Ysc84p proposed subsequent studies which remain incomplete. In order to investigate the localisation of the actin binding region of Ysc84p, and following initial F-actin high speed sedimentation assays which localised the actin binding region of Ysc84p to the N-terminus of the protein, a third GST tagged fusion was generated. A 293 bp region of the Ysc84p coding sequence was amplified by PCR, corresponding to amino acids 87 – 184 of Ysc84p (figure 4-17). This fragment was amplified from plasmid pKA259 using oligonucleotides oKA366 and oKA251. Amplification engineered BamHI and EcoR1 restriction sites at product ends, allowing cloning of the fragments into the pGEX4T2 vector (pKA143) at corresponding sites; generating a plasmid pGEX4T1-*ysc84(259-552)* (pKA394) which encodes a 97 amino acid fragment of Ysc84p in fusion with an amino-terminal GST tag (GST-Ysc84-^{Nt}). Expression and purification of this fusion protein was successful, however due to the low yield of fusion protein obtained and limitations of time, the actin binding abilities of this construct remain untested. This construct lacks both predicted actin binding regions and it is proposed therefore that this fusion construct will not bind directly to F-actin. Further investigation must however be performed in order to ascertain the precise F-actin binding domain of Ysc84p, with the generation of further protein fragments. The actin binding ability of this fusion protein will however indicate whether the actin binding domain is lacking or incomplete in this construct.

While we have observed the binding, severing and capping activity of Ysc84p *in vitro*, the mechanism for these activities remains to be elucidated. Identification of capping activity *in vitro* is a however a significant development. Capping proteins are thought to play an important role in the regulation of actin dynamics by localising filament polymerisation to specific sites. By capping the ends of specific filaments, the availability of filament ends free to undergo polymerisation is affected, allowing polymerisation to be confined or ‘funnelled’ to filament sites which lack bound capping protein. This proposal has been strengthened by studies of *Listeria* (David *et al*, 1998). Capping protein is known to be a component of actin comet tails in *Listeria*. In a system comprising of pure proteins, decreasing the available amount of capping protein was shown to abolish the motility of *Listeria*, suggesting filament capping and ‘funnelling’ may drive motility (Loisel *et al* 1999). Studies have also shown that most cellular actin filament barbed ends are not freely

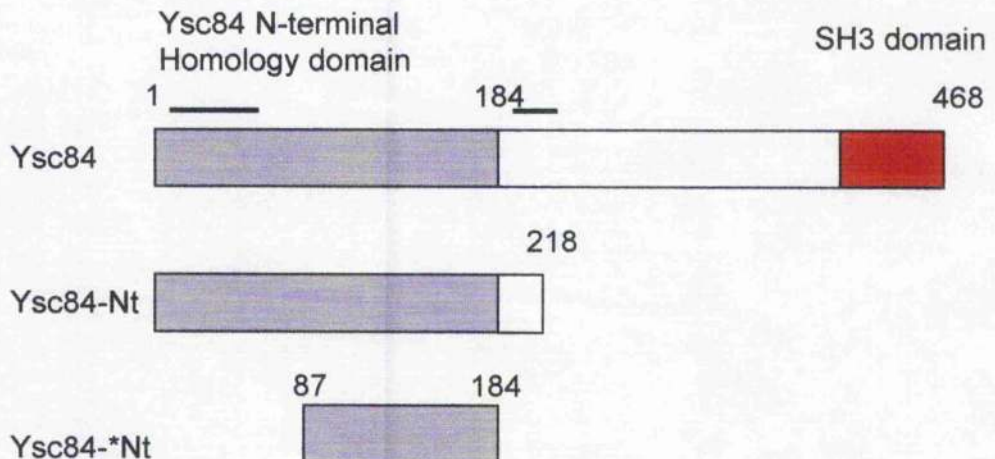


Figure 4-17. The Ysc84-*Nt fragment fused to GST. The highly conserved amino-terminal of Ysc84 encompasses residues 1-184. The Ysc84-Nt fragment encompassing residues 1 – 218 has previously been shown to bind, cap and sever actin filaments *in vitro*. Potential actin binding regions have been identified in Ysc84p and encompass residues 12-65 and 207-223 of Ysc84p (marked above). A small fragment, Ysc84-*Nt has been generated encompassing residues 87 – 184 and lacking both potential actin binding regions.

accessible, suggesting many may be capped. The low concentration of cellular actin in non-motile yeast cells (0.1% of total protein) compared to highly motile *Dictyostelium* (10% of total protein), suggests that the main function of actin regulating proteins in yeast may not be to hold back spontaneous polymerisation, but to act instead in the stabilisation and precise regulation of the actin network in yeast.

Capping protein (CP) has been shown to bind to the barbed ends of actin filaments in *S. cerevisiae*, preventing further monomer addition or monomer loss from filament ends (Karpova, 1995). Capping protein is conserved throughout the eukaryotes, with the heterodimeric protein being encoded by *CAP1* and *CAP2* in yeast. CP is known to co-localise with F-actin both at cortical actin patches and with actin cables (Amatruda *et al* 1992). CP deletion has been shown to affect the stability of actin, with a decrease in F-actin and increase in G-actin, and is lethal in conjunction with deletion of the actin filament binding protein yeast fimbrin (Sac6p). Deletion of Ysc84p appears not to affect the actin cytoskeleton of *S. cerevisiae* (Dewar *et al*, 2002) suggesting that the capping activity of Ysc84p is not a requirement for the control of actin dynamics in the yeast, or that functional redundancy with other proteins exists.

The co-localisation of Ysc84p with cortical actin patches (Dewar *et al*, 2002) and newly determined actin binding, severing and capping activity of the protein *in vitro* strongly implicate Ysc84p in the regulation of actin at endocytic sites *in vivo*. Actin is known to be recruited to endocytic sites in the later stages of vesicle development and is thought to be the driving force for endocytic vesicle fission and the movement of endocytic vesicles into the cell. The endocytic model proposed by Kaksonen and colleagues (Kaksonen *et al*, 2003) demonstrates the accumulation of Las17p, Sla2p and Sla1p at early endocytic sites, followed by recruitment of actin, Abp1p and the Arp2/3 complex (figure 1-12). Actin, Arp2/3 and Abp1p then dissociate from early endocytic proteins, moving off with newly endocytosed vesicles into the cytoplasm. A transient interaction between Ysc84p and Sla1p, and co-localisation of Ysc84p with actin, suggests Ysc84p is recruited to endocytic sites at the same time as actin, and is in close proximity to Sla1p for only a short time before moving off with actin, into the cell. The interaction between Ysc84p and Las17p suggested by 2-hybrid analysis may also occur at this time. The requirement of both Abp1p and Las17p for localisation of Ysc84p to cortical patch sites (Dewar *et al*, 2002) additionally suggests that the mechanism of Ysc84p recruitment to endocytic sites may involve these proteins.

Studies of actin comet tails which associate with the motile bacterial pathogens, *Listeria* and *Shigella* demonstrate the orientation of polarised actin filaments, by decoration of the filaments with the S1 fragment of myosin. These studies reveal that filament barbed ends are orientated towards the bacterial surface, indicating that polymerisation occurs on or near to the bacterial surface (Gouin *et al.*, 1999). The barbed end capping protein CapZ has been shown to co-localise with actin comet tails in both *Listeria* and *Shigella* (David *et al.*, 1998; Gouin *et al.*, 1999). These studies support a role for the requirement of filament capping in promoting F-actin linked motility, as suggested by models proposing 'funnelling' of actin polymerisation. Ysc84p may therefore cap and sever actin filaments at cortical endocytic sites, promoting vesicle motility by the control of actin polymerisation. A model for Ysc84p recruitment and regulation of actin at endocytic sites is therefore proposed in figure 1-18.

Generation of Ysc84p specific antibodies was a significant development which was not exploited fully in this study, due to limitations of time. Studies performed following my departure from the lab have however made use of these antibodies, and have proved very successful. Antibodies were initially raised against the GST-Ysc84-Nt fusion protein and specifically recognise Ysc84p (section 4.2.8). Subsequent analysis has however shown that these antibodies also recognise a single band, by Western analysis of whole cell Ref52 and Hela extracts. The band identified has an approximate molecular weight of 38 kDa, similar to the 34.8 kDa Mwt predicted for the Ysc84p human homologue hSH3yl-1. Antibodies were therefore used for immunofluorescence studies in Ref52 cells and identified a protein which localises both to membrane ruffles and focal adhesions (Steve Winder, unpublished data). A GFP-hSH3yl-1 construct generated during the course of this study has also been transfected into, and localised in Ref52 cells (Steve Winder, unpublished data). The tagged protein localises to focal adhesions, lamellipodia and filopodia (data not shown). These studies suggest that rabbit antibodies raised to Ysc84p in this study also specifically recognise hSH3yl-1, and in combination with GFP localisation of hSH3yl-1, demonstrate the localisation of hSH3yl-1 to sites of dynamic actin remodelling, suggesting that hSH3yl-1 may have similar actin regulating abilities as Ysc84p.

Endocytic site

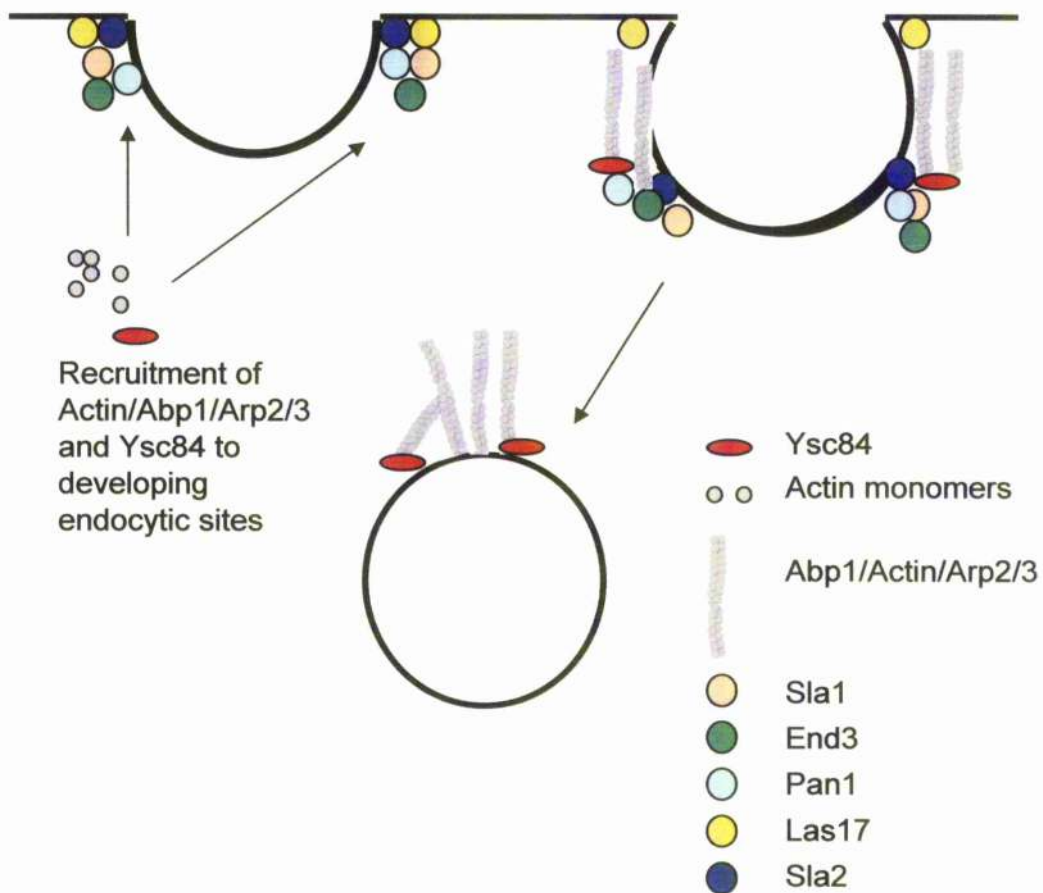


Figure 4-18. Proposed involvement of Ysc84p in endocytosis. Co-localisation of Ysc84p with cortical actin patches suggests this a role in the regulation of actin at endocytic sites. The mechanism of recruitment of Ysc84p to endocytic sites remains unknown, however Las17p and Abp1p have been implicated in this. The polymerisation of actin and formation of cortical actin patches at developing endocytic sites places Ysc84p at this location. Transient interactions with the cortical adaptor Sla1p may also occur at this time. Actin 'comet tails' are known to associate with vesicles following their release from the plasma membrane. The action of Ysc84p as an actin associated filament severing and capping protein strongly suggests an involvement in the generation of vesicle movement mediated by actin polymerisation.

**5 GTS1 IS AN Arf-GAP HOMOLOGY PROTEIN THAT INTERACTS WITH
SLA1 AND YSC84**

Abstract

Gts1p has been shown to have a role in the regulation of budding in *S. cerevisiae* and to contain regions of homology to both a ubiquitin associated domain (UBA) and to an ADP-ribosylation factor GTPase activating (Arf-GAP) motif. Using GFP-tagged Gts1p, our studies have localised Gts1p to punctuate patches at the cell cortex, a localisation which is independent of both Sla1p and F-actin. Yeast 2-hybrid analysis has also enabled confirmation and identification of domains of Sla1p and Ysc84p which interact with Gts1p by yeast 2-hybrid analysis. Additionally, *GTS1* deletion suggests the protein plays a role in the regulation of endocytic uptake, a role which is potentially mediated by interaction with Sla1p and Ysc84p.

5.1 Introduction

Gts1p/*YGL181W* has been shown to interact with the cortical patch proteins Pan1p and Ysc84p, the actin regulating adaptor protein Rvs167p, and the cortical adaptor protein Sla1p, by large scale yeast 2-hybrid screen (Uetz et al, 2000). This screen also reported a 2-hybrid interaction with Yap1802p, a member of the AP180 protein family known to bind both to clathrin and Pan1p (Uetz et al, 2000). Gts1p was originally described by Mitsui and colleagues, when overexpression of Gts1p was shown to delay budding in *S. cerevisiae* and consequently increased cell size (Mitsui et al, 1994). Disruption of the gene was in addition shown to accelerate budding and subsequently to reduce cell size.

In yeast, oscillations in the rate of energy metabolism have been identified during continuous cell culture in aerobic conditions. These oscillations are seen as periodic changes in oxygen metabolism, carbon dioxide production and glucose and ethanol levels. Response to stresses including heat shock, oxidative agents and cytotoxic chemicals has also been shown to induce oscillations of the same frequency (Wang et al, 2001b). Disruption or overexpression of *GTS1* affects growth rates in the presence of cytotoxic drugs and the life span of cells. Energy metabolism oscillations were seen to become irregular in a $\Delta gts1$ strain, suggesting Gts1p has an important role in the regulation of these oscillations (Akiyama and Tsurugi, 2003). Additionally, intracellular reactive oxygen species (ROS) levels are elevated in a $\Delta gts1$ strains, and following overexpression of Gts1p (Abudugupur et al, 2003). Cellular increases in ROS are known to correlate directly with a decrease in the life span of cells.

Gts1p was originally named due to the presence of glycine/threonine and serine repeats in the predicted amino acid sequence of the protein. Due to an error in the DNA sequence however, and subsequent frame shift, this G/T repeat has been replaced in the present version of the predicted amino acid sequence by an A/Q repeat. Gts1p also contains a CxxCx(16)CxxC motif in the N-terminus of the protein from residues 30-53, which resembles a zinc-finger (Zn-finger) motif. Additionally, the identification of a stretch of poly-Glutamine (Poly-Gln) in the C-terminus of the protein, commonly found in transcription factors and transcriptional activators, led to the protein originally being originally identified as a nuclear zinc-finger transcription factor (Bossier *et al*, 1997). The lack of a highly conserved nuclear localisation signal and homology to an Arf-GTPase activating (Arf-GAP) domain between residues 14 -141, however suggests that Gts1p is instead likely to be involved in cytoplasmic interactions with endocytic and actin regulating proteins. Reported 2-hybrid interactions with Ysc84p, Rvs167p and Sla1p support this suggestion, while a global GFP study in yeast suggested localisation of the Gts1p to cortical punctate patches (Huh *et al*, 2003). Analysis by Bossier and colleagues has shown that the Gts1p protein is generally hydrophilic, with a weakly hydrophobic stretch of amino acids in its N-terminal domain (Bossier *et al*, 1997). This data suggests Gts1p is not a transmembrane protein due to the lack of a strong hydrophobic domain.

The domains identified in Gts1p are shown in figure 5-1. Identification an Arf-GAP domain in the N-terminus of the protein, suggests that Gts1p may induce hydrolysis of GTP bound ADP-ribosylation factors (Arfs) (for review see Randazzo and Hirsch, 2004). Three Arf proteins have been identified in yeast: Arf1p, Arf2p and Arf3p (Lee *et al*, 1994; Stearns *et al*, 1990). Members of the Arf protein family regulate vesicular trafficking pathways by reversible association with membranes and recruitment of coat proteins to sites of vesicle development. The central region of Gts1p from residues 194-234, contains a UBA (Ubiquitin associated domain) or TS-N domain. Proteins which contain UBA domains have previous been shown to be involved in the ubiquitination of membrane proteins. UBA domains consist of three alpha helices and are approximately 45 amino acids in length. Additionally, a glutamine rich region has been identified in the C-terminus of the protein from residues 311-360.

A)

1 MRFRSSSHSLKHVDRELKELINSSENANKCGECGNFYPTWCSVNLGVFLCGRCASVHRKV
61 **FGSRDDDAFSNVKSLSMDRWTR**EIDDELVSLGGNKGNAWFNPKNVPFPFDGDDDKAIVE
121 **HYIRDKYILGKF**RYDEIKP**EDFGS**RMDDFDGESDRFDERNRSRSRSRSHSFYKGHHNRSD
181 YGGSRDSFQSSGSRYSRQLAELKDMGFGDTNKNLDALSSAHGNINRAIDYLEKSSSSRNS
241 VSAAATTSTPPLPRRRATTSGPQPAIFDGTNVITPDFTNSASFVQAKPAVFDGTLQQYY
301 DPATGM**IYVDQQQYAMAMQQQQQQQLAVAQA**QAQQAQQAQVQAQQAQQAQQAQQAQ
361 QMQQLQM**QQQQAPLSFQQMSQGGNLPQGYFYTQ**

B)

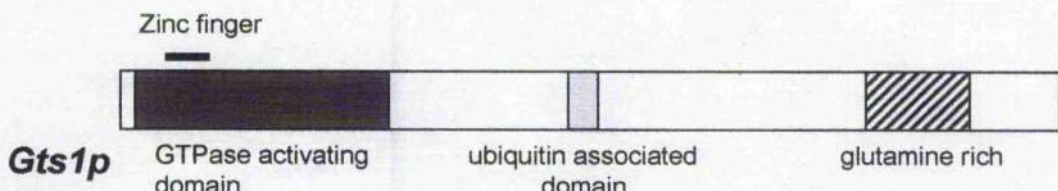


Figure 5-1. Predicted domains of Gts1p. A) The 393 amino acid protein sequence is shown. Residues 14 – 141 form a putative GTPase activating domain (underlined and shown in bold). Residues 27 – 57 were originally reported as a zinc finger domain. Residues 311-360 form a glutamine rich region (underlined), while residues 194-234 (italicised) reportedly form a ubiquitin associated domain (or TS-N domain). Domains identified using the motif scan at <http://hits.isb-sib.ch/cgi-bin/PFSCAN>. B) The putative GTPase activating domain is shown (dark grey). Reported zinc finger domain is also shown. The glutamine rich region is shown (crosshatched), and the ubiquitin associated domain (or TS-N domain) (light grey).

5.2 Results

5.2.1 Gts1p interacts with Sla1p and Ysc84p, as determined by yeast two hybrid analysis

Previous large scale 2-hybrid screens have identified interactions between Gts1p, the cortical patch protein Ysc84p, and the cortical adaptor protein Sla1p (Uetz *et al*, 2000). My aim was to confirm these interactions, and to further define the interacting regions in both Sla1p and Ysc84p. 2-hybrid analysis is described in detail in sections 2.5.1 - 2.5.3 of the Materials and Methods. *GTS1* was initially cloned in-frame into the Gal4-binding domain plasmid (pGBDU-C1). Correct integration of *GTS1* was confirmed by sequencing and a plasmid encoding an N-terminal Gal4-binding domain Gts1 fusion protein (Gal4-BD-Gts1) generated. This plasmid was then transformed into yeast two-hybrid strain, pJ69-4a. Gal4-activation domain plasmid (pGAD-C2) constructs, encoding regions of both Ysc84p and Sla1p fused N-terminally to the Gal4-activation domain, had previously been generated and are summarised in table 5-1. Plasmids encoding these N-terminal Gal4-activation domain fusions were then individually transformed into the yeast two-hybrid stain pJ69-4α. pJ69-4α strains containing plasmids encoding full-length, N-terminal Gal4-activation domain tagged Sla1p and Ysc84p (KAY750 and KAY751, respectively) were also obtained commercially (Invitrogen). The 2-hybrid strain pJ69-4a, containing the Gal4-BD-Gts1 encoding plasmid was then sequentially mated with pJ69-4α strains containing plasmids encoding the N-terminal Gal4-activation domain Ysc84p and Sla1p fusions, and also with the pJ69-4α strains encoding full length Ysc84p and Sla1p fusions. Following mating, diploids containing both plasmid constructs were selectively grown on drop-out leucine and tryptophan synthetic media to ensure retention of both plasmids (figure 5-2A). Diploid strains were then assayed for interaction of the Gal4-BD-Gts1 fusion protein with N-terminal Gal4-activation domain fusions proteins; by growth of the strains on drop-out leucine, tryptophan and histidine synthetic media, to which adenine had been added (figure 5-2B). Interaction between the two Gal4-domain fusion constructs brings the Gal4-binding and activation domains into close proximity, allowing expression of the *HIS3* gene and subsequent growth on media lacking histidine. The addition of adenine to this selective media increased the stringency of this selection.

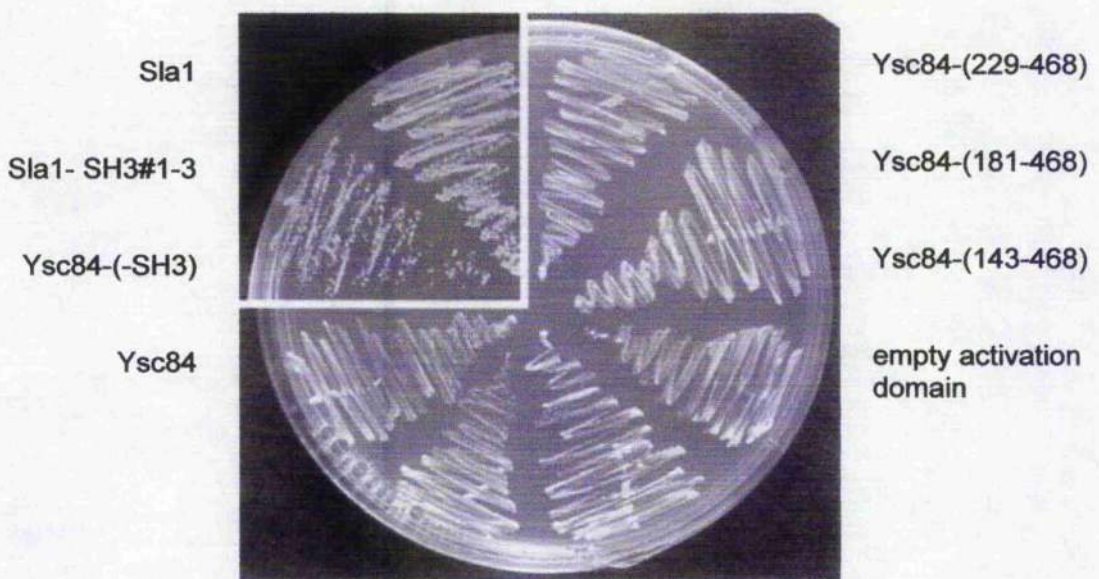
Figure 5-2B demonstrates the growth of diploid strains on drop-out leucine, tryptophan and histidine media containing adenine. Results confirm previous reports of a 2-hybrid interaction between Gts1p and Ysc84p, with substantial growth of a diploid strain expressing Gal4-BD-Gts1 and Gal4-AD-Ysc84 seen. Additionally, analysis of the

interaction of Gts1p with various Ysc84p fragments demonstrates the importance of the C-terminal SH3 domain of Ysc84p for interaction with Gts1p. A diploid strain expressing Gal4-BD-Gts1 and a Ysc84p construct which lacks the C-terminal SH3 domain (Gal4-AD-Ysc84-(-SH3)) did not grow on drop-out leucine, tryptophan and histidine media with adenine. Strong growth was however seen in diploids expressing Gal4-BD-Gts1 with Ysc84p constructs: Gal4-AD-Ysc84-(143-468), Gal4-AD-Ysc84-(181-468) and Gal4-AD-Ysc84-(229-468). These Ysc84p fragments decrease in size, with sequential removal of N-terminal residues. All fragments constructs however contained the C-terminal SH3 domain of Ysc84p. Data also confirms previous reports of a 2-hybrid interaction between Gts1p and Sla1p, with strong growth of a diploid strain expressing Gal4-BD-Gts1 and Gal4-AD-Sla1 shown. Additionally, interaction between the Gts1p and a fragment of Sla1p which encompasses the three N-terminal SH3 domains was assayed, by growth of a diploid strain expressing Gal4-BD-Gts1 and Gal4-AD-Sla1-SH3#1-3. Slow growth of this diploid strain suggested that while this region of Sla1p could mediate interaction with Gts1p, additional domains of Sla1p may strengthen this interaction.

Plasmid	Description
pKA388	Gal4-BD-Gts1
pKA328	Gal4-AD-Sla1-SH3#1-3
pKA251	Gal4-AD-Ysc84-(-SH3)
pKA241	Gal4-AD-Ysc84-(229-468)
pKA242	Gal4-AD-Ysc84-(181-468)
pKA243	Gal4-AD-Ysc84-(143-468)
pKA163	Gal4-AD empty activation domain (pGAD)

Table 5-1 2-hybrid constructs assayed

A)



B)

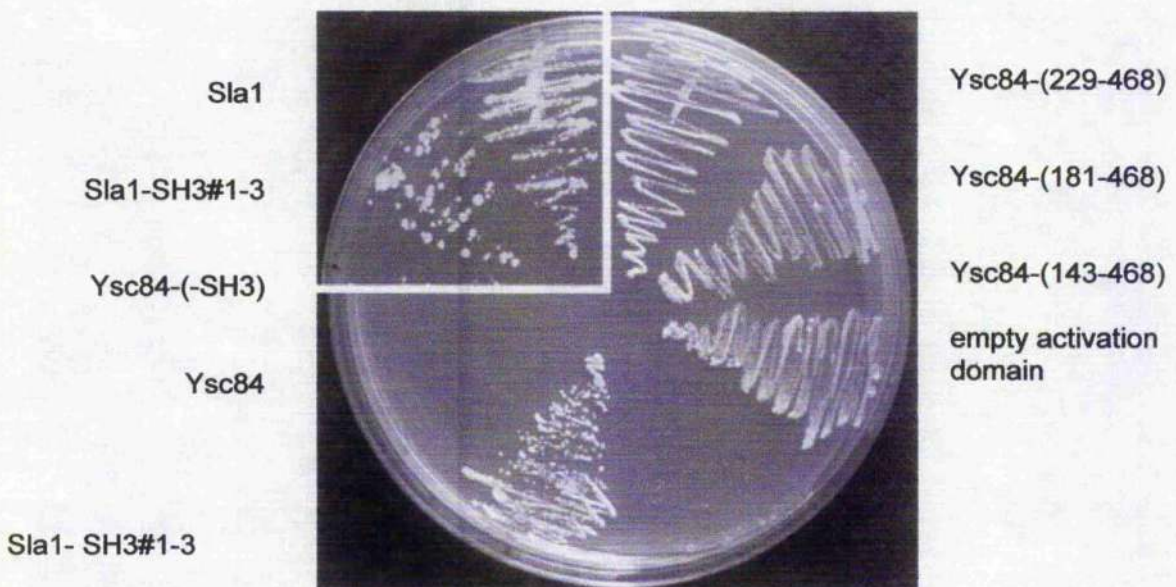


Figure 5-2. Gts1p interacts with Ysc84p and Sla1p by 2-hybrid.

Diploid strains containing both the Gal4-BD-Gts1 encoding plasmid and fusion constructs detailed in table 5-1 and obtained commercially were grown on A) drop-out leucine and tryptophan synthetic media ensure retention of both fusion construct plasmids, and B) drop-out leucine, tryptophan and histidine synthetic media containing adenine, to assay interaction of the proteins of interest.

5.2.2 Gts1p interacts with the N-terminal SH3 domains of Sla1p and the SH3 domain of Ysc84p

Following confirmation of 2-hybrid interactions between Gts1p, Ysc84p and Sla1p, and identification of domains able to mediate these interactions, the strength of these 2-hybrid interactions was investigated using the β -galactosidase assay (section 2.5.3). Expression levels of the reporter gene, *lacZ* (which encodes β -galactosidase) can be measured by following the catalytic hydrolysis of the ONPG (*o*-nitrophenyl- β -D-galactopyranoside); a substrate cleaved by β -galactosidase to the bright yellow product, *o*-nitrophenol (ONP). The strength of this colour change is used to determine the strength of yeast 2-hybrid interactions in β -galactosidase units. β -galactosidase assays were performed in triplicate on the diploid strains previously described (section 5.2.2). Results of these assays are shown in figure 5-3.

The basal level of *lacZ* expression was determined using a strain containing the Gal4-BD-Gts1 plasmid (pKA388) and a control, empty Gal4-activation domain plasmid (pKA163). The basal level was determined as 1.69 ± 0.66 β -galactosidase units. A strong interaction between Gts1p and full length Sla1p was also determined, following calculation of the strength of interaction in a diploid strain expressing Gal4-BD-Gts1 and Gal4-AD-Sla1 as 10.80 ± 0.96 β -galactosidase units. Deletion of the central and C-terminal domains of Sla1p from residues 415 to 1244 however produced a substantial drop in this reading to a basal level of 1.99 ± 0.47 β -galactosidase units, suggesting the importance of the central and C-terminal domains of Sla1p in mediating a strong interaction with Gts1p.

The interaction between Gts1p and full-length Ysc84p was recorded as 3.65 ± 0.06 β -galactosidase units, substantially weaker than the interaction of Gts1p with full-length Sla1p. This interaction was lost following deletion of the C-terminal SH3 domain of Ysc84p, and assays generated readings of 2.49 ± 0.34 β -galactosidase units, close to basal levels. Additionally, analysis of the interaction between Gts1p and the shortest Ysc84p fragment Ysc84-(229-468), produced a decrease in reporter gene expression compared to that recorded for full-length Ysc84p, a reading of 3.14 ± 0.11 β -galactosidase units. Interactions between Ysc84p fragments, Ysc84-(181-468) and Ysc84-(143-468) however showed a small increase in β -galactosidase expression when compared to the full length protein with levels of 4.02 ± 0.34 and 4.65 ± 0.70 β -galactosidase units respectively. These results confirm the importance of the SH3 domain of Ysc84p for interaction with Gts1p. Analysis of Ysc84p fragments

additionally suggests that the interaction mediated by the C-terminal domains of Ysc84p, may be strengthened by the inclusion of N-terminal domains.

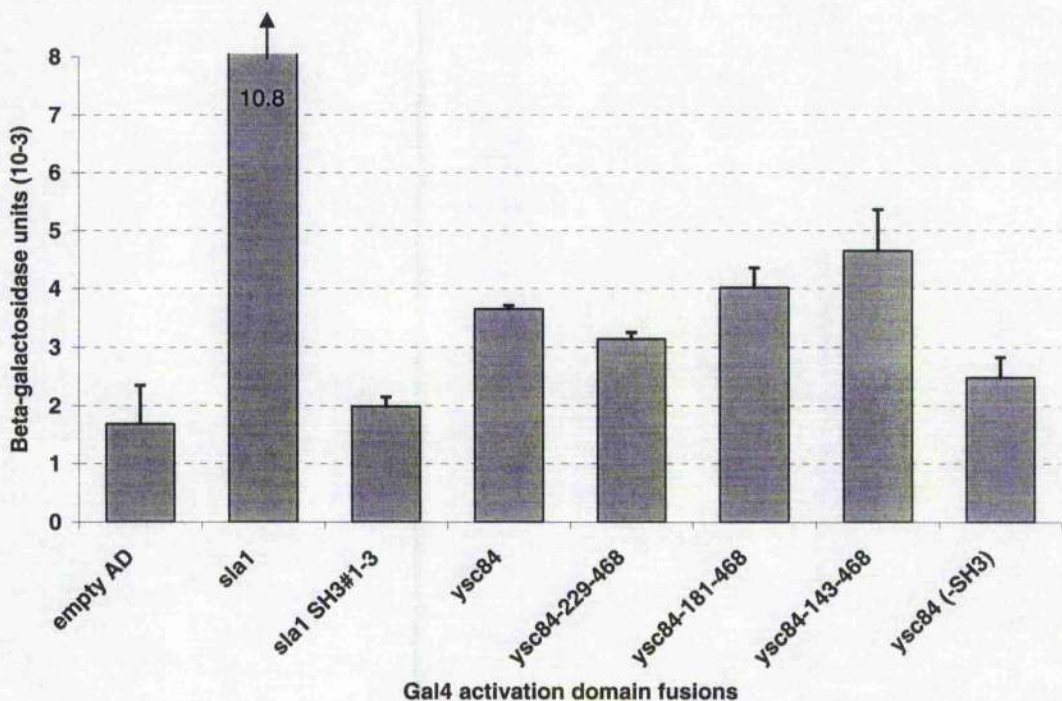


Figure 5-3. Testing the strength of interaction between Gts1p, Ysc84p and Sla1p by β -Galactosidase assay

β -galactosidase assays were performed on diploid strains containing both the Gal4-BD-Gts1 encoding plasmid and fusion constructs detailed in table 5-1 and obtained commercially. Results are shown graphically in β -galactosidase units.

5.2.3 Gts1p localises to punctate structures at the plasma membrane, independently of both Sla1p and F-actin

Identification of an N-terminal region of Gts1p which shows homology to an Arf-GAP motifs, suggests a cytoplasmic localisation for Gts1p and regulation of members of the small GTPase ADP-ribosylation factor (Arf) family. Two hybrid interactions with the cortical patch protein Ysc84p and the adaptor protein Sla1p; a protein which localises to both punctuate patches at the cell cortex and to the nucleus, also suggest that Gts1p may be found in the cytoplasm. In order to identify the cellular localisation of Gts1p, a green fluorescent protein (GFP) tagged Gts1p construct was obtained (Research Genetics) in a wild-type background (KAY725). GFP-tagged Gts1p was localised by microscopy and direct observation of GFP fluorescence following growth of the strain in YPAD media. Images obtained are shown in figure 5-4. Gts1-GFP is seen to localise to punctuate patches at the cell cortex. These patches polarise during budding and accumulate in the newly developing bud. Polarisation of these patches suggests a possible co-localisation or overlapping localisation with cortical actin patches.

The yeast 2-hybrid interaction between Gts1p and Sla1p, suggests Sla1p may be involved in the recruitment of Gts1p to punctate patches at the cell cortex. To investigate the role of Sla1p in the localisation of Gts1p, Gts1-GFP was localised in a $\Delta sla1$ strain (KAY752). The localisation of Gts1-GFP to punctate patches at the cell cortex was unaffected in a $\Delta sla1$ strain (figure 5-5).

Given that *sla1* deletion has been shown to produce yeast cells with a distinct actin phenotype of fewer and enlarged cortical actin patches, mislocalisation of Gts1-GFP in a $\Delta sla1$ strain would be expected if the localisation of Gts1p was dependent on actin. In order to confirm that Gts1p localises independently of the actin cytoskeleton, localisation of Gts1-GFP in a Latrunculin-A treated wild-type strain (KAY725) was performed (section 2.7.6). Latrunculin-A treatment causes rapid depolymerisation of F-actin. Following Latrunculin-A treatment, this strain was examined for complete disruption of actin structures by rhodamine phalloidin staining (Ayscough *et al*, 1997). The localisation of Gts1-GFP in this strain is shown in figure 5-6. Gts1-GFP was seen to localise to punctuate structures at the cell cortex, demonstrating that Gts1p localises to these sites independently of F-actin. Polarisation of Gts1-GFP in both $\Delta sla1$ cells and latrunculin-A treated cells was seen during budding, suggesting recruitment to sites of cell growth occurs independently of both F-actin and Sla1p.

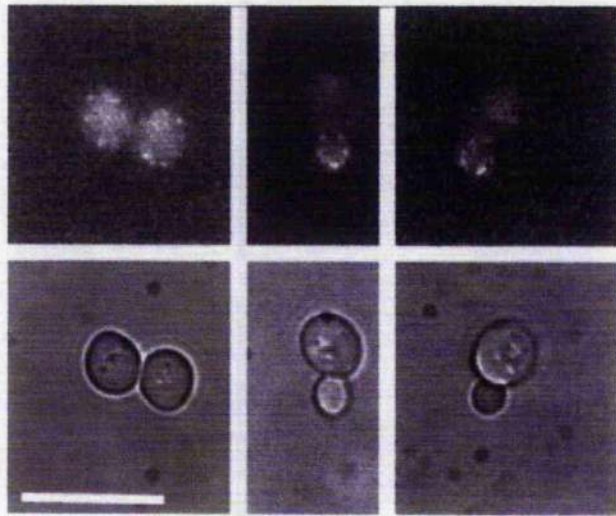


Figure 5-4. GFP-Gts1 localises to punctuate patches at the cell cortex.

The strain KAY725 expresses an N-terminal GFP-tagged Gts1 construct. The GFP tagged protein was localised in this strain by direct fluorescence (upper panels). Nomarski images are shown in the lower panels.

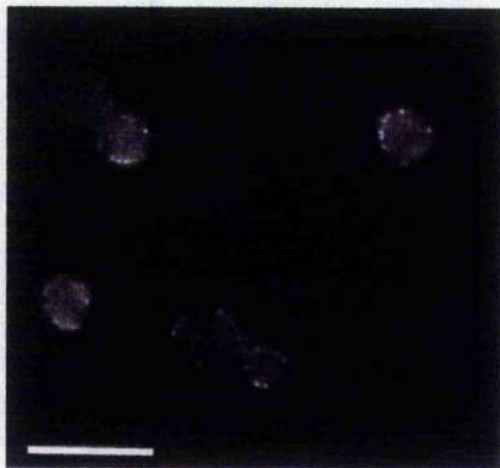


Figure 5-5. GFP-Gts1p localisation is unaffected in a Δ sla1 strain.

The Δ sla1 strain KAY752 expressed a genomically tagged N-terminal GFP-Gts1 construct. GFP-Gts1 was localised by direct fluorescence.

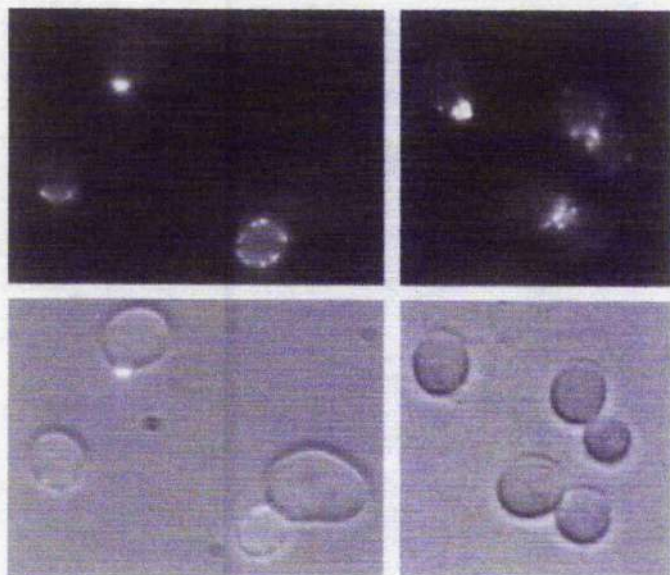


Figure 5-6. GFP-Gts1p localises to punctuate patches at the cell cortex in Latrunculin-A treated cells. The strain KAY725 expresses a GFP-Gts1 construct. Latrunculin-A was added to the strain during log-phase growth 15 minutes. Complete disruption of the actin cytoskeleton was visualised by rhodamine phalloidin staining. GFP-Gts1 localisation was performed by direct fluorescence. Nomarski images are shown in the panels below.

5.2.4 GTS1 deletion indicates that the protein plays a role in endocytosis and actin organisation

Given that Gts1p interacts with the endocytic proteins Ysc84p and Sla1p by yeast 2-hybrid, and that Gts1p localises to punctuate structures at cortical sites which polarise during budding, data suggested a role for Gts1p in the regulation of endocytosis. The study of a *gts1* deletion mutant was therefore undertaken in order to provide insight into the role of the Gts1p at the cell cortex.

Haploid and diploid $\Delta gts1$ strains (KAY709 and KAY710 respectively) were obtained (Invitrogen) and phenotypic analysis of these mutants performed, in conjunction with their respective parental wild-type strains (KAY 446 and KAY 480). $\Delta gts1$ strains demonstrated a mild defect in the organisation of the actin cytoskeleton as determined by rhodamine phalloidin staining (section 2.7.3). Polarisation of actin towards a new bud site was seen to occur before completion of cytokinesis in 10% of the cells examined (figure 5-7), demonstrating that *gts1* deletion has only a subtle effect on actin organisation. This budding defect may however be linked to the reported acceleration of budding and associated reduction in cell size following disruption of *gts1* (Mitsui *et al*, 1994). Additionally, Nomarski images (figure 5-8) suggested an elongation of cells in the diploid $\Delta gts1$ strain during budding and cytokinesis. Lucifer yellow uptake assays identified a reduction in uptake of the dye in $\Delta gts1$ strains, demonstrating defects in fluid phase endocytosis (figure 5-8). Uptake was reduced by approximately 60% in 70% of $\Delta gts1$ haploid cells examined and decreased by approximately 50% in 85% of $\Delta gts1$ diploid cells examined, as determined qualitatively. Additionally, a decrease in the uptake of the lipophilic styryl dye FM4-64 ((N-triethylammoniumpropyl)-4-(p-diethylaminophenylhexatrienyl) pyridinium dibromide) in both $\Delta gts1$ haploid and diploid strains suggested further endocytic defects, characterised by a decrease in internalisation of the cell membrane (figure 5-7). An approximately 80% decrease in FM4-64 uptake was identified in 62% of $\Delta gts1$ haploid cells and 71% of $\Delta gts1$ diploid cells examined, as determined qualitatively. The methods for assaying both lucifer yellow and FM4-64 uptake are described in sections 2.7.4 and 2.7.5 respectively.

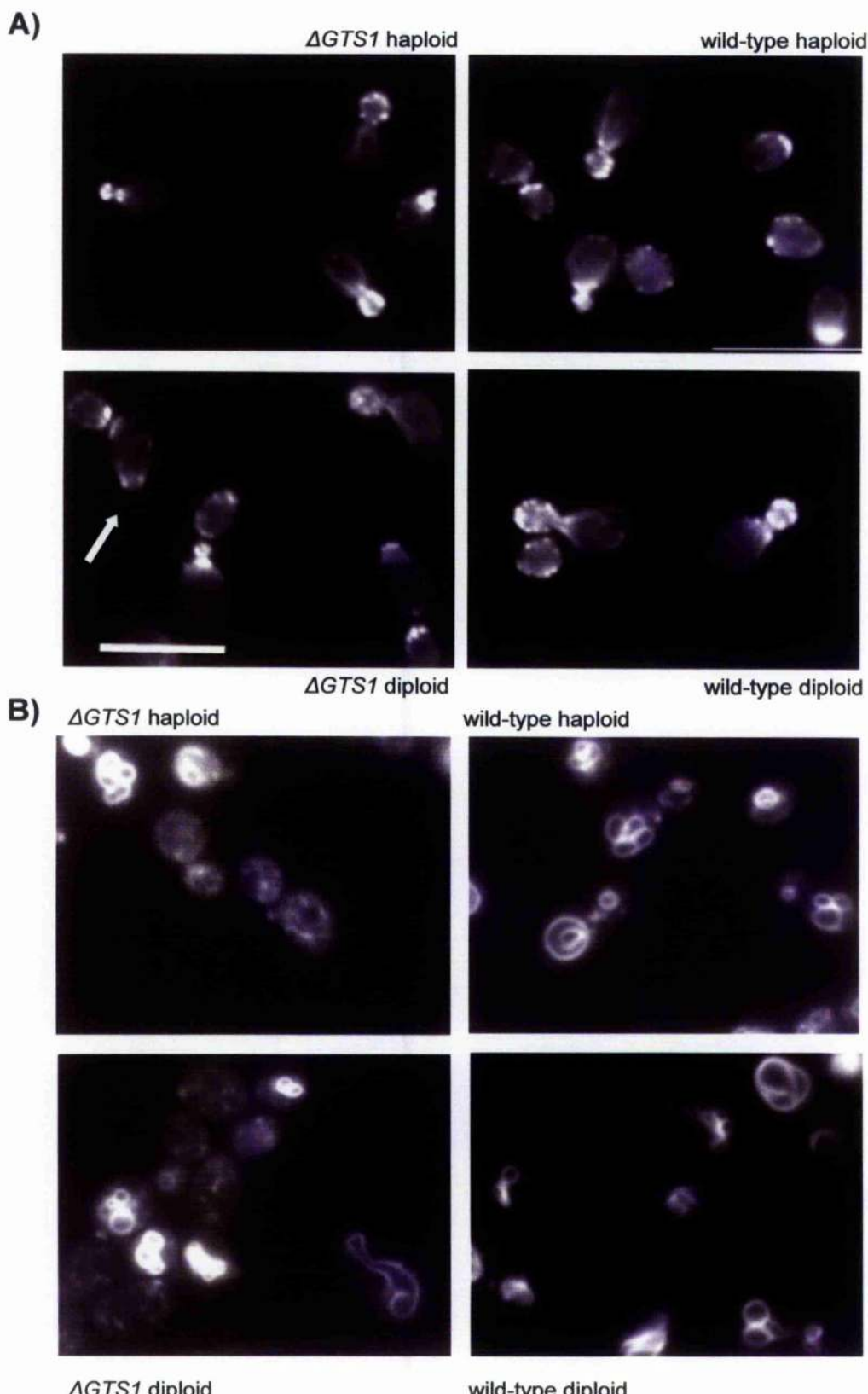


Figure 5-7. Deletion of *GTS1* causes a mild actin defect and defects in the endocytic internalisation of membranes. A) Rhodamine phalloidin staining was performed on a haploid $\Delta gts1$ strain (KAY 709), diploid $\Delta gts1$ deletion strain (KAY 710), and parental wild-type haploid (KAY446) and diploid (KAY480) strains. Accumulation of actin at a new bud site was seen to occur early, before cytokinesis had concluded in the diploid *GTS1* deletion strain (arrow). B) FM4-64 uptake assays were also performed on the haploid $\Delta gts1$ deletion strain, diploid $\Delta gts1$ /deletion strain, and parental wild-type haploid and diploid strains. 10 μ M bars are shown.

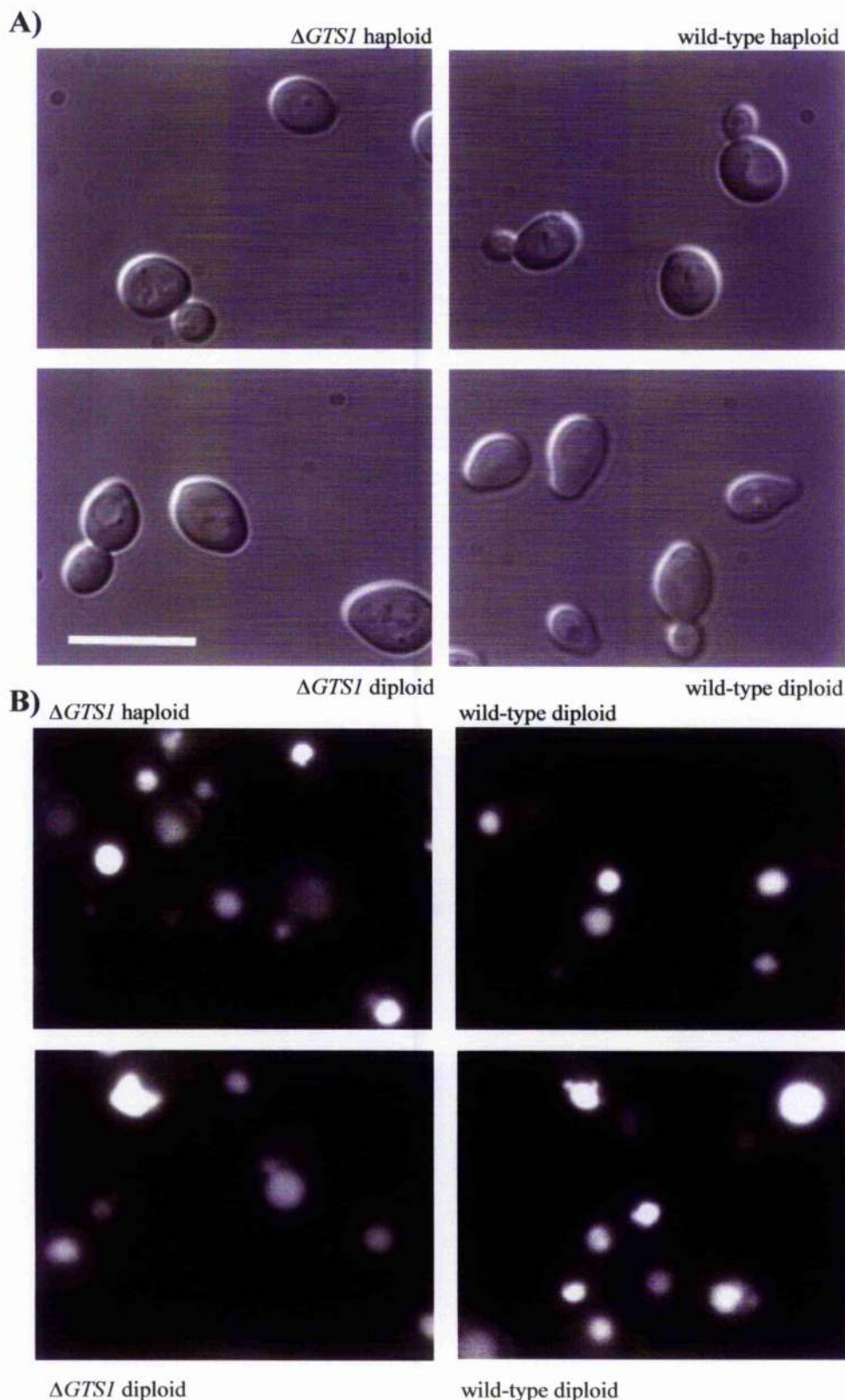


Figure 5-8. Deletion of *GTSI* causes defects in fluid phase endocytosis. A) Nomarski images of haploid $\Delta gts1$ strain (KAY709), diploid $\Delta gts1$ strain (KAY710), and parental wild-type haploid (KAY446) and diploid (KAY480) strains. B) Lucifer yellow uptake assays were also performed on these strains.

5.3 Discussion

Data presented in this chapter confirms that the initial identification of Gts1p as a nuclear transcription factor was incorrect. Cellular analysis has demonstrated that Gts1p localises to the cell cortex in punctate patches and has a role in the regulation of actin and endocytic uptake. Consistent with previous reports (Uetz et al, 2000), we also find that Gts1p interacts with Sla1p and Ysc84p by yeast 2-hybrid. Our yeast 2-hybrid and β -galactosidase assays additionally demonstrate that the C-terminal SH3 domain of Ysc84p is important for mediating the interaction with Gts1p, and that the N-terminal domains of Sla1p mediate interaction with Gts1p.

A previous yeast 2-hybrid screen has also demonstrated interactions between Gts1p and Rvs167p, Pan1p, Sla1p and Ysc84p (Uetz et al, 2000). Given that Pan1p, Sla1p and Ysc84p localised to endocytic sites (Dewar et al, 2002; Kaksonen et al, 2003), yeast 2- hybrid interactions with these proteins suggested that Gts1p may also localise to endocytic sites or have a role in the regulation of actin. In this study, I have confirmed the interaction of Gts1p with the cortical patch proteins Ysc84p and Sla1p by yeast 2-hybrid analysis and determined the regions mediating these interactions to be located in the N-terminal domains of Sla1p and the C-terminal SH3 domain of Ysc84p (sections 5.2.1 and 5.2.2). The interaction of the N-terminal domain of Sla1p with Gts1p was however substantially weaker than that seen with full-length Sla1p, as determined by β -galactosidase assay. This suggests that additional domains may strengthen the interaction mediated by the N-terminal domains of Sla1p. These interactions must however be confirmed biochemically.

Significant progress has also been made in the characterisation of the cellular role of Gts1p. Gts1p was localised to punctuate structures at the cell cortex which polarised to sites of cell growth during budding (section 5.2.3). This localisation and potential *in vivo* interactions with Sla1p and Ysc84p, suggested a role for Gts1p in the regulation of endocytosis. Localisation of the protein to cortical sites was however shown to occur independently of both Sla1p and F-actin; two integral endocytic components required for endocytic uptake (section 5.2.3). Localisation of Gts1p to the cell cortex therefore occurs via an as yet undefined mechanism. Potentially however, localisation may be mediated through interaction with Pan1p or Rvs167p as suggested by 2-hybrid analysis (Uetz et al, 2000) or by interaction with additional membrane

associated or endocytic proteins. Consistent with a role in the regulation of endocytosis, deletion of *gts1* in both haploid and diploid strains generated defects in fluid phase endocytosis and mild actin defects. Uptake of the lipophilic dye FM4-64 was also aberrant in $\Delta gts1$ strains, indicating an inhibitory effect on later endocytic events and internalisation of the cell membrane (section 5.2.4).

Biochemical analysis must be performed to confirm interaction between Gts1p, Ysc84p and Sla1p, initial data however suggests that Gts1p may link Sla1p and Ysc84p at the cell cortex and may also regulate proteins of the Arf family. Regulation of Gts1p has been investigated in a study by Yaguchi and colleagues. Two forms of Gts1p were identified by SDS-page gel electrophoresis and the slower migrating form of Gts1p lost upon treatment with protein phosphatase (Yaguchi *et al*, 2000). This data identifies a phosphorylated form of Gts1p and suggests that Gts1p may be regulated by phosphorylation.

One potential mechanism for Gts1p recruitment and interaction with endocytic components is via Arf3p. The ADP-ribosylation factors (Arfs) are a family of small ubiquitously expressed Ras-like GTPases that are central to many vesicular transport processes. Like other GTPases, these proteins cycle between the active, GTP-bound form and the inactive GDP-bound form, and require accessory factors to mediate the conversion between GTP and GDP bound states. Arf guanine-nucleotide exchange factors (GEFs) catalyse the exchange of GDP for GTP, while Arf GTPase activating factors (GAPs) induced hydrolysis of GTP to GDP (for review see Randazzo *et al*, 2004). The identification of an Arf-GAP domain in Gts1p suggests the ability of Gts1p to induce hydrolysis of GTP-bound ADP-ribosylation factors (Arfs). Arf3p has been shown to localise primarily to the cell periphery in *S. cerevisiae*, exhibiting a punctate fluorescence at the cell periphery and an evenly distributed cytoplasmic staining which polarises towards sites of cell growth during budding (Huang *et al*, 2003). Arf1p and Arf2p are primarily Golgi localised. The mammalian homologue of Arf3p is Arf6. Arf6 retains a high level of sequence conservation, showing 60% identity at the amino acid level. Arf6 localises to the plasma membrane and has been implicated in early endocytic events (Millar *et al*, 1999; Altschulter *et al*, 1999; for review see Donaldson, 2003). Recent data from our lab has disproved initial findings that Arf3p is not linked to endocytosis (Huang *et al*, 2003). Lsb5p interacts with Sla1p, which regulates both actin structures and endocytic components at the plasma membrane (Dewar *et al*, 2002; Costa *et al*, 2005). By demonstrating a biochemical

interaction between Arf3p and Lsb5p, a link between Arf3p and endocytic uptake has been shown (Costa *et al*, 2005). Endocytosis is however unaffected in *arf3* mutant cells (Huang *et al*, 2003). The mammalian Arf3p homologue, Arf6 activates PIP5-kinase *in vivo*, which generates phosphatidylinositol 4,5-bisphosphate (PIP₂) a key phosphoinositide at the cell cortex which is involved in membrane trafficking and actin regulation (Yin and Janmey, 2003). Arf3p was therefore proposed to regulate actin in a similar mechanism, however recent studies suggest that Arf3p does not directly regulate actin but instead has a role in polarisation and bud site selection (Huang *et al*, 2003). Intriguingly, the mild actin defect demonstrated in our $\Delta gts1$ diploid strain also suggests role for Gts1p in bud development (section 5.2.4). Disruption of the *GTS1* has previously been shown to accelerate budding (Mitsui *et al*, 1994).

The presence of an Arf-GAP domain in Gts1p and the localisation of both Gts1p and Arf3p at the cell periphery suggest Gts1p may inactivate Arf3p. The active form of Arf3p and other Arf proteins have been shown to be membrane associated (Gaschet and Hsu, 1999; Huang *et al*, 2003), while the GDP bound form remains primarily cytoplasmic. The action of Gts1p may therefore inactivate and release Arf3p from the plasma membrane. However, while Gts1p has homology to the Arf GAP domain, previous analysis has demonstrated that Gts1p lacks the ability to rescue growth of an *arf1-3* mutant at 37°C when overexpressed on a high-copy number plasmid. Overexpression of other known Arf-GAPs: *SAT1*, *GCSI*, *GLO3*, and *YIL044C/SAT2* have been shown to compensate for the loss of Arf function associated with *arf1-3* (Zhang *et al*, 1998). This questions the ability of Gts1p to act as an Arf-GAP. The potential Arf-GAP activity of Gts1p therefore should be examined in future work.

Data presented in this chapter has enabled us to propose several potential Gts1p interactions which may occur *in vivo* (figure 5-9). We propose that Gts1p interacts with Sla1p and Ysc84p at the cell cortex, as suggested by yeast 2-hybrid analysis (sections 5.2.1 and 5.2.2). Additionally, homology to an Arf-GAP domain suggests Gts1p may regulate Arf proteins, and specifically Arf3p which localises predominantly to the plasma membrane in yeast. Arf3p, through homology to mammalian Arf6 is proposed to interact with adaptor proteins and coat proteins at plasma membrane (Austin *et al*, 2002). While Arf6 is not involved in recruitment of GGAs to the trans-golgi network (TGN), it does however appear to recruit GGA1 to

putative early endosomes (Takatsu *et al*, 2002), suggesting that Arf6 may be involved in the recruitment of specific proteins to compartments other than the TGN. Interestingly, Arf3p has recently been shown to interact with Lsb5p at the cell cortex; a protein which shows significant similarity to the GGA proteins (Costa *et al*, 2005). Yeast Ggalp and Gga2p proteins interact with Arf1p and Arf2p but not Arf3p (Zhdanina *et al*, 2001; Huang *et al*, 2003)). Recruitment of Lsb5p to the cell cortex is dependent on Arf3p and in turn, Lsb5p binds to Sla1p (Costa *et al*, 2005). Through homology to the GGA proteins therefore, Lsb5p may be recruited to the plasma membrane by Arf3p in its GTP bound form, potentially stabilising Arf3p, as stabilisation of Arf1p by several GGAs has been demonstrated, possibly by direct competition with Arf-GAP proteins for a binding site (Puertollano *et al*, 2001). The action of Arf3p in the GTP bound form additionally may be regulated by the recruitment of Gts1p which potentially promotes hydrolysis of GTP through its Arf-GAP domain.

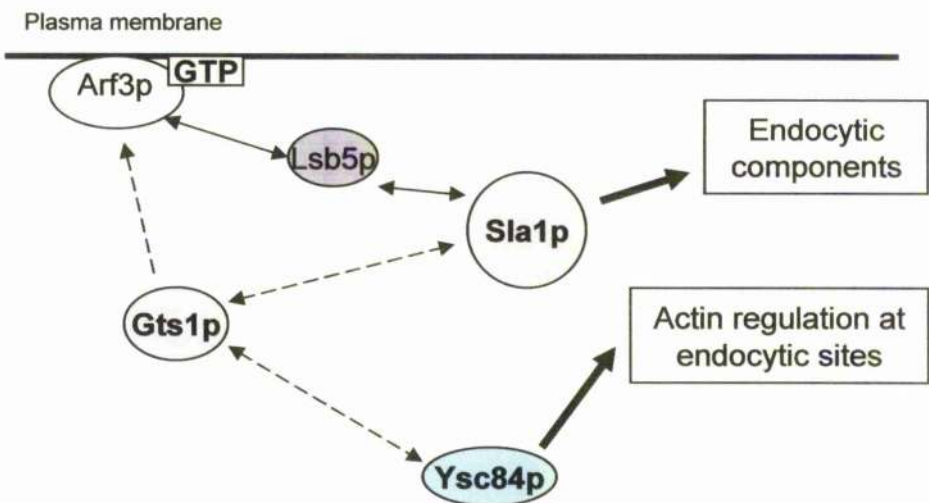


Figure 5-9. Proposed Gts1p interactions at the cell cortex. Gts1p may regulate Arf3p at the plasma membrane via its Arf-GAP domain. In addition, 2-hybrid interactions suggest Gts1p interacts with both Ysc84p and Sla1p *in vivo*. Sla1p has been previously shown to interact with Lsb5p which interacts with Arf3p. Known roles are linked by block arrows, while proposed interactions are demonstrated with dashed arrows.

6 THESIS SUMMARY AND FUTURE DIRECTIONS

6.1

Thesis Summary

The filamentous structure assumed by polymerised cytoplasmic actin is utilised in the cell by the organisation of such filaments into a diverse array of structures. These structures include both actin cables and patches in *S. cerevisiae*, and filopodial and lamellipodial structures in motile mammalian cells. To achieve this organisation, actin regulating proteins regulate filaments on an individual scale, while also co-ordinating the integration of filaments into complex filamentous networks. Elucidation of the mechanisms controlling the dynamic rearrangements of the actin network is therefore a significant challenge to researchers. The activity and function of many specific actin regulating proteins have however been the focus of a multitude of studies which are enabling the wider picture of cellular actin control to become clear. The focus of my work was an investigation of specific proteins which were known to regulate, or were proposed to regulate actin in *S. cerevisiae*. By enabling further insights into the activities and regulation of such proteins, I hope to contribute to the overall understanding of actin dynamics in *S. cerevisiae* and in other organisms.

Sla1p was previously known as a multifunctional cortical adaptor protein. In Chapter 3 however, I present data which details my investigation of nuclear Sla1p. This analysis has allowed the proposal of a mechanism for the regulated nuclear translocation of Sla1p. The aberrant nuclear localisation of two *sla1* mutants, was shown to correlate with the loss of specific nuclear transport signals, suggesting specific regions of the protein which were important for mediating nuclear translocation of Sla1p. Subsequent studies of nuclear transport receptor mutants also enabled the identification of an importin mutant which inhibited nuclear translocation of Sla1p. Finally, the microarray analysis of a wild-type and a Δ *sla1* strain was detailed and the results considered. These microarray results may provide crucial clues which may enable the role of nuclear Sla1p to be identified. Chapter 3 therefore defines the nuclear localisation of a protein previously known to localise only to the cellular cytoplasm. This work is the first detailed analysis of such a protein in *S. cerevisiae*.

A mechanism for the nuclear translocation of phosphorylated Sla1p has been proposed. The proposed recognition of phosphorylated Sla1p by the importin Rsl1p, is supported by the detection of Sla1-myc in an *rsl1* mutant strain. Sla1-myc exhibits a higher molecular weight in this mutant strain than was seen our wild-type strain (figure 3-12), suggesting that Sla1p exists primarily in a modified, and potentially

phosphorylated form when nuclear translocation by Rsl1p is blocked. It is proposed therefore that the nuclear translocation, and potentially the nuclear role of Sla1p may be dependent on protein modification, similar to the role of Sla1p in the Sla1p/End3p/Pan1p endocytic complex. Accumulation of a potentially phosphorylated form of Sla1p upon inhibition of nuclear uptake by *rsll* mutation, also suggests that dephosphorylation of Sla1p may occur in the nucleus. PP1 is known to localise to the nucleus and has been reported to interact with Sla1p by yeast 2-hybrid analysis. Nuclear PP1 may therefore potentially dephosphorylate Sla1p.

Microarray analysis of a wild-type and a Δ sla strain identified gene expression changes in a number of genes which encoded nuclear proteins. While this study failed to directly identify a role for nuclear Sla1p, microarray data may be used to promote further investigations into nuclear Sla1p. The identification of nuclear actin and suggestion that actin continues to play a structural role in the nucleus, implies a continuing requirement for the regulation and nucleation of actin polymers, and therefore potential conservation of the regulatory mechanisms of actin and Sla1p activity at this location. Additionally however, the potential of Sla1p to perform a transcriptional role in the nucleus should also be investigated.

The dynamic nature of the actin cytoskeleton is a consequence of the coordinated control of filament polymerisation, disassembly and nucleation. Ysc84p associates with cortical actin patches, which are composed of over 30 patch proteins and an integral branched, filamentous actin network (Pruyne and Bretscher 2000b, Young et al 2004). In Chapter 4, I demonstrate the interaction of Ysc84p with actin filaments *in vitro*. Additional analysis also reveals both the filament severing and capping activity of Ysc84p *in vitro*. Finally, by localising these activities to an amino-terminal region of Ysc84p, and demonstrating a loss of capping activity associated with the full length protein, a possible regulatory mechanism for Ysc84p was considered. This *in vitro* data suggests an exciting role for Ysc84p in the regulated control of branched actin filaments at cortical patches in *S. cerevisiae*. Actin patches are integral components of the endocytic machinery in *S. cerevisiae* and I therefore proposed that the capping and severing activity of Ysc84p may be central to the co-ordinated control of actin regulation at the cell cortex. Ysc84p may influence actin dynamics both during the early stages of endocytic uptake, and during the generation of an actin based propulsive force, which is thought to be harnessed to enable the movement of endocytosed vesicles. Additionally, the localisation of the Ysc84p homologue, hSH3yl-1, to sites of dynamic actin remodelling, and demonstration of the ability of hSH3yl-1 to partially functionally

replace Ysc84p in *S. cerevisiae*, suggests that this Ysc84p homologue may also perform an important role in the regulation of actin in higher cells. The *in vitro* actin regulating abilities of hSH3yl-1 however remain to be examined.

The actin binding, severing and capping activities of the conserved N-terminal region of Ysc84p suggest a previously unidentified functional domain. This region of Ysc84p fails to show significant homology to known domains or motifs upon investigation, and Ysc84p itself does not show significant homology to known actin severing and capping proteins. Initial secondary structural predictions of Ysc84p however identify several regions of predicted alpha helical and beta sheet structures in the N-terminal region which in combination with actin binding, capping and severing activities, suggests an as yet uncharacterised conserved functional domain in Ysc84p. Ysc84p and its homologues may therefore constitute a new class of actin severing/capping proteins. Additionally it is also suggested by our analysis that Ysc84p may preferentially bind to phalloidin stabilised filaments. Binding of both full length and Ysc84p N-terminal fusions to unstabilised F-actin was demonstrated by F-actin sedimentation, however a lack of severing activity exhibited by GST-Ysc84 in the absence of phalloidin suggests that Ysc84p may require stabilisation of filaments in order to exhibit strong binding to F-actin. Phalloidin does not inhibit the hydrolysis of ATP-actin following incorporation into actin filaments, but has been shown to inhibit the release of the product of hydrolysis, inorganic phosphate from filaments. This effect may therefore stabilise the interaction of Ysc84p with F-actin and should therefore be investigated.

The generation of cellular phenotypes upon deletion of both *YSC84* and *LSB5* suggests a partial overlap the function of these proteins. Endocytic and actin defects, a temperature dependent growth defect and slow growth phenotype, are seen in a Δ *ysc84* Δ *lsb5* mutant; phenotypes which are not apparent in single deletions. EM studies of this double mutant also demonstrate vesicle accumulation and thickening of the cell wall, which suggest trafficking defects in this strain. The potentially involvement of Lsb5p in the regulation of actin through interaction with the Arp2/3 regulating protein, Las17p (Madania et al, 1999), recent studies which suggest that Lsb5p may regulate endocytic uptake and vesicle trafficking at the cell cortex, and the identification of the actin regulating abilities of Ysc84p, suggest Lsb5p and Ysc84p may both play roles in endocytic regulation, although a specific functional overlap has yet to be identified.

Both Ysc84p and Sla1p localise predominantly to the cell cortex, where they are proposed to transiently interact. This interaction may function as a recruiting or

regulatory mechanism in the control of endocytic uptake at the cell cortex. An additional link between Ysc84p and Sla1p may be Gts1p. In chapter 5, I confirmed the previously reported interaction between Gts1p, and both Sla1p and Ysc84p, as determined by yeast 2-hybrid analysis. I also identified domains in both Sla1p and Ysc84p which were involved in mediating these interactions. These interactions suggest that Gts1p, Sla1p and Ysc84p may interact *in vivo* at the cell cortex, potentially linking the inactivation of Arf3p with endocytosis, via the proposed Arf-GAP activity of Gts1p. The potential Arf regulating ability of Gts1p should therefore be investigated in subsequent studies. Gts1p may act in the recruitment of specific components to sites of Arf3p mediated vesicle formation or in the recruitment of components important for bud growth and development to specific sites.

The work which I have presented in chapters 3 – 5 provides further insights into the regulatory mechanisms controlling remodelling of the actin cytoskeleton in *S. cerevisiae* and higher organisms. While this study has concentrated specifically on the roles of Sla1p, Ysc84p and Gts1p, information gathered during the course of this work can be regarded as pieces of a larger actin puzzle, the understanding of which will eventually enable a better understanding of cellular regulation. Knowledge gained from this study may also be extrapolated and applied to regulatory networks in other systems, which in many cases show a high degree of conservation. This thesis therefore provides a body of research which can be regarded as incomplete and which raises many further questions. With these questions in mind, I propose several experiments in section 6-2 to address some interesting possibilities which have arisen from my studies.

6.2 Future Directions

6.2.1 Investigating the nuclear translocation of Sla1p

Cellular and protein analysis suggests that Sla1p cycles through the nucleus (chapter 3). By undertaking point-mutagenesis of potential signal sequences located between residues 118-511 and 507-1008 of Sla1p, the identification of precise signal sequences which specified the nuclear translocation of the Sla1p could be made. Additionally, Sla1p point-mutants which were deficient in nuclear translocation may retain the functionality lost by domain deletion in the *sla1-Δ188-511* and *sla1-ΔG2* mutants. Such strains would potentially therefore identify cellular defects specific to the inhibition of Sla1p nuclear translocation only. Successful inhibition of Sla1p nuclear translocation would be detected by immunofluorescence of the tagged mutant protein, with cellular analysis undertaken in strains demonstrating Sla1p mislocalisation.

6.2.2 Examining the regulatory mechanism of Sla1p

A model for the phosphorylation dependent cycling of Sla1p through the nucleus has been proposed. 2-Dimensional gel analysis of our *sla1-Δ188-511* and *sla1-ΔG2* mutant strains, followed by Sla1p detection with Sla1p specific antibodies, would provide insight into the modification and regulation of Sla1p. Previously unpublished data from our lab has identified four modified forms of Sla1p by 2-Dimensional gel analysis of the wild type strain (KAY 302) during log phase growth. The study of *sla1-Δ188-511* and *sla1-ΔG2* mutants by 2-Dimensional gel analysis would identify modified forms of these Sla1p mutants, and may suggest whether a specifically modified form of the protein predominates in these strains. Our model proposes the nuclear entry of a phosphorylated form of Sla1p. Analysis of the *sla1-ΔG2* strain would therefore be of particular interest, as our model predicts that this mutant protein would be predominantly phosphorylated.

A previous screen has identified an interaction between Sla1p and Glc7p, the catalytic subunit of protein phosphatase 1 (PP1) by yeast 2-hybrid analysis (Venturi *et al.*, 2000). In order to further investigate the regulatory mechanisms of Sla1p, confirmation of this interaction both by 2-hybrid and biochemical analysis could be undertaken, while additionally undertaking a study of Sla1p localisation and modification in PP1 mutant strains.

6.2.3 Identifying Sla1p protein-protein interactions

To further investigate the function and regulation of Sla1p, GST pull-down assays should be used to identify proteins in crude yeast extracts which physically interact with Sla1p. GST tagging, expression and purification of GST-Sla1p would enable immobilisation of the purified fusion protein on glutathione sepharose beads. Subsequent incubation of both a control GST column and a column containing immobilised GST-Sla1p with yeast extracts, followed by column washing, elution and SDS-page gel analysis of the eluted proteins, would identify protein bands which specifically bound to the GST-Sla1p. Analysis of such bands could then be undertaken by mass spectrometry, following identification of known or potential binding partners by western blotting. The tandem affinity purification (TAP) tagging method may also be useful in purifying Sla1p complexes under native conditions. Prior purification of Sla1p has however proved difficult due to degradation of the protein.

6.2.4 Investigating the effect of Ysc84p on actin polymerisation

To further investigate the actin severing and capping activities of Ysc84p, the effect of Ysc84p on the kinetics of actin polymerisation should be measured by following the polymerisation of pyrene labelled actin, in both the presence and absence of untagged Ysc84p and Ysc84p fragments. The pyrene conjugated G-actin monomer is weakly fluorescent, but upon polymerisation fluorescence is substantially enhanced. The speed of polymerisation can therefore be followed by measuring the increase in fluorescence in a spectrofluorimeter (Cooper and Pollard 1982). From these studies the binding affinity and kinetic rate constants of Ysc84p and Ysc84p fragments could be determined. Additionally the actin severing activities of Ysc84p could be studied by following the time course of depolymerisation upon incubation with pre-formed actin filaments. Polymerised pyrene labelled actin filaments could also be incubated with various concentrations of free Ca^{2+} , in the presence of Ysc84p, and the intensity of fluorescence recorded. This study would allow the depolymerising effects of Ysc84p to be compared to that of known actin severing and capping proteins, and the effects of calcium addition to be quantified.

6.2.5 Investigating the *in vivo* function of Ysc84p and protein-protein interactions

Overexpression of hSH3yl-1 in *S. cerevisiae* is known to affect the actin cytoskeletal network. Additionally, overexpression of capping protein (CP) in *S. cerevisiae* is known to generate cells which demonstrate a loss of heterogeneous morphology; with many showing abnormally thickened cell walls, loss of actin cables or an altered actin cytoskeleton, in addition to aberrant bud morphology (Amatruda et al 1992). Overexpression studies of Ysc84p may therefore yield important information as to the effects of the protein *in vivo*. The ability of Ysc84p overexpression to rescue defects associated with capping protein deletion could also be tested, which may suggest a functional overlap between these two proteins. Genetic screens to identify suppressors of *YSC84* overexpression phenotypes could additionally be performed, in order to identify proteins which may physically interact with Ysc84p.

The generation of antibodies specific to Ysc84p was a significant development which was not utilised fully in this study. Ysc84p has been shown to immunoprecipitate with Abp1p, and to potentially interact with Las17p and Gts1p by two-hybrid analysis. Ysc84p specific antibodies could therefore be used to perform immunoprecipitation assays in which the proposed interactions between Ysc84p, Las17p, and Gts1p could be confirmed biochemically.

6.2.6 Analysis of the Arf-GAP activity of Gts1p

In order to confirm the proposed Arf-GAP activity of Gts1p, subsequent analysis must be performed. The Arf-GAP activity of Gts1p could be assayed in total cell lysates as described by Randazzo and colleagues (Randazzo and Kahn, 1994). Cloning of Gts1p to engineer a myc epitope at the C-terminus of the protein could be undertaken, and the fusion expressed in yeast cells on a high copy number plasmid. Total cell lysates from this strain and a control untransformed strain could then be assayed by immunoblotting with anti-myc antibodies to identify the tagged protein, and to ensure expression of the fusion protein at the correct molecular weight. Arf-GAP activity would then be assayed by incubating total cell lysates with known concentrations of [³²P] GTP loaded, purified Arf1. Untransformed yeast would exhibit low background levels of GAP activity, from endogenous Arf-GAP proteins. However, in strains

overexpressing Gts1p a marked increase in Arf-GAP activity would potentially be seen. Protein bound nucleotides are then trapped on nitrocellulose filters from which they are extracted. Analysis is then performed by chromatography to separate the nucleotides, from which [³²P]-containing nucleotides can be visualised and quantified using a phosphoimager.

6.2.7 Investigating protein-protein interactions and the localisation of Gts1p

2-hybrid data indicates interactions between Gts1p and both Slalp and Ysc84p. Purification of tagged Gts1p would enable these proposed interactions to be confirmed biochemically. GST tagging, expression and purification of GST-Gts1p would enable immobilisation of the fusion protein on glutathione sepharose beads, and subsequent incubation with purified proteins of interests or with yeast extracts from strains expressing tagged proteins of interest, in order to confirm these interactions. The tandem affinity purification (TAP) tagging method may also be useful in purifying Gts1p complexes under native conditions.

7 REFERENCES

- Abraham, V. C., Krishnamurthi, V., Taylor, D. L., & Lanni, F. (1999). The Actin-Based Nanomachine at the Leading Edge of Migrating Cells. *Biophys. J.*, 77(3), 1721-1732.
- Abudugupur, A., Xu, Z., Mitsui, K., Hisaki, H., Ueda, N., Amemiya, T., & Tsurugi, K. (2003). Severe reduction of superoxide dismutase activity in the yeast *Saccharomyces cerevisiae* with the deletion or overexpression of GTS1. *FEMS Microbiology Letters*, 223(1), 141-145.
- Adams, A., & Pringle, J. (1984). Relationship of actin and tubulin distribution to bud-growth in wild-type and morphogenic-mutant *Saccharomyces cerevisiae*. *Journal of Cell Biology*, 98, 934-945.
- Adams, A. E., & Pringle, J. R. (1991). Staining of actin with fluorochrome-conjugated phalloidin. *Methods in Enzymology*, 194, 729-731.
- Adams, A. E. M., Botstein, S., & Drubin, D. G. (1989). A yeast actin-binding protein is encoded by SAC6, a gene found by suppression of an actin mutation. *Science*, 243, 231-233.
- Aguilar, R. C., Watson, H. A., & Wendland, B. (2003). The Yeast Epsin Ent1 Is Recruited to Membranes through Multiple Independent Interactions. *J. Biol. Chem.*, 278(12), 10737-10743.
- Aizawa, H., Sutoh, K., Tsubuki, S., Kawashima, S., Ishii, A., & Yahara, I. (1995). Identification, Characterization, and Intracellular Distribution of Cofilin in *Dictyostelium discoideum*. *J. Biol. Chem.*, 270(18), 10923-10932.
- Akiyama, S., & Tsurugi, K. (2003). The GTS1 gene product facilitates the self-organization of the energy metabolism oscillation in the continuous culture of the yeast *Saccharomyces cerevisiae*. *FEMS Microbiology Letters*, 228(1), 105-110.
- Alberts, A. S. (2001). Identification of a Carboxyl-terminal Diaphanous-related Formin Homology Protein Autoregulatory Domain. *J. Biol. Chem.*, 276(4), 2824-2830.
- Alberts, B., Johnson, A., Lewis, J., Raff, M., Roberts, K., & Walter, P. (2002). *Molecular Biology of the Cell* (3rd Edition ed.): Garland Publishing.
- Altschuler, Y., Liu, S.-H., Katz, L., Tang, K., Hardy, S., Brodsky, E., Apodaca, G., & Mostov, K. (1999). ADP-ribosylation Factor 6 and Endocytosis at the Apical Surface of Madin-Darby Canine Kidney Cells. *J. Cell Biol.*, 147(1), 7-12.
- Amatruda, J., Gattermeir, D., Karpova, T., & Cooper, J. (1992). Effects of null mutations and overexpression of capping protein on morphogenesis, actin distribution and polarized secretion in yeast. *J. Cell Biol.*, 119(5), 1151-1162.
- Amberg, D. C., Basart, E., & Botstein, D. (1995). Defining protein interactions with yeast actin in vivo. *Nature Structural Biology*, 2(1), 28-35.
- Aoki, N., Ito, K., & Ito, M. (2000). A Novel Mouse Gene, Sh3yl1, is Expressed in the Anagen Hair Follicle. *J Invest Dermatol*, 114(5), 1050-1056.
- Austin, C., Boehm, M., & Tooze, S. A. (2002). Site-Specific Cross-Linking Reveals a Differential Direct Interaction of Class 1, 2, and 3 ADP-Ribosylation Factors with Adaptor Protein Complexes 1 and 3. *Biochemistry*, 41(14), 4669-4677.
- Auty, R., Steen, H., Myers, L. C., Persinger, J., Bartholomew, B., Gygi, S. P., & Buratowski, S. (2004). Purification of Active TFIID from *Saccharomyces cerevisiae*: Extensive Promoter Contacts and Co-activator Function. *J. Biol. Chem.*, 279(48), 49973-49981.
- Ayscough, K. R. (1998). *In vivo* functions of actin-binding proteins. *Current opinion in Cell Biology*, 10, 102-111.
- Ayscough, K. R. (2000). Endocytosis and the development of cell polarity in yeast require a

- dynamic F-actin cytoskeleton. *Current Biology*, 10(24), 1587-1590.
- Ayscough, K. R., & Drubin, D. G. (1996). Actin: general Principles from Studies in Yeast. *Annual Review of Cell Developmental Biology*, 12, 129-160.
- Ayscough, K. R., Eby, J. J., Lila, T., Dewar, H., Kozminski, K. G., & Drubin, D. G. (1999). Sla1p Is a Functionally Modular Component of the Yeast Cortical Actin Cytoskeleton Required for Correct Localization of Both Rho1p-GTPase and Sla2p, a Protein with Talin Homology. *Mol. Biol. Cell*, 10(4), 1061-1075.
- Ayscough, K. R., Stryker, J., Pokala, N., Sanders, M., Crews, P., & Drubin, D. G. (1997). High Rates of Actin Filament Turnover in Budding Yeast and Roles for Actin in Establishment and Maintenance of Cell Polarity Revealed Using the Actin Inhibitor Latrunculin-A. *J. Cell Biol.*, 137(2), 399-416.
- Bailly, M., Macaluso, F., Cammer, M., Chan, A., Segall, J. E., & Condeelis, J. S. (1999). Relationship between Arp2/3 Complex and the Barbed Ends of Actin Filaments at the Leading Edge of Carcinoma Cells after Epidermal Growth Factor Stimulation. *J. Cell Biol.*, 145(2), 331-345.
- Barden, J. A., Miki, M., Hambly, B. D., & Dos Remedios, C. G. (1987). Localization of the phalloidin and nucleotide-binding sites on actin. *European Journal of Biochemistry*, 162(3), 583-588.
- Bénédetti, H., Raths, S., Crausaz, F., & Riezman, H. (1994). The END3 gene encodes a protein that is required for the internalization step of endocytosis and for actin cytoskeleton organization in yeast. *Molecular Biology of the Cell*, 5(9), 1023-1037.
- Bengtsson, L., & Wilson, K. L. (2004). Multiple and surprising new functions for emerin, a nuclear membrane protein. *Current Opinion in Cell Biology*, 16(1), 73-79.
- Bettinger, B. T., Gilbert, D. M., & Amberg, D. C. (2004). Actin Up in the Nucleus. *Nature Reviews Molecular Cell Biology*, 5(5), 410-415.
- Blessing, C. A., Ugrinova, G. T., & Goodson, H. V. (2004). Actin and ARPs: action in the nucleus. *Trends in Cell Biology*, 14(8), 435-442.
- Blondel, M., Alepuz, P. M., Huang, L. S., Shaham, S., Ammerer, G., & Peter, M. (1999). Nuclear export of Far1p in response to pheromones requires the export receptor Msn5p/Ste21p. *Genes Dev.*, 13(17), 2284-2300.
- Boman, A. L. (2001). GGA proteins: new players in the sorting game. *J Cell Sci.*, 114(19), 3413-3418.
- Borisy, G. G., & Svitkina, T. M. (2000). Actin machinery: pushing the envelope. *Curr Opin Cell Biol.*, 12(1), 104-112.
- Bossier, P., Goethals, P., & Rodrigues-Pousada, C. (1997). Constitutive flocculation in *Saccharomyces cerevisiae* through overexpression of the GTS1 gene, coding for a 'Glo'-type Zn-finger-containing protein. *Yeast*, 13(8), 717-725.
- Burtnick, L. D., Koepf, E. K., Grimes, J., Jones, E. Y., Stuart, D. I., McLaughlin, P. J., & Robinson, R. C. (1997). The crystal structure of plasma gelsolin: implications for actin severing, capping, and nucleation. *Cell*, 90(4), 661-670.
- Buzan, J. M., & Frieden, C. (1996). Yeast actin: Polymerization kinetic studies of wild type and a poorly polymerizing mutant. *PNAS*, 93(1), 91-95.
- Cairns, B., Henry, N., & Kornberg, R. (1996). TFG/TAF30/ANC1, a component of the yeast SWI/SNF complex that is similar to the leukemogenic proteins ENL and AF-9. *Mol. Cell Biol.*, 16(7), 3308-3316.
- Care, A., Vousden, K. A., Binley, K. M., Radcliffe, P., Trevethick, J., Mannazzu, I., &

- Sudbery, P. E. (2004). A Synthetic Lethal Screen Identifies a Role for the Cortical Actin Patch/Endocytosis Complex in the Response to Nutrient Deprivation in *Saccharomyces cerevisiae*. *Genetics*, 166(2), 707-719.
- Carlier, M. F. (1998). Control of actin dynamics. *Curr Opin Cell Biol.*, 10(1), 45-51.
- Carlier, M.-F., Laurent, V., Santolini, J., Melki, R., Didry, D., Xia, G.-X., Hong, Y., Chua, N.-H., & Pantaloni, D. (1997). Actin Depolymerizing Factor (ADF/Cofilin) Enhances the Rate of Filament Turnover: Implication in Actin-based Motility. *J. Cell Biol.*, 136(6), 1307-1322.
- Carlier, M.-F., & Pantaloni, D. (1997). Control of actin dynamics in cell motility. *Journal of Molecular Biology*, 269(4), 459-467.
- Carlsson, A. E., Shah, A. D., Elking, D., Karpova, T. S., & Cooper, J. A. (2002). Quantitative Analysis of Actin Patch Movement in Yeast. *Biophys. J.*, 82(5), 2333-2343.
- Carlsson, A. E., Wear, M. A., & Cooper, J. A. (2004). End versus Side Branching by Arp2/3 Complex. *Biophys. J.*, 86(2), 1074-1081.
- Carlsson, L., Nyström, L. E., Sundkvist, I., Markey, F., & Lindberg, U. (1977). Actin polymerizability is influenced by profilin, a low molecular weight protein in non-muscle cells. *J Mol Biol.*, 115(3), 465-483.
- Cestra, G., Castagnoli, L., Dente, L., Minenkova, O., Petrelli, A., Migone, N., Hoffmuller, U., Schneider-Mergener, J., & Cesareni, G. (1999). The SH3 Domains of Endophilin and Amphiphysin Bind to the Proline-rich Region of Synaptojanin 1 at Distinct Sites That Display an Unconventional Binding Specificity. *J. Biol. Chem.*, 274(45), 32001-32007.
- Chang, J. S., Henry, K., Wolf, B. L., Geli, M., & Lemmon, S. K. (2002). Protein Phosphatase-1 Binding to Scd5p Is Important for Regulation of Actin Organization and Endocytosis in Yeast. *J. Biol. Chem.*, 277(50), 48002-48008.
- Colwill, K., Field, D., Moore, L., Friesen, J., & Andrews, B. (1999). In Vivo Analysis of the Domains of Yeast Rvs167p Suggests Rvs167p Function Is Mediated Through Multiple Protein Interactions. *Genetics*, 152(3), 881-893.
- Cooper, J. (1987). Effects of cytochalasin and phalloidin on actin. *J. Cell Biol.*, 105(4), 1473-1478.
- Cooper, J. A., & Pollard, T. D. (1982). Methods to measure actin polymerization. *Methods in Enzymology*.
- Cope, M., T.V., J., Yang, S., Shang, C., & Drubin, D. G. (1999). Novel Protein Kinases Ark1p and Prk1p Associate with and Regulate the Cortical Actin Cytoskeleton in Budding Yeast. *J. Cell Biol.*, 144(6), 1203-1218.
- Costa, R., Warren, D. T., & Ayscough, K. R. (2005). Lsb5p interacts with actin regulators Sla1p and Las17p, ubiquitin and Arf3p to couple actin dynamics to membrane trafficking processes. *Biochemical Journal*, 385(2).
- Daelemans, D., Costes, S. V., Lockett, S., & Pavlakis, G. N. (2005). Kinetic and Molecular Analysis of Nuclear Export Factor CRM1 Association with Its Cargo In Vivo. *Mol. Cell. Biol.*, 25(2), 728-739.
- Dang, C. V., & Lee, W. M. (1988). Identification of the human c-myc protein nuclear translocation signal. *Mol. Cell. Biol.*, 8(10), 4048-4054.
- David, V., Gouin, E., Troys, M. V., Grogan, A., Segal, A. W., Ampe, C., & Cossart, P. (1998). Identification of cofilin, coronin, Rac and capZ in actin tails using a Listeria affinity approach. *J Cell Sci.*, 111(19), 2877-2884.
- de Arruda, M., Watson, S., Lin, C., Leavitt, J., & Matsudaira, P. (1990). Fimbrin is a

- homologue of the cytoplasmic phosphoprotein plastin and has domains homologous with calmodulin and actin gelation proteins. *J. Cell Biol.*, 111(3), 1069-1079.
- de Beer, T., Hoofnagle, A. N., Enimon, J. L., Bowers, R. C., Yamabhai, M., Kay, B. K., & Overduin, M. (2000). Molecular mechanism of NPF recognition by EH domains. *Nature Structural Biology*, 7(11), 1018 - 1022.
- DeVit, M. J., & Johnston, M. (1999). The nuclear exportin Msn5 is required for nuclear export of the Mig1 glucose repressor of *Saccharomyces cerevisiae*. *Current Biology*, 9(21), 1231-1241.
- Dewar, H., Warren, D. T., Gardiner, F. C., Gourlay, C. G., Satish, N., Richardson, M. R., Andrews, P. D., & Ayscough, K. R. (2002). Novel Proteins Linking the Actin Cytoskeleton to the Endocytic Machinery in *Saccharomyces cerevisiae*. *Mol. Biol. Cell*, 13(10), 3646-3661.
- Dingwall, C., & Laskey, R. A. (1991). Nuclear targeting sequences--a consensus? *Trends in Biochemical Sciences*, 16(12), 478-481.
- Dominguez, R. (2004). Actin-binding proteins - a unifying hypothesis. *Trends in Biochemical Sciences*, 29(11), 572-578.
- Donaldson, J. G. (2003). Multiple Roles for Arf6: Sorting, Structuring, and Signaling at the Plasma Membrane. *J. Biol. Chem.*, 278(43), 41573-41576.
- Doyle, T., & Botstein, D. (1996). Movement of yeast cortical actin cytoskeleton visualized in vivo. *PNAS*, 93(9), 3886-3891.
- Drees, B. L., Sundin, B., Brazeau, E., Caviston, J. P., Chen, G.-C., Guo, W., Kozminski, K. G., Lau, M. W., Moskow, J. J., Tong, A., Schenkman, L. R., McKenzie, A., III, Brennwald, P., Longtine, M., Bi, E., Chan, C., Novick, P., Boone, C., Pringle, J. R., Davis, T. N., Fields, S., & Drubin, D. G. (2001). A protein interaction map for cell polarity development. *J. Cell Biol.*, 154(3), 549-576.
- Drubin, D., Miller, K., & Botstein, D. (1988). Yeast actin-binding proteins: evidence for a role in morphogenesis. *J. Cell Biol.*, 107(6), 2551-2561.
- Drubin, D. G. (1990). Actin and actin-binding proteins in yeast. *Cell Motility and the Cytoskeleton*, 15(1), 5-11.
- Drubin, D. G. (1991). Development of cell polarity in budding yeast. *Cell*, 65(7), 1093-1096.
- Drubin, D. G., & Ayscough, K. R. (1998). *Immunofluorescence Microscopy of Yeast Cells* (2nd edition ed.): Academic Press.
- Dubreuil, R. R. (1991). Structure and Evolution of the Actin-Crosslinking Proteins. *Bioessays*, 13(5), 219-226.
- Dulic, V., Egerton, M., Elguindi, I., Raths, S., Singer, B., & Riezman, H. (1991). Yeast endocytosis assays. *Methods in Enzymology*, 194, 697-710.
- Duncan, M. C., Cope, M. J., Goode, B. L., Wendland, B., & Drubin, D. G. (2001). Yeast Eps15-like endocytic protein, Pan1p, activates the Arp2/3 complex. *Nature Cell Biology*, 3, 687-690.
- Dunn, R., & Hicke, L. (2001). Domains of the Rsp5 Ubiquitin-Protein Ligase Required for Receptor-mediated and Fluid-Phase Endocytosis. *Mol. Biol. Cell*, 12(2), 421-435.
- Engel, J., Fasold, H., Hull, F. W., Waechter, F., & Wegner, A. (1977). The polymerization reaction of muscle actin. *Mol. Cell Biochem.*, 18(1), 3-13.
- Engqvist-Goldstein, A. E. Y., & Drubin, D. G. (2003). Actin Assembly and Endocytosis: From Yeast to Mammals. *Annual Review of Cell and Developmental Biology*, 19(1), 287-332.

- Engqvist-Goldstein, A. E. Y., Kessels, M. M., Chopra, V. S., Hayden, M. R., & Drubin, D. G. (1999). An Actin-binding Protein of the Sla2/Huntingtin Interacting Protein 1 Family Is a Novel Component of Clathrin-coated Pits and Vesicles. *J. Cell Biol.*, 147(7), 1503-1518.
- Evangelista, M., Klebl, B. M., Tong, A. H. Y., Webb, B. A., Leeuw, T., Leberer, E., Whiteway, M., Thomas, D. Y., & Boone, C. (2000). A Role for Myosin-I in Actin Assembly through Interactions with Vrp1p, Bee1p, and the Arp2/3 Complex. *J. Cell Biol.*, 148(2), 353-362.
- Evangelista, M., Pruyne, D., Amberg, D. C., Boone, C., & Bretscher, A. (2002). Formins direct Arp2/3-independent actin filament assembly to polarize cell growth in yeast. *Nature Cell Biology*, 4(1), 32-41.
- Ficarro, S. B., McCleland, M. L., Stukenberg, P. T., Burke, D. J., Ross, M. M., Shabanowitz, J., Hunt, D. F., & White, F. M. (2002). Phosphoproteome analysis by mass spectrometry and its application to *Saccharomyces cerevisiae*. *Nature Biotechnology*, 20(3), 301-305.
- Fornerod, M., Ohno, M., Yoshida, M., & Mattaj, I. W. (1997). CRM1 Is an Export Receptor for Leucine-Rich Nuclear Export Signals. *Cell*, 90(6), 1051-1060.
- Fujimoto, L. M., Roth, R., Heuser, J. E., & Schmid, S. L. (2000). Actin Assembly Plays a Variable, but not Obligatory Role in Receptor-Mediated Endocytosis. *Traffic*, 1(2), 161-171.
- Fukuda, M., Asano, S., Nakamura, T., Adachi, M., Yoshida, M., Yanagida, M., & Nishida, E. (1997). CRM1 is responsible for intracellular transport mediated by the nuclear export signal. *Nature*, 390(6657), 308-311.
- Galan, J. M., Moreau, V., Andre, B., Volland, C., & Haguenauer-Tsapis, R. (1996). Ubiquitination Mediated by the Npi1p/Rsp5p Ubiquitin-protein Ligase Is Required for Endocytosis of the Yeast Uracil Permease. *J. Biol. Chem.*, 271(18), 10946-10952.
- Gallwitz, D., & Sures, I. (1980). Structure of a split yeast gene: complete nucleotide sequence of the actin gene in *Saccharomyces cerevisiae*. *PNAS*, 77(5), 2546-2550.
- Gancedo, J. M. (2001). Control of pseudohyphae formation in *Saccharomyces cerevisiae*. *FEMS Microbiology Reviews*, 25(1), 107-123.
- Gaschet, J., & Hsu, V. W. (1999). Distribution of ARF6 between Membrane and Cytosol Is Regulated by Its GTPase Cycle. *J. Biol. Chem.*, 274(28), 20040-20045.
- Gavin, A.-C., Bosche, M., Krause, R., Grandi, P., Marzioch, M., Bauer, A., Schultz, J., Rick, J. M., Michon, A.-M., Cruciat, C.-M., Remor, M., Hofert, C., Schelder, M., Brajenovic, M., Ruffner, H., Merino, A., Klein, K., Hudak, M., Dickson, D., Rudi, T., Gnau, V., Bauch, A., Bastuck, S., Huhse, B., Leutwein, C., Heurtier, M.-A., Copley, R. R., Edelmann, A., Querfurth, E., Rybin, V., Drewes, G., Raida, M., Bouwmeester, T., Bork, P., Seraphin, B., Kuster, B., Neubauer, G., & Superti-Furga, G. (2002). Functional organization of the yeast proteome by systematic analysis of protein complexes. *Nature*, 415(6868), 141-147.
- Giffard, R., Weeds, A., & Spudich, J. (1984). Ca²⁺-dependent binding of severin to actin: a one-to-one complex is formed. *J. Cell Biol.*, 98(5), 1796-1803.
- Goode, B. L., Drubin, D. G., & Lappalainen, P. (1998). Regulation of the Cortical Actin Cytoskeleton in Budding Yeast by Twinfilin, a Ubiquitous Actin Monomer-sequestering Protein. *J. Cell Biol.*, 142(3), 723-733.
- Goode, B. L., Rodal, A. A., Barnes, G., & Drubin, D. G. (2001). Activation of the Arp2/3 complex by the Actin Filament Binding Protein Abp1p. *Journal of Cell Biology*, 153(3), 627-634.

- cerevisiae by mass spectrometry. *Nature*, 415 (6868), 180-183.
- Holaska, J. M., Kowalski, A. K., & Wilson, K. L. (2004). Emerin Caps the Pointed End of Actin Filaments: Evidence for an Actin Cortical Network at the Nuclear Inner Membrane. *PLoS Biology*, 2(9), e231.
- Holmes, K. C., Popp, D., Gebhard, W., & Kabsch, W. (1990). Atomic model of the actin filament. *Nature*, 347(6288), 44-49.
- Holtzman, D., Yang, S., & Drubin, D. (1993). Synthetic-lethal interactions identify two novel genes, SLA1 and SLA2, that control membrane cytoskeleton assembly in *Saccharomyces cerevisiae*. *J. Cell Biol.*, 122(3), 635-644.
- Howard, J. P., Hutton, J. L., Olson, J. M., & Payne, G. S. (2002). Slalp serves as the targeting signal recognition factor for NPFX(1,2)D-mediated endocytosis. *J. Cell Biol.*, 157(2), 315-326.
- Huang, C.-F., Liu, Y.-W., Tung, L., Lin, C.-H., & Lee, F.-J. S. (2003). Role for Arf3p in Development of Polarity, but Not Endocytosis, in *Saccharomyces cerevisiae*. *Mol. Biol. Cell*, 14(9), 3834-3847.
- Huang, S., Robinson, R. C., Gao, L. Y., Matsumoto, T., Brunet, A., Blanchard, L., & Staiger, C. J. (2005). Arabidopsis VILLIN1 Generates Actin Filament Cables That Are Resistant to Depolymerization. *Plant Cell*, 17(2), 486-501.
- Hug, C., Jay, P. Y., Reddy, I., McNally, J. G., Bridgman, P. C., Elson, E. L., & Cooper, J. A. (1995). Capping protein levels influence actin assembly and cell motility in *Dictyostelium*. *Cell*, 81(4), 591-600.
- Huh, W., Falvo, J., Gerke, L., Carroll, A., Howson, R., Weissman, J., & O'Shea, E. K. (2003). Global analysis of protein localization in budding yeast. *Nature*, 425, 686-691.
- Humphries, C. L., Balcer, H. I., D'Agostino, J. L., Winsor, B., Drubin, D. G., Barnes, G., Andrews, B. J., & Goode, B. L. (2002). Direct regulation of Arp2/3 complex activity and function by the actin binding protein coronin. *J. Cell Biol.*, 159(6), 993-1004.
- Hurley, J. H., & Wendland, B. (2002). Endocytosis: Driving Membranes around the Bend. *Cell*, 111(2), 143-146.
- James, P., Halladay, J., & Craig, E. A. (1996). Genomic Libraries and a Host Strain Designed for Highly Efficient Two-Hybrid Selection in Yeast. *Genetics*, 144(4), 1425-1436.
- Jans, D. A., Xiao, C. Y., & Lam, M. H. C. (2000). Nuclear targeting signal recognition: a key control point in nuclear transport? *Bioessays*, 22(6), 532 - 544.
- Jung, U. S., & Levin, D. E. (1999). Genome-wide analysis of gene expression regulated by the yeast cell wall integrity signalling pathway. *Mol Microbiol*, 34(5), 1049-1057.
- Kabsch, W., Mannherz, H. G., Suck, D., Pai, E. F., & Holmes, K. C. (1990). Atomic structure of the actin:DNase I complex. *Nature*, 347(6288), 37-44.
- Kaffman, A., Rank, N. M., O'Neill, E. M., Huang, L. S., & O'Shea, E. K. (1998). The receptor Msn5 exports the phosphorylated transcription factor Pho4 out of the nucleus. *Nature*, 396(6710), 482-486.
- Kaksonen, M., Peng, H. B., & Rauvala, H. (2000). Association of cortactin with dynamic actin in lamellipodia and on endosomal vesicles. *J Cell Sci*, 113(24), 4421-4426.
- Kaksonen, M., Sun, Y., & Drubin, D. G. (2003). A Pathway for Association of Receptors, Adaptors, and Actin during Endocytic Internalization. *Cell*, 115(4), 475-487.
- Kalderon, D., Richardson, W. D., Markham, A. F., & Smith, A. E. (1984). Sequence requirements for nuclear location of simian virus 40 large-T antigen. *Nature*, 311(5981), 33-38.

- Karpova, T. S., McNally, J. G., Moltz, S. L., & Cooper, J. A. (1998). Assembly and Function of the Actin Cytoskeleton of Yeast: Relationships between Cables and Patches. *Journal of Cell Biology*, 142, 1501-1517.
- Karpova, T. S., Reck-Peterson, S. L., Elkind, N. B., Mooseker, M. S., Novick, P. J., & Cooper, J. A. (2000). Role of Actin and Myo2p in Polarized Secretion and Growth of *Saccharomyces cerevisiae*. *Mol. Biol. Cell*, 11(5), 1727-1737.
- Karpova, T. S., Tatchell, K., & Cooper, J. A. (1995). Actin filaments in yeast are unstable in the absence of capping protein or fimbrin. *J. Cell Biol.*, 131(6), 1483-1493.
- Kelleher, J. F., Atkinson, S. J., & Pollard, T. D. (1995). Sequences, structural models, and cellular localization of the actin-related proteins Arp2 and Arp3 from Acanthamoeba. *J. Cell Biol.*, 131(2), 385-397.
- Kinosian, H. J., Newman, J., Lincoln, B., Selden, L. A., Gershman, L. C., & Estes, J. E. (1998). Ca²⁺ Regulation of Gelsolin Activity: Binding and Severing of F-actin. *Biophys. J.*, 75(6), 3101-3109.
- Kiseleva, E., Drummond, S. P., Goldberg, M. W., Rutherford, S. A., Allen, T. D., & Wilson, K. L. (2004). Actin- and protein-4.1-containing filaments link nuclear pore complexes to subnuclear organelles in Xenopus oocyte nuclei. *J Cell Sci*, 117(12), 2481-2490.
- Kowanetz, K., Husnjak, K., Holler, D., Kowanetz, M., Soubeyran, P., Hirsch, D., Schmidt, M. H. H., Pavelic, K., De Camilli, P., Randazzo, P. A., & Dikic, I. (2004). CIN85 Associates with Multiple Effectors Controlling Intracellular Trafficking of Epidermal Growth Factor Receptors. *Mol. Biol. Cell*, 15(7), 3155-3166.
- Kowanetz, K., Szymkiewicz, I., Haglund, K., Kowanetz, M., Husnjak, K., Taylor, J. D., Soubeyran, P., Engstrom, U., Ladbury, J. E., & Dikic, I. (2003). Identification of a Novel Proline-Arginine Motif Involved in CIN85-dependent Clustering of Cbl and Down-regulation of Epidermal Growth Factor Receptors. *J. Biol. Chem.*, 278(41), 39735-39746.
- Kumar, N., & Khurana, S. (2004). Identification of a Functional Switch for Actin Severing by Cytoskeletal Proteins. *J. Biol. Chem.*, 279(24), 24915-24918.
- Lamb, J., Allen, P., Tuan, B., & Janmey, P. (1993). Modulation of gelsolin function. Activation at low pH overrides Ca²⁺ requirement. *J. Biol. Chem.*, 268(12), 8999-9004.
- Lee, F., Stevens, L., Kao, Y., Moss, J., & Vaughan, M. (1994). Characterization of a glucose-repressible ADP-ribosylation factor 3 (ARF3) from *Saccharomyces cerevisiae*. *J. Biol. Chem.*, 269(33), 20931-20937.
- Lew, D. J. (2002). Formin' actin filament bundles. 4(2), E29-E30.
- Li, R. (1997). Bee1, a Yeast Protein with Homology to Wiscott-Aldrich Syndrome Protein, Is Critical for the Assembly of Cortical Actin Cytoskeleton. *J. Cell Biol.*, 136(3), 649-658.
- Lila, T., & Drubin, D. G. (1997). Evidence for physical and functional interactions among two *Saccharomyces cerevisiae* SH3 domain proteins, an adenylyl cyclase-associated protein and the actin cytoskeleton. *Mol Biol Cell*, 8(2), 367-385.
- Liu, H. P., & Bretscher, A. (1989). Disruption of the single tropomyosin gene in yeast results in the disappearance of actin cables from the cytoskeleton. *Cell*, 57(2), 233-242.
- Loisel, T. P., Boujemaa, R., Pantaloni, D., & Carlier, M. F. (1999). Reconstitution of actin-based motility of *Listeria* and *Shigella* using pure proteins. *Nature* 401, 613 - 616 (07 October 1999); doi:10.1038/44183, 401(613 - 616), 1038 - 44183.
- Longtine, M. S., McKenzie, A., Demarini, D. J., Shah, N. G., Wach, A., Brachat, A., Philippse, P., & Pringle, J. R. (1998). Additional modules for versatile and economical PCR-based gene deletion and modification in *Saccharomyces cerevisiae*. *Yeast*, 14(10),

953-961.

- Lorenz, M., Popp, D., & Holmes, K. C. (1993). Refinement of the F-Actin Model against X-ray Fiber Diffraction Data by the Use of a Directed Mutation Algorithm. *Journal of Molecular Biology*, 234(3), 826-836.
- Ma, L., Rohatgi, R., & Kirschner, M. W. (1998). The Arp2/3 complex mediates actin polymerization induced by the small GTP-binding protein Cdc42. *PNAS*, 95(26), 15362-15367.
- Machesky, L. M., Atkinson, S. J., Ampe, C., Vandekerckhove, J., & Pollard, T. D. (1994). Purification of a cortical complex containing two unconventional actins from Acanthamoeba by affinity chromatography on profilin-agarose. *J. Cell Biol.*, 127(1), 107-115.
- Macias, M. J., Wiesner, S., & Sudol, M. (2002). WW and SH3 domains, two different scaffolds to recognize proline-rich ligands. *FEBS Letters*, 513(1), 30-37.
- Maciver, S., Zot, H., & Pollard, T. (1991). Characterization of actin filament severing by actophorin from Acanthamoeba castellanii. *J. Cell Biol.*, 115(6), 1611-1620.
- Maciver, S. K. (1998). How ADF/cofilin depolymerizes actin filaments. *Current Opinion in Cell Biology*, 10(1), 140-144.
- Madania, A., Dumoulin, P., Grava, S., Kitamoto, H., Scharer-Brodbeck, C., Soulard, A., Moreau, V., & Winsor, B. (1999). The *Saccharomyces cerevisiae* Homologue of Human Wiskott-Aldrich Syndrome Protein Las17p Interacts with the Arp2/3 complex. *Molecular Biology of the Cell*, 10, 3521-3538.
- McCann, R. O., & Craig, S. W. (1997). The I-LWEQ module: a conserved sequence that signifies F-actin binding in functionally diverse proteins from yeast to mammals. *Proc. Natl. Acad. Science*, 94, 5679-5684.
- McGough, A. M., Staiger, C. J., Min, J. K., & Simonetti, K. D. (2003). The gelsolin family of actin regulatory proteins: modular structures, versatile functions. *FEBS Letters*, 552(2-3), 75-81.
- McLaughlin, P. J., Gooch, J. T., Mannherz, H. G., & Weeds, A. G. (1993). Structure of gelsolin segment 1-actin complex and the mechanism of filament severing. *Nature*, 364(6439), 685-692.
- McPherson, P. S. (1999). Regulatory Role of SH3 Domain-mediated Protein-Protein Interactions in Synaptic Vesicle Endocytosis. *Cellular Signalling*, 11(4), 229-238.
- Mejillano, M. R., Kojima, S.-i., Applewhite, D. A., Gertler, F. B., Svitkina, T. M., & Borisy, G. G. (2004). Lamellipodial Versus Filopodial Mode of the Actin Nanomachinery: Pivotal Role of the Filament Barbed End. *Cell*, 118(3), 363-373.
- Merrifield, C. J., Feldman, M. E., Wan, L., & Almers, W. (2002). Imaging actin and dynamin recruitment during invagination of single clathrin-coated pits. *Nature Cell Biology*, 4(9), 691-698.
- Merrifield, C. J., Moss, S. E., Ballestrem, C., Imhof, B. A., Giese, G., Wunderlich, I., & Almers, W. (1999). Endocytic vesicles move at the tips of actin tails in cultured mast cells. *Endocytic vesicles move at the tips of actin tails in cultured mast cells*, 1(1), 72-74.
- Miki, H., Sasaki, T., Takai, Y., & Takenawa, T. (1998). Induction of filopodium formation by a WASP-related actin-depolymerizing protein N-WASP. *Nature*, 391(6662), 93-96.
- Millar, C. A., Powell, K. A., Hickson, G. R. X., Bader, M.-F., & Gould, G. W. (1999). Evidence for a Role for ADP-ribosylation Factor 6 in Insulin-stimulated Glucose Transporter-4 (GLUT4) Trafficking in 3T3-L1 Adipocytes. *J. Biol. Chem.*, 274(25),

17619-17625.

- Milligan, R. A., Whittaker, M., & Safer, D. (1990). Molecular structure of F-actin and location of surface binding sites. *Nature*, 348(6298), 217-221.
- Mitsui, K., Yaguchi, S., & Tsurugi, K. (1994). The GTS1 gene, which contains a Gly-Thr repeat, affects the timing of budding and cell size of the yeast *Saccharomyces cerevisiae*. *Molecular Biology of the Cell*, 14(8), 5569-5578.
- Moon, A., & Drubin, D. G. (1995). The ADF/Cofilin Proteins: Stimulus-responsive Modulators of Actin Dynamics. *Molecular Biology of the Cell*, 6(11), 1423-1431.
- Moon, A., Janmey, P., Louie, K., & Drubin, D. (1993). Cofilin is an essential component of the yeast cortical cytoskeleton. *J. Cell Biol.*, 120(2), 421-435.
- Moores, C. A., Keep, N. H., & Kendrick-Jones, J. (2000). Structure of the utrophin actin-binding domain bound to F-actin reveals binding by an induced fit mechanism. *Journal of Molecular Biology*, 297(2), 465-480.
- Moreau, V., Galan, J. M., Devilliers, G., Haguenauer-Tsapis, R., & Winsor, B. (1997). The yeast actin-related protein Arp2p is required for the internalization step of endocytosis. *Molecular Biology of the Cell*, 8(7), 1361-1375.
- Moreau, V., Madania, A., Martin, R., & Winson, B. (1996). The *Saccharomyces cerevisiae* actin-related protein Arp2 is involved in the actin cytoskeleton. *J. Cell Biol.*, 134(1), 117-132.
- Morton, W. M., Ayscough, K. R., & McLaughlin, P. J. (2000). Latrunculin alters the actin-monomer subunit interface to prevent polymerisation. *Nature Cell Biology*, 2, 376-378.
- Mosammaparast, N., & Pemberton, L. F. (2004). Karyopherins: from nuclear-transport mediators to nuclear-function regulators. *Trends in Cell Biology*, 14(10), 547-556.
- Mulholland, J., Preuss, D., Moon, A., Wong, A., Drubin, D. G., & Botstein, D. (1994). Ultrastructure of the yeast actin cytoskeleton and its association with the plasma membrane. *J. Cell Biol.*, 125(2), 381-391.
- Mumberg, D., Muller, R., & Funk, M. (1995). Yeast vectors for the controlled expression of heterologous proteins in different genetic backgrounds. *Gene*, 156(1), 119-122.
- Munn, A. L. (2000). The Yeast Endocytic Membrane Transport System. *Microscopy Research and Technique*, 51, 547-562.
- Munn, A. L., Stevenson, B. J., Geli, M. I., & Riezman, H. (1995). end5, end6, and end7: mutations that cause actin delocalization and block the internalization step of endocytosis in *Saccharomyces cerevisiae*. *Mol Biol Cell*, December; 6(12), 1721-1742.
- Nakayasu, H., & Ueda, K. (1985). Association of rapidly-labelled RNAs with actin in nuclear matrix from mouse L5178Y cells. *Experimental cell research*, 160(2), 319-330.
- Nefsky, B., & Bretscher, A. (1992). Yeast actin is relatively well behaved. *European Journal of Biochemistry*, 206(3), 949-955.
- Nern, A., & Arkowitz, R. A. (2000). Nucleocytoplasmic Shuttling of the Cdc42p Exchange Factor Cdc24p. *J. Cell Biol.*, 148(6), 1115-1122.
- Nossal, R., & Zimmerberg, J. (2002). Endocytosis: Curvature to the ENTH Degree. *Current Biology*, 12(22), R770-R772.
- Ohta, Y., Nishida, E., Sakai, H., & Miyamoto, E. (1989). Dephosphorylation of cofilin accompanies heat shock-induced nuclear accumulation of cofilin. *J. Biol. Chem.*, 264(27), 16143-16148.
- Olave, I. A., Reck-Peterson, S. L., & Crabtree, G. R. (2002). Nuclear Actin and Actin-Related Proteins in Chromatin Remodelling. *Annual Review of Biochemistry*, 71(1), 755-781.

- Onoda, K., Yu, F. X., & Yin, H. L. (1993). gCap39 is a nuclear and cytoplasmic protein. *Cell Motility and the Cytoskeleton*, 26(3), 227-238.
- Otterbein, L. R., Graceffa, P., & Dominguez, R. (2001). The Crystal Structure of Uncomplexed Actin in the ADP State. *Science*, 293, 708-711.
- Pantaloni, D., Boujemaa, R., Didry, D., Gounon, P., & Carlier, M. F. (2000). The Arp2/3 complex branches filament barbed ends: functional antagonism with capping proteins. *Nature Cell Biology*, 2(7), 385-391.
- Pendleton, A., Pope, B., Weeds, A., & Koffer, A. (2003). Latrunculin B or ATP Depletion Induces Cofilin-dependent Translocation of Actin into Nuclei of Mast Cells. *J. Biol. Chem.*, 278(16), 14394-14400.
- Philimonenko, V. V., Zhao, J., Iben, S., Dingova, H., Kysela, K., Kahle, M., Zentgraf, H., Hofmann, W. A., de Lanerolle, P., Hozak, P., & Grummt, I. (2004). Nuclear actin and myosin I are required for RNA polymerase I transcription. *advanced online publication*.
- Pollard, T. (1986). Rate constants for the reactions of ATP- and ADP-actin with the ends of actin filaments. *J. Cell Biol.*, 103(6), 2747-2754.
- Pollard, T. D. (1982). A falling ball apparatus to measure filament cross-linking. *Methods in Cell biology*(24), 301-311.
- Pollard, T. D., Blanchoin, L., & Mullins, R. D. (2000). Molecular Mechanisms Controlling Actin Filament Dynamics in Non-muscle Cells. *Annual Review of Biophysics and Biomolecular Structure*, 29(1), 545-576.
- Pollard, T. D., & Borisy, G. G. (2003). Cellular Motility Driven by Assembly and Disassembly of Actin Filaments. *Cell*, 112(4), 453-465.
- Pruyne, D., & Bretscher, A. (2000a). Polarization of cell growth in yeast. I. Establishment and maintenance of polarity states. *J Cell Sci*, 113(3), 365-375.
- Pruyne, D., & Bretscher, A. (2000b). Polarization of cell growth in yeast. II. *J Cell Sci*, 113(4), 571-585.
- Pruyne, D., Evangelista, M., Yang, C., Bi, E., Zigmond, S., Bretscher, A., & Boone, C. (2002). Role of Formins in Actin Assembly: Nucleation and Barbed-End Association. *Science*, 297(5581), 612-615.
- Pruyne, D., Gao, L., Bi, E., & Bretscher, A. (2004). Stable and Dynamic Axes of Polarity Use Distinct Formin Isoforms in Budding Yeast. *Mol. Biol. Cell*, 15(11), 4971-4989.
- Pruyne, D. W., Schott, D. H., & Bretscher, A. (1998). Tropomyosin-containing Actin Cables Direct the Myo2p-dependent Polarized Delivery of Secretory Vesicles in Budding Yeast. *J. Cell Biol.*, 143(7), 1931-1945.
- Puertollano, R., Randazzo, P. A., Presley, J. F., Hartnell, L. M., & Bonifacino, J. S. (2001). The GGAs Promote ARF-Dependent Recruitment of Clathrin to the TGN. *Cell*, 105(1), 93-102.
- Qualmann, e. a. (2000). Molecular Links between Endocytosis and the Actin Cytoskeleton. *Journal of Cell Biology*, 150(5), F111-F116.
- Randazzo, P., & Kahn, R. (1994). GTP hydrolysis by ADP-ribosylation factor is dependent on both an ADP-ribosylation factor GTPase-activating protein and acid phospholipids [published erratum appears in J Biol Chem 1994 Jun 10;269(23):16519]. *J. Biol. Chem.*, 269(14), 10758-10763.
- Randazzo, P. A., & Hirsch, D. S. (2004). Arf GAPs: multifunctional proteins that regulate membrane traffic and actin remodelling. *Cellular Signalling*, 16(4), 401-413.
- Rando, O. J., Zhao, K., & Crabtree, G. R. (2000). Searching for a function for nuclear actin.

Trends in Cell Biology, 10(3), 92-97.

- Raths, S., Rohrer, J., Crausaz, F., & Riezman, H. (1993). end3 and end4: two mutants defective in receptor-mediated and fluid-phase endocytosis in *Saccharomyces cerevisiae*. *J. Cell Biol.*, 120(1), 55-65.
- Reizman, H. (1985). Endocytosis in yeast: several of the yeast secretory mutants are defective in endocytosis. *Cell*, 40(4), 1001-1009.
- Robbins, J., Dilworth, S. M., Laskey, R. A., & Dingwall, C. (1991). Two interdependent basic domains in nucleoplasmin nuclear targeting sequence: identification of a class of bipartite nuclear targeting sequence. *Cell*, 64(3), 615-623.
- Robinson, R. C., Mejillano, M., Le, V. P., Burtnick, L. D., Yin, H. L., & Choe, S. (1999). Domain Movement in Gelsolin: A Calcium-Activated Switch. *Science*, 286(5446), 1939-1942.
- Robinson, R. C., Turbedsky, K., Kaiser, D. A., Marchand, J., Higgs, H. N., Choe, S., & Pollard, T. D. (2001). Crystal Structure of Arp2/3 Complex. *Science*, 294(5547), 1679-1684.
- Rodal, A. A., Tetreault, J. W., Lappalainen, P., Drubin, D. G., & Amberg, D. C. (1999). Aip1p Interacts with Cofilin to Disassemble Actin Filaments. *J. Cell Biol.*, 145(6), 1251-1264.
- Roelants, F. M., Torrance, P. D., Bezman, N., & Thorner, J. (2002). Pkh1 and pkh2 differentially phosphorylate and activate ypk1 and ykr2 and define protein kinase modules required for maintenance of cell wall integrity. *Molecular Biology of the Cell*, 13(9), 3005-3028.
- Rosenblatt, J., Agnew, B. J., Abe, H., Bamburg, J. R., & Mitchison, T. J. (1997). Xenopus Actin Depolymerizing Factor/Cofilin (XAC) Is Responsible for the Turnover of Actin Filaments in *Listeria monocytogenes* Tails. *J. Cell Biol.*, 136(6), 1323-1332.
- Rothkegel, M., Mayboroda, O., Rohde, M., Wucherpfennig, C., Valenta, R., & Jockusch, B. (1996). Plant and animal profilins are functionally equivalent and stabilize microfilaments in living animal cells. *J Cell Sci*, 109(1), 83-90.
- Sagot, I., Klee, S. K., & Pellman, D. (2002a). Yeast formins regulate cell polarity by controlling the assembly of actin cables. *4*(1), 42-50.
- Sagot, I., Rodal, A. A., Moseley, J., Goode, B. L., & Pellman, D. (2002b). An actin nucleation mechanism mediated by Bni1 and Profilin. *4*(8), 626-631.
- Sazer, S., & Dasso, M. (2000). The ran decathlon: multiple roles of Ran. *J Cell Sci*, 113(7), 1111-1118.
- Schaerer-Brodbeck, C., & Riezman, H. (2000). Functional Interactions between the p35 Subunit of the Arp2/3 Complex and Calmodulin in Yeast. *Molecular Biology of the Cell*, 11(4), 1113-1127.
- Schaerer-Brodbeck, C., & Riezman, H. (2003). Genetic and biochemical interactions between the Arp2/3 complex, Cmd1p, casein kinase II, and Tub4p in yeast. *FEMS Yeast Research*, 4(1), 37-49.
- Schafer, D. A., Jennings, P. B., & Cooper, J. A. (1996). Dynamics of capping protein and actin assembly in vitro: uncapping barbed ends by polyphosphoinositides. *J. Cell Biol.*, 135(1), 169-179.
- Schutt, C. E., Myslik, J. C., Rozycki, M. D., Goonesekere, N. C., & Lindberg, U. (1993). The structure of crystalline profilin-beta-actin. *Nature*, 365(6449), 810-816.
- Seedorf, M., & Silver, P. A. (1997). Importin/karyopherin protein family members required for mRNA export from the nucleus. *PNAS*, 94(16), 8590-8595.

- Shaw, J. D., Cummings, K. B., Huyer, G., Michaelis, S., & Wendland, B. (2001). Yeast as a Model System for Studying Endocytosis. *Experimental cell research*, 271(1), 1-9.
- Silacci, P., Mazzolai, L., Gauci, C., Stergiopoulos, N., Yin, H. L., & Hayoz, D. (2004). Gelsolin superfamily proteins: key regulators of cellular functions. *Cellular and Molecular Life Sciences (CMLS)*, 61(19 - 20), 2614-2623.
- Smith, M. G., Swamy, S. R., & Pon, L. A. (2001). The Life Cycle of Actin Patches in Mating Yeast. *Journal of Cell Science*, 114, 1505-1513.
- Smythe, E., & Ayscough, K. R. (2003). The Ark1/Prk1 family of protein kinases. *EMBO reports*, 4(3), 246-251.
- Stamenova, S. D., Dunn, R., Adler, A. S., & Hicke, L. (2004). The Rsp5 Ubiquitin Ligase Binds to and Ubiquitinates Members of the Yeast CIN85-Endophilin Complex, Sla1-Rvs167. *J. Biol. Chem.*, 279(16), 16017-16025.
- Stearns, T., Kahn, R. A., Botstein, D., & Hoyt, M. A. (1990). ADP ribosylation factor is an essential protein in *Saccharomyces cerevisiae* and is encoded by two genes. *Mol Cell Biol.*, 10(12), 6690-6699.
- Stüven, T., Hartmann, E., & Görlich, D. (2003). Exportin 6: a novel nuclear export receptor that is specific for profilin-actin complexes. *The EMBO Journal*, 22, 5928-5940.
- Svitkina, T. M., & Borisy, G. G. (1999). Arp2/3 Complex and Actin Depolymerizing Factor/Cofilin in Dendritic Organization and Treadmilling of Actin Filament Array in Lamellipodia. *J. Cell Biol.*, 145(5), 1009-1026.
- Symons, M., Derry, J. M., Karlak, B., Jiang, S., Lemahieu, V., McCormick, F., Francke, U., & Abo, A. (1996). Wiskott-Aldrich syndrome protein, a novel effector for the GTPase CDC42Hs, is implicated in actin polymerization. *Cell*, 84(5), 723-734.
- Takatsu, H., Yoshino, K., Toda, K., & Nakayama, K. (2002). GGA proteins associate with Golgi membranes through interaction between their GGAH domains and ADP-ribosylation factors. *Biochemical Journal*, 365, 369-378.
- Tang, H., Xu, J., & Cai, M. (2000). Pan1p, End3p, and Sla1p, Three Yeast Proteins Required for Normal Cortical Actin Cytoskeleton Organization, Associate with Each Other and Play Essential Roles in Cell Wall Morphogenesis. *Mol. Cell. Biol.*, 20(1), 12-25.
- Tang, H. Y., & Cai, M. (1996). The EH-domain-containing protein Pan1 is required for normal organization of the actin cytoskeleton in *Saccharomyces cerevisiae*. *Mol. Cell. Biol.*, 16(9), 4897-4914.
- Tang, H. Y., Munn, A. L., & Cai, M. (1997). EH domain proteins Pan1p and End3p are components of a complex that plays a dual role in organization of the cortical actin cytoskeleton and endocytosis in *Saccharomyces cerevisiae*. *Mol. Cell. Biol.*, 17(8), 4294-4304.
- Theriot, J. A. (1997). Accelerating on a Treadmill: ADF/Cofilin Promotes Rapid Actin Filament Turnover in the Dynamic Cytoskeleton. *J. Cell Biol.*, 136(6), 1165-1168.
- Theriot, J. A., Rosenblatt, J., Portnoy, D. A., Goldschmidt-Clermont, P. J., & Mitchison, T. J. (1994). Involvement of profilin in the actin-based motility of *L. monocytogenes* in cells and in cell-free extracts. *Cell*, 76(3), 505-517.
- Tilney, L. G., Connelly, P. S., & Portnoy, D. A. (1990). Actin filament nucleation by the bacterial pathogen, *Listeria monocytogenes*. *J. Cell Biol.*, 111(6), 2979-2988.
- Tolliday, N., VerPlank, L., & Li, R. (2002). Rho1 Directs Formin-Mediated Actin Ring Assembly during Budding Yeast Cytokinesis. *Current Biology*, 12(21), 1864-1870.
- Tong, A. H. Y., Lesage, G., Bader, G. D., Ding, H., Xu, H., Xin, X., Young, J., Berriz, G. F.,

- Brost, R. L., Chang, M., Chen, Y., Cheng, X., Chua, G., Friesen, H., Goldberg, D. S., Haynes, J., Humphries, C., He, G., Hussein, S., Ke, L., Krogan, N., Li, Z., Levinson, J. N., Lu, H., Menard, P., Munyana, C., Parsons, A. B., Ryan, O., Tonikian, R., Roberts, T., Sdicu, A.-M., Shapiro, J., Sheikh, B., Suter, B., Wong, S. L., Zhang, L. V., Zhu, H., Burd, C. G., Munro, S., Sander, C., Rine, J., Greenblatt, J., Peter, M., Bretscher, A., Bell, G., Roth, F. P., Brown, G. W., Andrews, B., Bussey, H., & Boone, C. (2004). Global Mapping of the Yeast Genetic Interaction Network. *Science*, 303(5659), 808-813.
- Tusher, V. G., Tibshirani, R., & Chu, G. (2001). Significance analysis of microarrays applied to the ionizing radiation response. *PNAS*, 98(9), 5116-5121.
- Uetz, P., Giot, L., Cagney, G., Mansfield, T. A., Judson, R. S., Knight, J. R., Lockshon, D., Narayan, V., Srinivasan, M., Pochart, P., Qureshi-Emili, A., Li, Y., Godwin, B., Conover, D., Kalbfleisch, T., Vijayadamodar, G., Yang, M., Johnston, M., Fields, S., & Rothberg, J. M. (2000). A comprehensive analysis of protein-protein interactions in *Saccharomyces cerevisiae*. *Nature*, 403(6770), 623-627.
- Venturi, G. M., Bloecher, A., Williams-Hart, T., & Tatchell, K. (2000). Genetic Interactions Between GLC7, PPZ1 and PPZ2 in *Saccharomyces cerevisiae*. *Genetics*, 155(1), 69-83.
- Verna, J., Lodder, A., Lee, K., Vagts, A., & Ballester, R. (1997). A family of genes required for maintenance of cell wall integrity and for the stress response in *cerevisiae*. *PNAS*, 94(25), 13804-13809.
- Vida, T. A., & Emr, S. D. (1995). A new vital stain for visualizing vacuolar membrane dynamics and endocytosis in yeast. *J. Cell Biol.*, 128(5), 779-792.
- Vignjevic, D., Yarar, D., Welch, M. D., Peloquin, J., Svitkina, T., & Borisy, G. G. (2003). Formation of filopodia-like bundles in vitro from a dendritic network. *J. Cell Biol.*, 160(6), 951-962.
- Volkmann, N., Amann, K. J., Stoilova-McPhie, S., Egile, C., Winter, D. C., Hazelwood, L., Heuser, J. E., Li, R., Pollard, T. D., & Hanein, D. (2001). Structure of Arp2/3 Complex in Its Activated State and in Actin Filament Branch Junctions. *Science*, 293(5539), 2456-2459.
- Volkmann, N., Hanein, D., Ouyang, G., Trybus, K. M., DeRosier, D. J., & Lowey, S. (2000). Evidence for cleft closure in actomyosin upon ADP release. *Nature Structural Biology*, 7(12), 1147-1155.
- Waddle, J. A., Karpova, T. S., Waterston, R. H., & Cooper, J. A. (1996). Movement of cortical actin patches in yeast. *J. Cell Biol.*, 132(5), 861-870.
- Wang, G., McCaffery, J. M., Wendland, B., Dupre, S., Haguenauer-Tsapis, R., & Huibregtse, J. M. (2001a). Localization of the Rsp5p Ubiquitin-Protein Ligase at Multiple Sites within the Endocytic Pathway. *Mol. Cell. Biol.*, 21(10), 3564-3575.
- Wang, J., Liu, W., Mitsui, K., & Tsurugi, K. (2001b). Evidence for the involvement of the GTS1 gene product in the regulation of biological rhythms in the continuous culture of the yeast *Saccharomyces cerevisiae*. *FEBS Letters*, 489(1), 81-86.
- Wang, Q., Xie, Y., Du, Q.-S., Wu, X.-J., Feng, X., Mei, L., McDonald, J. M., & Xiong, W.-C. (2003). Regulation of the formation of osteoclastic actin rings by proline-rich tyrosine kinase 2 interacting with gelsolin. *J. Cell Biol.*, 160(4), 565-575.
- Warren, D. T., Andrews, P. D., Gourlay, C. W., & Ayscough, K. R. (2002). Sla1p couples the yeast endocytic machinery to proteins regulating actin dynamics. *J Cell Sci*, 115(8), 1703-1715.
- Way, M., Pope, B., & Weeds, A. G. (1992). Evidence for functional homology in the F-actin

- binding domains of gelsolin and alpha-actinin: implications for the requirements of severing and capping. *J. Cell Biol.*, 119(4), 835-842.
- Weis, K. (2003). Regulating Access to the Genome: Nucleocytoplasmic Transport throughout the Cell Cycle. *Cell*, 112(4), 441-451.
- Welch, M. D., & Drubin, D. G. (1994). A nuclear protein with sequence similarity to proteins implicated in human acute leukemias is important for cellular morphogenesis and actin cytoskeletal function in *Saccharomyces cerevisiae*. *Molecular Biology of the Cell*, 5(6), 617-632.
- Welch, M. D., Iwamatsu, A., & Mitchison, T. J. (1997). Actin polymerization is induced by Arp2/3 protein complex at the surface of *Listeria monocytogenes*. *Nature*, 385(6613), 165-269.
- Welch, M. D., Vinh, D. B. N., Okamura, H. H., & Drubin, D. G. (1993). Screens for Exogenous Mutations That Fail to Complement *act1* Alleles Identify Genes That Are Important for Actin Function in *Saccharomyces cerevisiae*. *Genetics*, 135(2), 265-274.
- Wendland, B., Emr, S. D., & Riezman, H. (1998). Protein Traffic in the Yeast Endocytic and Vacular Protein Sorting Pathways. *Current Opinion in Cell Biology*, 10, 513-522.
- Wendland, B., McCaffery, J. M., Xiao, Q., & Emr, S. D. (1996). A novel fluorescence-activated cell sorter-based screen for yeast endocytosis mutants identifies a yeast homologue of mammalian eps15. *J. Cell Biol.*, 135(6), 1485-1500.
- Wesp, A., Hicke, L., Palecek, J., Lombardi, R., Aust, T., Munn, A. L., & Riezman, H. (1997). End4p/Sla2p Interacts with Actin-associated Proteins for Endocytosis in *Saccharomyces cerevisiae*. *Mol. Biol. Cell*, 8(11), 2291-2306.
- Wiederkehr, A., Meier, K. D., & Riezman, H. (2001). Identification and characterisation of *Saccharomyces cerevisiae* mutants defective in fluid-phase endocytosis. *Yeast*, 18, 759-773.
- Winder, S. J., Jess, T., & Ayscough, K. R. (2003). SCP1 encodes an actin-bundling protein in yeast. *Biochemical Journal*, 375, 287-295.
- Winter, D., Lechler, T., & Li, R. (1999a). Activation of the yeast Arp2/3 complex by Bee1p, a WASP-family protein. *Current Biology*, 9(9), 501-505.
- Winter, D., Podtelejnikov, A. V., Mann, M., & Li, R. (1997). The complex containing actin-related proteins Arp2 and Arp3 is required for the motility and integrity of yeast actin patches. *Current Biology*, 7(7), 519-529.
- Winter, D. C., Choe, E. Y., & Li, R. (1999b). Genetic dissection of the budding yeast Arp2/3 complex: A comparison of the *in vivo* and structural roles of individual subunits. *PNAS*, 96(13), 7288-7293.
- Xu, C., Craig, R., Tobacman, L., Horowitz, R., & Lehman, W. (1999). Tropomyosin Positions in Regulated Thin Filaments Revealed by Cryoelectron Microscopy. *Biophys. J.*, 77(2), 985-992.
- Yaguchi, S.-i., Mitsui, K., Iha, H., & Tsurugi, K. (2000). Phosphorylation of the GTS1 gene product of the yeast *Saccharomyces cerevisiae* and its effect on heat tolerance and flocculation. *FEMS Microbiology Letters*, 187(2), 179-184.
- Yang, S., Cope, M. J., & Drubin, D. G. (1999). Sla2p is Associated with the Yeast Cortical Actin Cytoskeleton via Redundant Localisation Signals. *Molecular Biology of the Cell*, 10, 2265-2283.
- Yin, H. L., & Janmey, P. A. (2003). Phosphoinositide Regulation of the Actin Cytoskeleton. *Annual Review of Physiology*, 65(1), 761-789.

- Yoneda, Y. (2000). Nucleocytoplasmic protein traffic and its significance to cell function. *Genes Cells*, 5(10), 777-787.
- Yonezawa, N., Nishida, E., Maekawa, S., & Sakai, H. (1988). Studies on the interaction between actin and cofilin purified by a new method. *Biochemical Journal*, 251(1), 121-127.
- Yoshida, K., & Blobel, G. (2001). The Karyopherin Kap142p/Msn5p Mediates Nuclear Import and Nuclear Export of Different Cargo Proteins. *J. Cell Biol.*, 152(4), 729-740.
- Young, M. E., Cooper, J. A., & Bridgman, P. C. (2004). Yeast actin patches are networks of branched actin filaments. *J. Cell Biol.*, 166(5), 629-635.
- Zeng, G., & Cai, M. (1999). Regulation of the Actin Cytoskeleton Organisation in Yeast by a Novel Serine/Threonine Kinase Prk1p. *Journal of Cell Biology*, 144(1), 71-82.
- Zeng, G., Yu, X., & Cai, M. (2001). Regulation of Yeast Actin Cytoskeleton-Regulatory Complex Pan1p/Sla1p/End3p by Serine/Threonine Kinase Prk1p. *Molecular Biology of the Cell*, 12(12), 3759-3772.
- Zhang, C.-j., Cavenagh, M. M., & Kahn, R. A. (1998). A Family of Arf Effectors Defined as Suppressors of the Loss of Arf Function in the Yeast *Saccharomyces cerevisiae*. *J. Biol. Chem.*, 273(31), 19792-19796.
- Zhdankina, O., Strand, N. L., Redmond, J. M., & Boman, A. L. (2001). Yeast GGA proteins interact with GTP-bound Arf and facilitate transport through the Golgi. *Yeast*, 18, 1-18.
- Zu, T., Verna, J., & Ballester, R. (2001). Mutations in WSC genes for putative stress receptors result in sensitivity to multiple stress conditions and impairment of RIM1-dependent gene expression in *Saccharomyces cerevisiae*. *Molecular Genetics and Genomics*, 266(1), 142-155.

